OXYGEN AND CARBON ISOTOPES IN INDIAN OCEAN SEDIMENTS AND THEIR PALAEOCLIMATIC IMPLICATIONS

by

ANINDYA SARKAR

A THESIS
SUBMITTED FOR THE DEGREE OF

DOCTOR OF PHILOSOPHY

TO THE
GUJARAT UNIVERSITY

AUGUST 1989

PHYSICAL RESEARCH LABORATORY
AHMEDABAD 380 009
INDIA

CERTIFICATE

I hereby declare that the work presented in this thesis is original and has not formed the basis for the award of any degree or diploma by any University or Institution.

Anindya Sarkar

(Anindya Sarkar)
Author

Certified by:

S. K. Bhattacharya

Professor S.K. Bhattacharya
Thesis Supervisor

Date: August 25, 1989

To

Bapi, Ma and little Rim

CONTENTS

SYNOPSIS

The most important feature in the climatic system of the northern Indian ocean and adjoining regions is the 'monsoon'. Due to its profound impact on the economy of the Indian subcontinent,it has received enormous attention from climatologists and planners alike.For predicting the future behaviour of monsoon, it has therefore been crucial to understand its variation in the past.For recovering the short term variations in the past monsoon,natural recorders like tree rings, coastal sediments etc. act as proxy meteorological 'observatories'. However, in order to know long term climatic changes related to the monsoon,spanning time scales from a few thousand years to a few million years, deep sea sediments are the ideal repositories.This is because, apart from the Indian sub-continent,the monsoon also has a pronounced effect on the northern Indian ocean.

The strong SW monsoon during the summer months brings heavy rainfall over the Indian subcontinent and produces a huge river discharge in the Bay of Bengal and the Arabian sea. Pronounced coastal upwelling takes place off Arabia and along the west coast of India due to this monsoon.During winter the SW monsoon disappears and the NE monsoon is activated, producing winter precipitation in NE India and along the east coast of peninsular India.The signatures of these monsoons are attested in the ocean by a variety of physico-chemical changes namely changes in temperature,

salinity, nutrient supply and so on and can be traced by stable isotopes of oxygen and carbon in marine calcitic shells of foraminifera from the sediments of this ocean.The oxygen isotopic composition ($\delta^{18}O$) of the foraminiferal shells depend on (i) the temperature of the ocean water in which these organisms grow;and (ii) the $\delta^{18}O$ composition of the sea water,which in turn is related to its salinity.

Similarly, the carbon isotopic composition ($\delta^{13}C$) of foraminiferal shells depends on the $\delta^{13}C$ composition of total dissolved CO_2 in the ocean.From the stable isotope studies on sediment cores from the other oceans viz. the Atlantic and the Pacific,it has been possible to know about the glacial (cold) and interglacial (warm) climatic changes for at least the last 2 million years.Variation in the oceanic carbon cycle and its nature has also been studied. It is then a pertinent question to ask what was the response of local monsoonal system to such global climatic changes. Monsoon induced upwelling largely controls the biological productivity in the northern Indian ocean.Any change in monsoon intensity therefore is capable of perturbing the oceanic productivity. The timing and the causative mechanisms of these changes form an important part of such inquiries.To know the timing of these climatic events for last 40, 000 years (40 kyr),radiocarbon (^{14}C, $t_{1/2}$~5.73 kyr) dating is necessary and has been widely used. In addition, the chronology based on ^{230}Th ($t_{1/2}$~75.2 kyr) can also be used to date sediments as old as 300 kyr.Many of these climatic changes are transient in nature and hence

high resolution (~1000 years) studies are necessary to get a detailed picture.

This thesis is an attempt to study palaeoclimatic and palaeo-oceanographic conditions in the northern Indian ocean based on precise measurements of $\delta^{18}O$ and $\delta^{13}C$ of foraminiferal shells in the sediments from this region.Aim of this work was to:-

1. Fabricate an experimental system of CO_2 extraction for precise measurement of $\delta^{18}O$ and $\delta^{13}C$ (expressed in terms of per mil, $^{o}/oo$) in minute (~ 0.5 mg) quantities of foraminiferal carbonate.

2. Study of long term changes of monsoon-intensity with a high resolution of 1000 years, and its effect on upwelling and oceanic productivity.

3. Obtain ^{14}C and ^{230}Th measurements for dating these climatic events as well as calculation of the accumulation rates of sediments.

Important findings of the present study based on sediment cores from the Arabian sea and the Indian ocean are:

1. During last glacial maximum (~ 18 kyr B.P.),the entire Arabian sea was more saline than today.However,the northern Arabian sea was characterised by higher salinity than southern part caused by an excessive evaporation due to dry trade winds of the stronger NE

monsoon circulation. This, coupled with a low river discharge (due to a weak SW-monsoon) increased the salinity gradient in the Arabian sea.

2. The NE monsoon oceanic circulation was stronger than today ~ 20-16 kyr back.

3. Oceanic productivity increased around 14 kyr B.P. due to an increased upwelling, which perhaps has an important role in controlling $\delta^{13}C$ of ΣCO_2 in ocean water.

4. Local reducing condition within the sediment column or low oxygenated bottom water condition during the LGM prevailed in the eastern Arabian sea leading to the removal of uranium from the sea water.

This thesis is divided into four chapters.

In Chapter I, a brief introduction is given about the application of stable isotope systematics in marine sediments. Deep sea sediments have yielded important information about the past changes in the global build up of continental ice, sea surface temperature (SST), ocean circulation, sea level changes as well as changes in the concentration of atmospheric CO_2. $\delta^{18}O$ and $\delta^{13}C$ changes in formainifera of the ocean sediments yield information about both global and local changes in climate. By subtracting the global effects one can determine the local climatic changes.

This chapter also gives a brief review of the earlier work done in the Indian ocean sediments, particularly the

Arabian sea. Stable isotope studies in this part have shown that beside the normal global signature of glacial-interglacial cycles, marked changes in local hydrography had taken place in the past. These studies revealed that:-

1. The SW monsoon was weaker than today at around 18 kyr B.P. coinciding with the last glacial maximum (LGM).

2. As a consequence the upwelling in the western Arabian sea was much less intense during LGM.

3. The sea surface temperature (SST) was warmer by about $1^{o}C$ during LGM in some locations of the Arabian sea.

4. A CO_2 rich, O_2 poor water characterised the deep sea (> 2000 m) during LGM.

These studies though did not yield a detailed picture of the climatic changes, served as a basis for conducting the present investigation. Along with the weak SW monsoon during LGM, the possibility of a stronger NE monsoon was indicated by earlier studies but no oxygen isotope evidence was available for it. Excepting $\delta^{18}O$, other climatic parameters namely $\delta^{13}C$, calcium carbonate were not measured by earlier workers. Additionally, the absolute chronologies for these events were not available. The present work aims at providing these information together so as to make a better picture of climatic changes in the northern Indian ocean. For this purpose, five deep sea cores have been raised

namely SK-20-185,SK-20-186,CD-17-15,CD-17-30 and CD-17-32.

The cores CD-17-30, CD-17-15 and CD-17-32 are representatives of the northern Arabian sea where salinity is high and coastal upwelling plays a dominant role today. Core SK-20-185 is located in the eastern Arabian sea,close to the region where some salinity reduction takes place during winter time due to the NE monsoon current but is not affected by coastal processes.The core SK-20-186 comes from the equatorial Indian ocean and represents an open ocean condition.

Chapter II deals with the experimental techniques employed viz., preparation of foraminiferal samples, extraction of CO_2 by acid reaction and its mass-spectrometric measurements for $\delta^{18}O$ and $\delta^{13}C$, radiochemical purification for U-Th isotopes and their assay, ^{14}C measurements and estimation of $CaCO_3$ and coarse fraction (> 150 μ m). $\delta^{18}O$-$\delta^{13}C$ measurements in deep sea cores require a rapid analysis of large number of samples. Towards this an on-line CO_2 extraction system has been fabricated which could analyse minute quantities (~ 0.5 mg) of foraminiferal shells. The reproducibility of the measurements in this system is better than $\pm$ 0.1 $^{o}/oo$.This is about a factor of two better than the conventional extraction system earlier employed at PRL,where we achieved a reproducibility of $\pm$ 0.2 $^{o}/oo$. An interlaboratory comparison of standard carbonates between PRL and the stable isotope laboratory (Godwin Lab.) at the University of Cambridge shows that the absolute $\delta^{18}O$-$\delta^{13}C$ values agree

within $\pm$ 0.1 $^{o}/_{oo}$. For the present work, about 600 samples have been analysed routinely accompanied by standard calcium carbonate measurements.

Before mass-spectrometric analysis foraminiferal shells are generally cleaned by ultrasonication, H_2O_2 treatment as well as roasting at 400°C under vacuum. These are done to avoid contamination from extraneous carbonates as well as organic matter. However it has been shown in the present study that neither H_2O_2 treatment nor roasting at high temperatures, is required to get reproducible δ-values as long as pure and near 100% orthophosphoric acid is used. However, ultrasonication was routinely employed to remove extraneous particles though the present experiment did not show any difference between ultrasonicated and non-ultrasonicated samples.

In Chapter III, results of various studies are presented and discussed.

Chapter III is divided into three sections. In Section III.1 geochronological studies of the sediment cores are presented. The dating of various levels of sediments from the cores based on different dating methods viz. ^{14}C, U-Th series isotopes and $\delta^{18}O$ stratigraphy, is discussed in this section. Twelve ^{14}C dates were obtained for SK-20-185. These data give a constant sedimentation rate of 2.2 $\pm$ 0.1 cm/10^3 yrs, for the last 30,000 years. A dozen measurements on U-Th series radionuclides have been made on this core. There is a significant uranium enrichment (authigenically precipitated) at certain levels, by and large coinciding

with the glacial periods.After correcting for both detrital and authigenic uranium, the ^{230}Th (excess) (on bulk sediments) based sedimentation rate is ~ 2.5 $\pm$ 0.5 cm/10^3 yrs.

In the core SK-20-186, ten ^{14}C measurements have been made. In this core a change in sedimentation rate is noted. The Holocene rate is 2.4 $\pm$ 0.1 cm/10^3 yrs in comparison to 0.6 $\pm$ 0.1 cm/10^3 yrs prevalent during the glacial period. ^{230}Th measurement at ten levels gives a rate of 0.6 $\pm$ 0.1 cm/10^3 yrs (both on bulk and $CaCO_3$ free basis).The ^{230}Th rate does not show any break in rate.In both the cores SK-20-185 and SK-20-186, ^{230}Th (excess) based rates agree with ^{14}C based rates within a factor of two.

However, since these cores are mostly calcareous oozes, ^{14}C dates and sedimentation rates are taken to be closer to the real age and sedimentation rates. Considering the SPECMAP stage boundaries as true ages,the sedimentation rates have been calculated based on $\delta^{18}O$ stratigraphy.For SK-20-185 this gives a rate of 2.0 cm/10^3 yrs which is close to ^{14}C based rate.For SK-20-186,however,this yields a rate ~ 1.1 cm/kyr and agrees only with gross ^{14}C based rate (~ 1.3 $\pm$ 0.1 cm/kyr) which does not consider the breaks. Four ^{14}C dates have been generated for core CD-17-30,which gives a sedimentation rate ~ 7.7 cm/kyr.This core comes from the strong upwelling zone in the western Arabian sea and hence has a higher sedimentation rate due to a high productivity.

The oxygen isotope data obtained on the five cores from

the Arabian sea and the equatorial Indian ocean, are presented in Section III.2.An intercomparison among them is attempted and palaeoclimatic interpreation is derived therefrom. It has been shown in the present work that,though analysis of a few individuals from large size fractions of foraminifera, shows a significant intrasample variability, analysis of a large number of individuals per aliquot, picked up from a very narrow size range (e.g. 250-400μm) exhibits much less variability. A mean intrasample variability of $\pm$ 0.15 $^{o}/oo$ has been found in these ocean cores. For the long term $\delta^{18}O$ stratigraphy,G. sacculifer alone has been analysed in all the cores.The core top $\delta^{18}O$ values of this species indicate that they grow most likely in isotopic equilibrium with the ambient sea water.

A correlation has been attempted between climatic stages obtained in these cores and those obtained from the global data of SPECMAP. This correlation, along with ^{14}C dates, shows that core SK-20-185 has a well preserved oxygen isotope stratigraphy.Its length spans from the present upto stage 5e corresponding to an age of 120 kyr,including all the oxygen isotope substages. $\delta^{18}O$ stratigraphy of core SK-20-186 goes upto stage 11 i.e. upto 430 kyr. Core CD-17-30 goes upto stage 3 i.e. a record for 30 kyr.In SK-20-185 and SK-20-186, glacial-interglacial amplitudes beyond last glacial maximum (LGM) are reduced. By $\delta^{18}O$ analyses of solution resistant and solution susceptible species it has been shown that dissolution is unimportant in core SK-20-185 (also,it is located at a depth shallower

than Calcium Carbonate Compensation Depth, CCD). Core SK-20-186, though comes from a depth closer to CCD, has a high $CaCO_3$ content throughout its length indicating the near absence of dissolution. It has also been shown that bioturbation is not significant in SK-20-185. Hence the $\delta^{18}O$ amplitude reduction is attributed to the coarse sampling where few kyr signals are averaged out. In SK-20-186, however, bioturbation may have some role in this regard, owing to its lesser sedimentation rate in the deeper section of the core.

Holocene-LGM amplitude (analysed at close intervals in all the cores) shows a difference between southern core SK-20-185 and northern cores CD-17-30 and CD-17-15. The amplitudes in these cores are 2.12, 2.28 and 2.33 $^{o}/oo$ respectively. Such large amplitudes in the Arabian sea indicate that the salinity during the LGM was higher than today. Core top foraminifera in these cores show an enrichment ($\sim$ 0.4 $^{o}/oo$) from south to north in Arabian sea, explained by increasing salinity and decreasing temperature in the same direction. During the LGM this gradient increased ($\sim$ 0.6 $^{o}/oo$) with the excess enrichment in northern cores, thereby making the difference in the LGM-Holocene amplitudes in these cores and is consistent with the earlier observation by Duplessy (1982). This is explained by excessive evaporation over the northern Arabian sea during the LGM mainly due to the stronger dry trade winds caused by a reinforced NE-monsoon. This, coupled with a low river discharge in the Arabian sea due to a

weaker SW-monsoon,increased the salinity gradient.

Against these values in the Arabian sea,Holocene-LGM amplitude in the equatorial core SK-20-186 is much less i.e. 1.5 $^{o}/oo$. This is explained by either increased precipitation over this oceanic region during LGM or a reduced ice volume effect (~ 1.1 $^{o}/oo$) coupled with ~ 2^{o}C decrease in SST.

Apart from the long term $\delta^{18}O$ stratigraphies in various cores, high resolution $\delta^{18}O$ analysis in multiple species of planktonic foraminifera were performed from the core SK-20-185 in order to find out short term transient climatic events,especially during the LGM.While determining the sedimentation rate by U-Th series isotopes in this core, high authigenic precipitation of uranium was observed at the glacial levels.This is probably due to the fixation of uranium from pore water under a locally reducing condition or removal of uranium from sea water under a low oxygenated bottom water condition during the glacial period.This in turn indicates that benthic mixing was probably less and the original $\delta^{18}O$ signals are not seriously affected.Along with the bulk sample,different fractions of sediments from same layers were also dated by ^{14}C.All the fractions show almost the same age indicating no contamination in the ^{14}C concentrations. Hence short term climatic signals could be reliably recovered from this core if high resolution analyses are done. The purpose of such analyses along with the salient results obtained,are described below.

Earlier work in this region showed that the SW monsoon

and related coastal upwelling was weaker during the LGM. However, there was no $\delta^{18}O$ evidence for the increased activity of the NE monsoon,a suggestion which came mainly from pollen and mineralogical studies.To find this,the core SK-20-185 was analysed from the Holocene to the LGM level with a high resolution (1-2 cm).Core SK-20-185 was chosen for the following reasons: At present the NE monsoon,a relatively weaker monsoon, brings low salinity water from the western Bay of Bengal to the west coast of India and along $5^{o}N$. If during the glacial time,the NE monsoon was stronger, this salinity reduction would have been more pronounced, perhaps reaching further north upto the present location of core SK-20-185.Three surface dwelling and two deeper dwelling planktonic foraminifera were analysed. Surface dwelling species show a strong negative excursion of $\delta^{18}O$ of upto ~ 1 $^{o}/oo$ during LGM between 20-16 kyr (^{14}C dates). This is explained by a combination of $2^{o}C$ relative warming of SST in the Arabian sea (due to the weaker upwelling and mixed layer thickening since upwelling brings up cooler, nutrient rich bottom water) and reduction in salinity by 2 $^{o}/oo$. Since the temperature coefficient of calcitic $\delta^{18}O$ is ~ 0.2 $^{o}/oo/^{o}C$,warming would decrease $\delta^{18}O$ by 0.40 $^{o}/oo$. Additionally 2 $^{o}/oo$ salinity decrease will reduce $\delta^{18}O$ by 0.60 $^{o}/oo$ (for 1 $^{o}/oo$ salinity change,$\delta^{18}O$ change in the Arabian sea is about 0.32 $^{o}/oo$),thus making the total reduction in $\delta^{18}O$ close to ~ 1 $^{o}/oo$.

The salinity reduction has been attributed to a stronger NE monsoon current which transported low salinity

water from the western Bay of Bengal to the eastern Arabian sea. Deeper species however do not show this change since the salinity change is essentially a surface phenomenon.

Another core SK-20-186 has also been analysed with a similar high resolution from the LGM to the Holocene.But the negative excursion during the LGM (as found in SK-20-185) is absent in this core.This is because the NE monsoon current did not reach this equatorial region during the LGM;it does not reach this region even today.

During LGM, increased amount of low salinity water was brought by the reinforced NE monsoon current in the southern Arabian sea. This water was driven further northward by a stronger thermohaline circulation caused by the enhanced salinity gradient between the northern and the southern parts.

The data on $\delta^{13}C$, $CaCO_3$, coarse fraction, etc. are presented in section III.3 and their palaeoclimatic significance discussed. A high resolution $\delta^{13}C$ analysis of multiple species of planktonic foraminifera shows that the $\delta^{13}C\ \Sigma CO_2$ in the Arabian sea was depleted by upto ~ 0.5 $^{o}/_{oo}$ relative to the present around 9 kyr back.Also an enrichment of upto ~ 0.6 $^{o}/oo$ relative to 9 kyr is observed during the LGM. This is explained by strong upwelling (and perhaps strong SW-monsoon) around 9 kyr B.P. which brought the $\delta^{13}C$ depleted water from the deeper levels to the surface. Consequently the enrichment during the LGM represents a weaker upwelling (and a weaker SW monsoon). This is further corroborated by the fact that the glacial

period was characterised by a lower $CaCO_3$ productivity relative to the Holocene (due to a weaker upwelling and less nutrient supply).

Both the $CaCO_3$ and the coarse fraction (> 150 μm, mainly foraminifera) in the core SK-20-185 decrease by a factor of two from the Holocene to the glacial value, indicating that most of the $CaCO_3$ is biogenic. In core SK-20-186 too, $CaCO_3$ decreases from Holocene 90% to glacial 80% ($CaCO_3$ estimation has an error of $\pm$ 1%). Such changes in the productivity has also been found from the northern and the western Arabian sea. This low glacial productivity increased around 14 kyr B.P., and was almost coincidental with the onset of deglaciation.

A power spectrum analysis of the $\delta^{18}O$ and the $CaCO_3$ variation indicates that both of them are in phase and their variations are controlled probably by the orbital change in the obliquity (41 kyr) and the precessional (23 kyr) cycles of the earth. Chapter IV highlights the important conclusions derived from the present work and the recommendations for future work in this region.

ACKNOWLEDGEMENTS

I am extremely indebted to Professor S.K. Bhattacharya for his invaluable guidance throughout the course of this work. His great insight into experimental physics,helped me a lot to carry out the present work.I am grateful to Dr. R. Ramesh for continuous help in the laboratory and critical suggestions on data-interpretation.

I am particularly beholden to Prof. B.L.K. Somayajulu and Prof. S. Krishnaswami who have been a constant source of inspiration and transformed a structural geologist into a palaeo-oceanographer.

I thank Dr. M.M. Sarin who patiently taught the U-Th geochemistry to a novice like me.My sincere thanks are due to Dr. G. Rajagopalan of BSIP,Lucknow,for ^{14}C measurements.

The present work came into fruition by the financial support from Department of Ocean Development (DOD).In this respect, I extend my thanks to DOD and the National Institute of Oceanography for giving the ship time and other related help.

The efficient help of the Chief Scientist,Mr. V.P.C. Rao (NIO) on board R/V Sagarkanya during cruise No. 20 is thankfully acknowledged.

It is a pleasure recalling the name of Dr. N.B. Price who helped a lot for collecting cores from the northern Arabian sea during a NERC cruise of R/V Charles Darwin.

The help of Dr. N.J. Shackleton and Mr.Mike Hall of

Cambridge in providing the internal standards, interlaboratory calibration as well as guidance during the fabrication of the experimental system, immensely benefitted me.

Valuable suggestions by Dr. J.C. Duplessy (Gif-sur-Yvette), Dr. W.H. Berger (UCSD,SIO) and Mr. D.S. Introne (UCSD,SIO) during various stages of experiments are also acknowledged.

Special thanks are due to Mr. R. Bhushan, R.A. Jani and J.P. Bhavsar for their help in sampling and laboratory work.

I greatfully acknowledge the help provided at some stage or the other by Drs. J.N. Goswami, P.N. Shukla, A.K. Singhvi, D. Sengupta, N. Bhandari, T.R. Venkatesan, R.K. Pant, S.V.S. Murthy, K. Dilli, Kanchan Pande and M/s. S.K. Shah, J.T. Padia, V.G. Shah, S. Chakraborty, D. Majumdar, J.R. Trivedi, G. Kori, K.R. Nambiar and K.V. Haridas.

This work would almost never have been done but for the excellent glass-blowing support provided by M/s. M.P.K. Kurup and K.K. Sivasankaran. M/s. A.R.S. Pandian, N.R. Manchanda and G.D. Panchal helped me a lot in maintaining the electronic units.

I thank Mr. S.C. Bhavsar, Mr. D.R. Ranpura and the entire Library staff for help with draughting, photography and xeroxing.

Company of my friends Mr. A.K. Sen, A. Dutta, B.P. Pandey, N. Juyal, and other fellow students kept me jolly during all these six strenuous years. Thanks to them.

I owe a special word of praise for Mr. V.T. Viswanathan

for giving this thesis its looks.

Finally, I convey my deep gratitude to Prof. A.K. Saha and Prof. K. Gopalan who inspired me to take a career in Isotope Geology.

A. Sarkar

CHAPTER I

INTRODUCTION

CHAPTER I

INTRODUCTION

Most elements of lower atomic masses occur in nature as mixtures of stable isotopes, for example, hydrogen (^{1}H, ^{2}H), carbon (^{12}C, ^{13}C) and oxygen (^{16}O, ^{17}O, ^{18}O). Harold Urey (1947) showed that significant differences in physico-chemical properties exist among these isotopes due to their finite mass differences resulting in their fractionation during chemical reactions. In nature, the fractionation or partitioning of these isotopes is caused mainly by equilibrium isotope exchange reactions or kinetic reaction processes (Hoefs 1980). Of these two processes, isotope exchange reactions can be considered as special cases of general chemical reactions. The present work deals with a particular exchange reaction system, $CaCO_3$-H_2O system. In such a system, where $CaCO_3$ (calcium carbonate) is precipitating from H_2O (water), the relevant exchange

reaction can be written as:

$$1/3\ CaC^{16}O_3 + H_2{}^{18}O \underset{}{\overset{K}{\rightleftharpoons}} 1/3\ CaC^{18}O_3 + H_2{}^{16}O \qquad (1)$$

where K is the equilibrium constant. The partitioning of two oxygen isotopes in the two phases namely $CaCO_3$ and H_2O can be expressed by introducing the concept of fractionation factor which is defined as:

$$\alpha = \frac{R_{CaCO_3}}{RH_2O}$$

where R_{CaCO_3} and R_{H_2O} are $^{18}O/^{16}O$ ratios in $CaCO_3$ and H_2O respectively. If the isotopes are randomly distributed over all possible positions in each of these two compounds, then

$$\alpha = K^{1/n}$$

where n = number of atoms exchanged. For the exchange reaction given in (1), where monoatomic exchange occurs,

$$\alpha = K = \frac{\left[CaC^{18}O_3\right]^{1/3}\left[H_2{}^{16}O\right]}{\left[CaC^{16}O_3\right]^{1/3}\left[H_2{}^{18}O\right]}$$

$$= \frac{(^{18}O/^{16}O)\ CaCO_3}{(^{18}O/^{16}O)\ H_2O}$$

Since equilibrium constant (K) or α depends on temperature (T), carbonates precipitated from water of a constant isotopic composition but at different temperatures, will have different $^{18}O/^{16}O$ ratios. This idea is the basic

concept behind the attempt for a quantitative determination of palaeotemperatures of ocean water.

Isotopic ratios are usually reported in terms of δ-values, defined as the relative deviation of the sample isotope ratio from that of an international standard and is expressed in per mil ($^{o}/oo$):

$$\delta = (R_s/R_{std} - 1)\ 10^3\ ^{o}/oo$$

where $R_s = {}^{18}O/{}^{16}O$ in sample

$R_{std} = {}^{18}O/{}^{16}O$ in standard

Empirical relation between $\delta^{18}O$ of precipitating $CaCO_3$ from a given water solution and solution temperature was first determined by McCrea (1950) and has the following form:

$$T = a + b\ (\delta_c - \delta_w) + c\ (\delta_c - \delta_w)^2 \qquad (2)$$

where T = temperature in ^{o}C, $\delta_c = \delta^{18}O$ of CO_2 obtained from carbonate by reaction with 100% orthophosphoric acid at $25^{o}C$, $\delta_w = \delta^{18}O$ of CO_2 (tank gas) equilibrated isotopically at $25^{o}C$ with water from which the carbonate was precipitated. Both δ_c and δ_w are measured against the same mass spectrometer standard gas.

McCrea's calibration was made on inorganic $CaCO_3$. But it was not clear whether the same equation can be applied to fossil $CaCO_3$ for determining temperatures of ancient ocean water (Emiliani 1981). Subsequent investigators measured $\delta^{18}O$ in $CaCO_3$ of both biogenic (e.g. mollusks, foraminifera,

etc.) and abiogenic nature as a function of temperature. Table I.1 gives different values for the coefficients a, b and c obtained by different investigators. It can be seen that most of the equations have similar slopes indicating a temperature coefficient, $\partial\delta^{18}O/\partial T$, of about -0.2 °/oo per °C and hence any one of them can be used for calculating relative temperature change.

Emiliani (1955) first analysed $\delta^{18}O$ in planktonic foraminifera separated from different depths in a core from the Caribbean sea. He obtained a saw-tooth pattern in the value of $\delta^{18}O$ as a function of depth (or time). A straight forward interpretation of this signal in terms of sea surface temperature (SST) variation is not possible since the $\delta^{18}O$ of foraminiferal $CaCO_3$ not only depends on temperature (T) but also on isotopic composition of water in which the organisms grow. It is known that the $\delta^{18}O$ of sea water depends on global and local climatic effects. Extraction of a large amount of water from the oceans as ice on the continents during colder periods change the isotopic composition of the water in the oceans and constitute the global effect whereas evaporation, river discharge, etc. are the local components. The difference in $\delta^{18}O$ between the glacial and interglacial, the glacial-interglacial amplitude (GIA) was ~ 1.8 °/oo in the Caribbean sea. Of this, Emiliani attributed about 0.4 °/oo to water-$\delta^{18}O$ change, while the remainder i.e. 1.4 °/oo of the signal was explained by glacial-interglacial SST change of about 6 °C. However, Shackleton (1967) based on simultaneous

Table 1.1

Empirical Equations for $CaCO_3$-H_2O $\delta^{18}O$ Equilibrium+

Nature of $CaCO_3$	a	b	c	Investigators
Inorganic	16.0	-5.1	0.09	McCrea (1950)
Mollusk	16.5	-4.3	0.14	Epstein et al. (1953)
Mollusk	16.9	-4.2	0.13	Craig (1965)
Inorganic	16.9	-4.68	0.10	O'Neil et al. (1969)
Mollusk	17.04	-4.34	0.16	Horibe and Oba (1972)
Core top benthics $< 16.9^{o}C$	16.9	-4.0	0.00	Shackleton (1974)
Extension of O'Neil et al. (1969) in $> 16.9^{o}C$ range	16.9	-4.38	0.10	Shackleton (1974)*
G. sacculifer	16.998	-4.52	0.028	Erez and Luz (1983)

+ These slightly differing relationships yield a range in temperature coefficients of $\delta^{18}O$ from -0.2 to -0.25 $^{o}/_{oo}$ per degree centrigrade.

* For the present work, the relationship of Shackleton (1974) i.e. $T = 16.9-4.38\ (\delta_c - \delta_w) + 0.1\ (\delta_c - \delta_w)^2$ has been used. This yields temperature coefficient for $CaCO_3$-$\delta^{18}O$ as $-0.2\ ^{o}/_{oo}/^{o}C$.

measurements of planktonic and benthic foraminifera from the same core, reinterpreted Emiliani's GIA of 1.8 °/oo to correspond mainly with the global ice volume effect.Several other studies have brought out further complications in the interpretation of $\delta^{18}O$ of foraminifera,e.g.,different depth habitats and vertical migration of forams (Emiliani 1954), seasonal variation in abundances (Williams et. al.,1981; Ganssen and Sarnthein 1983), disequilibrium fractionation (Shackleton et. al., 1973;Vergnaud-Grazzini 1976;Fairbanks et. al., 1982),gametogenic calcification (Duplessy et. al., 1981a),dissolution (Erez 1979) and bioturbation (Mix 1987).

Till these controversies are resolved, it seems difficult to accurately delineate the glacial-interglacial temperature change and the global ice volume effect.A possible solution is to look for other sources of climatological data to find out the temperature and/or ice volume effect. One such source is the $\delta^{18}O$ composition of ancient ice sheets and their correlation with the past sea level change. But controversies still exist among these various estimates of ice volume effect (Mix 1987).

Apart from these dominant global climatic effects of ice volume and temperature, down core $\delta^{18}O$ is considerably modified by small scale,local oceanographic processes,some of which are described below.

I.1 Local Effects in the $\delta^{18}O$ of Foraminifera

In Gulf of Mexico, a negative $\delta^{18}O$ spike (upto ~

1.5 °/oo) during the transition from the Last Glacial Maximum (LGM) to Holocene, superimposed on normal GIA, was observed. This was explained by the presence of a less saline water that originated from the melting of the Laurentide ice sheet (Kennett and Shackleton 1975) and was considered to be a local phenomenon. Berger et al. (1977a) and Berger (1978), however, proposed that such a meltwater lid during last deglaciation could have existed globally. Subsequent studies indicated presence of freshwater spike from melting of Fennoscandian and Barents ice sheets (Grosswald 1980; Jones and Keigwin 1988). If such an effect contributes to the total $\delta^{18}O$ signal, it becomes difficult to assess the global ice volume effect.

Inspite of these aforementioned problems, down core $\delta^{18}O$ analysis on various species of foraminifera from different oceans have yielded more or less similar signals. A large number of studies from various ocean cores suggest that about ~ 1/3 of the GIA is due to temperature variation while majority (~ 2/3) of the signal is due to ice volume effect. This makes the $\delta^{18}O$ stratigraphy as a proxy ice volume indicator. After about a decade of the initial work of Shackleton and Opdyke (1973, 1976), it is now firmly established that the entire pleistocene experienced more than 20 ice ages and not four (e.g. Wisconsin, Illinoian, Kansas, Nebraskan) as was thought by Quaternary geologists. The following section will address the cause of these ice ages.

I.2. $\delta^{18}O$ Cycle in the Ocean Cores : Causative Mechanism

Since oxygen isotopes in deep sea cores provide continuous palaeoclimatic record for a long period, much effort has been made to establish an absolute $\delta^{18}O$ chronology for the entire pleistocene. Initially the chronology was based on palaeomagnetic boundaries coupled with the assumption of constant sedimentation rates in between (Shackleton and Opdyke 1973).Subsequently Broecker and van Donk (1970) made the correlation between isotopic stages and coral terraces dated by U-series isotopes.

But Hays et al. (1976), for the first time,made a combined effort to produce a time scale tuned to orbital variations, which established the link between terrestrial climatic changes and astronomical forces, the so-called Milankovitch hypothesis. The currently available SPECMAP (Imbrie et al.,1984) time scale is the culmination of Hays et al's effort.which demonstrated that isotopic signatures are phase locked and are strongly coherent with orbital variations, in all the frequencies namely 19 and 23 kyr. (precessional), 41 kyr. (obliquity) and 100 kyr. (eccentricity). According to Imbrie et al. (1984), "85 percent of the observed isotopic variance is linearly related to orbital forcing". However, a detailed investigation of the last deglaciation i.e. 20 kyr. to the present, shows that the isotopic record is not strictly a linear function of orbital forcing.

Now we turn our attention to the significance of carbon

isotope changes in the foraminifera.

I.3 Carbon Isotope Records of Climatic Change

The carbon isotopic composition of calcium carbonate precipitated from sea water is controlled by (Faure,1986):

1. $\delta^{13}C$ value of the dissolved CO_2 gas, in equilibrium with the carbonate and bicarbonate ions in solution.

2. Fractionation of carbon isotopes between CO_2 gas, the carbonate and bicarbonate ions in the solution and solid $CaCO_3$.

3. Temperature of isotopic equilibration.

4. pH and eH values of the medium

where $$\delta^{13}C = \left[\frac{(^{13}C/^{12}C)_{sample}}{(^{13}C/^{12}C)_{standard}} - 1 \right] 10^3 \ ^o/_{oo}$$

The CO_2 gas is nothing but atmospheric CO_2 dissolved in ocean water, which produces several components thereafter. The total CO_2 can be represented as:

$$\sum CO_2 = CO_{3(aq.)}^{=} + CO_{2(dissolved)} + HCO_{3(aq.)}^{-}$$

Consequently, the exchange reactions among the various components can be written as:

$$^{13}C\,O_{2(dissolved)} + H^{12}CO_{3(aq.)}^{-} \rightleftharpoons {}^{12}CO_{2(diss.)} + H^{13}CO_{3(aq.)}^{-}$$

$$H\,{}^{13}CO_{3(aq.)}^{-} \longrightarrow H^{+} + {}^{13}CO_{3(aq.)}^{=}$$

$${}^{13}CO_{3(aq.)}^{=} + {}^{12}CO_{3(solid)}^{=} \rightleftharpoons {}^{12}CO_{3(aq.)}^{=} + {}^{13}CO_{3}^{=}(solid)$$

Among these steps, the bicarbonate-carbonate exchange reaction is the most important, because the HCO_3^- is the major component of the $\sum CO_2$. Hence by approximating $\sum CO_2$ by HCO_3^-, the relation between the $\delta^{13}C$ of $CaCO_3$ and HCO_3^- can be written as follows (Emrich et al.,1970):

$$\delta^{13}C \text{ calcite} = \delta^{13}C(HCO_3^-, aq.) + 1.85 + 0.035\ (T-20)$$

where $\alpha^{CaCO_3}_{HCO_3^-} = 1.00185$, T = temperature in degree centigrade. The temperature coefficient of calcite - $\delta^{13}C$ i.e. $\partial\delta^{13}C/\partial T \sim 0.035$ $^{o}/oo/^{o}C$, is quite small. Hence any change in $\delta^{13}C$ of foraminifera can be interpreted in terms of change in the $\sum CO_2$ reservoir alone.

In general, $\delta^{13}C$ of $\sum CO_2$ shows a stratification profile with depth in open ocean similar to those of nutrients like PO_4 and NO_3 (Kroopnick 1974).This profile is controlled by organic productivity in the ocean. In the euphotic zone, organic productivity is high. The preferential uptake of ^{12}C by organic matter through metabolic processes makes them depleted in ^{13}C and consequently enriches surface water in $\delta^{13}C$. When the organic matter sinks through the water column,it gets oxidised and releases ^{13}C depleted CO_2

in the deeper water.As a result,deep waters are depleted in $\delta^{13}C$ relative to surface.This $\delta^{13}C$ profile can be recorded in foraminiferal calcite-$\delta^{13}C$ and can be used as palaeo-oceanographic tracer,provided different species grow at different depths in isotopic equilibrium with the ambient. Departure from this equilibrium and its effect on $\delta^{18}O$ has been mentioned earlier. Such disequilibrium may affect the $\delta^{13}C$ values too.Disequilibrium precipitation may occur, if apart from HCO_3^- (ΣCO_2),some amount of respiratory CO_2 or CO_2 derived from oxidation of organic matter,takes part in the $CaCO_3$ shell building process.Hence it has to be assessed how reliable foraminiferal $\delta^{13}C$ are as palaeoclimatic indicator.

Evaluation of Foraminiferal $\delta^{13}C$

Majority of the work on $\delta^{13}C$ has been done on benthic foraminifera. Most of the benthics precipitate calcite out of isotopic equilibrium.The disequilibrium at a particular place is not constant but depends on taxonomic groups (Grossman 1984). For a particular species, however, this disequilibrium probably remains constant with time and can be approximately corrected;for example:

$$\delta^{13}C_{\underline{Cibicides}} = 0.954\ \delta^{13}C\ TCO_2 + 0.095$$
$$\delta^{13}C_{\underline{Uvigerina}} = 0.904\ \delta^{13}C\ TCO_2 - 0.805$$

where TCO_2 is total dissolved CO_2 (ΣCO_2) (Duplessy et al.,

1984). In general, $\delta^{13}C$ of these commonly used species like Cibicides, Uvigerina, Planulina, etc. record ΣCO_2 of bottom water quite reliably (Grossman 1984). Planktonic foraminifera in most cases, show a higher scatter in downcore $\delta^{13}C$ values than benthics (Williams et al.,1977; Broecker and Peng 1982). However many species from the open ocean (e.g., N. dutertrei, G.bulloides etc.) have yielded very similar $\delta^{13}C$ variation, indicating that they too record surface water ΣCO_2 property (Shackleton and Pisias 1985).

Summarising, it is clear that stable isotope palaeoclimatology has experienced multifarious developments in the last three decades. Our present understanding of the global isotope palaeoclimatology reveals the following important features:

1. There exists a cyclic $\delta^{18}O$ stratigraphy in the ocean sediments for at least the last 2 million years.

2. Such fluctuations in $\delta^{18}O$ are mainly controlled by the waxing and waning of continental ice sheets, which in turn is controlled by the sun-earth orbital geometry changes namely changes in eccentricity, obliquity and precession of the earth.

3. The average glacial-interglacial change in $\delta^{18}O$ (GIA) is between 1.1 $^{o}/oo$ and 1.6 $^{o}/oo$.

4. $\delta^{18}O$ signal and sea-level estimates show a fairly good agreement.

5. $\delta^{13}C$ difference between planktonics and benthics was maximum during LGM and is perhaps controlled by the change in the oceanic nutrient cycles, coupled with the deep sea circulation change.

Superimposed on these global effects, many local climatic changes modify the isotope patterns. By appropriately subtracting the global signals, one can decipher the local climatic variation. For example, in the Mediterranean and the Red sea GIA is ~4 °/oo against the global GIA of ~ 1.6 °/oo (Vergnaud-Grazzini, 1975; Thunell et al., 1988) and is explained by increased local evaporation in these marginal seas during LGM. Variations in coastal upwelling systems also show very complex local phenomena (Prell 1984a, b; Suess and Thiede, Thiede and Suess 1983). Such phenomena if present on a large scale ought to have influenced global cimate as well.

We now discuss the problems and prospects of palaeoclimatic studies in the northern Indian ocean and the objectives of the present study in this context.

I.4. Review of Earlier Work in the Northern Indian Ocean

One of the early systematic studies of stable isotopes in foraminifera from the northern Indian Ocean was carried out by Oba (1969). His study focussed on estimating the palaeotemperature of the ocean water in relation to faunal geography and identifying the depth habitats of different foram species. $\delta^{18}O$ stratigraphy was also tested against the

global climatic cycles. Subsequent to the work of CLIMAP group (1976) on world oceans,which included the northern Indian Ocean also, increasing attention was drawn towards this region. This is because, the Arabian sea,the Bay of Bengal and the adjacent oceans respond to a unique feature in the regional climate namely,"monsoon",which introduces important physico-chemical changes in these oceans. Characteristic long term changes of the Indian monsoon, their causes and effects have been the subject of numerous studies (Miller and Keshavamurty 1968;Lighthill and Pearce 1981; Fein and Stephens 1987).Broadly,the monsoon system has two dominant effects in the oceanic realm:

1. Heavy rainfall during June to September over the Indian subcontinent. This results in a large river water discharge to the Bay of Bengal and the Arabian sea.

2. Intense upwelling due to the prevailing wind system takes place in the coastal Arabia and the west coast of India.

Both these phenomena bring about significant changes in the sea water salinity and sea surface temperature,which,in principle, can be traced spatially and temporally by the stable isotope ratios of oxygen and carbon (by the productivity changes).

A pioneering work in this regard was done by Duplessy

(1982) who showed that apart from the general global climatic cycles, the $\delta^{18}O$ stratigraphy of foraminifera in the Bay of Bengal and the Arabian sea records important information about local oceanographic changes.His studies, based on Holocene core tops and LGM levels of several cores in the Arabian sea and Bay of Bengal,showed significant changes in water properties in the past.

At present the Arabian sea is dominated by strong evaporation. On the contrary the Bay of Bengal experiences large river discharges from the Ganges,Brahmaputra,Irrawady rivers. Consequently the mean annual surface salinity in the Arabian sea increases from south to north by 1.5 °/oo and decreases in the Bay of Bengal by 3 °/oo.Modern core top G. ruber species record this salinity gradient in their $\delta^{18}O$ composition; this shows a south to north increase in $\delta^{18}O$ by 0.6 °/oo in Arabian sea and decrease by 1.1 °/oo in the Bay of Bengal.Duplessy (1982) showed that this gradient in $\delta^{18}O$ during LGM time was higher in the Arabian sea (~ 1 °/oo) and considerably smaller in Bay of Bengal (~ 0.2 °/oo). This has been explained by enhanced evaporation and low river discharge during LGM, in these two basins respectively. Zonal nature of the iso-$\delta^{18}O$ contours and their similarities along particular latitude, indicated decreased runoff from west-bound peninsular rivers as well as weak upwelling conditions in the western Arabian sea (op. cit.). These conclusions supported the earlier observations of Prell et al (1980) in this region.Based on planktonic foraminiferal biogeography, Prell et al. showed

that the Arabian sea was characterised by warmer SST and weak-upwelling condition during LGM while increased salinity was prevailing in the Bay of Bengal. Thus glacial-interglacial changes in $\delta^{18}O$ (a function of only ice volume and temperature) are considerably modified by local climatic effects in the northern Indian ocean.

Since upwelling off the Arabian coast is coupled with monsoon, its variation through time has been the subject of many investigations. During summer months, upwelling brings up cold, nutrient-rich water from the deeper levels and creates a distinct temperature anomaly. The centre of this upwelling lies between $17^{o}N$ and $21^{o}N$ and is $4^{o}C$ cooler than the mid-ocean SST (Prell and Streeter 1982). If foraminifera, growing in this region, record such a temperature change, a total of ~ 0.8 $^{o}/oo$ change in the $\delta^{18}O$ values should be observed in their shells across this upwelling zone (considering the $CaCO_3$ temperature coefficient ~ 0.2 $^{o}/oo/^{o}C$). The study by Prell and Curry (1981) on Holocene core top planktonic foraminifera collected across this upwelling zone, indeed showed such a range in the $\delta^{18}O$. $\delta^{18}O$ compositions of any surface dwelling foraminifera such as G. sacculifer, G. ruber, G. bulloides, G. menardii show a total 0.8 $^{o}/oo$ change across the upwelling zone same as the predicted value. This prompted Prell and Curry to suggest that synoptic mapping of these shallow dwelling species across the upwelling zone can be a potential tool for studying its variation from LGM to the present. Due to the peculiar topographic configuration (Fig. 2.1), however,

obtaining undisturbed cores is quite difficult especially near the coast of Arabia,where the upwelling is maximum.

During the same investigation, Prell and Curry (1981) noticed that the percentage (%) of modern G.bulloides is directly correlated with PO_4 content of the surficial water (an index of upwelling) and inversely correlated with SST. Therefore, it was concluded that the abundance of G. bulloides can be used as an index of the intensity of upwelling. Subsequent investigation by Prell (1984a,b) on the down-core variation of G. bulloides from this region, showed that its abundance decreased during 18 kyr B.P. indicating a weak upwelling,while it increased around 9 kyr B.P., suggesting a stronger upwelling than today.This is consistent with the earlier observation of Duplessy (1982) which showed a weak SW-monsoon during LGM and a probable less intense upwelling off Arabia.

In addition, Duplessy proposed that a stronger NE monsoon existed during the same period but no oxygen isotope evidence was found for it.If true,such a stronger NE monsoon should presumably increase the evaporation in the northern Arabian sea due to the presence of dry NE winds over this region (op. cit.) during LGM.

Apart from the oxygen isotope studies,evidence for a weak monsoon during LGM and extreme aridity over south Asia comes from a number of other sources.Pollen studies in conjunction with $\delta^{18}O$ stratigraphy from the western Arabian sea have shown the prevalance of an extreme arid condition around 20 kyr. B.P. and a wet condition around 11 kyr. B.P.

(Van Campo et al.,1982).Increased glacial aridity is also indicated by high quartz content in Arabian sea (Kolla and Biscaye 1977), increase in sand dune activity (Sarnthein 1978) and stronger loess storms in the cold deserts of inner Asia (Huang 1973).Dessication took place in the large lakes from Rajasthan around 20 kyr. B.P. and recovered only at 13.6 kyr. B.P. (Singh et al.,1974;Wasson et al.,1983). Study of the fluvial deposits from the Deccan upland region shows river aggradation and drier climate around LGM whereas early Holocene was characterised by strong incisional stages of these rivers,when discharge was high (Kale and Rajaguru, 1987). Based on the abundance of planktonic foraminifera Globoquadrina dutertrei,as well as total planktonic assemblages,increased salinity in the Bay of Bengal during LGM has been proposed (Cullen 1981).This study also indicates a strong salinity reduction in the early Holocene.Such salinity changes have been explained by varying river run-off coupled with monsoon fluctuations for last 20 kyr.

It is of interest to know the chronological evolution of monsoon from a glacial weak condition to its Holocene strength. Pollen study by Van Campo (1986) suggests that the evolution of the monsoon was gradual.After LGM,rainfall started increasing along the west coast as early as 16 kyr. at $15^{o}N$ latitude. This produced extensive development of mangrove forests which culminated at 11 kyr. B.P. Monsoon reached its maximum strength around 10 kyr. B.P. at $10^{o}N$ latitude and 8 kyr. B.P. at $28^{o}N$. Such an evolution of

monsoon was explained by progressive northward movement of intertropical convergence zone (ITCZ) (op. cit). In the western Arabian sea (north of $10^{o}N$) G. bulloides reached its maximum abundance around 9 kyr. B.P. indicating the strongest upwelling which is consistent with the above proposition.

Unlike oxygen,carbon isotope studies in carbonates from these sediments are meagre.Prell and Curry (1981) attempted to study the effect of upwelling on $\delta^{13}C$ of modern planktonic foraminifera, based on the fact that the deeper water brought up by upwelling contains ΣCO_2 depleted in $\delta^{13}C$ arising from oxidation of organic matter.Consequently one would expect a correlation between $\delta^{13}C$ and various indices of upwelling. But $\delta^{13}C$ values showed very poor correlation with both PO_4 and SST (two strong upwelling indices). Prell and Curry explained the lack of such correlations by one or more of the following reasons:

1. Disequilibrium fractionation of carbon isotopes.

2. Dilution of upwelled water by the surrounding reservoir.

3. Quick equilibration between atmospheric CO_2 and dissolved ΣCO_2.

However, $\delta^{13}C$ of benthic foraminifera has been successfully used to reconstruct the hydrographic condition in the northern Indian ocean during LGM (Kallel et al 1988). Analysis of benthic Cibicides reveals significant

differences between the characteristics of intermediate and deep water masses during LGM.In the modern situation,the vertical decrease in $\delta^{13}C$ from 2000m to 2300m is less than 0.1 $^{o}/oo$. During LGM,a sharp discontinuity was found around this depth separating intermediate and the deep water masses. The deep water was depleted in $\delta^{13}C$ by as much as 1 $^{o}/oo$ against the intermediate water value of ~ 0 $^{o}/oo$. Similar discontinuity was observed in the $\delta^{18}O$ value also. GIA in the cores raised from the intermediate water depth, are ~ 1.1 $^{o}/oo$ whereas, in the deep waters GIA has values upto 1.5 $^{o}/oo$ (LGM levels being heavier).This was explained by the presence of a ventilated intermediate water mass (with same temperature as of today) and a cooler ($\delta^{18}O$ enriched), poorly ventilated (CO_2 rich and hence $\delta^{13}C$ depleted) deep water during LGM.Today's intermediate water originates from the Red Sea and the Persian Gulf region. During LGM, sea-level in this region was lower thus, significantly reducing their contribution to intermediate water. Consequently three probable sources for this ventilated intermediate water have been suggested:

1. Dense water formed by increased evaporation and reduced SST in the northern Arabian sea during LGM.

2. Expansion of Antartic intermediate water to the north of $10^{o}S$.

3. Increased flow of intermediate water from the Pacific Ocean through the Indonesian Archipelago.

Change in the $\delta^{13}C$ of the deep water has been explained by a strong stratification and development of a deep thermocline during the same period (Kallel et al.,1988).

A recent work on palaeomonsoon circulation which is of great significance has been reported by Fontugne and Duplessy (1986). They used the $\delta^{13}C$ of organic matter as a tracer. $\delta^{13}C$ in sedimentary organic matter is a mixture of contributions from marine and terrestrial sources.Since the average $\delta^{13}C$ values for these sources are -26 and -20 $^{o}/_{oo}$ (w.r.t. PDB) respectively,one can calculate the fraction of terrestrial and marine organic carbon in these sediments, provided the organic matter is not diagenetically altered. Their reconstruction showed a higher terrigenous carbon input to the Bay of Bengal along a NE-SW axis,indicating an increased NE monsoon activity during LGM.This was supported by the total organic carbon (TOC) content of the sediment which increased in the eastern Bay of Bengal.In the western Arabian sea TOC decreased during LGM indicating a weak upwelling. However,the increased NE monsoon activity was not indicated by any of the earlier $\delta^{18}O$ studies cited above.An enhanced input of terrestrial carbon,deep into the Bay of Bengal during LGM, is also supported by the measurement of sediment accumulation rate. In the Bay of Bengal this rate was higher during LGM (Foucalt and Fang 1987;J.C. Duplessy and R. Chesselet, preprint) while that in the Andaman sea and the Arabian sea was much lower (Van Campo 1986;Fontugne

and Duplessy 1986). A higher terrigenous flux during the glacial period is perhaps due to the direct pathways of rivers to the ocean cutting through the newly exposed shelf. Though terrigenous input controls the sedimentation rate in near coastal regions, in the deep ocean other factors such as productivity, eolian transport and dissolution play an important role.

The above discussion on the available isotopic and palaeontological data shows that significant changes in past climatic conditions have taken place in the northern Indian ocean and the adjacent regions.

In addition to these experimental studies,a significant amount of work has also been done to simulate the past climatic conditions based on theoretical modelling.These models take into account different boundary conditions provided by the geological data. The major boundary conditions, which control the climate over the northern Indian ocean and adjoining continents are SST,size and elevation of the Asian continent, surface albedo and the seasonal distribution of solar radiation over the Asian continent (Prell 1984b).A change in any of these parameters is potentially capable of perturbing the local climate.By using the GFDL general circulation model (GCM),Hahn and Manabe (1975) showed that the high elevation of the Tibetan plateau produces in part,an intensified monsoon.Absence of the mountains, in the simulation, produced a much weaker monsoon. However, the elevation of the Tibetan plateau is almost constant when one is concerned about the climatic

change over a 10^4 years timescale.Another GCM experiment by Manabe and Hahn (1977) demonstrated the effect of surface albedo and produced a weak monsoonal circulation during LGM due to the higher albedo over Asia.Presence of an extensive snow cover over the Tibetan plateau perhaps was responsible for such a higher albedo during the LGM,which reduced the land-ocean temperature contrast.CLIMAP's (1976) simulation with the modern terrestrial boundary conditions and the glacial SST produced a monsoon intensity similar to that of today. This indicates that the SST change is perhaps not very significant for the monsoon performance.Recent studies by Kutzbach and Guetter (1986) indicate that the response of the monsoon circulation and tropical precipitation to change in the solar radiation is much larger than the response to the changes of glacial-age boundary conditions. Their model predicts a higher aridity during LGM and 10-20% increase in the summer monsoon precipitation between 12-16 kyr. ago.

Relation between the terrestrial climatic change and the astronomical forcing (Milankovitch theory) has been mentioned earlier. Spectra of time series of $\delta^{18}O$ and % G. bulloides (index of upwelling) from the Arabian sea show distinct peaks around 12 kyr. and 23 kyr. respectively (Prell 1984a). Both these signals are coherent with the insolation curve over the orbital frequencies. This indicates that monsoonal upwelling is linearly correlated with the solar radiation over time scales of the precessional frequency (23 kyr).However $\delta^{18}O$ (ice volume)

and % G. bulloides (upwelling) lag insolation change by ~ 5.5 kyr. Such a delay of monsoonal circulation is probably due to the persistence of seasonal snow cover into the summer and its wide areal coverage over the Tibetan plateau which prevented low-level heating and the consequent pressure gradient (op. cit.).A latest review by Prell and Kutzbach (1987) using the GCM simulation based on diverse arrays of data (also see COHMAP members 1988) on the monsoon variability shows four distinct monsoon maxima during interglacials for the last 150 kyr.Such maxima are caused by changes in the northern hemispheric summer radiation controlled by the precession of the earth.In this simulation, the glacial age bc ndary conditions produced an increased precipitation on the western Indian ocean along with glacial aridity and a weak SW-monsoon over Asia. However, glacial age boundary conditions have much less effect on the monsoon intensity compared to the insolation changes.

Summarising all the geological evidences (ocean sediments, pollen, lake level data, etc.) and model simulations, several important conclusions can be drawn about the past climatic changes in this region:

1. Presence of a weak SW-monsoon and weak coastal upwelling and indications of a strong NE monsoon during LGM.

2. Extreme aridity over southern Asia during LGM.

3. Presence of an O_2-poor, CO_2 rich deep water and more ventilated intermediate water front in the northern Indian ocean.

4. Increased precipitation and SW-monsoon circulation around 12-6 kyr. B.P..

I.5. Plan of the Present Study

In the foregoing section it has been shown that important information on palaeoclimatic changes have been obtained by using stable isotope tracers and foraminifera from the northern Indian ocean.However,several questions remain. The actual geological data base in this ocean on which the abovementioned conclusions are based is sparse. There is no real evidence from the foraminiferal $\delta^{18}O$ data that the NE monsoon was stronger during LGM.Since most of the evidences lack absolute chronologies, it has not yet been possible to precisely date the glacial-interglacial transitions in the northern Indian ocean. In many cases oxygen-isotope stratigraphy itself is used to date the sediments. However, concurrence between the $\delta^{18}O$ based chronology and that obtained by the absolute dating techniques may not be always achieved (Prell et al 1980; Keigwin et al 1984).Even among the various absolute dating techniques serious discrepancy may arise (Ku et al.,1968; Goldberg 1968). Such discordances arise because different isotopes used to date the sediments,have different sources

and geochemical pathways. In addition their distributions are likely to be affected by various post depositional oceanographic processes viz. bioturbation, winnowing of bottom sediments, variation in redox condition etc. For example, earlier attempts of dating sediments of the Arabian sea by U-Th series isotopes did not prove very successful (Sarin et al.,1979;Sarin,M.M.,personal communication,1988, unpublished data; Borole 1980),while in the other oceans it proved to be a good technique (Goldberg and Koide 1962). Hence an intercomparison of these various methods can be made to ascertain their validity.

In the GCM simulation of Prell and Kutzbach (1987), influence of CO_2-change has not been taken into account and hence the question is,what role does the change in carbon cycle play in this ocean? Finally,the periodicities and the interrelationship of different climatic indices and their phase relation to the orbitally induced solar insolation should be tested.One such test has already been done for % of foraminifera,an upwelling index (Prell 1984a, b) and should be extended to other parameters e.g. $\delta^{18}O$, $CaCO_3$,etc.

The present work is an attempt to answer some of the queries cited above and has been focussed to:

1. study the geochronology of the sediments and put an absolute time bracket on the glacial-interglacial transitions by using ^{14}C (upto 30 kyr.) and ^{230}Th (beyond the range of ^{14}C and upto ~ 300 kyr) dating

methods.

2. find out the nature and extent of local climatic variations in the northern Indian ocean vis-a-vis global changes, based on the long term $\delta^{18}O$-stratigraphy.

3. find an oxygen isotope evidence of a stronger NE-monsoon during LGM, based on high resolution $\delta^{18}O$ stratigraphy.

4. find out $\delta^{13}C$ variation from LGM to present, vis-a-vis $\delta^{18}O$ stratigraphy, in relation to changes in upwelling and organic productivity.

5. test the periodicites, coherence and phase relationship between $\delta^{18}O$, an ice volume index and $CaCO_3$, a productivity index.

CHAPTER II

EXPERIMENTAL TECHNIQUES

CHAPTER II

EXPERIMENTAL TECHNIQUES

This chapter summarises the experimental procedures employed in the present work. These are:

1. Collection of sediment cores.

2. Separation of foraminiferal species from sediment cores for stable isotope analysis and estimation of the percentage of coarse fraction (> 150 μm).

3. Extraction of carbon-dioxide from foraminiferal calcite for $\delta^{18}O$ and $\delta^{13}C$ analysis.

4. Mass spectrometric measurements, their analytical precision and reproducibility.

5. Effect of sample pretreatment on $\delta^{18}O - \delta^{13}C$ values.

6. Estimation of calcium-carbonate ($CaCO_3$) in cores.

7. Radiochemical analysis of sediments for U-Th series isotopes.

8. Dating of sediments by the radiocarbon (^{14}C) method.

II.1. Collection of Sediment Cores

Sediment cores for this work were collected from the Arabian sea and the equatorial Indian ocean.Two cores were raised by ORV/SAGARKANYA belonging to the Department of Ocean Development (with the help of the scientists from the National Institute of Oceanography,Goa) during the cruise no. 20 in November,1985.The other three cores were raised by the ship ORV/CHARLES DARWIN of National Environmental Research Council (NERC), U.K., with the help of the scientists from the University of Edinburgh, during the cruise no. 17 in 1986.Table 2.1 gives the relevant details of these cores.Locations of these cores along with a rough sketch of bottom topography is shown in Fig. 2.1.Two gravity cores i.e. SK-20-185 and SK-20-186 were subsampled by thin perspex sheets at 1-2 cm interval for the top 50 cm and at 5-10 cm intervals for the rest of the core lengths. The piston core CD-17-15 and the box core CD-17-32 were split into two halves and subsampled at 5 cm intervals. Samples of CD-17-30 were kindly provided by Dr. N.B. Price of University of Edinburgh,again at 5 cm intervals.All the samples were kept in zip lock bags and brought to the

Table 2.1

Descriptions of the Sediment Cores

Core No.	Location Lat./Long.	Water Depth (m)	Core Length (cm)	Type
SK-20-185*	10°N71°50'E	2523	300	Gravity Core
SK-20-186*	0° 68°30'E	3564	500	Gravity Core
CD-17-30+	19°56'N 61°39'E	3850	800#	Piston Core
CD-17-15+	16°38'N 60°39'E	4012	600#	Piston Core
CD-17-32+	21°45'N 60°49'E	3150	50	Box Core

* SK: Sagar Kanya, an Indian Ship, Department of Ocean Development

\+ CD: Charles Darwin, a British Ship, NERC, U.K.

\# Analysed only upto ~ 300 cm.

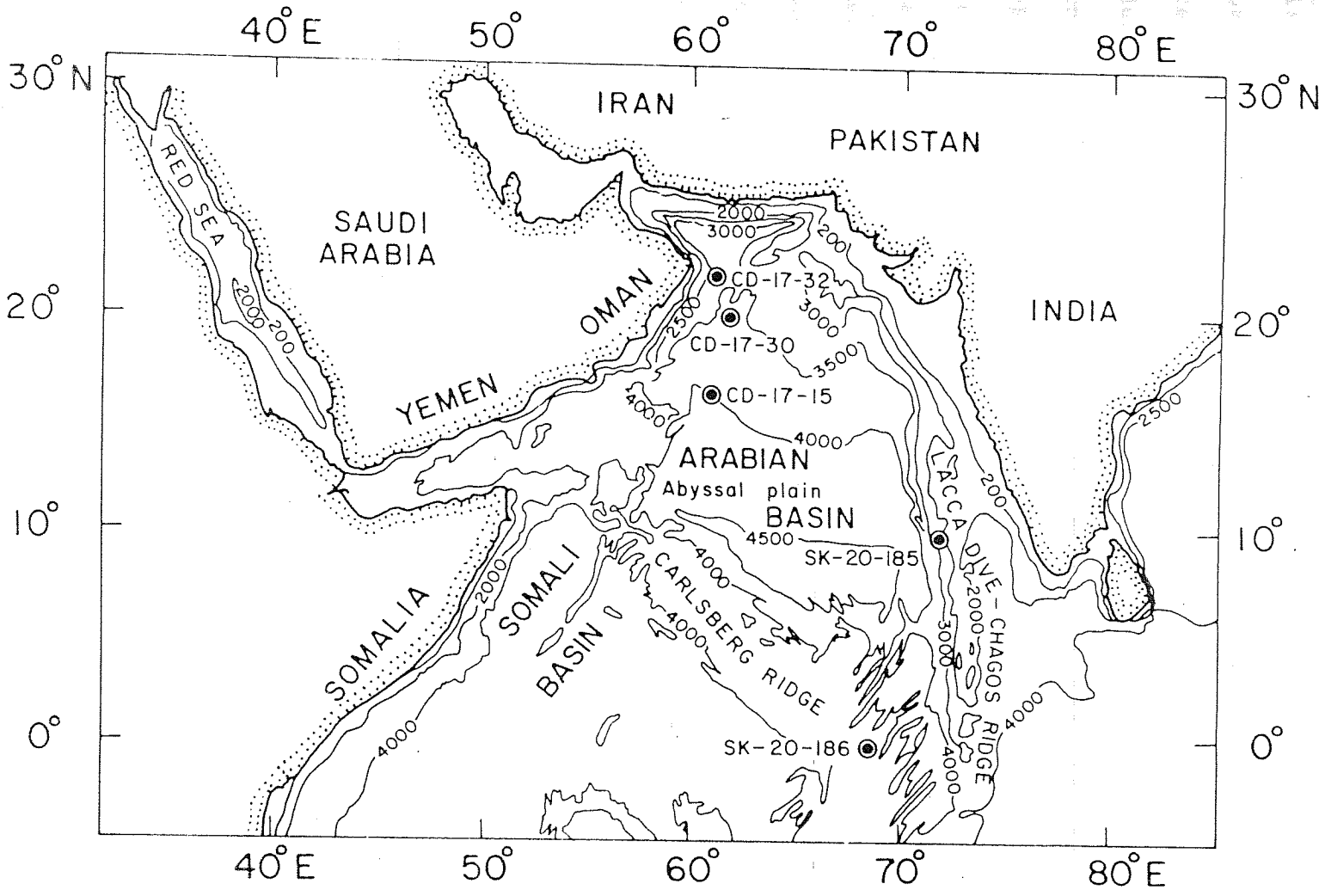

Fig. 2.1 : Locations of sediment cores along with rough sketches of bottom topography.

laboratory. All the cores were collected from the regions where bottom topography was reasonably flat.Core SK-20-185 is located in the eastern Arabian sea to the west of the Laccadive-Chagos ridge. A minor but significant salinity reduction due to the NE monsoon circulation,takes place during winter time close to this region.In this respect it is a strategically located core because an important objective of the present study was to look for evidences of the stronger NE monsoon, if any, during the last glacial maximum (~ 18 kyr. back, see Chapter 1).Such a salinity reduction also takes place near the west coast of India. However, the present location was chosen in order to avoid the influence of coastal processes and the Laccadive-Chagos ridge probably acts as a barrier in this regard.Core SK-20-186, on the other hand, comes from the equatorial Indian ocean and represents an open ocean condition where the glacial-interglacial amplitude should be dominated by global effects of the ice volume signal and a minor temperature change with little or no contributions from the local effects. Cores CD-17-15 and CD-17-30 come from the south of the Murray ridge but above the Arabian sea abyssal plain. Interestingly, the former one shows several turbidite sequences in its litholog (prepared by the author), eventhough it was raised outside the southern fringes of the Indus fan. The latter (i.e. CD-17-30) core seems to be free of any disturbance albeit it is closer to the Indus fan. Core CD-17-32 was raised from the Oman basin.These three CD cores come from the northern Arabian sea where the

salinity is high and coastal upwelling plays a dominant role. If in the past these local oceanographic conditions had changed, their glacial-interglacial amplitude would have been modified and can be compared with the southern cores SK-20-185 and SK-20-186.

We think that during retrieval some of the core top (a few cm) was lost in our piston and gravity corers. While in the Charles Darwin (CD) cores the loss could not be estimated (owing to the small diameter (~ 10 cm) of piston cores), in SK-20-185 and SK-20-186 (giant gravity cores), this estimation was made. After retrieval of these two cores, the top part was found to be sloshy and some amount of sediment was slumped, at the top when the corer was made horizontal. Considering the cross sectional area of the corers and the total weight of sediment slumped, the loss was estimated to be atleast 1-2 cm (knowing the density of sediments ~ 0.7 gm/cc). Consequently the depths given to different levels of the corers are apparent depths. However, it is difficult to exactly know the amount of sediments lost during retrieval.

II.2. Separation of Foraminifera and Estimation of the Coarse Fraction

Sediment samples were soaked in 10% calgon solution overnight in glass beakers, and subsequently washed through 150 μm sieve with a distilled water jet. The fraction >150 μm was kept in beakers, supernatant decanted and oven-dried

at 60°C. The dry coarse fraction (> 150 μm), consisting mainly the mature foraminifera, is then kept in plastic vials. These samples were dry-sieved to obtain different size fractions. Each size fraction of interest was spread on a black plate provided with a suitable grid. Foraminifera were picked up under a binocular microscope and kept in pyrex thimbles for isotopic measurements.

Based on test results (discussed later) we avoided roasting of the samples and cleaned the forams only by ultrasonic treatment. The distilled water, the medium of ultrasonic treatment, was then absorbed by tissue papers. Foraminifera (in pyrex thimbles) were subsequently dried at 150°C in vacuum, and taken for mass spectrometric analysis.

For estimating the coarse fraction (> 150 μm), sediment samples were dried at 200°C in an oven. The dried sediment was weighed and subsequently wet sieved to collect the > 150 μm fraction. Care was taken not to use a strong jet for sieving since it might break foram-shells into fine fragments. The dried coarse fraction was reweighed and its percentage in the total sediment was calculated.

II.3. Extraction of CO_2 from Foraminiferal Calcite

In 1950, McCrea developed a technique to analyse oxygen and carbon isotopes in carbonates which involves the reaction of $CaCO_3$ with 100% orthophosphoric acid (H_3PO_4). The reaction can be written as,

$$3CaCO_3 + 2H_3PO_4 \xrightarrow{25^\circ C} Ca_3(PO_4)_2 + 3H_2O + 3CO_2\uparrow$$

Evolved CO_2 and H_2O are equilibrated at 25°C.

This method requires a considerable time for equilibration and the precision of isotopic measurement is not high (see Section II.4). Analysis of foraminera from ocean cores requires the rapid analysis of a large number of samples with a high precision, since the total range in the $\delta^{18}O$ signal obtained from ocean cores is about ~ 2 °/oo. Shackleton (1967) developed a procedure, which, unlike the McCrea-method, is an on-line extraction system and capable of analysing a large number of samples with a high precision (see Section II.4). An extraction line was constructed for the present work, following the design of Shackleton. The present system is based on the $CaCO_3$-H_3PO_4 reaction at 50°C followed by the immediate removal of CO_2 from H_2O. This is a kinetic process where the evolved CO_2 and H_2O are not allowed to interact as in the case of the 25°C equilibration method.

100 % orthophosphoric acid was prepared from commercially available Analar grade H_3PO_4 with specific gravity 1.75. The method of acid preparation is shown in Fig. 2.2. A flask containing commercial acid is connected to a glass vacuum line pumped through rotary pump. The acid is continuously stirred by a magnetic stirrer. Water of the acid is collected by a liquid nitrogen (LN_2) trap. No heating was employed while removing the water from H_3PO_4. Eventhough McCrea suggested 100% H_3PO_4 as the best acid to get a highly reproducible isotopic data, Mook (1968) reported that 95% H_3PO_4 gives a better reproducibility.

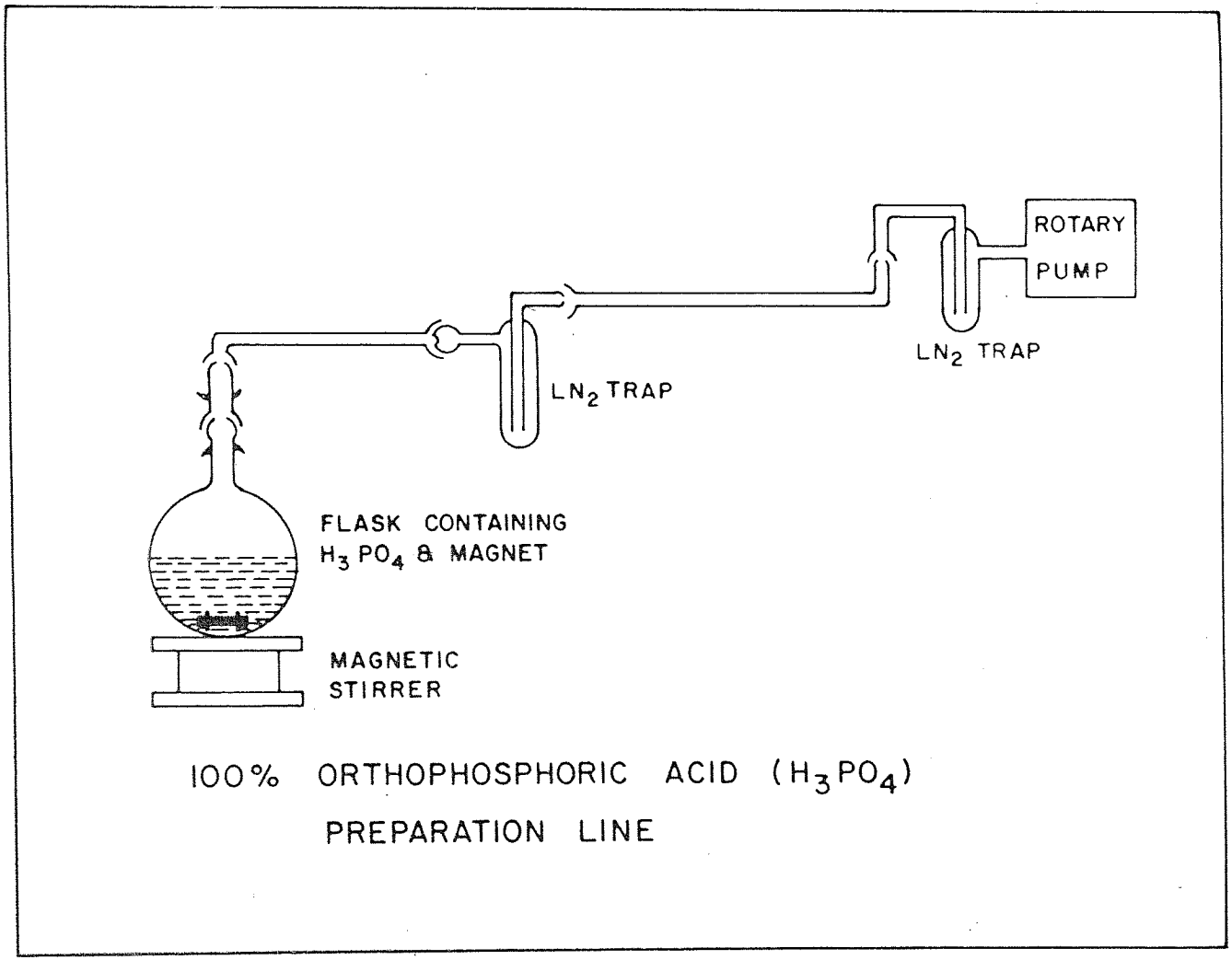

Fig. 2.2 : Orthophosphoric acid preparation line

Shackleton and Opdyke (1973) recommended the use of 100 % H_3PO_4. Recently Coplen et al (1983) suggested that H_3PO_4 of density 1.9-1.92 should be used and this is equivalent to 103-105% H_3PO_4. It is known that as the percentage of H_3PO_4 in a solution, approaches 100% level, polymerization starts (Such 1971). In fact, polymerization starts well before it reaches 100% (Wachter and Hayes 1985). The common steps involved are:

$$2H_3PO_4 \rightleftharpoons H_4P_2O_7 + H_2O$$

$$H_4P_2O_7 + H_3PO_4 \rightleftharpoons H_5P_3O_{10} + H_2O$$

$$H_5P_3O_{10} + H_3PO_4 \rightleftharpoons H_6P_4O_{13} + H_2O$$

The most serious effect of this polymerization is production of H_2O molecule which may exchange with CO_2 evolved from the phosphorolysis of carbonates, thus affecting the reproducibility. However, in the present case, this is not very important, because CO_2 and H_2O are immediately separated. But if the H_3PO_4 has lot of H_2O molecules in it, the trap efficiency may be reduced. As a result the separation of H_2O and CO_2 will not be complete and some H_2O may be carried through to the mass spectrometer along with CO_2, thus affecting the reproducibility. For the present study density of H_3PO_4 is kept at 1.86 gm/cc such that its concentration is 99%.

Preparation of Mass Spectrometer Reference CO_2 Gas

For higher accuracy in experimental measurement of

δ-values, it is preferable to use a mass spectrometer reference gas whose δ-values fall well within the range of δ-values of the samples.Owing to the non-avaibaility of a $CaCO_3$ reference standard close to PDB (since sample values are close to zero on PDB scale),it was decided to use CO_2 extracted from a bulk foraminiferal assemblage in an Arabian sea core top. Consequently, (0-2) cm. section (Holocene) of the core SK-20-185 was taken and wet seived to collect > 150 μm fraction consisting mainly of foraminiferal shells.This fraction was soaked in 30% dilute H_2O_2 and kept in a beaker overnight to remove the organic matter. Subsequently it was filtered through a coarse (54) Whatman filter paper,rinsed repeatedly with deionised water and oven-dried at 60°C.Approximately 10 g. of this fraction was taken for preparing the CO_2 reference gas. The extraction and clean up system for this are shown in Fig. 2.3. Foraminiferal carbonate (> 150 μm) is kept in a flask provided with a side arm.Approximately 45 ml of 99% H_3PO_4 is taken in the side arm.The flask is connected to a glass vacuum line and pumped through diffusion and rotary pumps for 3 hours.After evacuating,the side arm vessel is tilted to drop H_3PO_4 on the carbonate sample to initiate the $CaCO_3$-H_3PO_4 reaction. The reaction was performed at room temperature (~ 30°C). The acid-carbonate mixture was magnetically stirred continuously so as to facilitate complete reaction. Equilibration of CO_2 and H_2O was allowed to proceed for 24 hours.To extract the CO_2 thus produced the flask was connected to the glass vacuum line.After

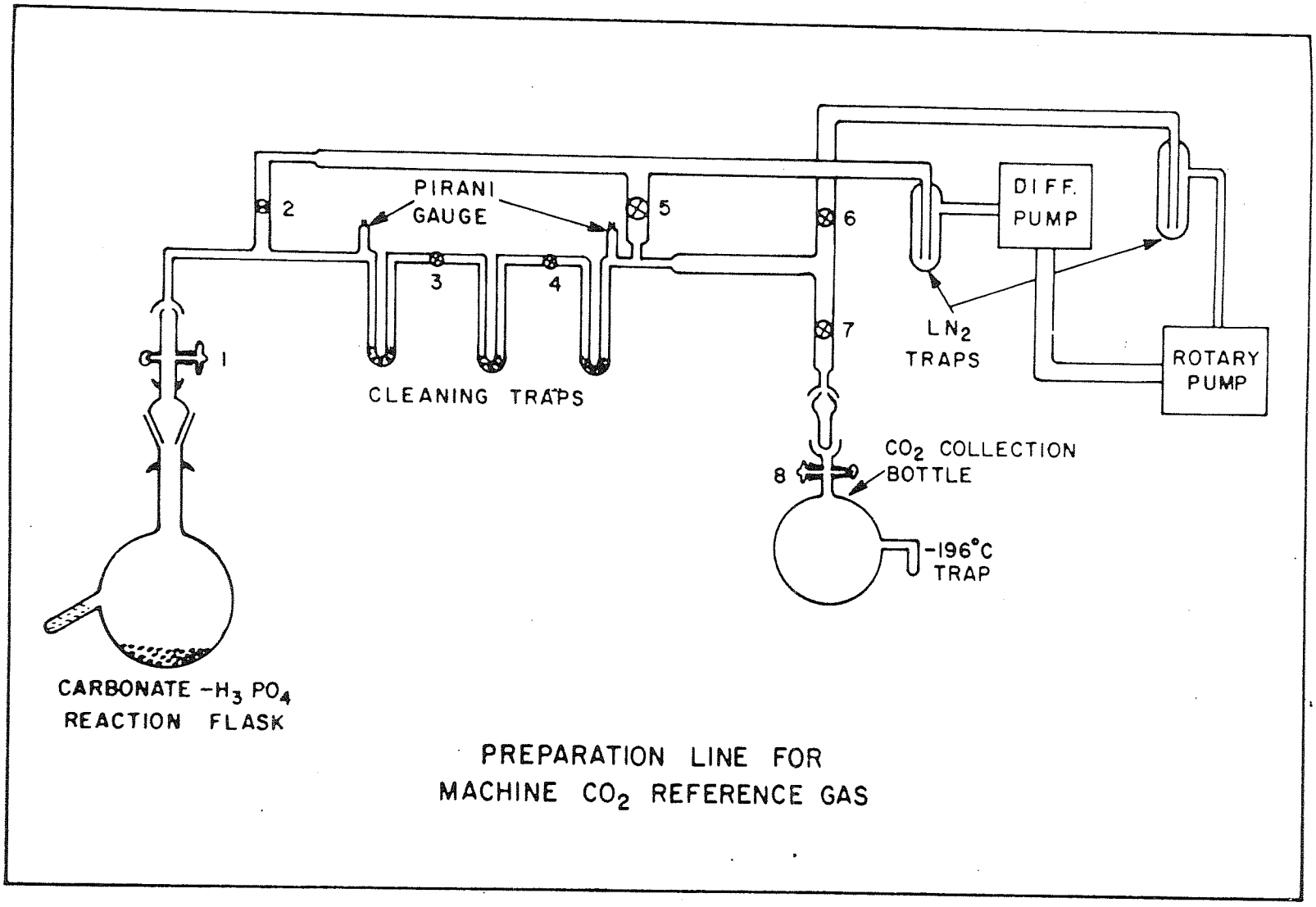

Fig. 2.3 : Extraction-clean up system for Mass Spectrometer CO_2 reference gas

evacuation, the CO_2 was released by opening stop-cock 1 and collected in the cleaning trap between valves 2 and 3 with the aid of LN_2 (-196^oC). All non-condensible gases were pumped out through valve 2.After all CO_2 was trapped,the -196^oC trap was replaced by an alcohol-acetone slurry,kept at -80^oC and LN_2 is put in the trap between valves 3 and 4. Stopcock 1 is closed,3 is opened and only CO_2 is absorbed in the second trap while H_2O remains trapped in -80^oC slurry. The CO_2 is thus cleaned repeatedly through 3 consecutive traps as shown in Fig. 2.3 and finally collected in a bottle by opening valves 7 and 8.This purified CO_2 is expected to be free of water.This CO_2 is then transferred into the machine-reference CO_2 reservoir of 5 litre volume,fixed on top of the mass-spectrometer so as to give ~ 10 cm pressure. This gas is named as Foram-standard CO_2 (FC). The purity of the gas is checked routinely by mass spectrometer and its δ-values are close to zero on (PDB) scale as expected.

On Line CO_2 Extraction from Small Samples

The gas extraction line designed and fabricated in PRL, for the preparation and purification of CO_2 from small amount of carbonates, is shown in Fig. 2.4.The thermally insulated box was made out of Bakelite boards.After putting 99% H_3PO_4 in the acid vessel,it was pumped through valve 13 for 1 hour, so that the acid does not absorb or exchange with H_2O molecules present in the air.Carbonate sample,kept in a small pyrex thimble, is put in the reaction chamber

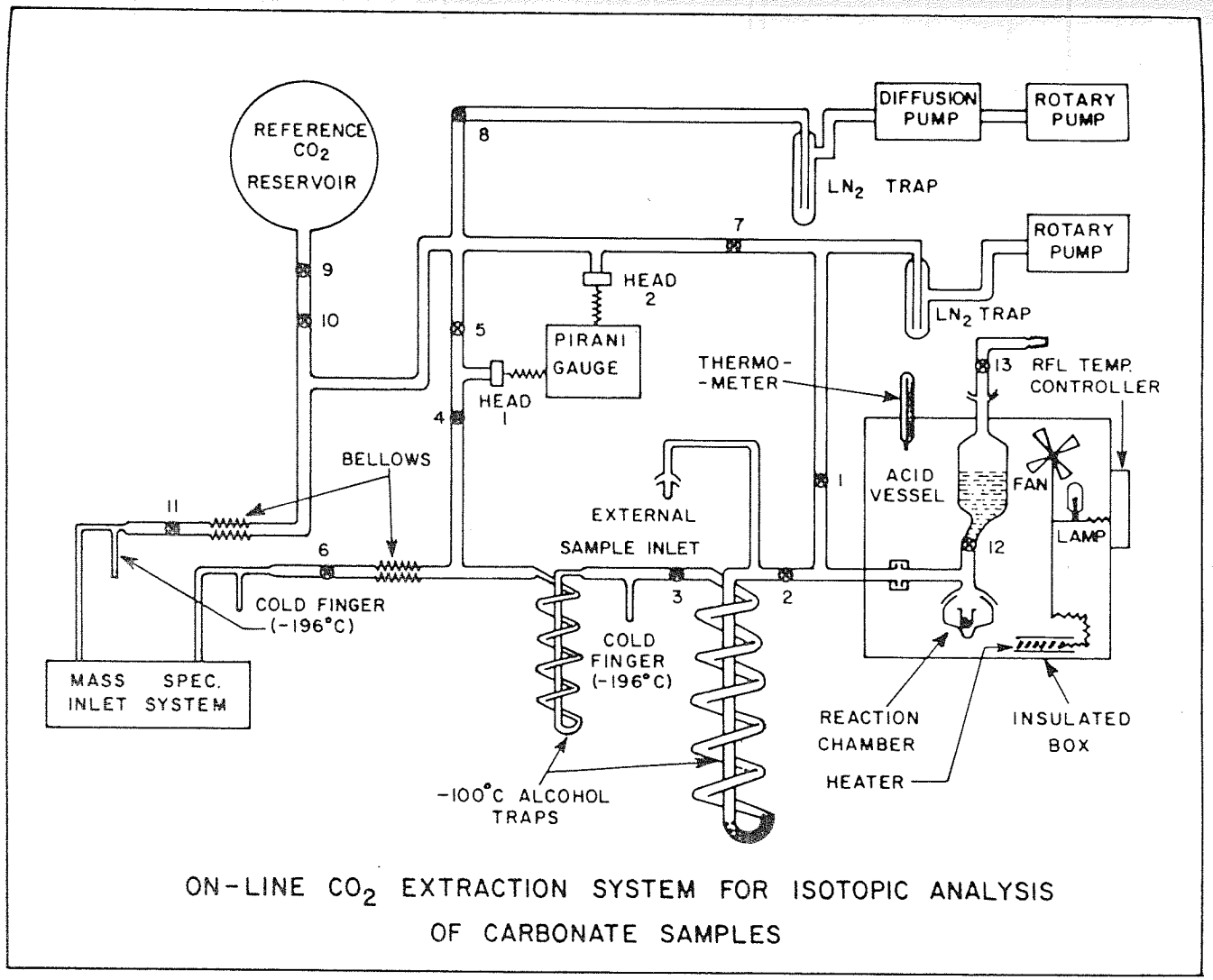

ON-LINE CO_2 EXTRACTION SYSTEM FOR ISOTOPIC ANALYSIS OF CARBONATE SAMPLES

Fig. 2.4 : On-line CO_2 extraction system for isotopic analysis of small carbonate samples.

connected below the acid vessel.The insulated box is kept at constant temperature $50^{o} \pm 0.1^{o}C$ with the aid of a thermistor coupled to a RFL temperature controller (model 70A) and a heater. A fan inside the box,circulates air to maintain the temperature uniform,which is monitored by an indicator lamp as well as a thermometer. The reaction chamber is evacuated through valve 1 by a rotary pump and subsequently by a diffusion pump for 10 minutes through valve 2,till the pressure goes down below 10^{-4} torr.

Afterwards valve 12 is opened to release a few drops of acid on the carbonate samples and immediately closed before the actual contact of acid with sample takes place.Reaction starts and the evolved gas is made to pass through a large spiral kept in a slush made of pure alcohol at $-100^{o}C$.The spiral separates H_2O from CO_2 and CO_2 is collected in a cold finger at $-196^{o}C$. The entire reaction is completed within 5 minutes and takes place at a very low pressure ~ 10^{-5} torr.For porous foraminiferal shells the reaction time was about 5 minutes while solid coarser carbonate (> 125 μm) particles generally take 10 minutes for complete reaction.

After CO_2 was collected,valves 2 and 3 are closed,non condensible gases are pumped out (via valve 4) by a diffusion pump. Subsequently valve 4 is closed and the LN_2 trap in cold finger is replaced by another small $-100^{o}C$ alcohol trap. This is a second cleaning after majority of H_2O is trapped in the big spiral.The CO_2 then is passed through another smaller $-100^{o}C$ alcohol spiral (3rd

cleaning) and collected in a LN_2 cold finger,next to valve 6.After all the CO_2 is collected in this second cold finger, valve 6 is closed and LN_2 trap is removed.The cold finger is heated by a hot air-gun.CO_2 is refrozen by LN_2 and again checked for non-condensible gases.Finally,fourth cleaning step by the small $-100^{o}C$ alcohol trap is employed here before taking the CO_2 into the mass-spectrometer inlet cold finger.

During the initial stages of analysis a major problem was encountered. A pure CO_2 gas shows typical 3 peaks of masses 44, 45 and 46 in the spectrum.At the early phase of work, the CO_2 gas was cleaned in three steps and in the mass spectrum, one more additional peak of mass 43 appeared (having the same peak height as mass 46).Some simulation experiments were done to identify the species of mass 43,by running pure CO_2 as well as CO_2 contaminated with water. While, the former did not show any extra peak,the latter did show a 43 peak.However,the species could not be identified properly, though it was concluded that water (H_2O) is responsible in some way for the production of the mass 43 peak.This had 2 bad effects:

1. After a prolonged contamination with H_2O vapour,the source current stability became poor.Upon opening the source, the filament was found to have a black coating, which might have been responsible for fluctuating electron emissions (source current fluctuation of 0.2 to 0.3 mA was observed).

2. Presence of H_2O and the associated 43 mass drastically affects $\delta^{13}C$ value but not the $\delta^{18}O$. It has been observed that a contaminated CO_2 gives a highly depleted $\delta^{13}C$ value.

The cause of this minute H_2O contamination was the inefficient trapping of water vapour by the big spiral trap. For the present work the cooling was done by adding LN_2 continuously in the slurry to keep it at $-100^{o}C$. If a thermal gradient is produced in the trap and temperature is not $-100^{o}C$ all over the spiral, its efficiency would not be 100%. Consequently some amount of H_2O might be carried through to cold finger along with CO_2.

However, this problem was overcome by introducing a 4th cleaning step. Often CO_2-H_2O form clathrets and by merely putting a $-100^{o}C$ trap, it is not possible to separate them. Hence in the final stage, gas was heated by hot-air gun, refrozen in cold finger by LN_2 and subsequently released by putting the cold finger at $-100^{o}C$ to introduce pure CO_2 into mass spectrometer. At this stage the H_2O amount is extremely small and does not cause any significant isotopic exchange with CO_2. In all the measurements reported in this thesis the CO_2 gas was dried thoroughly and the 43 mass peak did not show up. For every sample the mass spectrum was taken with a chart recorder.

The present system is capable of analysing as small as 0.5 mg carbonate, but in general 1.5 to 2 mg of carbonate

sample have been analysed on a regular basis.In most cases, it was difficult to weigh the carbonate samples due to their small quantity.However,the yield of CO_2 in all cases are presumably close to 100%, since the reaction is completed very quickly (~ 5 minutes).About 10-15 samples were analysed per day routinely. Reproducibility of the δ-values in the daily run of one or two standards as well as occasional replicate analysis of pure homogeneous marble acted as a check on the overall procedure.Blanks were also checked periodically and found to be negligible.

II.4. Mass Spectrometric Measurements, Their Analytical Precision and Reproducibility

Machine Standard

$\delta^{18}O$ and $\delta^{13}C$ were measured using a VG Micromass 602D mass-spectrometer, relative to the foram-standard CO_2 (FC), which served as an internal standard.

Most of the measurements were done in the second half of 1987 and in 1988.Initially one aliquot of FC of volume ~ 10 cc at p ~ 10 cm (between valves 9 and 10,Fig. 2.4) was taken in the mass spectrometer's variable reservoir (VR). This was sufficient to give major 44 current in the range $2x10^{-9}$A to $5x10^{-9}$A. In the later stage of experiments two aliquots were taken, since the pressure of FC in the reservoir decreased due to its continuous use.Once the FC was taken in VR, it was used for 2 to 3 days.During the period of measurements i.e. from July 1987 to September

1988, the standard carbonate gave reproducible values (discussed later).

Calibration to PDB via Secondary Standard

Prof. N.J. Shackleton kindly provided two standard marbles, Z-Carrara and Marble-V (125-180 μm) used in Cambridge as internal standard and whose δ-values w.r.t. PDB are known. In the present work we used these δ-values for calibrating the laboratory standard against PDB.The values are, Z-Carrara $\delta^{18}O = -1.79$, $\delta^{13}C = 2.18$ ($^{o}/oo$) and Marble-V $\delta^{18}O = -1.02$, $\delta^{13}C = 2.38$ ($^{o}/oo$).An internal carbonate standard was also prepared from pure (MAKMARB) Makrana marble of Rajasthan (< 150 μm).In the present work Z-Carrara and Marble-v have always been routinely analysed along with every set of samples. To check the reproducibility of the extraction system from time to time, replicate samples of MAKMARB standard were also run in a single day. All the standards were stored in glass bottles with air-tight screw caps and kept in an evacuated dessicator.

δ-values of replicate MAKMARB runs on two different days are listed in Table 2.2 and the δ-values of standards, Z-Carrara and Marble-V,over a period of more than one year, are listed in Table 2.3. The δ-values in single day replicate runs of MAKMARB, as well as standard carbonates analysed over a long period show that the overall reproducibility of the system is $\pm$ 0.1 $^{o}/oo$ for both $\delta^{18}O$ and $\delta^{13}C$. As can be seen from Table 2.3 that even after a

lapse of one year, the standard carbonate Z-Carrara and Marble-V had not changed isotopically and yielded the same δ-values as in the beginning. This shows that (i) the machine reference gas remained fairly unchanged despite use and depletion over the year, and (ii) carbonate standards can give reproducible values over quite a long period if care is taken to avoid ambient humidity. A comparison of the two methods of CO_2 extraction and analysis was made. Table 2.4 gives values of MAKMARB analysed in the 25°C conventional McCrea technique, before the on-line 50°C system was fabricated. Comparing values between Table 2.3 and 2.4 it is clear that reproducibility of δ-values in the present system is better by about a factor of two.

All the raw data are subjected to Craig (1957) correction and then converted to PDB through the following equations:

$$\delta^{18}O^{x}_{PDB} = \delta^{18}O^{x}_{FC} + \delta^{18}O^{FC}_{PDB} + \delta^{18}O^{x}_{FC} \cdot \delta^{18}O^{FC}_{PDB} \cdot 10^{-3}$$

$$\delta^{18}O^{FC}_{PDB} = \delta^{18}O^{FC}_{M-V/Z-C} + \delta^{18}O^{M-V/Z-C}_{PDB} + \delta^{18}O^{FC}_{M-V/Z-C} \cdot \delta^{18}O^{M-V/Z-C}_{PDB} \cdot 10^{-3}$$

where x = $^{18}O/^{16}O$ ratio in the sample, FC = Foram Standard CO_2, M-V = Marble-V, Z-C = Z-Carrara. $\delta^{18}O^{x}_{FC}$ is measured, $\delta^{18}O^{FC}_{M-V/Z-C}$ is also measured everyday along with a set of samples. $\delta^{18}O^{M-V/Z-C}_{PDB}$ values are known and hence $\delta^{18}O^{x}_{PDB}$ can be calculated. For the sample data generated between 31-7-87 to 7-9-88, grand mean values of Z-C or M-V with respect to

Table 2.2

Typical Examples of Delta Values of Standard MAKMARB Carbonate Run on Single Day

Date	$\delta^{18}O_{PDB}$ °/oo	$\delta^{13}C_{PDB}$ °/oo
1-3-88	-10.39	3.77
	-10.10	3.97
	-10.30	3.79
	-10.16	3.90
	-10.39	3.95
	-10.24	3.98
	-10.29	3.99
	-10.24	4.02
	-10.33	3.93
	-10.28	4.01
Mean[1]	-10.27±0.09	3.93±0.09
13-4-88	-10.31	3.91
	-10.39	3.84
	-10.61	3.99
	-10.21	4.03
	-10.24	3.86
	-10.40	3.79
	-10.29	3.98
	-10.39	3.84
Mean[1]	-10.36±0.1	3.91±0.09

[1] Uncertainties given are one sigmas.

Table 2.3

$\delta^{18}O$, $\delta^{13}C$ Values of Carbonate Standard Z-Carrara* and Marble-V*

(provided by N.J. Shackleton) analysed in PRL

Date	Z-Carrara		Marble-V	
	$\delta^{13}C$ ‰	$\delta^{18}O$ ‰	$\delta^{13}C$ ‰	$\delta^{18}O$ ‰
From 31-7-87 to 7-9-88	0.38	-1.96	0.53	-1.16
	0.58	-1.98	0.65	-1.24
	0.40	-2.00	0.52	-1.20
	0.51	-2.03	0.60	-1.36
	0.54	-1.81	0.59	-1.35
	0.48	-1.84	0.59	-1.32
	0.55	-1.78	0.58	-1.26
	0.59	-1.79	0.62	-1.07
	0.60	-1.93	0.65	-1.08
	0.47	-1.94	0.62	-1.05
	0.60	-1.90	0.68	-1.31
	0.53	-1.80	0.68	-1.20
	0.43	-1.70	0.57	-1.10
	0.48	-2.07	0.52	-1.10
	0.43	-1.74	0.72	-1.10
	0.57	-1.77	0.73	-1.13
	0.54	-1.81	0.73	-1.28
	0.51	-1.91	0.58	-1.18
	0.51	-1.71	0.70	-1.20
	0.51	-1.80	0.69	-1.11
	0.46	-1.77	0.58	-1.13
	0.58	-1.66	0.49	-1.18
	0.54	-1.83	0.61	-1.03
	0.47	-1.78	0.47	-1.12
	0.50	-1.65		
	0.50	-1.81		
Mean[1]	0.51±0.06	-1.83±0.1	0.61±0.08	-1.18±0.1

* With respect to Foram-standard CO_2 (FC)

[1] Uncertainties given are one sigmas.

Table 2.4

Run of Standard MAKMARB[#] IN 25°C (McCrea) System

Date	$\delta^{13}C$ °/oo	$\delta^{18}O$ °/oo	$\delta^{13}C$ °/oo	$\delta^{18}O$ °/oo
	1.74	-7.56	1.41	-8.34
	1.50	-7.98	1.46	-8.43
	1.56	-8.02	1.40	-8.01
	1.60	-7.77	1.42	-8.19
	1.60	-7.81	1.28	-8.48
	1.80	-7.36	1.43	-8.06
	1.29	-8.20	1.35	-8.31
From	1.38	-8.31	1.26	-8.60
1-1-85	1.48	-8.05	1.37	-8.67
to	0.88	-8.85	1.43	-8.95
27-2-86	0.97	-8.91	1.30	-8.06
	1.52	-8.27	1.22	-8.29
	1.60	-7.75	1.38	-8.36
	1.58	-8.03	1.02	-9.18
	1.46	-8.22	1.61	-8.54
	1.63	-8.03	1.60	-8.54
	1.39	-8.41	1.68	-8.39
	0.90	-9.37	1.39	-8.62
	1.43	-8.40	1.33	-8.32
	1.49	-8.09	1.51	-8.38
	1.48	-8.43	1.53	-8.45
	1.52	-8.79	1.49	-8.76
	1.46	-8.42	1.64	-8.47
	1.44	-8.41	1.36	-8.89
	1.45	-8.42	1.33	-8.89
	1.59	-8.06	1.28	-8.89
	1.41	-8.35	1.54	-8.60

Mean[1] $\delta^{18}O = -8.38 \pm 0.30$ $\delta^{13}C = 1.43 \pm 0.20$

$\delta^{18}O_{PDB}^{MAKMARB} = -10.58 \pm 0.3$, $\delta^{13}C_{PDB}^{MAKMARB} = 3.43 \pm 0.2$

Against Toilet Seat Limestone Standard

[1] Uncertainties given are one sigmas.

FC were taken to calculate sample δ-values w.r.t. PDB.

This conversion method does not require the direct calibration of Foram-Standard and takes care of any fractionation in reference CO_2 gas.Thus two sets of values with respect to PDB were obtained.One via Z-Carrara and the other via Marble-V. In most cases,these values were pretty close and an average was taken (see section on interlaboratory comparison). All data in this thesis are reported with respect to PDB.Errors given in tables are one standard deviation. The measurements were done with a variety of controls and checks,some of which are described below:

1. Z-Carrara and Marble-V standards were run regularly, along with every set of 10-15 samples.

2. Replicate measurements were made for most of the samples.

3. Blanks were measured periodically and kept at a minimum by cleaning the extraction line regularly.The extraction line has an inherently low blank since only greaseless stop cocks with viton 'O' rings (Kontes) were used.

4. The machine performance was checked routinely (capillary balance, zero enrichment, through valve leakage and cross-mixing in the change over valve etc.).

5. Since water contamination during acid extraction of CO_2 proved to be the only major problem during initial testing of the line, mass spectrum of each sample was taken as a routine check to see the presence of mass 43 species. If 43 mass was found, the run was rejected.

Interlaboratory Comparison of Standards

In addition to the tests cited above, it was necessary to check our measurements for systematic errors. It has been done in two ways:

1. Knowing the Z-Carrara and Marble-v values w.r.t. PDB, Foram-CO_2 standard was calibrated through both these marble standards and compared. Additionally NBS-20 and Paris sirap were also run to calibrate FC gas. This calibration of FC was, however, not used for converting sample values with respect to PDB.

2. Also the standard (MAKMARB) prepared in our laboratory was sent to another laboratory for measurement.

Table 2.5 gives a list of such an interlaboratory comparison of MAKMARB standard and comparison of gas reference standard through different standard carbonates.

It is seen that calibration of gas reference standard against PDB via several secondary standards agrees well among themselves within experimental errors; also the PRL value of MAKMARB standard agrees well with value quoted by Godwin Laboratory (Cambridge) of Dr. Shackleton. Calibration

Table 2.5

Comparison of Gas Reference Standard and Interlaboratory Comparison of δ-values (°/oo)

Values	Reference CO_2 gas	Via Z-Carrara[2]	Via Marble-V[3]	Via NBS-20[4]	Via Paris Sirap[5]
$\delta^{18}O$	FC	0.04±0.1(26)[1]	0.16±0.1(24)	-0.19(1)	-0.01±0.1(2)
$\delta^{13}C$	FC	1.67±0.1(26)	1.77±0.1(24)	1.54(1)	1.8±0.1(2)

Carbonate standard	Quoted value[6]	PRL value
MAKMARB	$\delta^{18}O$ = -10.5±0.2(28)	$\delta^{18}O$ = -10.3±0.1(18)
	$\delta^{13}C$ = 3.9±0.1(28)	$\delta^{13}C$ = 3.9±0.1(18)

1 No. of measurements given in parenthesis.

2,3 Supplied by N.J. Shackleton

4,5 Supplied by IAEA

6 Analysed in N.J. Shackleton's Laboratory, Cambridge.

via Z-Carrara and Marble-V gives very close values for same samples. The $\delta^{18}O$ values of Foram-Standard (CO_2) (FC) are very close to those of sample foraminifera i.e. close to zero.

A Few Notes on the Mass Spectrometric Measurement of CO_2

1. During the analysis of small amount of carbonate sample it was observed that the depletion of sample CO_2 gas was faster than that of reference, over a period of time when using machine cold-finger. By eliminating the chance of through valve leakage and introducing the same amount of gas on either side cold fingers, it was found that sample cold finger had ~ 15% less volume than that of reference cold finger. To overcome this, a circular groove of 0.075 ml was made between the raised head and knife edge on cu-seat valve of sample inlet side. This extra volume made the sample cold finger volume equal to that of the reference cold finger. In this condition both reference and sample gas depleted equally even after a long period i.e. major current (44) difference was within the prescribed limit of 1%.

2. Since it was not feasible in this on-line system, to weigh and measure the yield of CO_2 from small carbonate samples, the ion-gauge pressure (IGP) and corresponding major current intensity could not be

predetermined accurately for each sample. The major current could vary anywhere between 1.5 x 10^{-9}A to 5 x 10^{-9}A range. Possible effect of this variation on the δ-value was studied by noting the change of isotope ratio with the variation in the major current and the variation of major current with the change in pressure of gas in the mass spectrometer determined by the ion gauge. Fig. 2.5 shows the plot of IGP vs. major current as well as major current vs. 46/44 ratio.As can be seen, the isotope ratio remains essentially constant between current 3 x 10^{-9}A to 5 x 10^{-9}A.Major current increases linearly in this range with respect to IGP and the isotope ratio remains constant.Hence samples were usually taken in such quantities that the extracted CO_2 gives a current between 3 x 10^{-9} and 5 x 10^{-9}A.

3. In some samples current in the above range could not be obtained by using the cold finger (either too low or too high) and the ion repeller,electron voltage were adjusted to get the proper current.

4. To calculate the final δ-value,3 sets of reference and sample isotopic ratios were printed out from a set of isotopic measurements. A microcomputer fabricated in our laboratory was attached to the machine, which enabled a quick calculation of the δ-values and the standard deviation for each run. This standard deviation (1σ), which was the precision of mass

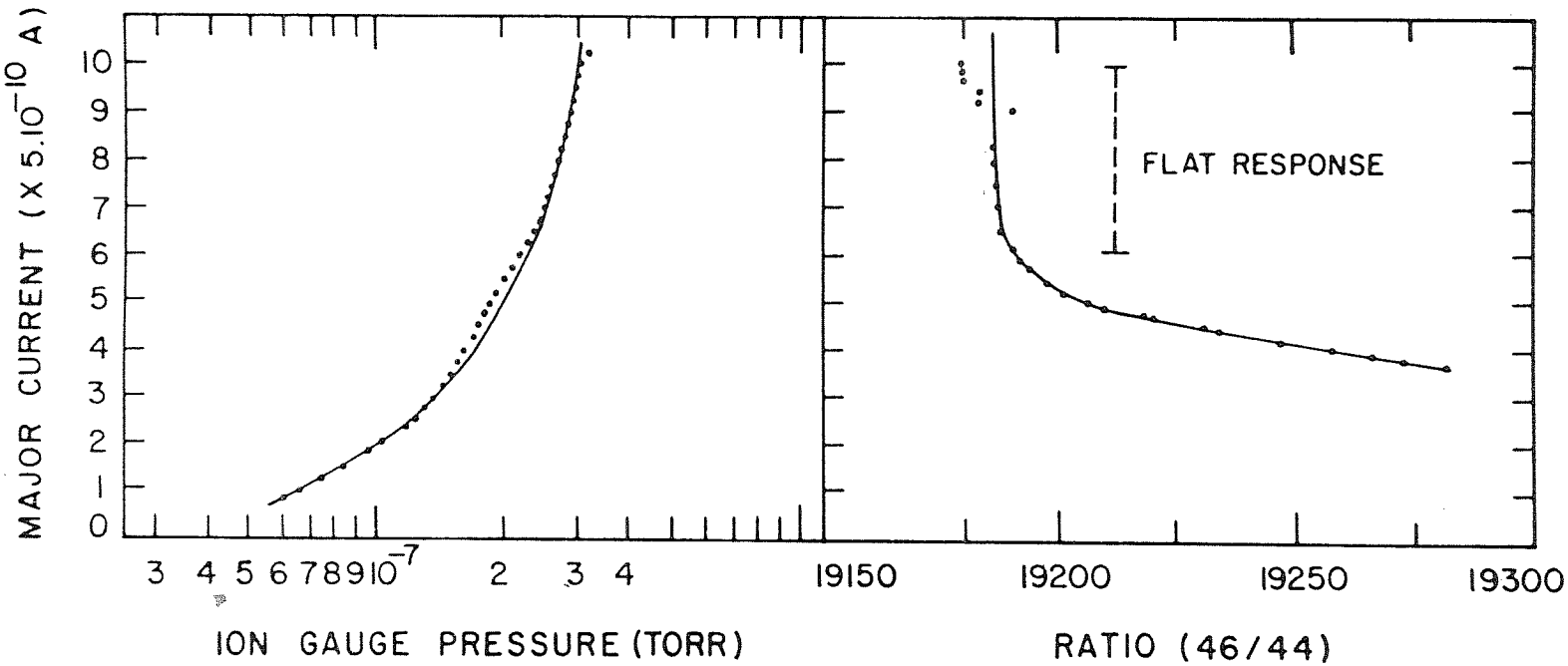

Fig. 2.5 : Variation of major current (44) with change in IGP and variation of ratio (46/44) with change in major current (44).

spectrometric measurement, was better than $\pm$ 0.01 $^{o}/_{oo}$ for $\delta^{13}C$ and $\pm$ 0.02 $^{o}/_{oo}$ for $\delta^{18}O$ for samples of reasonably large amount ($\sim$ 0.07 litre at 4 cm. pressure). When same gas was run several times (e.g. laboratory check standard) the reproducibility of the measurements was same as the precision of the individual run, given above. However,when cold finger was used, reproducibility was better if six sets of sample and reference isotopic ratios were taken.Table 2.6 gives the reproducibility obtained by running same gas in cold finger condition but with variable number of sets of ratios. These results clearly show the effect of statistics on data reproducibility.In VG Micromass 602D version,45/44 and 46/44 mass ratios are measured one after the other,not simultaneously as in the triple collector VG Micromass 903.While measuring small samples the sample depletion was considerable and it was not possible to take six sets of ratios; instead 3 sets of ratios were taken. This is the probable reason of having an overall reproducibility of $\pm$ 0.1 $^{o}/_{oo}$.

II.5. Effect of Sample Pretreatment on $\delta^{18}O$-$\delta^{13}C$ Values

Effect of sample pretreatment on $\delta^{18}O$-$\delta^{13}C$ has been discussed at length by Duplessy (1970). The techniques adopted by different laboratories are not always the same but in general comprise of:

Table 2.6

Reproducibility of Small Amount of Gas[#]

Gas	$\delta^{13}C$*	$\delta^{18}O$*	No. of sets	Remarks
Check standard(10)[+]	-0.19 ±0.06	0.95 ±0.11	3	Poor reproducibility
CO_2 " (6)[+]	-0.05 ±0.03	1.07 ±0.04	6	Good reproducibility

[#] 25 μl at 4 cm pressure.

* Measured against some arbitrary standard.

+ No. of measurements in parenthesis.

(i) Soaking in dilute H_2O_2/Chlorox

(ii) Ultrasonic treatment for a few seconds

(iii) Roasting at high temperature (~ 400°C) in vacuum.

Apparently no difference is seen between treated and untreated samples when one is dealing with pure $CaCO_3$ (Duplessy 1970), while impure $CaCO_3$ like Fletton and NBS-20 show significant difference. It is also not known whether 100% H_3PO_4 has any effect on organic matter which can produce mass species in the mass range 43-47 and bias isotopic ratios of carbonates. However, some laboratories use so-called "green acid" i.e. H_3PO_4 containing crystals of chromium trioxide. Chromium trioxide changes to chromic acid,which is highly oxidative and reacts with organic matter to produce CO_2 (D.S. Introne, U.C.S.D., personal communication, 14.1.88). In general, pure H_3PO_4 is unlikely to produce any CO_2 from organic matter. Nevertheless, almost all laboratories try to remove organic matter by some treatment. Some roast under vacuum at 400°C (J.C. Duplessy,personal communication, 3.1.88), while others roast under helium (Epstein et. al., 1953). Other methods include soaking the sample in dilute chlorox (Emiliani 1966), or in 10% H_2O_2 (N.J. Shackleton, personal communication, 30.12.88) both of

which may partially dissolve the carbonate (op. cit.). In contrast a few laboratories do not treat the samples at all for removing organic matter (W.H. Berger, personal communication, 14.1.88). However,all laboratories employ ultrasonic treatment to remove adhering carbonate particles inside the foraminifera which may have very different isotopic composition (for example, coccolith particles within benthic shells), thus biasing the actual ratio.The sample is soaked either in methanol or distilled water and ultrasonic treatment is given to dislodge extraneous particles. The time of ultrasonic treatment is kept nearly constant (a few seconds) since strong agitation may break the shells and some part of the sample may be physically lost.

During the course of this investigation, some experiments were done to determine the effect of various types of pretreatments on $\delta^{18}O$-$\delta^{13}C$ values of carbonates. Samples were soaked in H_2O_2 for 1/2 hour. After adsorbing the H_2O_2,sample was rinsed thrice with methanol and roasted at high temperature (~ 420°C) under vacuum (~ 10^{-6} torr).Fig. 2.6 shows the roasting system. Samples in pyrex thimbles are kept on a steel holder and inserted in a quartz tube.A heater provided with a temperature controller (APLAB,model 9601) is mounted on a trolley and can be moved back and forth. The quartz tube is inserted within the heater after it acquires the required temperature.The quartz tube is

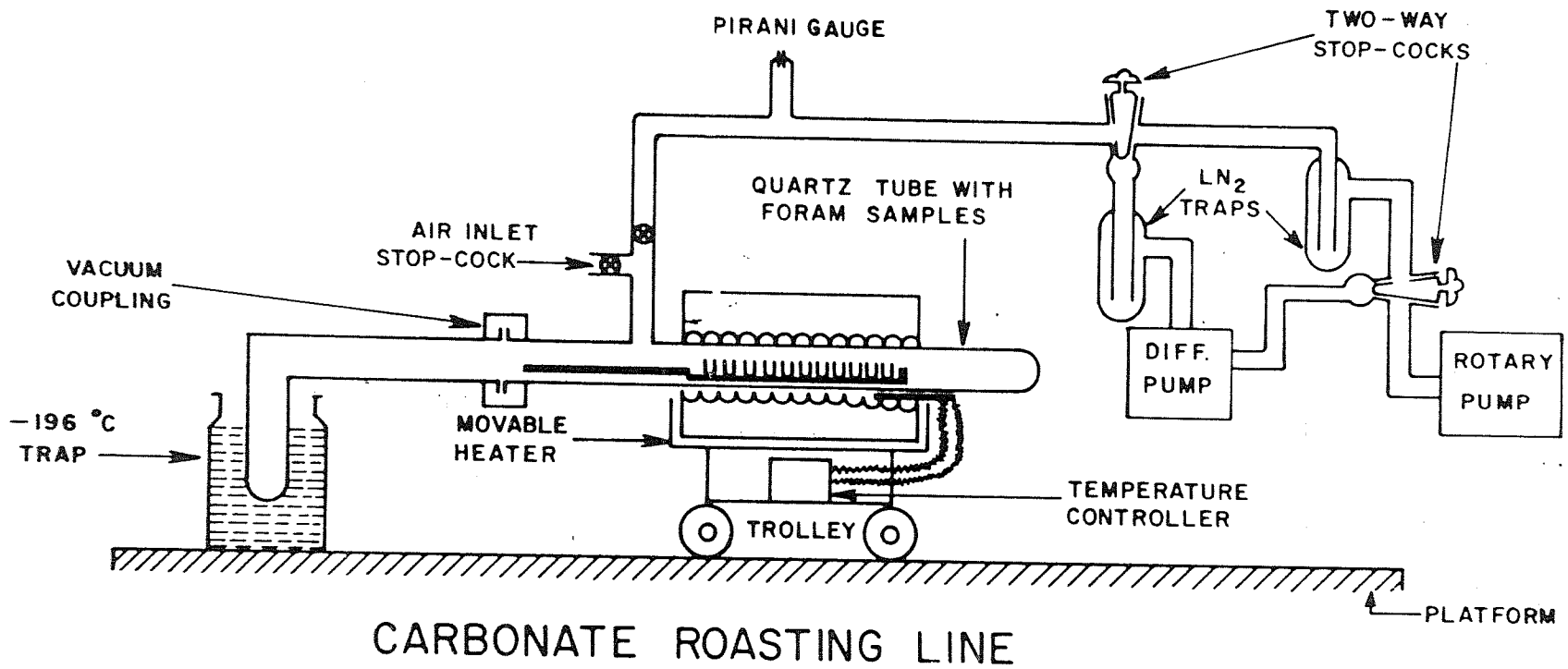

Fig. 2.6 : Foraminifera/small carbonate roasting system

connected to a glass line evacuated by rotary and diffusion pumps.Evolved gases from roasting of organic matter is collected in a LN_2 trap.The average roasting time is about one hour.Samples have also been analysed without roasting. Analyses have been done on samples with and without ultrasonic treatment.In addition an experiment was carried out to see the effect of organic matter on sample values.Results (along with pretreatment technique employed) of these analyses are given in Table 2.7.

It is evident from Table 2.7 that there is no difference in $\delta^{18}O$ between treated (roasted) and untreated (unroasted) samples on pure marbles as well as powdered and homogenised foraminifera samples from Holocene and deeper levels of both the cores SK-20-185 and SK-20-186. Organic matter does not react with pure H_3PO_4 to produce CO_2 and therefore no difference was observed between treated and untreated mixtures of organic matter and carbonate. Hence it is concluded that roasting of forams is probably not necessary when one is using pure H_3PO_4.Also no difference in δ-values was seen between samples with and without ultrasonic treatment, perhaps indicating that for planktonic foraminifera, secondary carbonate particles do not bias their isotopic composition. However,this might not be always true and hence for the present study following procedures have been routinely employed:

1. Ultrasonic treatment of foram-tests in distilled water and subsequent absorption of water by a tissue paper.

2. Drying the tests under vacuum, at 150°C for one hour in the roasting system.

Finally the problem of grain size has to be discussed in some detail. Various workers have shown that different grain size fractions of the same carbonate tend to show different values for $\delta^{18}O$ and $\delta^{13}C$. The variation may be from 0.2 to as large as 0.7 °/oo (Duplessy 1970). Most of these workers have used McCrea's 25°C method. In Shackleton's 50°C method, however, no systematic variation is observed with grain size. At 50°C, reaction rate is very fast and all carbonates get quickly digested, where the evolved CO_2 probably has an isotopic composition irrespective of grain size.

Recently Barrera and Savin (1987) have reported marked changes in isotopic composition in fine grained carbonates (< 10 μm), when dried from distilled water. This has been observed when carbonates were dried even at room temperature. However, the effect is not seen when carbonate samples were dried from acetone. Foraminiferas are composed of the fine calcite particles (< 0.5 μm). Aggregation of these particles significantly reduces the surface area/volume ratio. When a foram test is subjected to internal dissolution, this surface area and corresponding porosity and permeability increases. In that case the drying of foram samples from distilled water may offset the

Table 2.7

Results of the Sample Pre-Treatment Experiments

Sample	Pretreatment	$\delta^{18}O$ °/oo PDB	$\delta^{13}C$ °/oo PDB
SK-20-185,(0-2) cm. level, Holocene, 100 (>400 μm) *G. sacculifer*, powdered and homogenised	No ultrasonic treatment pretreated with H_2O_2, methanol and roasted	-1.7±0.1(10)+	2.17±0.1(10)
"	No treatment, no roasting	-1.79±0.1(10)	2.23±0.1(10)
SK-20-185,(70-75) cm. level, 100 (>400 μm) *G. sacculifer* powdered and homogenised	No ultrasonic treatment, pretreated with H_2O_2, methanol and roasted	-0.72±0.1(6)	2.0±0.1(6)
"	No treatment, no roasting	-0.56±0.1(8)	2.1±0.1(8)
SK-20-186,(6-7) cm. level, Holocene, 100 (>400 μm) *G. sacculifer*, powdered and homogenised	No ultrasonic treatment, pretreated with H_2O_2 methanol and roasted	-1.68±0.1(9)	2.0±0.1(9)
"	No treatment, no roasting	-1.5±0.1(11)	1.98±0.1(11)
SK-20-186, (6-7) cm level, Holocene, 130 *G.sacculifer* (>400 μm)	With ultrasonic treatment (all the shells), pretreated with H_2O_2, methanol, roasted and subsequently powedered and homogenised	-1.68±0.1(8)	2.05±0.1(8)

SK-20-186,(25-26) cm. level, 150 (>400 μm) G. sacculifer powdered and homogenised	No ultrasonic treatment, pretreated H_2O_2, methanol and roasted	-0.79±0.1(8)	2.01±0.1(8)
"	No treatment, no roasting	-0.68±0.1(9)	1.98±0.1(9)
SK-20-186,(25-26) cm level, Holocene, 130 G. sacculifer (>400 μm)	With ultrasonic treatment (all the shells), pretreated with H_2O_2, methanol, roasted and subsequently powedered and homogenised	-0.64±0.1(10)	1.97±0.1(10)
Pure Marble (MAKMARB)	With ultrasonic treatment, pretreated with H_2O_2, methanol, roasted	-10.3±0.1(7)	3.91±0.1(7)
"	No treatment, no roasting	-10.3±0.1(6)	3.89±0.1(6)
Pure Marble (MAKMARB) mixed with organic matter*	With ultrasonic treatment, pretreated with H_2O_2, methanol, roasted	-10.44±0.1(5)	3.89±0.1(5)
"	No treatment, no roasting	-10.37±0.1(5)	3.88±0.1(5)

+ Number in parenthesis is the number of measurements.

* Organic matter is obtained from Prof. S. Krishnaswami, (300-600) μm marine plankton, pretreated with mild HCl to remove $CaCO_3$, if any, and dried before mixing with marble powder.

isotopic values (op. cit.).In the experiments of Table 2.7, foram-tests have been powdered, homogenised, treated with H_2O_2-methanol and subsequently roasted. No difference in δ-values is seen between such treated and untreated foram-powder. These have been done at several levels from two different cores,along with pure marbles.It appears that these pretreatments do not change the isotopic composition of a complete test by dissolution - reprecipitation mechanism of isotopic exchange.

II.6. Estimation of Calcium Carbonate

Calcium carbonate estimation was done, following the standard procedure (Barnes 1959). A known amount of dry, powdered sediment sample (~ 100 mg) was taken for analysis and subjected to 2% acetic acid leaching in batches. Centrifuged, clear solution was made to 100 ml. and titrated against 0.01 M standardised EDTA. The reproducibility of $CaCO_3$ measurement,estimated from both replicate analyses of standard carbonate and sample is $\pm$ 1%.

II.7. Radiochemical Analysis of Sediments for U-Th Series Isotopes

A known quantity of sample (~ 5 gms),finely powdered and ovendried at 110°C was brought into solution by HF, $HClO_4$, HCl and HNO_3 treatment and finally taken in a 9M HCl solution. Prior to acid digestion, $^{228}Th/^{232}U$ equilibrated

spike was added to monitor the chemical yields of Th and U fractions respectively. Approximately 250 μl of this spike (containing ~ 17.7 dpm $^{232}U/_{ml}$) was used.From the solution, Th and U were separated on an anion exchange column (DOWEX-1x8 100-200 mesh, Cl^- form) and purified following the procedure of Krishnaswami and Sarin (1976).Chemical yields for both Th and U fractions were above 70%.The Th and U were electroplated on platinum planchets. Concentrations of Th and U isotopes were determined by alpha-counting on a solid state silicon surface barrier detector, coupled to a ND100 pulse height analyser.Standard U-Th sources were periodically counted to check the stability of the system.Overall counting efficiency of the system was 27.2 $\pm$ 0.7%.Error associated with the data was only due to uncertainty in counting. Fig. 2.7 gives the flow-chart of U-Th extraction.

II.8. ^{14}C Measurements

^{14}C measurements were done on bulk samples at the Birbal Sahni Institute of Palaeobotany (BSIP),Radiocarbon Laboratory, Lucknow. Sediment samples were hydrolysed using 10% HCl.Evolved CO_2 was purified,converted to methane (CH_4) and assayed for its ^{14}C activity in gas proportional counter (Rajagopalan and Vishnu-Mittre 1977).Since most of the samples were calcareous ooze,enough CO_2 was available

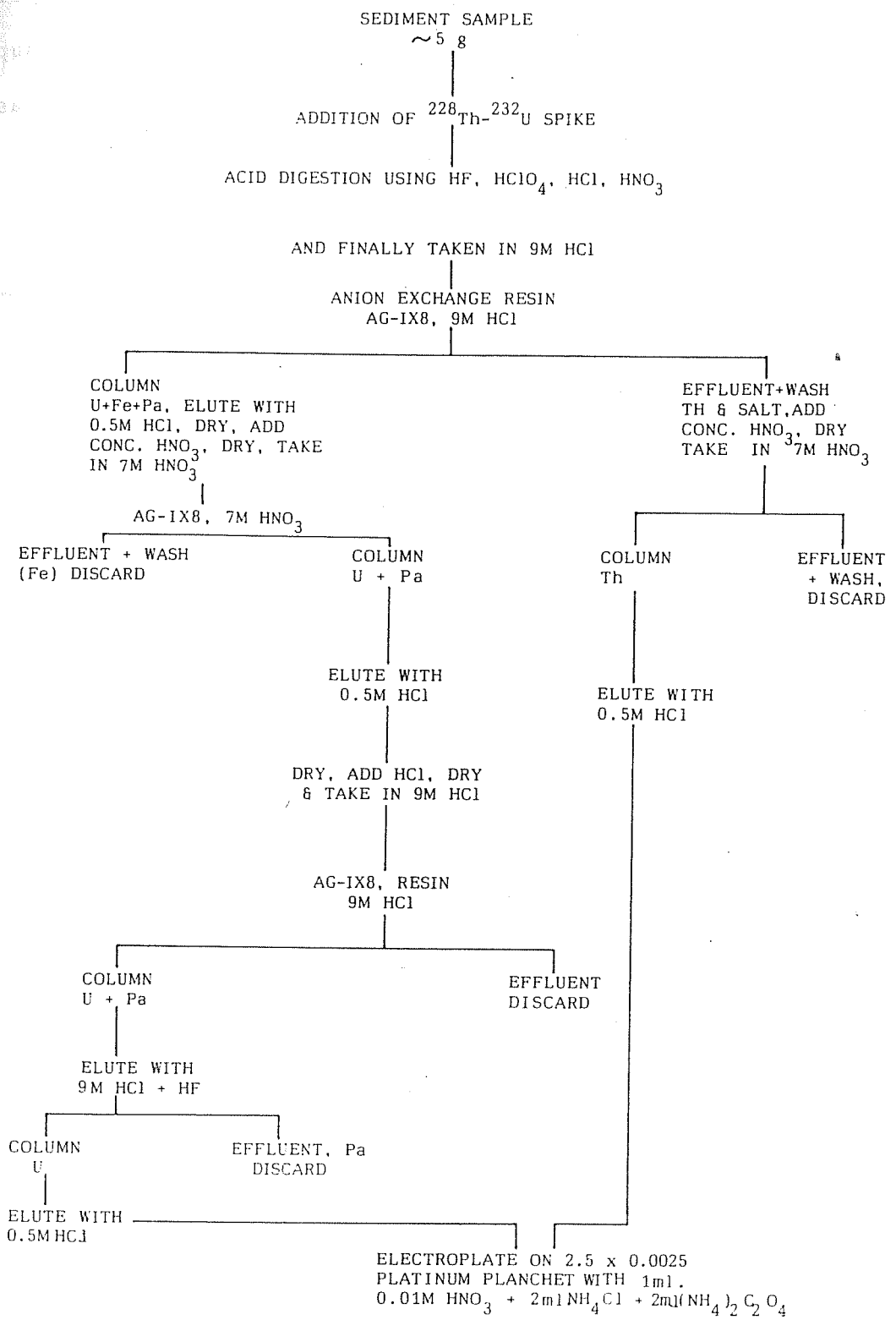

Fig. 2.7 : Ion exchange separation and purification

for counting.In case of clayey sediments and/or less sample quantities, dead CO_2 was mixed and counted.Error in the age estimation is typically 1 to 5%.

CHAPTER III

RESULTS AND DISCUSSION

CHAPTER III

RESULTS AND DISCUSSION

Results of various measurements carried out in the present work are presented in this chapter and their implications are discussed.For the sake of convenience,this chapter is broadly divided into three sections.The dating of sediment cores based on different methods viz. ^{14}C,U-Th series isotopes and $\delta^{18}O$ stratigraphy,is discussed in the first section. Oxygen isotope results of samples from the cores and important palaeoclimatic results obtained from these data are discussed in the second section.The third section deals with carbon isotope variation in the samples and down core calcium carbonate measurements and their relation to oceanic carbon cycle and productivity.

III.1. Geochronological Studies of the Sediment Cores

III.1.1. Determination of Accumulation Rates from ^{14}C and $\delta^{18}O$ Stratigraphy

^{14}C dates on cores SK-20-185, SK-20-186 and CD-17-30, are presented in Tables 3.1 to 3.3.

A plot of ^{14}C ages against depth for core SK-20-185 is shown in Fig. 3.1. The best fit line through the data points, taking into account the measurement error in ^{14}C ages and the spread in sampling depths, gives a sedimentation rate (S) of 2.2±0.1 cm/kyr. The goodness of fit shows that the average sedimentation rate can be considered to be constant over the last 30 kyr at this location. A similar plot of ^{14}C ages versus depth for core SK-20-186 is shown in Fig. 3.2. In this core, a distinct change in accumulation rate is observed at 22.5 cm, corresponding to about 14 kyr., (glacial-Holocene transition). The observed sedimentaiton rate during the Holocene is 2.4 ± 0.1 cm/kyr, an increase by a factor of 4 compared to that observed during the glacial period (S = 0.6 ± 0.1 cm/kyr). Another change is observed at 30.5 cm (i.e. ~ 27 kyr), the sedimentation rate at the deeper levels being 1.6 ± 0.4 cm/kyr. The ^{14}C age of top samples in cores SK-20-185 and SK-20-186 are 4.0 ± 0.1 and 5.2 ± 0.1 kyr respectively. Such older ages are typical of cores with bioturbation. However, in both these cores, ^{14}C activity shows a continuous decay and no plateau in the ages is found near the core top. This observation argues

Table 3.1

Radiocarbon* Ages on Core SK-20-185

Depth (cm)	Age (kyr)+
0-2	4.0 ± 0.1, 4.2 ± 0.1[1]
2-3	4.8 ± 0.1
6-7	6.4 ± 0.2
12-13	8.8 ± 0.4
15-17	12.9 ± 0.4
21-23	13.3 ± 0.2
23-25	15.6 ± 0.2, 16.5 ± 0.3[2], 15.2 ± 0.7[3]
29-31	18.2 ± 0.3
35-40	20.0 ± 0.4
40-45	22.8 ± 0.5, 19.7 ± 0.8[2], 23.5 ± 0.5[3]
45-50	25.3 ± 0.7
65-70	27.7 ± 1.2

* Measurements made on bulk samples

1 > 150 μm fraction-ages

2 > 63 μm fraction-ages

3 < 63 μm fraction-ages

\+ A half life of 5730 ± 40 years was used to calculate the age.

Table 3.2

Radiocarbon* Ages on Core SK-20-186

Depth (cm)	Age (kyr)+
0-2	5.2 ± 0.1
5-6	6.6 ± 0.1
14-15	10.2 ± 0.1
22-23	13.6 ± 0.2
26-27	19.8 ± 0.3
30-31	27.4 ± 0.7
37-38	31.1 ± 1.3
42-44	36.1 ± 2.2
72-77	>40
97-102	>40

Table 3.3

Radiocarbon* Ages on Core CD-17-30

Depth (cm)	Age (kyr)+
30-35	10.4 ± 0.2
50-60	14.8 ± 0.6
95-105	18.1 ± 0.5
175-185	30.0 ± 1.9

* Measurements made on bulk samples.

\+ A half life of 5730 ± 40 years was used to calculate the age.

Table 3.4

Data of U-Th[1] Isotopes in Core SK-20-185

Depth interval (cm)	$CaCO_3$ (%)	^{232}Th (dpm/gm)	^{238}U (dpm/gm)	Th/U (weight ratio)	^{230}Th (dpm/gm)[2]	^{230}Th excess[3] (dpm/gm)	$\frac{^{234}U}{^{238}U}$
0-1	67.5	0.71±0.02	0.5±0.02	4.26±0.21	5.84±0.09	5.34±0.25	1.18±0.04
1-2	67.5	0.70±0.02	0.45±0.02	4.67±0.28	5.72±0.08	5.27±0.24	1.11±0.04
2-3	67.5	0.75±0.01	0.58±0.02	3.75±0.19	6.40±0.10	5.82±0.20	1.03±0.03
15-17	51.6	1.18±0.03	0.81±0.03	4.50±0.18	5.96±0.10	5.15±0.20	1.00±0.03
29-31	41.0	1.33±0.02	0.87±0.02	4.43±0.17	4.65±0.04	3.78±0.10	1.06±0.03
40-45	39.0	1.52±0.02	4.83±0.06	0.94±0.03	5.16±0.05	3.42±0.30	1.09±0.01
45-50	38.5	1.60±0.03	3.54±0.07	1.33±0.03	5.00±0.06	3.39±0.30	1.12±0.02
50-55	39.0	1.66±0.03	2.87±0.03	1.74±0.05	4.95±0.08	3.43±0.30	1.08±0.01
65-70	42.8	1.36±0.0	1.26±0.02	3.26±0.06	4.54±0.04	3.51±0.35	1.00±0.02
85-90	45.6	1.33±0.04	1.48±0.02	2.80±0.08	4.16±0.09	3.05±0.30	1.05±0.02
105-110	46.0	1.23±0.02	3.47±0.07	1.06±0.03	4.62±0.04	2.70±0.30	1.09±0.02
130-125	45.0	1.27±0.03	2.27±0.03	1.68±0.05	4.18±0.07	2.70±0.35	1.10±0.02
140-145	41.4	1.56±0.03	1.58±0.02	3.00±0.06	3.74±0.06	2.35±0.52	1.05±0.02

1 Errors are given as one sigmas

2 Total ^{230}Th

3 ^{230}Th excess calculated on bulk samples

Table 3.5

Data of U-Th[1] Isotopes in Core SK-20-186

Depth interval (cm)	$CaCO_3$ (%)	^{238}U (dpm/gm)	^{232}Th (dpm/gm)	Th/U (weight ratio)	^{230}Th[2] (dpm/gm)	^{230}Th excess[3] (dpm/gm)	$\frac{^{230}Th}{^{232}Th}$[4] (AR)
0-1	88.0	0.22±0.01	0.29±0.02	3.95±0.30	9.10±0.10	8.90±0.89	30.60±3.70
1-2	88.0	0.23±0.01	0.33±0.02	4.30±0.30	10.83±0.10	10.60±1.00	32.10±3.80
2-3	87.8	0.16±0.01	0.23±0.02	4.31±0.50	6.83±0.07	6.70±0.50	29.10±3.40
12-13	84.9	0.23±0.01	0.34±0.02	4.43±0.30	9.82±0.10	9.60±0.96	28.20±3.30
21-22	81.8	0.25±0.01	0.44±0.02	5.28±0.30	8.10±0.09	7.90±0.72	17.95±1.80
32-33	83.7	0.20±0.01	0.47±0.02	7.05±0.50	7.30±0.07	7.10±0.50	15.10±1.20
50-52	84.5	0.25±0.01	0.46±0.02	5.52±0.30	5.26±0.08	5.00±0.40	10.80±0.95
72-77	84.2	0.25±0.01	0.43±0.02	5.16±0.30	4.27±0.05	4.00±0.20	9.30±0.70
87-92	79.6	0.34±0.02	0.53±0.02	4.68±0.30	3.80±0.04	3.50±0.15	6.60±0.40
142-147	84.9	0.30±0.02	0.39±0.02	3.90±0.30	1.60±0.04	1.37±0.06	3.50±0.23

1 On bulk samples (errors are given as one sigmas).

2 Total ^{230}Th.

3 ^{230}Th excess, calculated after correcting for uranium-supported ^{230}Th.

4 AR denotes activity ratio.

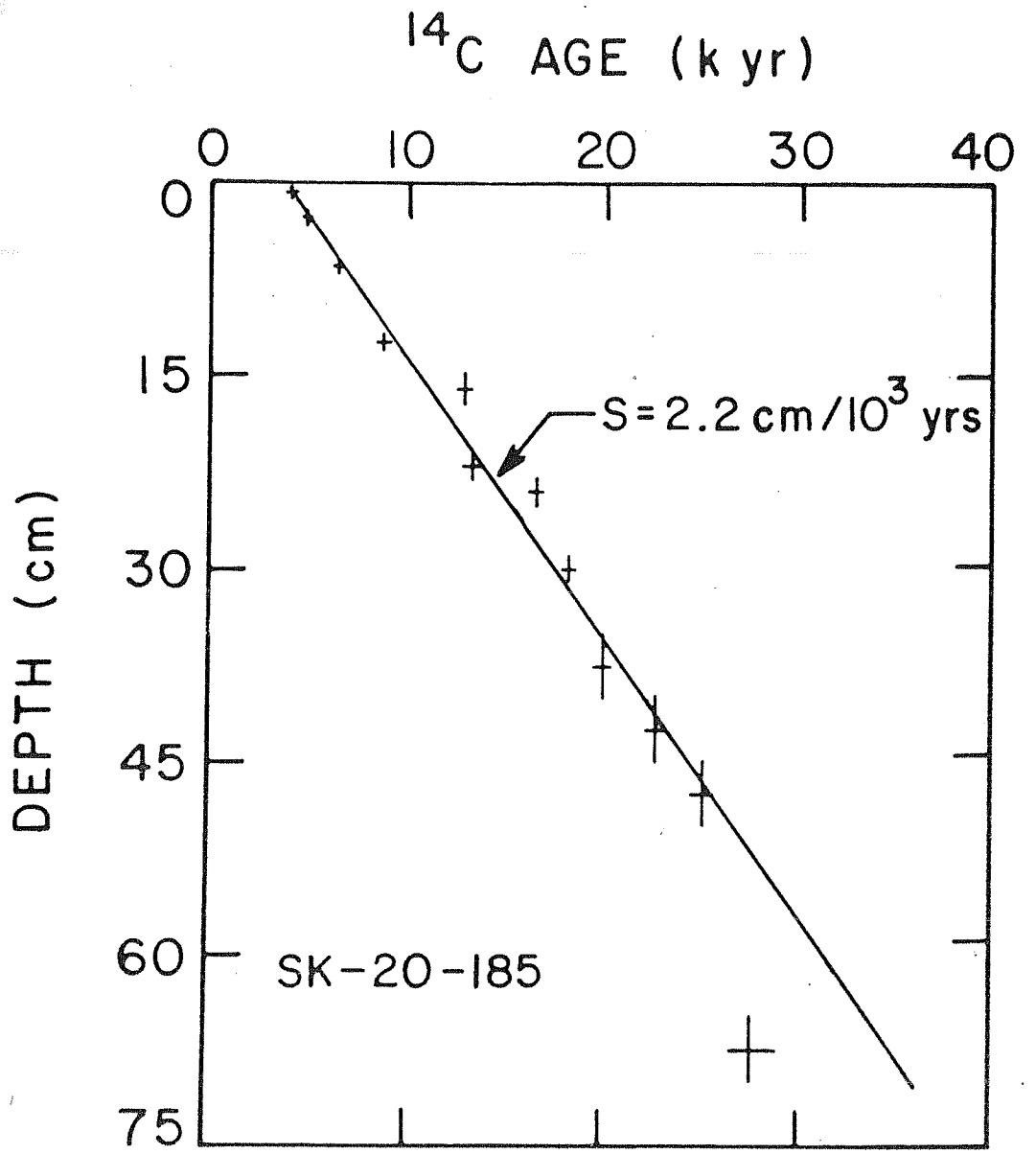

Fig. 3.1 : ^{14}C ages with depth in core SK-20-185. Sedimentation rate (S) is obtained by drawing the best fit line through the data sets (S = 2.2 ± 0.1 cm/kyr)

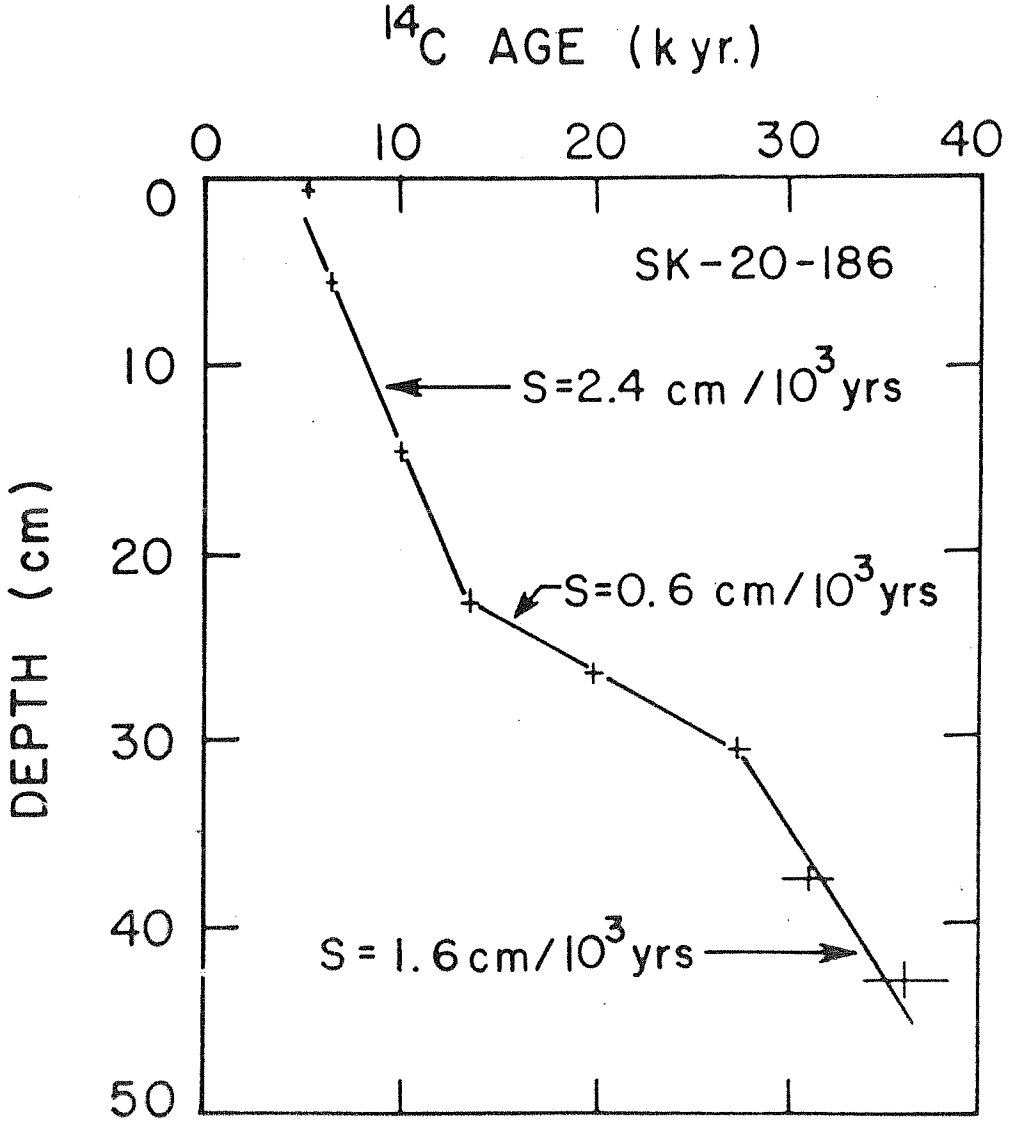

Fig. 3.2 : ^{14}C ages with depth in core SK-20-186. Note the breaks in sedimentation rate (S = 2.4 ± 0.1, 0.6 ± 0.1, 1.6 ± 0.4 cm/kyr)

against bioturbation/particle mixing as a cause for the older surface ages.The only other explanation for the older ages would be to hypothesise that some part of the core top was indeed lost during retrieval as mentioned before.

In core SK-20-185,various fractions of sediments namely bulk, > 63 μm and < 63 μm fractions have been dated by radiocarbon method, the significance of which will be discussed later. In core SK-20-186 only bulk sediment was dated. For the sake of uniformity,in all cases only bulk ^{14}C ages have been used to calculate sedimentation rates. However, the data in Table 3.1 indicate that bulk ages and coarse fraction ages are nearly the same in the core SK-20-185. Both these cores are foraminiferal oozes and hence ^{14}C ages should approximate the true ages of the sediments. This is corroborated when accumulation rates based on radiocarbon dates are compared with those obtained by $\delta^{18}O$ stratigraphy. For all stage boundaries in $\delta^{18}O$ stratigraphies (see next section),SPECMAP dates have been plotted against depth. For the core SK-20-185,this method yields an accumulation rate ~ 2 cm/kyr for the past 120 kyr (Fig. 3.3) and for the core SK-20-186, an average sedimentation rate of 1.1 cm/kyr is obtained for the past 400 kyr (Fig. 3.4).The best fit lines in both the figures do not pass through the origin,indicating that this method gives the average sedimentation rates over a long time period but not the rates over past few kyrs.Though in the core SK-20-185, $\delta^{18}O$ based rate and ^{14}C rate agree fairly well (2 cm/kyr against 2.2 cm/kyr),in the core SK-20-186,

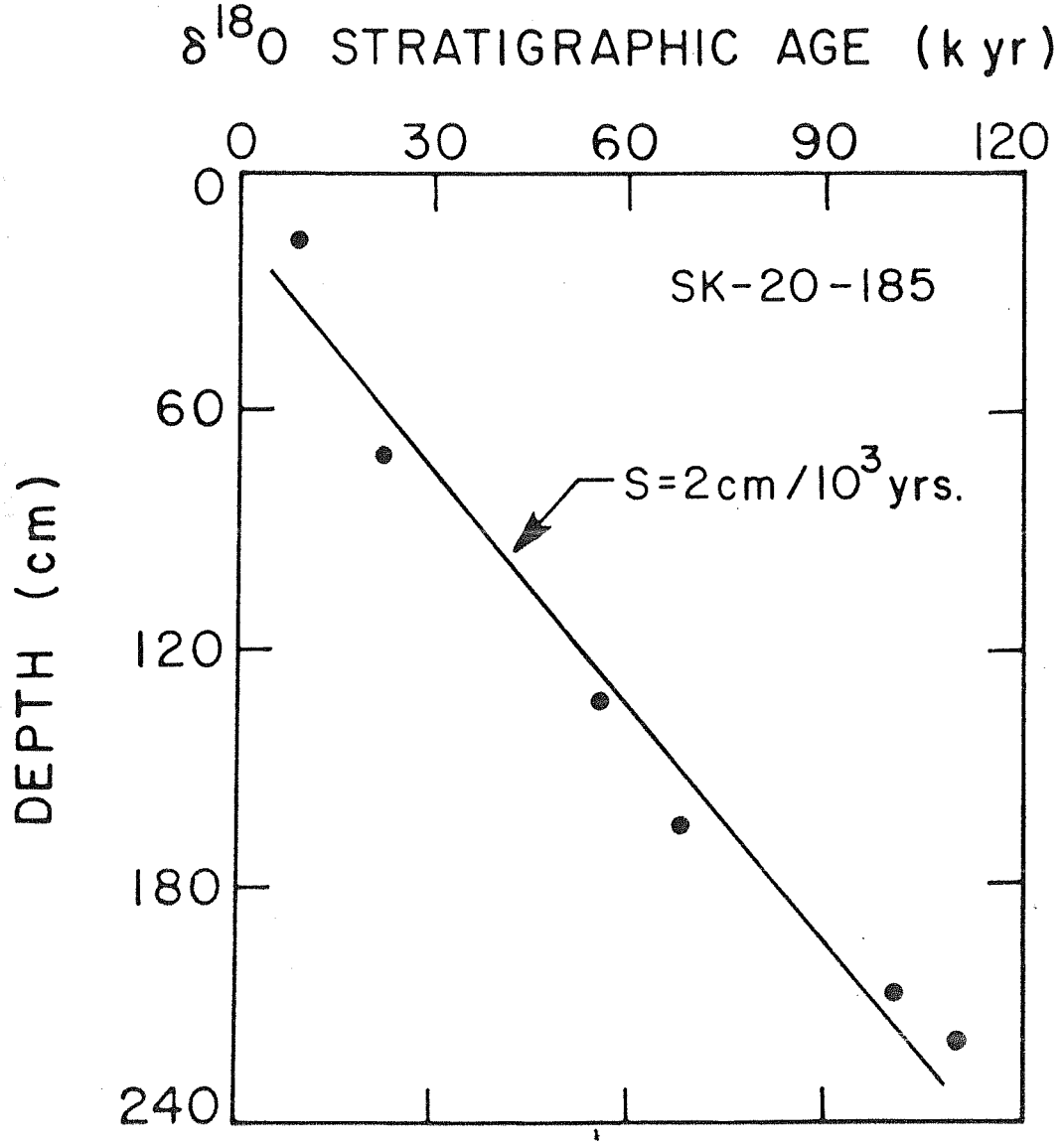

Fig. 3.3 : Sedimentation rate based on the ages of $\delta^{18}O$ stage boundaries at different depths for core SK-20-185

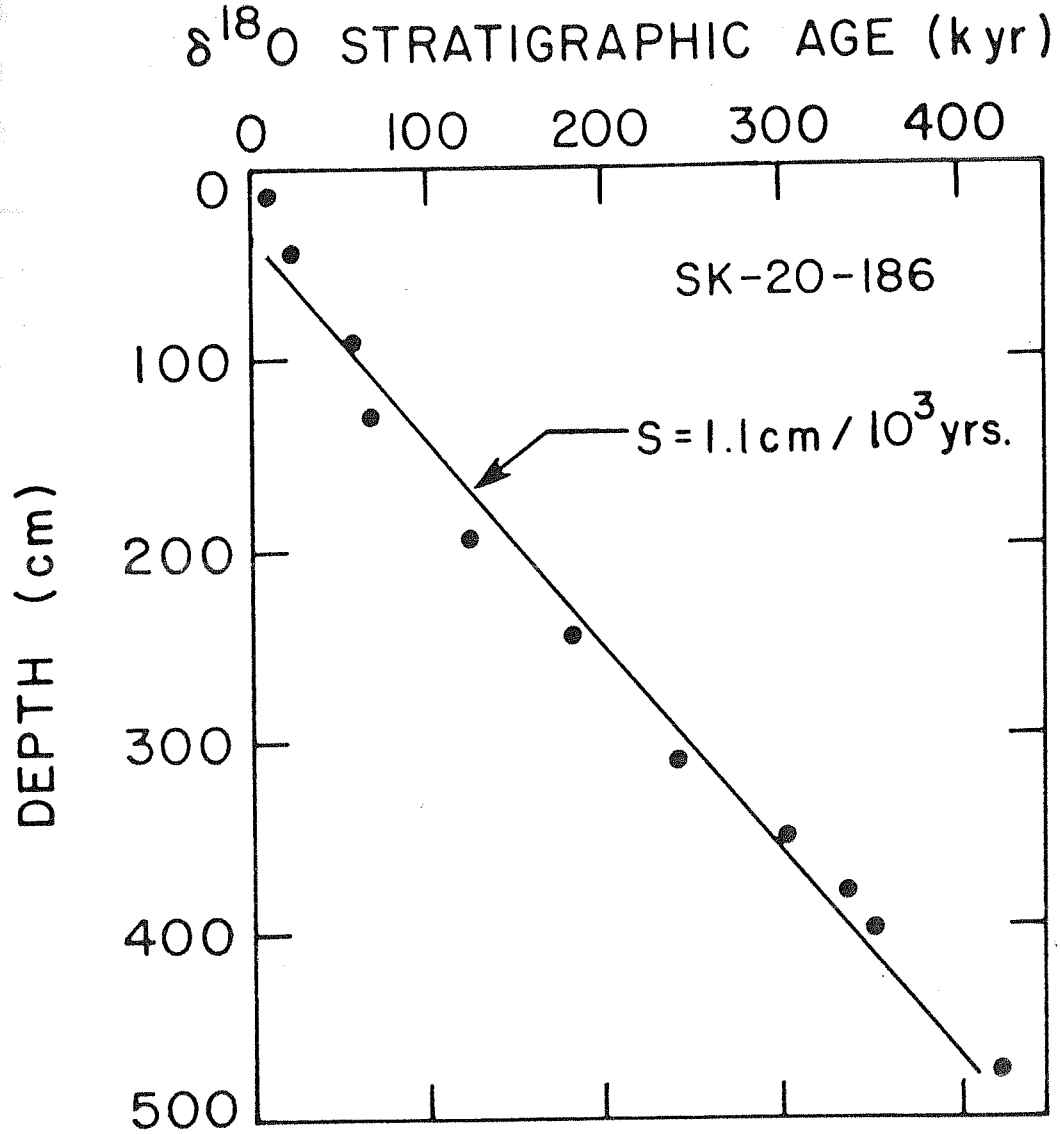

Fig. 3.4 : Sedimentation rate based on the ages of $\delta^{18}O$ stage boundaries at different depths for core SK-20-186

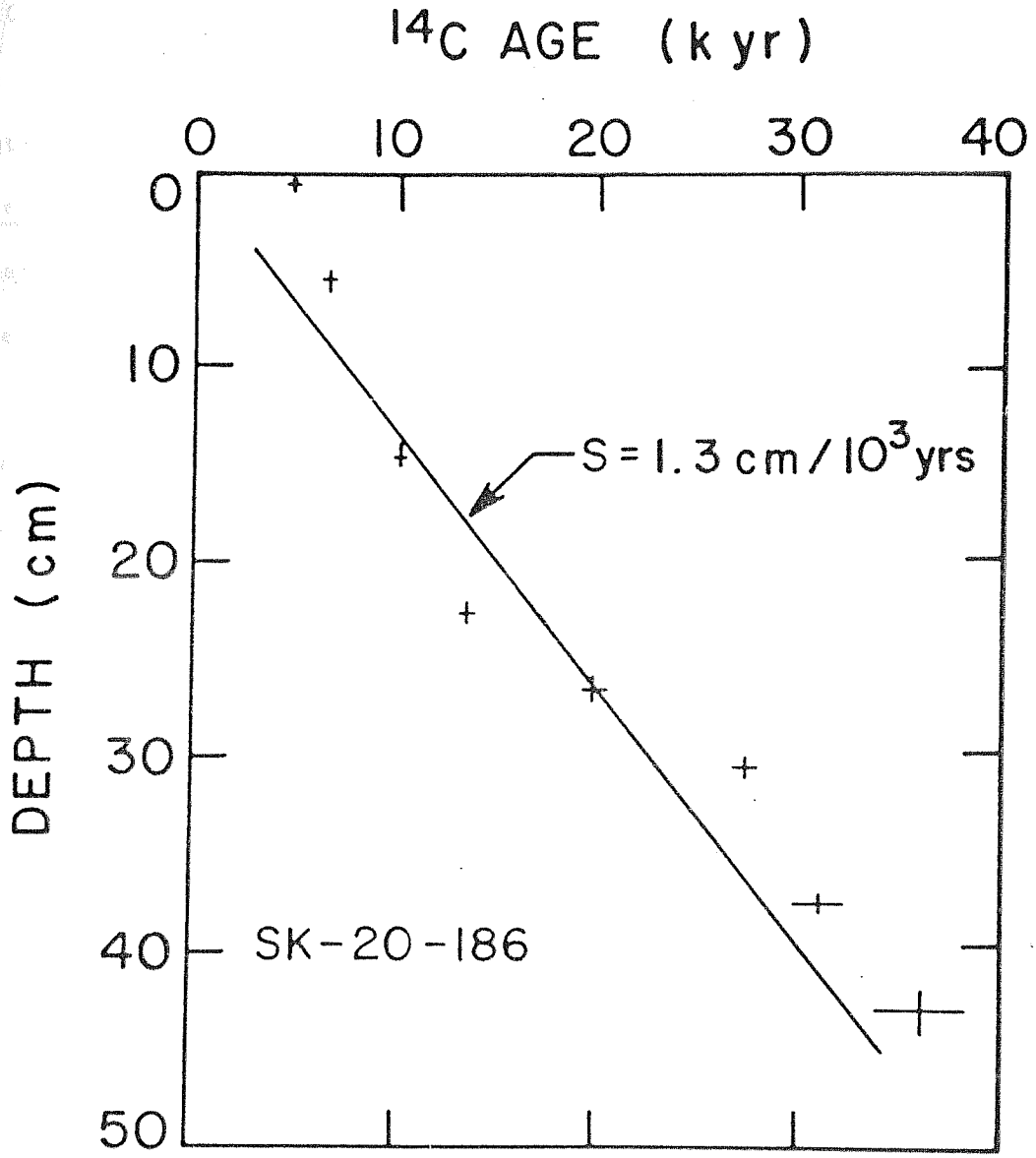

Fig. 3.5 : ^{14}C ages with depth in core SK-20-186. The gross sedimentation rate has been calculated by drawing a best fit line through all the data points, neglecting the breaks (S = 1.3 ± 0.1 cm/kyr)

$\delta^{18}O$ based sedimentation rate yields a lower value than that obtained by ^{14}C in the upper part (1.1 cm/kyr against 2.4 cm/kyr). But if a best fit line is drawn through all the ^{14}C data points, neglecting the breaks (Fig. 3.5), it gives an accumulation rate of 1.3 ± 0.1 cm/kyr, similar to that obtained by the $\delta^{18}O$ method. However, it is recognized that the sedimentation rates based on $\delta^{18}O$ chronology give average rates over past several hundred thousand years; whereas the ^{14}C rates are for the past ~ 35 kyr, the limit of conventional radiocarbon method. The similarity in accumulation rates between ^{14}C and $\delta^{18}O$ methods is an indication that in these cores average sediment accumulation rates have probably remained same over the past ~ 400 kyr.

The radiocarbon dates have been obtained for four different sections of core CD-17-30. ^{14}C dates against depth for this core are plotted in Fig. 3.6. The best fit line gives a sedimentation rate of 7.7 ± 0.6 cm/kyr. This rate is a factor of three higher than those of SK-20-185 and SK-20-186. Core CD-17-30 comes from the western Arabian sea. The high sedimentation rate can be interpreted in terms of higher productivity associated with the monsoonal upwelling in this area.

III.1.2. Determination of Accumulation Rates based on ^{230}Th (Excess) Method

To determine the sedimentation rate radiometrically beyond the limit by ^{14}C method (~ 35 kyr) another method

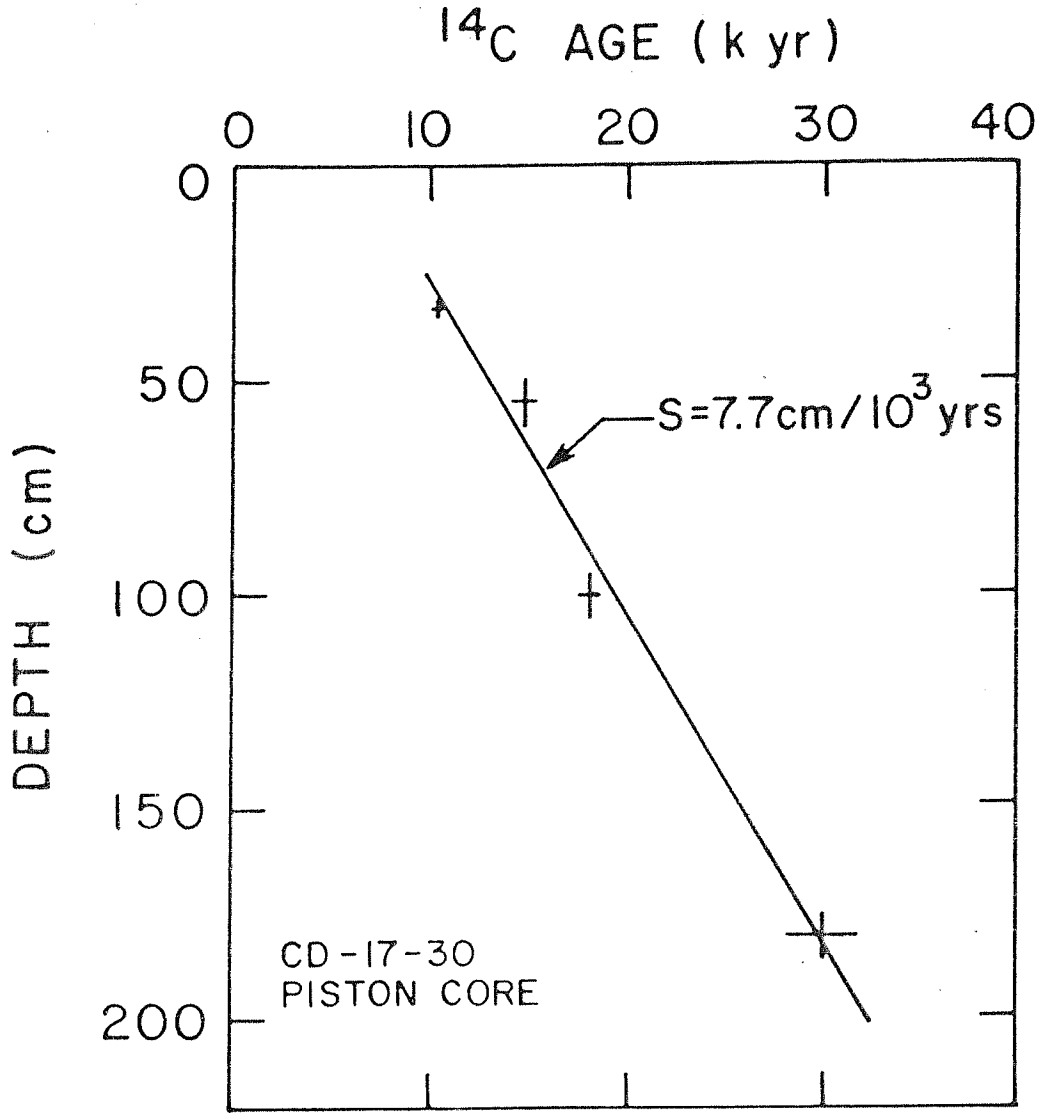

Fig. 3.6 : ^{14}C ages with depth in core CD-17-30. Note a high sedimentation rate compared to other cores. (S = 7.7 ± 0.6 cm/kyr)

namely ^{230}Th (excess) has been used.Similar to the oxygen isotope stratigraphy, the ^{230}Th(excess) method provides data on average sedimentation rate for the past ~ 300 kyr. ^{230}Th is a radioactive isotope,produced by the decay of ^{234}U present in the ocean.Being particle reactive,^{230}Th is removed from sea water to sediments on time scales of a few tens of years.If the flux of ^{230}Th to sediment surface has remained constant over the dating interval (~ 300 kyr),then its activity would show an exponential decrease with depth (time) provided ^{230}Th has not migrated in the sediments i.e. the change in the ^{230}Th concentration with depth in the sediment is only due to its radioactive decay.The half life of ^{230}Th is 7.52×10^4 years and hence it can be used to determine the chronology of sediments deposited upto 300 kyr (Goldberg and Koide 1962). In addition to its contribution from sea water, ^{230}Th in sediments can also come from other sources, such as the radioactive decay of ^{234}U contained in them. ^{234}U in sediments arise from ^{238}U inherited by them from their parent rocks/soils (commonly termed as detrital uranium) and ^{238}U precipitated/removed from sea water (termed as authigenic uranium).The ^{230}Th produced by these uranium sources (termed as ^{230}Th supported) in the sediment ought to be accounted for,in order to derive sedimentation rates based on ^{230}Th excess method. The detrital uranium component typically would have $^{234}U/^{238}U$ activity ratio (AR) 0.95 - 1.00.The $^{234}U/^{238}U$ AR of authigenic uranium derived from sea water would have a value 1.14 $\pm$ 0.01 same as the activity ratio of the sea

water. Therefore, the $^{234}U/^{238}U$ AR can serve as a tool to determine the source of uranium contained in the sediment. Along with ^{238}U, detrital phases entering the oceans also bring finite amount of ^{232}Th. This isotope has a long half-life $1.4x10^{10}$ years and is brought to oceans primarily on particulate phases.In addition to ^{230}Th excess discussed above, the ^{230}Th (excess)/^{232}Th ratio is also used to determine the sedimentation rate of deep sea cores.

Criteria for identifying detrital and authigenic component of ^{238}U in sediments

Eventhough ^{232}Th and ^{238}U concentrations in crustal materials vary, the Th/U weight ratio centre around ~ 4 (Faure 1986). Hence, a sediment made primarily of detrital materials should have a Th/U ratio close to 4. These detrital materials also transport ^{230}Th,at levels close to that in radioactive equilibrium with ^{238}U.Therefore,the amount of detrital ^{230}Th in sediments is assumed to be equal to the activity of ^{238}U in them.

In cases, where sediments contain ^{238}U derived from sea water, over and above the detrital component,the Th/U ratios will be lower than that of the crustal value.In this case, ^{230}Th excess should be calculated by subtracting the contributions from both detrital and authigenic ^{238}U.Below, we compute the sedimentation rate for the cores SK-20-186 and SK-20-185 after making appropriate corrections for supported ^{230}Th.

Core SK-20-186

The data for total ^{230}Th, ^{232}Th, ^{238}U and ^{230}Th excess for various depths are given in Table 3.5.Also given are ^{230}Th (excess)/^{232}Th activity ratio and Th/U weight ratio. It is seen that ^{238}U concentration is quite small (~ 0.24 $\pm$ 0.05 dpm/gm) and approximately constant throughout the core. From these data the average Th/U ratio of the levels is calculated to be 4.9 $\pm$ 0.9 which is close to the crustal value. As can be seen at all depths the Th/U ratio is close to this value within experimental errors.Hence we can infer that the entire ^{238}U in this core is of detrital origin. Consequently the ^{230}Th excess in this core has been computed, after correcting for ^{230}Th detrital contribution by assuming its activity to be equal to that of ^{238}U.Plots of ^{230}Th(excess) and ^{230}Th(excess)/^{232}Th activity ratio against depth are shown in Fig. 3.7. ^{230}Th(excess) is plotted on a $CaCO_3$ free basis.Regression analysis of the data for the depth interval 12 to 147 cm yields a sedimentation rate of 0.6 $\pm$ 0.1 cm/kyr for ^{230}Th (excess) (Fig. 3.7a) which is close to that obtained from activity ratio of ^{230}Th(excess)/^{232}Th i.e. 0.7 $\pm$ 0.1 cm/kyr (Fig. 3.7b). Since $CaCO_3$% in this core does not vary much,bulk ^{230}Th excess rate is also same as that obtained on $CaCO_3$ free basis i.e. 0.6 $\pm$ 0.1 cm/kyr.The concentrations of ^{230}Th excess and ^{230}Th excess/^{232}Th activity ratio in the top four sections (0-1),(1-2),(2-3) and (12-13) are quite similar.^{230}Th scatter around a value of ~ 9 dpm/gm, a result which can arise either due to bioturbation/particle mixing

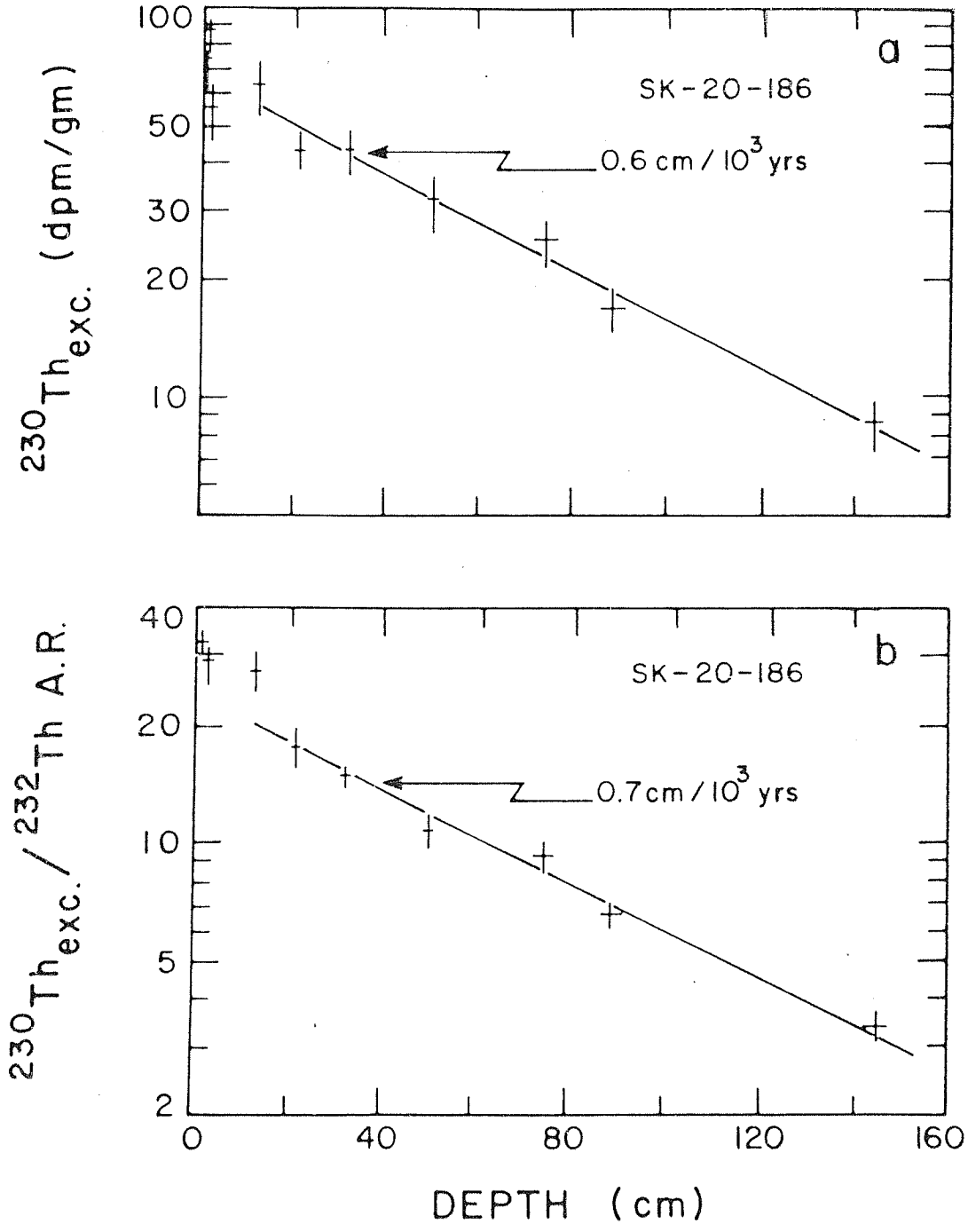

Fig. 3.7 : Variations of ^{230}Th excess (a) and ^{230}Th (excess)/^{232}Th activity ratio (b) with depth in SK-20-186. Best fit lines yield lower sedimentation rate than ^{14}C i.e. 0.6 ± 0.1 and 0.7 ± 0.1 cm/kyr.

or rapid sedimentation.The sedimentation rate based on ^{14}C for the top 22.5 cm core length is (2.4 $\pm$ 0.1) cm/kyr.For such a high sedimentation rate, ^{230}Th excess is not expected to show a measurable decay in these top sections,consistent with our observations. The ^{230}Th based accumulation rates, 0.6 - 0.7 cm/kyr for this depth interval i.e. 12 to 147 cm is about 50% lower than the ^{14}C based rate of 1.0 $\pm$ 0.05 cm/kyr for the depth interval 14 to 44 cm.

Core SK-20-185

The U-Th isotope data for this core are given in Table 3.4. The Th/U weight ratio in these samples scatters considerably and at many depths it is as low as ~ 1.The core sections with low Th/U ratio also have high ^{238}U with $^{234}U/^{238}U$ activity ratio of ~ 1.14,close to sea water value. This indicates the presence of authigenic uranium at several layers of cores SK-20-185.Presence of authigenic uranium in the coastal Arabian sea sediments was reported earlier (Borole et al.,1982b).

This authigenic uranium would also give rise to some ^{230}Th, in addition to its supply from uranium in the detrital phases. Consequently, the ^{230}Th (excess) has been computed by correcting for its contribution from both detrital and authigenic uranium. This has been done as follows:

The top 5 sections viz. (0-1),(1-2),(2-3),(15-17) and (29-31) cm all have similar Th/U ratios which are close to the crustal value.The average value of Th/U ratio in these

levels is 4.32 ± 0.35. The ^{230}Th excess concentrations at these levels have been calculated by assuming that all ^{238}U is of detrital origin. In the layers below (29-31) cm where Th/U ratios are much lower than the crustal value, detrital uranium activity (U_D) has been calculated using the following relation:

$$U_D = \frac{^{232}Th}{4.32 \pm 0.35} \times 3$$

The measured ^{232}Th concentration in each level was used to calculate U_D.

The authigenic uranium activity (dpm/g) (U_A) was calculated by subtracting U_D from total uranium U_T, i.e. $U_A = U_T - U_D$. Both the uranium phases (U_D and U_A) would contribute to ^{230}Th. The U_D supported ^{230}Th activity is equal to U_D. Since U_A is deposited with $^{234}U/^{238}U$ ratio ~ 1.14, the ^{230}Th grown from authigenic uranium (U_A) has been calculated using the following relation (Ivanovich and Harmon 1982):

$$^{230}Th = {}^{238}U_A \left[\left(e^{-\lambda_{238} t} - e^{-\lambda_{230} t} \right) + \frac{\lambda_{230}}{\lambda_{230} - \lambda_{234}} \left(e^{-\lambda_{234} t} - e^{-\lambda_{230} t} \right) \times 0.14 \right]$$

where $^{238}U_A$ = activity of authigenic uranium

λ = Decay constant

t = Age of sediment sections calculated based on ^{14}C sedimentation rate (2.2 cm/10^3 yrs) and sampling depth.

The supported ^{230}Th (grown from detrital and authigenic

phases) was subtracted from the measured ^{230}Th, to get ^{230}Th(excess).

Fig. 3.8a gives the plot of ^{230}Th(excess) concentration (on a $CaCO_3$ free basis) against depth.In the top 3 layers i.e. upto (2-3) cm the ^{230}Th(excess) is nearly the same and considerably higher than the values at (15-17) and (29-31) cm. The data in this depth range (0-31) cm indicate a very slow accumulation rate. Thereafter, the activity of ^{230}Th(excess) changes gradually with depth,indicating that an apparent break in sedimentation rate may be considered at (29-31) cm depth. However, ^{14}C based rate does not show any such change (Fig. 3.1) at this depth.The best fit line through all the data points (below 15-17 cm) yields a sedimentation rate 3.4 $\pm$ 1.3 cm/kyr. Fig. 3.8b shows the plot of ^{230}Th(excess) concentration in bulk sediments against depth. Here too top 4 levels were not taken for calculating the rate. The best fit line gives an accumulation rate 2.5 $\pm$ 0.5 cm/kyr.It is to be noted that the scatter in the plot 3.8a is higher than the 3.8b.

III.1.3. Intercomparison of Sedimentation Rates Calculated by Different Methods

The sedimentation rates of cores SK-20-185 and SK-20-186 by three different methods are given below:

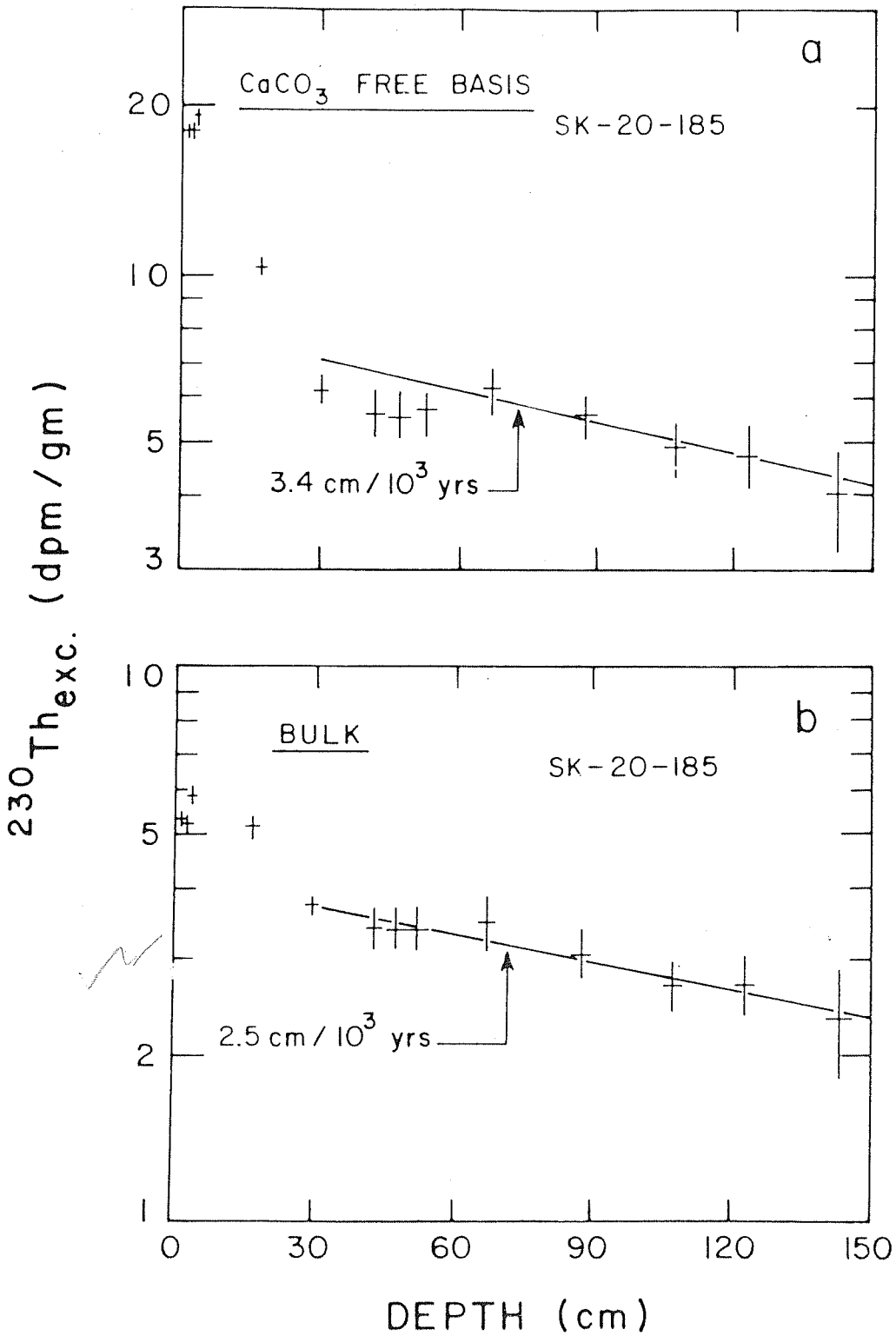

Fig. 3.8 : Variation of ^{230}Th excess with depth in SK-20-185.

a) On $CaCO_3$ free basis (S = 3.4 ± 1.3 cm/kyr)

b) On bulk sediments (S = 2.5 ± 0.5 cm/kyr)

Method	SK-20-185 Depth Interval(cm)	SK-20-185 Rate(S) cm/kyr	SK-20-186 Depth Interval(cm)	SK-20-186 Rate(S) cm/kyr
^{14}C	0-70	2.2±0.1	0-44	1.3±0.1 (gross)
^{230}Th excess (bulk)	29-145	2.5±0.5	12-147	0.6±0.1
^{230}Th excess ($CaCO_3$ free basis)	29-145	3.4±1.3	12-147	0.6±0.1
$\delta^{18}O$ stratigraphy	0-290	2.0	0-487	1.1

In core SK-20-185, the sediment accumulation rate based on all the three methods are in reasonable agreement with each other. The ^{14}C and $\delta^{18}O$ methods show a better agreement with each other. The ^{230}Th excess method yields a slightly higher sedimentation rate, however, the associated errors are large and hence the derived rates are probably compatible with those derived from ^{14}C and $\delta^{18}O$. In core SK-20-186, similar to that in SK-20-185, the ^{14}C and $\delta^{18}O$ methods yield results which are in close agrement. The ^{230}Th excess method on the other hand yields an accumulation rate, ~ 50% lower than that based on ^{14}C. It is not clear why in both these cores the ^{230}Th derived sedimentation rates are slightly at variance with those derived from ^{14}C and $\delta^{18}O$. Nevertheless, the sedimentation rates of each of these cores by all the methods yield values which are within ± 50% of each other. For climatic interpretation, however, ^{14}C based rates are used.

In addition to sediment accumulation rate, the ^{230}Th

excess data also provides information on the focussing/erosion of sediments for a given core site. These can be done by comparing the observed ^{230}Th excess flux at site with that expected from its production in the overlying water column. The flux of ^{230}Th precipitation is given by the following relation (Cochran and Osmond, 1976):

$$F_p = DCR\ \lambda_{230}\ \frac{A_{234}}{A_{238}}$$

where F_p = ^{230}Th production rate (dpm/cm^2/10^3 yrs)

D = water depth in cm

C = uranium concentration in sea water = 3.3 μg/l

R = uranium mass activity conversion factor

= 7.42 x 10^5 dpm ^{238}U/gm

λ_{230} = Decay constant of ^{230}Th = 9.2x10^{-3}/(10^3 yrs)

$\frac{A_{234}}{A_{238}}$ = Activity ratio of $^{234}U/^{238}U$ in sea water

= 1.14

Substituting the constant gives,

$$F_p = 2.6D$$

where D is water depth in km.

In a steady state condition, all ^{230}Th produced in water column should be deposited in the sediment and the accumulation rate of ^{230}Th in sediments can be calculated from the following relation:

$$F_a = A_o S \rho$$

where F_a is predicted ^{230}Th excess accumulating on surface sediment,

A_o is the concentration of ^{230}Th excess observed on surface sediment

S is the sedimentation rate, and

ρ is the in situ density of sediment.

In cores SK-20-185 and SK-20-186, the recent deposition flux of ^{230}Th has been calculated based on measured ^{230}Th excess concentrations and ^{14}C based (Holocene) sediment accumulation rates.

Calculated F_p and observed F_a values for these two cores are given below:

	SK-20-185	SK-20-186
Depth interval (cm)	0-1	0-1
S (cm/kyr)	2.2	2.4
A_o (dpm/gm)	5.34(bulk)	8.9(bulk)
$CaCO_3$(%)	67.5	88.0
F_p(dpm cm^{-2} kyr^{-1})	6.5	9.1
F_a(dpm cm^{-2} kyr^{-1})	8.22	14.95

For both the cores, F_a was calculated on the basis of ^{230}Th concentration in surface sediments i.e. (0-1) cm depth. In core SK-20-185, the ^{230}Th accumulation is close to that calculated for a standing crop of ^{230}Th in the overlying water column. In core SK-20-186, however, ^{230}Th accumulation is higher than the calculated F_p value. But, calculation of F_a based on the gross sedimentation rate

(i.e. 1.3 cm/kyr) gives a value of 8.1 dpm cm^{-1} kyr^{-1}, which is close to the calculated F_p value. This indicates that during the Holocene the ^{230}Th flux is higher, either due to bottom focussing of clay particles or due to the scavenging of ^{230}Th even by the $CaCO_3$ particles at the site of core SK-20-186.

III.2. Oxygen Isotope Studies of the Ocean Cores

The oxygen isotope data obtained on the five sediment cores from the Arabian sea and the equatorial Indian Ocean are presented in this section. An attempt is made to intercompare the results from these cores and to derive palaeoclimatic information from them. The $\delta^{18}O$ data are given in Table 3.6 to Table 3.13. For the sake of convenience $\delta^{13}C$ data are also given in these tables but their implications are discussed in a later section. Before we discuss the isotopic data for palaeoclimatic interpretatons, it is important to delineate the nature of intrasample variability and the ways to overcome it.

III.2.1. Sample Variability and Reliability of Isotopic Data as Climatic Indicators

In Chapter II, it has been shown that in the present work, a typical experimental precision of $\pm$ 0.1 °/oo has been achieved. However, in natural samples of oceanic sediments, foraminifera often show a variability in $\delta^{18}O$ and $\delta^{13}C$ much greater than that resulting from the experimental errors. In the initial phase of this work, only 5-6

individuals per aliquot were analysed from a relatively large size fraction i.e. > 400 μ m. The intrasample variability for both $\delta^{18}O$ and $\delta^{13}C$ obtained from the analysis of few individuals was as high as 1 °/oo.This is clearly undesirable, particularly when the climatic signal is only ~ 2 °/oo in deep sea cores.

As a first approximation, when one considers only two sources of error viz. analytical precision and intrasample variability, the total variance associated with these errors can be expressed as:

$$\sigma^2 = \sigma_m^2 + \frac{\sigma_i^2}{n} \qquad \text{(Killingley et al 1981)}$$

where σ_m^2 is variance contributed by mass-spectrometer and σ_i^2 is variance contributed by the individual shells of foraminifera. When σ_m = 0.1 °/oo, σ = 0.25 °/oo (taking 1 °/oo spread as 2σ),and n=5 (since 5 shells/aliquot were analysed), σ_i = 0.5 °/oo i.e. about 2 °/oo spread (at 2σ level) in δ-values can be obtained in core SK-20-185,if single shells of foraminifera are analysed.Causes of such intraspecific variability are not very clear, though sediment mixing by bioturbation, seasonal changes in the water column properties,depth stratification and metabolic effects have been proposed for such variations (Fairbanks et al. 1982, Williams et al. 1979;Killingley et al. 1981). While it is difficult to delineate the actual mechanism of such variability, in practice it is overcome by analysing a large number of individuals of a foraminiferal population

(Killingley et al. 1981; N.J. Shackleton, personal communication,30.12.1987;W.H. Berger,personal communication, 14.1.1988).

Consequently in the second phase of the present work, about 30-40 individuals have been picked up for each sample, from narrow size ranges. Analysis of such large number of individuals in a single aliquot, gives a signal which is averaged over wide seasonal and hydrographic variations and the effects of the possible occurrence of discrete individual foraminifera with very different isotopic composition, produced in different environmental conditions are also minimised. Table 3.6 gives the results of such analyses (replicates) for several depths in core SK-20-185. As can be seen, this reduced the effect of intrasample variability. In the present study,the results of $\delta^{18}O$ and $\delta^{13}C$ used for delineating palaeoenvironmental information are all based on analysis of 30-40 individuals,run at least in duplicates. Mean intrasample variability for 300 such duplicate analyses is about $\pm$ 0.15 $^{o}/_{oo}$ for both $\delta^{18}O$ and $\delta^{13}C$. All the data on various cores presented in later tables are the mean values of duplicates.

Besides choosing a large number of individuals for analysis it is also important to pick up shells of a given size since isotopic composition is different for different size fractions (Berger et al. 1978b).Such differences arise due to the vertical migration of foraminifera through the water column during the ontogenic development.Since the physico-chemical properties of sea water change

Table 3.6

Oxygen and Carbon Isotope Data[#] on Core SK-20-185

Depth (cm)	$\delta^{18}O_{PDB}$ [*] (‰)	$\delta^{13}C_{PDB}$ [*] (‰)	$\Delta^{18}O$ [+]	$\Delta^{13}C$ [+]
2.5	-1.23,-1.44	1.75,1.74	0.21	0.01
4.5	-1.65,-1.78	1.8,1.72	0.13	0.08
8.5	-1.38,-1.43	1.58,1.48	0.05	0.10
10.5	-1.23,-1.24,-1.03,-1.03	1.33,1.44,1.49,1.41	0.21	0.16
12.5	-0.75,-0.44	1.47,1.52	0.31	0.05
16.0	-0.49,-0.43	1.0,1.1	0.06	0.10
20.0	-0.11,-0.21	1.42,1.29	0.10	0.13
26.0	0.29,0.23,0.24,0.17	1.51,1.41,1.44,1.37	0.12	0.14
52.5	0.47,0.33	1.94,1.9	0.14	0.04
67.5	-0.05,0.01	1.83,1.84	0.06	0.01
92.5	-0.28,-0.17	1.52,1.54	0.11	0.02
137.5	-0.12,-0.16	1.55,1.54	0.04	0.01
157.5	-0.15, -0.09	1.4, 1.52	0.06	0.12
200.0	-0.74,-0.86	1.6, 1.65	0.12	0.05

Measured on G.sacculifer, 30-40 individuals (250-400 μm) per aliquot.

* Values of replicate measurements are given.

+ $\Delta^{18}O$ and $\Delta^{13}C$ are the differences between two extreme values at each level.

significantly within the upper few hundred metres, vertical migration of foraminifera results in the secretion of their tests in different temperature conditions. Consequently different size fractions representing various stages of ontogenic development can yield different isotopic values. Alternatively, disequilibrium fractionation can give rise to such differences, as mentioned in the first chapter. Emiliani (1954) first studied the relationship between various size fractions and isotopic composition. He showed that apart from Orbulina universa, no other species had any appreciable difference between different size fractions. Subsequent studies showed that, in general, larger size fractions are enriched in $\delta^{18}O$ and $\delta^{13}C$ (Emiliani 1971; Berger et al. 1978b). In the present study, two different size fractions viz. > 400 μm and 250-400 μm of G. sacculifer have been analysed for the entire length of core SK-20-185. Relative difference of these two fractions are shown in Table 3.7. The $\delta^{18}O$ values of these two fractions from different levels are plotted in Fig. 3.8c. All the points should fall on the 45° line in case there is no difference in $\delta^{18}O$. But the best fit line through the data points indicates that the larger (> 400 μm) fraction is depleted in $\delta^{18}O$ by about ~ 0.5 °/oo compared to the smaller fractions (250-500 μm). Fig. 3.8d shows the plot of $\delta^{13}C$ in > 400 μm against (250-400) μm fraction. Though no significant trend is observed, by and large, in most of the levels $\delta^{13}C$ in > 400 μm fraction is enriched compared to the (250-400) μm fraction. This observation is in contradiction with that of

Table 3.7

Oxygen# and Carbon# Isotope Data* on Core SK-20-185

Depth (cm)	> 400 μm		(250-400) μm		$\Delta^{18}O^{+}$	$\Delta^{13}C^{+}$
	$\delta^{18}O$ PDB (‰)	$\delta^{13}C$ PDB (‰)	$\delta^{18}O$ PDB (‰)	$\delta^{13}C$ PDB (‰)		
2.5	-2.22	1.13	-1.34	1.74	-0.88	-0.61
10.5	-1.75	1.77	-1.17	1.42	-0.58	0.35
12.5	-1.3	1.93	-0.6	1.5	-0.70	0.43
18.0	-1.12	1.41	-0.16	1.5	-0.96	-0.09
22.0	-0.87	1.75	-0.09	1.48	-0.78	0.27
24.0	0.41	2.13	0.08	1.49	0.33	0.64
26.0	-0.31	1.68	0.23	1.40	-0.08	0.28
28.0	-0.75	1.89	-0.14	1.54	-0.61	0.25
30.0	-1.09	1.74	-0.30	1.36	-0.79	0.38
32.0	-1.55	2.22	-0.97	1.66	-0.58	0.56
34.0	-0.58	1.57	-0.88	1.62	0.30	-0.05
37.5	-0.46	1.66	0.34	1.54	-0.80	0.12
42.5	-0.21	1.88	0.26	1.73	-0.47	0.15
47.5	-0.21	1.77	0.26	1.65	-0.47	0.12
52.5	0.34	2.25	0.40	1.92	-0.06	0.33
57.5	-0.12	2.55	0.22	1.88	-0.34	0.67
62.5	-0.79	1.83	0.11	1.83	-0.90	0.0
67.5	-0.40	2.25	-0.02	1.84	-0.38	0.41
72.5	-0.31	2.47	-0.25	1.79	-0.06	0.68
77.5	-0.78	2.08	-0.17	1.69	-0.61	0.39
92.5	-0.54	1.67	-0.23	1.53	-0.31	0.14
97.5	-0.84	1.51	-0.21	1.71	-0.63	-0.2
107.5	-0.75	1.62	-0.21	1.75	-0.54	-0.13
112.5	-0.86	1.38	-0.67	1.5	-0.19	-0.12
122.5	-0.64	1.83	-0.49	1.48	-0.15	0.35
127.5	-0.83	1.65	-0.42	1.52	-0.41	0.13
137.5	-1.13	1.28	-0.14	1.54	-0.99	-0.26
142.5	-0.73	1.67	-0.07	1.49	-0.66	0.18
147.5	-1.12	1.31	0.03	1.65	-1.15	-0.34
152.5	-0.63	1.25	-0.24	1.32	-0.39	-0.07
157.5	-0.82	1.48	-0.12	1.46	-0.70	0.02

Table 3.7 contd.

Depth (cm)	>400 μm		(250-400) μm		$\Delta^{18}O^{+}$	$\Delta^{13}C^{+}$
	$\delta^{18}O$ PDB	$\delta^{13}C$ PDB	$\delta^{18}O$ PDB	$\delta^{13}C$ PDB		
167.5	-0.9	1.71	-0.68	1.50	-0.22	0.21
172.5	-0.92	1.48	-0.34	1.41	-0.58	0.07
182.5	-1.01	1.72	-0.90	1.36	-0.11	0.36
190.0	-1.11	1.58	-0.51	1.53	-0.60	0.05
200.0	-1.44	1.99	-0.80	1.63	-0.64	0.36
210.0	-1.67	1.59	-1.09	1.87	-0.58	-0.28
220.0	-1.06	1.92	-0.60	1.82	-0.46	0.10
230.0	-1.46	1.3	-0.87	1.42	-0.59	-0.12
240.0	-1.15	1.64	-0.89	1.47	-0.26	0.17
250.0	-1.38	1.6	-1.05	1.48	-0.33	0.12
260.0	-1.53	1.89	-1.18	1.76	-0.35	0.13
270.0	-1.67	1.5	-1.10	1.71	-0.57	-0.21
280.0	-1.44	1.65	-1.13	1.45	-0.31	0.20
290.0	-1.3	1.58	-0.84	1.55	-0.46	0.03

In case of replicate analysis, mean values are given.

* Measured on G.sacculifer. 30-40 individuals per aliquot.

+ $\Delta^{18}O$ and $\Delta^{13}C$ are the respective difference between large (>400 μm) and small (250-400 μm) size fractions.

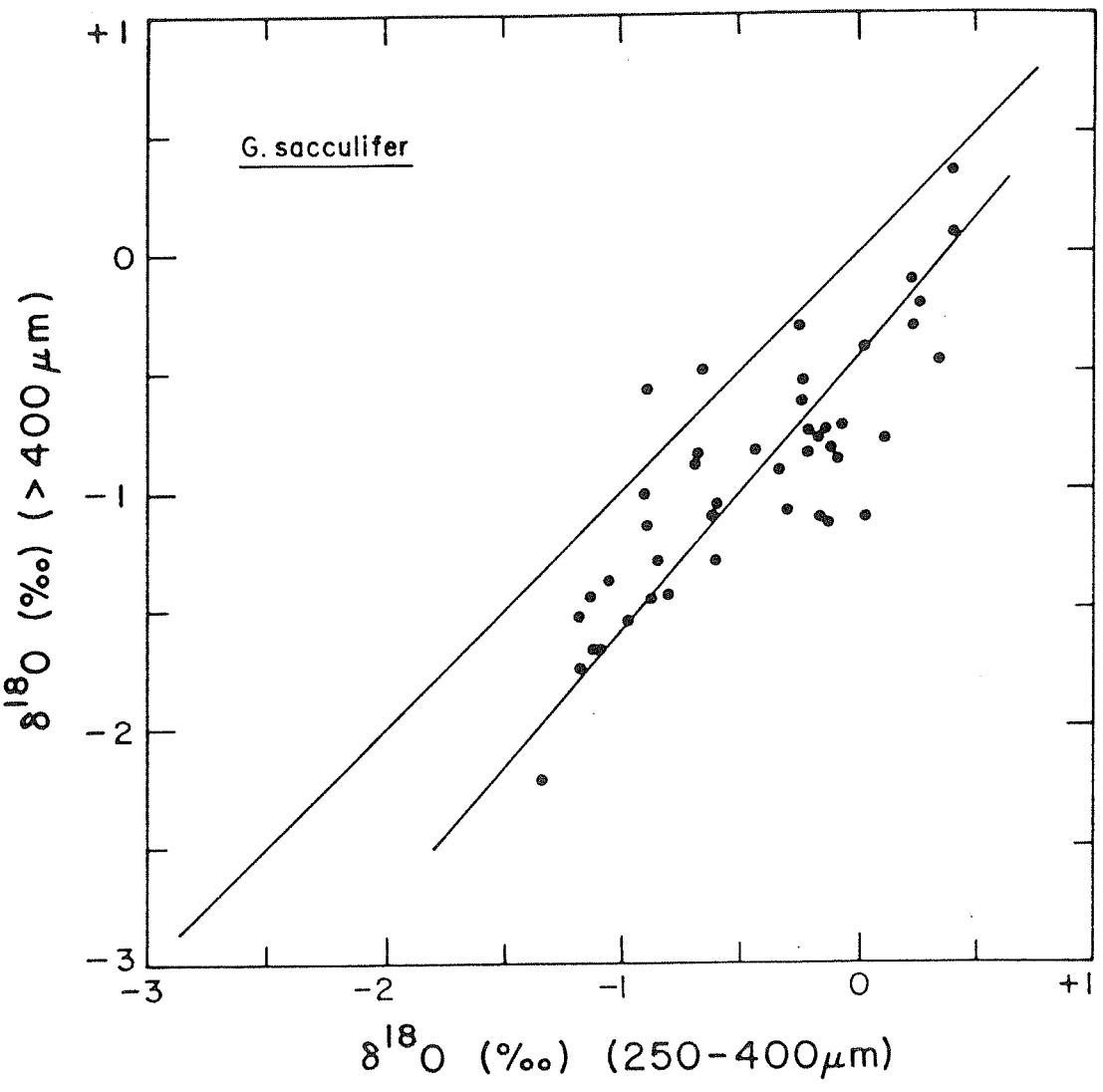

Fig. 3.8c : $\delta^{18}O$ values of two different size fractions of G.sacculifer from SK-20-185.

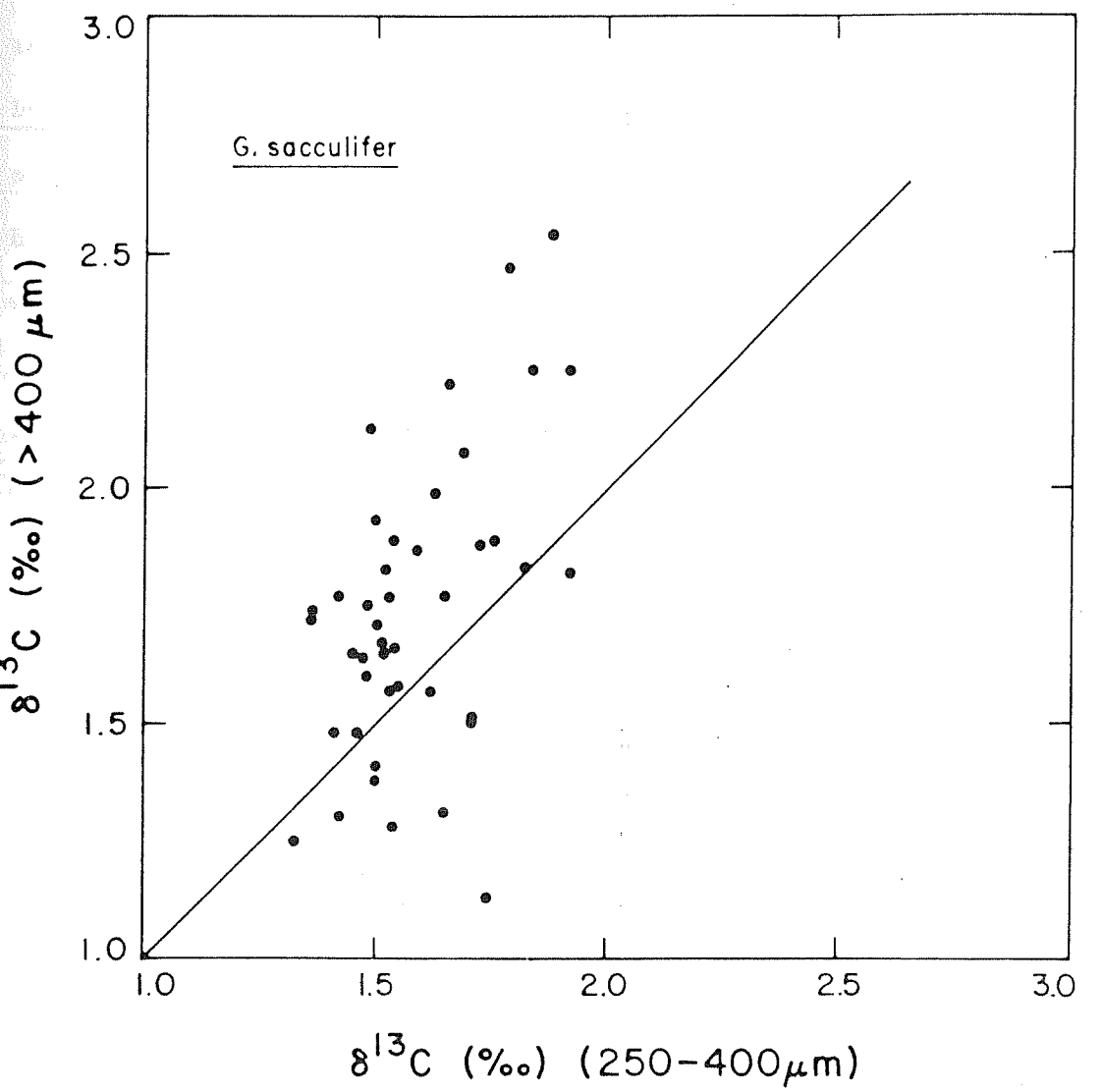

Fig. 3.8d : $\delta^{13}C$ values of two different size fractions of G.sacculifer in SK-20-185.

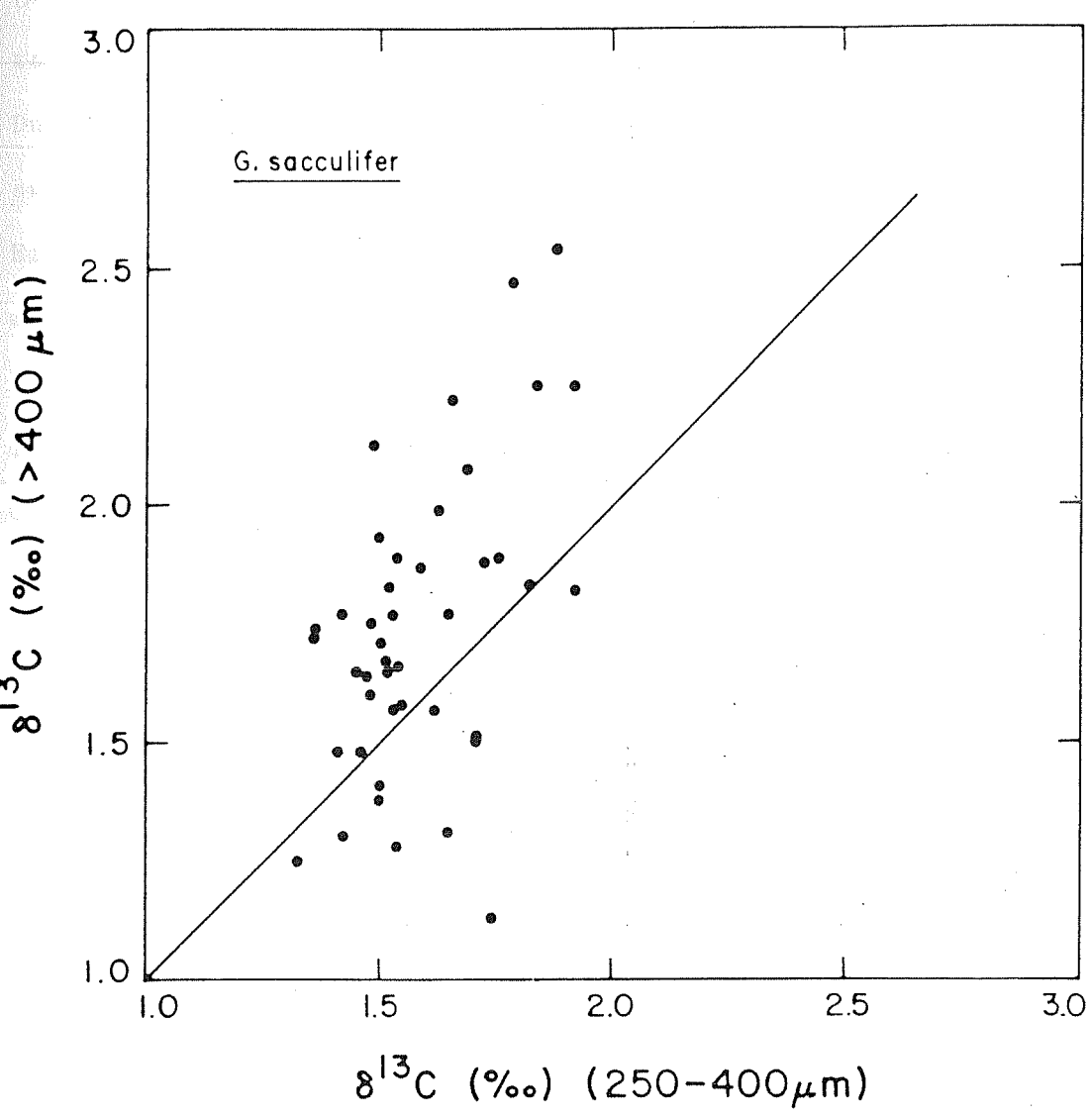

Fig. 3.8d : $\delta^{13}C$ values of two different size fractions of G.sacculifer in SK-20-185.

Berger et al (1978b). Recently Duplessy et al (1981a) have analysed different size fractions from plankton tows in the Arabian sea. Their study does not show any difference in $\delta^{18}O$ among various size fractions in G. sacculifer. However, $\delta^{13}C$ in large specimens are significantly enriched relative to smaller ones, consistent with our observations. Be and Duplessy (1976) noted a direct correlation between sea surface temperature and the size of Orbulina universa. Higher SST can presumably deplete $\delta^{18}O$, a mechanism which might have been responsible for producing $\delta^{18}O$ depletion in large size fraction of G. sacculifer if we assume that the larger forams migrate upwards due to their buoyancy. Conversely, the smaller tests can be grown during summer period when SST is lowered, thereby enriching the $\delta^{18}O$ (Berger 1969).

The depletion of $\delta^{13}C$ in the smaller fraction can be explained either by

1. the use of carbon derived from oxidation of organic matter while building $CaCO_3$ shells, or

2. the kinetic fractionation operating due to rapid $CaCO_3$ production in initial ontogenic stage, thereby enriching ^{12}C (Berger et al 1978b).

Since considerable differences exist in the isotopic values of different size fractions, it is pertinent to test whether these fractions grow in isotopic equilibrium or not. This requires measurement of the $\delta^{18}O$ of water in which the

foraminifera calcifies and the $\delta^{13}C$ of bicarbonate dissolved in water. Duplessy et al. (1981a) have earlier measured water-$\delta^{18}O$ in the Arabian sea. But their measurements are limited in number and restricted to a small transect off west-coast of India, where the sea water-$\delta^{18}O$ has a strong influence of the large amount of continental river water input. Measurements of Craig and Gordon (1965) were made at places,far away from present core locations. Consequently these salinity-$\delta^{18}O$ relations cannot be used for calculating equilibrium values in the present case. As an alternative, GEOSECS (1987) data of stations 416, 417 and 418 have been taken for calculating $\delta^{18}O$ and $\delta^{13}C$ values of equilibrium calcite.These stations cover a north-south transect in central Arabian sea, spanning $6^{o}N$ to $20^{o}N$ and hence could be taken to represent the present core locations. Unfortunately, however, only station 416 has data on water-$\delta^{18}O$.Stations 417 and 418 have only $\delta^{13}C$ data on aquous bicarbonate.Hence the $\delta^{18}O$ of equilibrium calcite was calculated only for cores CD-17-30, 15, 32, for which surface water-$\delta^{18}O$ was available from nearby station 416 ($19^{o}45'N$ $64^{o}37'E$).$\delta^{13}C$ is calculated for all the core locations.

Equilibrium calcite-$\delta^{18}O$ has been calculated from the following equation:

$$T^{o}C = 16.9-4.38(\delta_c - \delta_w) + 0.10(\delta_c - \delta_w)^2$$

(Shakleton 1974; This Thesis, Chapter I)

value of δ_c for given $T^{o}C$ and δ_w, is obtained

from above as:

$$(\delta_c - \delta_w) = \frac{4.38 - \sqrt{19.18 - 0.4(16.9+T)}}{0.2}$$

where δ_c and δ_w are both expressed with respect to CO_2 derived from PDB. Normally, δ_w is measured w.r.t. CO_2 equilibrated with SMOW. So, δ_w (SMOW) has been converted to δ_w(PDB) through the following relation:

$$\delta_w(\text{PDB}) = \delta_w(\text{SMOW}) - 0.22 \text{ (Friedman and O'Neil, 1977)}$$

Similarly, equilibrium $\delta^{13}C$ value of calcite is calculated from the following relation, based on the assumption that $\delta^{13}C(\Sigma CO_2)$ can be approximated by $\delta^{13}C$-bicarbonate (Williams et al. 1977):

$$\delta^{13}C \text{ calcite} = \delta^{13}C(HCO_3^-, \text{aq.}) + 1.85 + 0.035\ (T-20)$$

(Emrich et al. 1970, Chapter 1)

where T = Temperature (^oC)

The calculated equilibrium values for $\delta^{18}O$ and $\delta^{13}C$ and those observed on core top G. sacculifer are given in Table 3.8. As can be seen, there is virtually no difference between the calculated and the core top $\delta^{18}O$ values, indicating that G. sacculifer, (250-400)μm fraction probably grows in isotopic equilibrium. However, this conclusion should be viewed with caution because GEOSECS data on surface water $\delta^{18}O$ was obtained at a particular time of the year and does not represent the mean annual $\delta^{18}O$ composition. Earlier, from

Table 3.8

$\delta^{18}O$, δ^{13} values of calcite* and the observed values of core top G.sacculifer (250-400 m)

Core No.	Mean Annual SST(°C)	$\delta^{18}O_{calc.}$ (°/oo) PDB [1]	$\delta^{18}O_{GS}$ (°/oo) PDB [2]	$\delta^{13}C_{calc.}$ (°/oo) PDB [3]	$\delta^{13}C_{GS}$ (°/oo) PDB [4]	$\Delta^{18}O$ (°/oo) [5]	$\Delta^{13}C$ (°/oo) [6]
CD-17-32	24.5	-1.1	-1.22	3.78	1.11	0.12	2.67
CD-17-30	25.5	-1.32	-1.28	3.81	1.35	-0.04	2.46
CD-17-15	26.0	-1.43	-1.43	3.83	1.27	0.0	2.56
SK-20-185	27.5	-	-1.72	3.77	1.76	-	2.01
SK-20-186	28.5	-	-1.39	3.91	1.79	-	2.12

* Calculated using equations (Shackleton, 1974 and Emrich et al., 1970) discussed in the text.

1 $\delta^{18}O$ values, for all the 3 core locations are calculated, taking surface $\delta^{18}O$ of water as 0.56 °/oo (PDB) (Station 416, GEOSECS 1987).

2,4 $\delta^{18}O$ and $\delta^{13}C$ values of core top G.sacculifer (250-400) μ m respectively.

3 $\delta^{13}C$ values are calculated based on bicarbonate- $\delta^{13}C$ data of GEOSECS (1987). For first 3 core locations, data from closest location i.e. station 416 are used. For the other two (185 and 186) cores, values of stations 417 and 418 are used respectively.

5,6 Difference in $\delta^{18}O$ and $\delta^{13}C$ between calculated and observed core top δ values respectively.

plankton tow studies in the Arabian sea Duplessy et al (1981a) showed that for both G. sacculifer and G. ruber, the temperature coefficients of $^{18}O/^{16}O$ fractionation are same as that given by Epstein et al. (1953) but the absolute values of $\delta^{18}O$ are systematically depleted by 0.7 to 0.6 °/oo respectively. Duplessy et al. (1981a) also noted that significant (~ 20%) gametogenic calcification, takes place in G. sacculifer in this region, which leads to ^{18}O enrichment and probably balances the 0.7 °/oo disequilibrium depletion at surface water. Hence the observed equilibrium values in the present core top G. sacculifer might be a fortuitous coincidence. Duplessy et al. (1981a) report, core top G. sacculifer value for station 13.67, close to the core CD-17-30 and CD-17-32 as -1.25 °/oo. This value is same as the values of core top G. sacculifer from CD-17-30 and CD-17-32, and this demonstrates the reliability of our measurements in a natural sample, which is not affected by any systematic error.

However, the core top $\delta^{13}C$ values in G. sacculifer show a depletion of 2 °/oo or more (Table 3.8) than the calculated value. This observation (also noted by Duplessy et al. 1981a) indicates a very strong disequilibrium effect in planktonic foraminifera as far as carbon isotopes are concerned. In the following discussion it is assumed that $\delta^{18}O$ of G. sacculifer reliably records the temperature and salinity variation of the upper 100 m in the water column (Duplessy et al. 1981a) and the disequilibrium effect in $\delta^{13}C$ perhaps remained constant throughout the upper

Quaternary period. Hence this species can be used to reconstruct past climatic variations. Since the (250-400)μm fraction was found to give near isotopic equilibrium value, for all the 5 cores G. sacculifer from this size fraction has been analysed to construct a long term $\delta^{18}O$ stratigraphy.

III.2.2. Long Term $\delta^{18}O$ Stratigraphy

$\delta^{18}O$ values of G.sacculifer for the 5 cores are given in Tables 3.9 to 3.12 and plotted against depth in Fig. 3.9. Data of CD-17-32 are not plotted in this figure as this core does not reach Last Glacial Maximum (LGM). For SK-20-185 there is a negative spike corresponding to depths (28-34) cms. whose significance will be discussed later. This spike is not shown in this figure as it represents a local event. Based on the shape of the $\delta^{18}O$ curves and the radiocarbon dates for samples from several depths in the cores $\delta^{18}O$ stratigraphies for the cores have been made in comparison with the typical $\delta^{18}O$ curve of SPECMAP (Imbrie et al. 1984).

Core CD-17-30 has a sedimentation rate of 7.7 cm/kyr and has been analysed upto stage 3. Core SK-20-185 has a moderate sedimentation rate of 2.2 cm/kyr and goes upto stage 5e. Core SK-20-186 has a long climatic record upto stage 11. Bold arrows in these three cores indicate the 18 kyr level. In general, the $\delta^{18}O$ maximum in stage 2 is assigned as the LGM. When two maxima are present, the older one is selected as LGM level (Prell et al. 1980). Such a

Table 3.9

Oxygen and Carbon Isotope Data* on Core SK-20-185

Depth (cm)	$\delta^{18}O_{PDB}$ (°/oo)	$\delta^{13}C_{PDB}$ (°/oo)
2.50	-1.34	1.74
4.50	-1.72	1.76
6.50	-1.70	1.53
8.50	-1.41	1.53
10.50	-1.17	1.42
12.50	-0.60	1.50
14.50	-0.94	1.31
16.00	-0.46	1.05
18.00	-0.16	1.50
20.00	-0.16	1.36
22.00	-0.09	1.48
24.00	0.08	1.49
26.00	0.23	1.40
28.00	-0.14	1.54
30.00	-0.30	1.36
32.00	-0.97	1.66
34.00	-0.88	1.62
37.50	0.34	1.54
42.50	0.26	1.73
47.50	0.26	1.65
52.50	0.40	1.92
57.50	0.22	1.88

Table 3.9 contd.

62.50	0.11	1.83
67.50	-0.02	1.84
72.50	-0.25	1.79
77.50	-0.17	1.69
82.50	-0.48	1.65
87.50	-0.06	1.74
92.50	-0.23	1.53
97.50	-0.21	1.71
102.50	-0.44	1.62
107.50	-0.21	1.75
112.50	-0.67	1.50
117.50	-0.53	1.42
122.50	-0.49	1.48
132.50	-0.32	1.47
137.50	-0.14	1.54
142.50	-0.07	1.49
147.50	0.03	1.65
152.50	-0.24	1.32
157.50	-0.12	1.46
162.50	-0.44	1.52
167.50	-0.68	1.50
172.50	-0.34	1.41

Table 3.9 contd.

177.50	-0.90	1.36
182.50	-0.90	1.36
190.00	-0.51	1.53
200.00	-0.80	1.63
210.00	-1.09	1.87
220.00	-0.60	1.82
230.00	-0.87	1.42
240.00	-0.89	1.47
250.00	-1.05	1.48
260.00	-1.18	1.76
270.00	-1.10	1.71
280.00	-1.13	1.45
290.00	-0.84	1.55

* Measured on G. sacculifer (250-400) μm with 30-40 individuals per aliquot.

Table 3.10

Oxygen and Carbon Isotope Data* on Core SK-20-186

Depth (cm)	$\delta^{18}O_{PDB}$ (°/oo)	$\delta^{13}C_{PDB}$ (°/oo)
1.00	-1.37	1.67
2.50	-1.39	1.79
11.50	-1.10	1.68
13.50	-0.85	1.71
15.50	-0.51	1.74
17.50	-0.49	1.76
19.50	-0.57	1.82
21.50	-0.47	1.78
24.50	-0.32	1.65
26.50	0.00	1.99
28.50	0.13	1.84
30.50	-0.30	1.73
32.50	-0.31	1.76
43.00	-0.37	1.78
47.00	-0.46	1.79
53.00	-0.83	1.68
57.00	-0.70	1.91
64.50	-0.68	1.70
69.50	-0.84	1.57
74.50	-0.92	1.62
79.50	-0.71	1.42
84.50	-1.00	1.29

Table 3.10 contd.

89.50	-0.70	1.24
94.50	-0.07	1.48
104.50	0.01	1.43
114.50	0.00	1.39
124.50	-0.21	1.49
129.50	-0.35	1.32
134.50	-0.61	1.45
139.50	-0.42	1.46
144.50	-0.50	1.54
149.50	-0.52	1.71
154.50	-0.75	1.55
159.50	-0.60	1.48
164.50	-0.54	1.53
169.50	-0.35	1.51
174.50	-0.40	1.64
179.50	-0.60	1.51
184.50	-0.90	1.46
189.50	-0.62	1.46
197.00	-0.43	1.44
207.00	-0.18	1.31
217.00	-0.13	1.38
227.00	-0.39	1.67
237.00	-0.41	1.54
247.00	-0.56	1.52

Table 3.10 contd.

257.00	-0.66	1.33
267.00	-0.78	1.33
277.00	0.06	1.21
287.00	0.12	1.49
297.00	-0.48	1.37
307.00	-0.47	1.38
317.00	0.31	1.44
327.00	0.21	1.60
337.00	0.13	1.72
347.00	0.05	1.64
357.00	-0.38	1.65
367.00	-0.59	1.45
377.00	-0.40	1.62
387.00	-0.03	1.42
397.00	-0.22	1.56
407.00	-0.73	1.41
417.00	-0.46	1.53
427.00	-0.28	1.37
437.00	-0.47	1.46
447.00	-0.27	1.45
457.00	-0.45	1.27
467.00	-0.69	1.43
477.00	0.01	1.26
487.00	0.43	1.15

* Measured on G. sacculifer (250-400) μm with 30-40 individuals per aliquot.

Table 3.11

Oxygen and Carbon Isotope Data* on Core CD-17-30

Depth (cm)	$\delta^{18}O_{PDB}$ (°/oo)	$\delta^{13}C_{PDB}$ (°/oo)
5.0	-1.28	1.35
15.0	-1.21	1.13
25.0	-0.61	1.21
42.5	-0.36	1.14
50.0	0.21	1.36
55.0	0.14	1.06
65.0	0.87	1.13
75.0	0.69	1.07
85.0	0.87	1.34
92.5	0.28	0.82
100.0	0.61	1.27
112.5	0.35	0.95
130.0	1.01	1.13
150.0	0.90	0.90
165.0	1.03	1.17
195.0	0.74	1.22
212.5	0.42	1.02
235.0	0.58	1.02
250.0	0.52	1.13
262.5	0.26	0.86
277.5	0.18	0.64
307.5	0.15	0.78

* Measured on G. sacculifer (250-400) μm with 30-40 individuals per aliquot.

Table 3.12

Oxygen and Carbon Isotope Data* on Core CD-17-15

Depth (cm)	$\delta^{18}O_{PDB}$ (°/oo)	$\delta^{13}C_{PDB}$ (°/oo)
Box Core		
47.5	-1.43	1.27
Piston Core		
Disturbed Top	-0.08	0.81
1.0	0.73	1.18
11.0	0.76	1.11
20.5	0.52	1.00
26.5	-0.35	0.83
37.5	0.34	0.95
47.5	0.65	1.07
57.5	0.89	0.88
67.5	0.47	0.91
77.5	0.90	0.64
112.5	0.32	1.03
127.5	0.61	1.20
142.5	0.17	0.77
157.5	0.19	0.93
175.0	-0.51	0.98
182.5	0.19	0.73

Table 3.12 contd.

Depth (cm)	$\delta^{18}O_{PDB}$ (°/oo)	$\delta^{13}C_{PDB}$ (°/oo)
205.0	0.23	0.93
227.5	0.50	0.91
262.5	-0.49	0.20
297.5	0.41	1.15

Oxygen and Carbon Isotope Data* on Core CD-17-32

Depth (cm)	$\delta^{18}O_{PDB}$ (°/oo)	$\delta^{13}C_{PDB}$ (°/oo)
5.0	-1.22	1.11
15.0	-1.05	1.12
25.0	-0.65	1.22
32.0	-1.11	1.29
41.0	-0.89	1.13
49.0	-0.95	1.31

* Measured on G. sacculifer (250-400) μm with 30-40 individuals per aliquot.

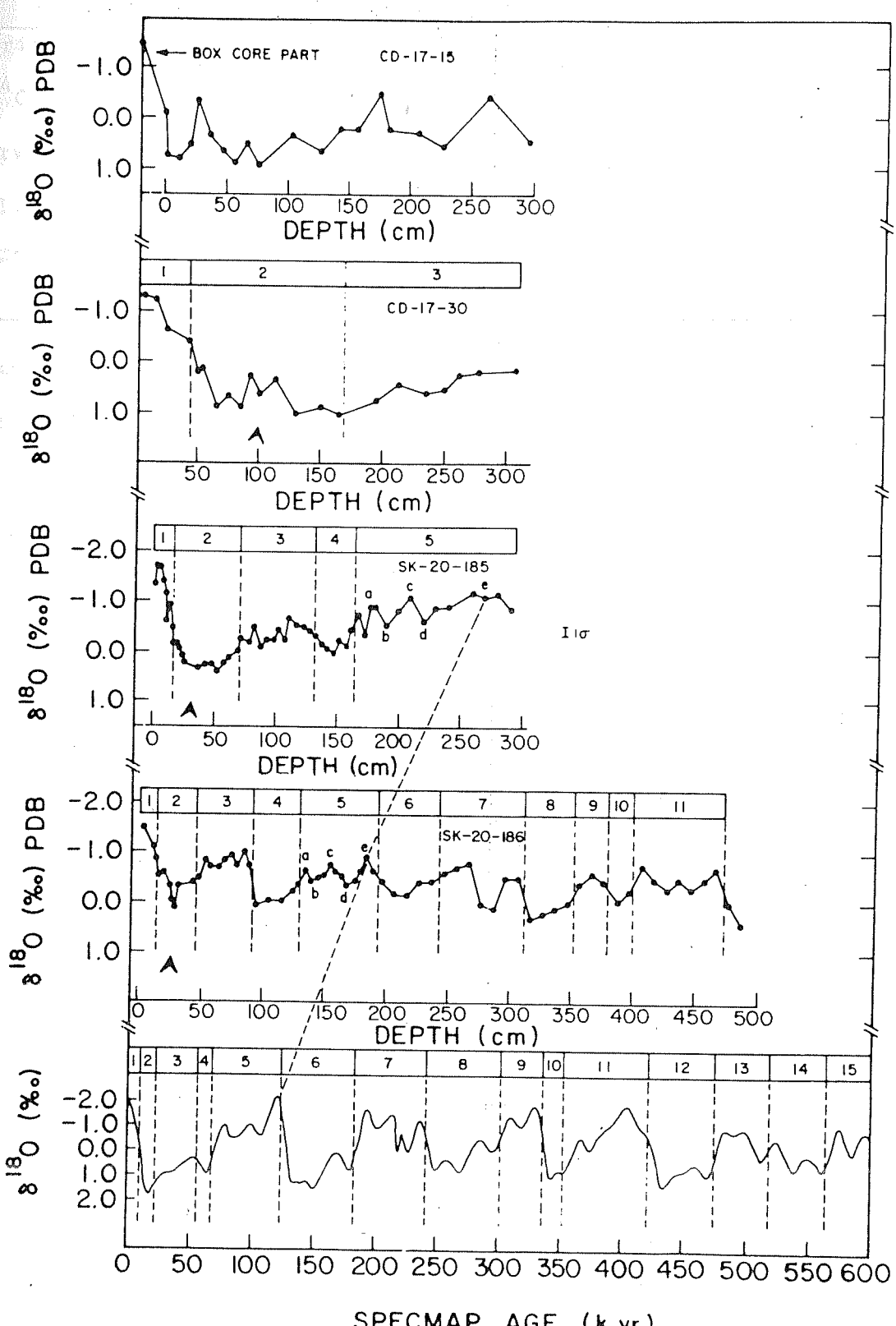

Fig. 3.9 : Variations of $\delta^{18}O$ in the sediment cores. For reference SPECMAP curve is also shown (data from Imbrie et al. 1984). For SK-20-185 data for depths (28-34) cm are not plotted. No stage boundary is shown for CD-17-15 due to its disturbed nature (see text).

* Here $(\delta^{18}O - \overline{\delta^{18}O})/\sigma$ has been plotted.

criterion for selecting the LGM level, however, does not strictly apply here. For example, in core CD-17-30, 18 kyr (^{14}C data) lies not on a maximum but on a minimum in between two maxima. In core SK-20-185 too (see section III.2.6), 18 kyr (^{14}C data) lies on a $\delta^{18}O$ minimum. While SK-20-185 has a moderate sedimentation rate, CD-17-30 has a relatively higher rate, and hence bioturbation is less likely to affect the position of the 18 kyr level. Hence fixing the 18 kyr level purely based on the shape of $\delta^{18}O$ curve may be erroneous. As will be discussed later, local hydrography can considerably modify the shape of the $\delta^{18}O$ curve.

When the ^{14}C based sedimentation rate is extrapolated, in SK-20-185, an excellent agreement is found with $\delta^{18}O$ stratigraphy. Considering the ^{14}C based sedimentation rate to be constant throughout the core length (2.2 cm/kyr), 122 kyr (stage 5e of SPECMAP) should occur at 263.5 cm level, which agrees with the peak of 5e stage in this core. For SK-20-186, however, the situation is different. Extrapolated ^{14}C dates do not match with the ages of $\delta^{18}O$ stage boundaries. This is related to the fact that sedimentation rate in this equatorial region has undergone significant changes for last 40 kyr. Glacial rate is about a factor of four lower than that of Holocene. Considering these breaks and putting the radiocarbon age constraint, 5e stage in this core lies at 184.5 cm. In both the cores, SK-20-185 and SK-20-186, substages are also well developed upto stage 5e (122 kyr). These include all the 3 substages in stage 3 and

5 substages (a,b,c,d,e) in stage 5.Beyond 5e stage,in core SK-20-186 substages are not very well preserved.Also it is noticeable that considerable modifications of the $\delta^{18}O$-amplitudes are found when one compares with global $\delta^{18}O$ data. Modification of Holocene-LGM amplitude and its significance will be discussed later. The following discussion pertains to the modification of $\delta^{18}O$-amplitudes and cycles beyond LGM.

III.2.3. Modification of $\delta^{18}O$ Cycles and Amplitudes

In SK-20-185,the amplitude between substages 3 and 4 is about 0.7 °/oo while in SK-20-186 it is ~ 1 °/oo and is higher than that noted in other oceans (Shackleton 1977), which record a value of ~ 0.25 °/oo to a maximum of about 0.5 °/oo. This cannot be explained either by bioturbation (which reduces the amplitude,see the following discussion) or by dissolution (which also reduces the amplitude in an interstadial stage, like 3,see next section).Considering a constant ice volume effect for all oceans,this increased amplitude in stage 3 perhaps indicates higher SST in this tropical ocean during this period.

The global average amplitude between stage 5e and 6,is seen to be about same as that between stage 1 and 2 (SPECMAP cycles,Fig. 3.9).The stage 5e event,normally taken as a super interglacial when perhaps less ice was stored in the continents than any other time (Shackleton and Opdyke, 1973), is however,represented by enriched δ values relative to Holocene in these cores.This reduces the amplitude of

5e-6 stage compared to 1-2.In core 185,the 5e stage in $\delta^{18}O$ is enriched by 0.5 °/oo relative to Holocene.In SK-20-186 too,5e stage shows 0.5 °/oo enrichment relative to Holocene, thus making 5e-6 amplitude ~ 0.8 °/oo.This is much less than Holocene-LGM (1-2) amplitude of 1.5 °/oo in this core. This core has a record of more than 400 kyr and its other stages beyond 5e, can be compared with SPECMAP cycles.In stage 7 finer structures (substages) are not well preserved and amplitude between stage 6 and stage 7 is only 0.6 °/oo. However, 7-8 amplitude is again 1 °/oo and that between 8 and 9 is 0.9 °/oo. Amplitude between stage 9 and stage 10 and between stage 10 and stage 11 are as small as 0.6 and 0.75 °/oo respectively. Both stage 8 and stage 9 do not contain finer substages.Possible causes of modification in $\delta^{18}O$ amplitude are discussed below.

III.2.4. Mechanisms for Modifications of $\delta^{18}O$ Amplitude

The original $\delta^{18}O$ amplitudes in deep sea cores can be modified by a variety of processes out of which two are most important, namely, bioturbation and dissolution. We discuss below features of these processes.

III.2.4.a. Bioturbation or Benthic Mixing

It has long been recognized that the upper few centimeters in the sediments are mixed by benthic organisms (Arrhenius 1963; Ruddiman and Glover 1972).As a result the original signals of chronology (e.g. ^{14}C) or of climatic indices (e.g. $\delta^{18}O$, $CaCO_3$, etc.) are modified.Bioturbation

acts as a low-pass filter which displaces and reduces the amplitudes of stratigraphic signals.Additionally it leads to a loss of high frequency events in the record (Bard et al., 1987).However,a reduction in the $\delta^{18}O$ amplitude is most serious, when one is interested in using glacial-interglacial $\delta^{18}O$ change (GIA) as an ice-volume indicator. This reduction in amplitude is more prominent in cores having a low sedimentation rate (Broecker 1986).The sedimentation rate in core SK-20-185 is moderate (2.2 cm/kyr), hence it can have some bioturbation effect.In the subsequent sections (III.2.6.a),however,we show by uranium analyses, that bioturbation (at least during the glacial period) is not very significant in this core.Additionally this core shows a laminated lithology all through indicating that benthic mixing was not intense. Core SK-20-186 might have some bioturbation effect more in the deeper section because sedimentation rate (~ 0.6, 1-6 cm/kyr) is lower during glacial period compared to Holocene (2.4 cm/kyr). In both the cores, however, estimation of bioturbation mixing length could not be done since top few cms of sediments are lost and no plateau age (of ^{14}C) were obtained in the top part of these cores.CD-17-30 has a high sedimentation rate and hence bioturbation is unlikely to change the amplitude in a major way.If it is assumed that bioturbation is insignificant for the entire length of SK-20-185, then the enrichment of 5e stage by 0.5 $^{o}/oo$ is most probably caused by some other mechanism.

III.2.4.b. Dissolution and $\delta^{18}O$ Amplitude

Savin and Douglas (1973) were the first to point out, that increasing dissolution not only progressively removes the species susceptible to dissolution but also preferentially removes the individuals which are thin-walled and calcified in the shallow-warm water. Berger and Killingley (1977) showed that this effect may increase $\delta^{18}O$ of dissolution susceptible species such as G. sacculifer by as much as 0.3 °/oo. Therefore, a dissolution effect in interglacial time will reduce GIA while an increase in dissolution during glacial period will enhance it (Erez 1979). This change in dissolution pattern in the past can be identified by analysing $\delta^{18}O$ in two different species having different dissolution susceptibility. One such study by Berger and Killingley (1977) in western equatorial pacific shows that $\Delta^{18}O$ i.e. difference in $\delta^{18}O$ between Pulleniatina obliquiloculata (a dissolution resistant species) and G. sacculifer (a solution susceptible species), increases during Holocene compared to glacial period (LGM), thus indicating greater Holocene dissolution. Similar analysis has been done in core SK-20-185 where $\Delta^{18}O$ has been calculated between P. obliquiloculata and G. ruber. G. sacculifer-$\delta^{18}O$ in this core has a strong influence of local hydrography (see section III.2.6) and therefore cannot be used for this purpose. The solution susceptibility of G. ruber has been shown to be same as that of G. sacculifer (Bonneau et al. 1980). Additionally, the difference in $\delta^{18}O$ of G. menardii

(another solution resistant,thick walled form) and G. ruber has also been calculated. $\Delta^{18}O$ values are given in Table 3.13. As can be seen,in both the cases $\Delta^{18}O$ remains more or less constant from LGM to Holocene,indicating possibly no major changes in dissolution pattern.Such a situation is not unexpected because SK-20-185 is located at a shallower level (~ 2.5 km) than the depth where calcium carbonate starts dissolving. This characteristic depth,termed as the calcium carbonate compensastion depth or CCD,in the Indian ocean and the Arabian sea is known to lie between 4.2 and 5 km water depths (Weser 1974).

In core SK-20-186, however, analysis of species other than G. sacculifer was not done.This core has a very high abundance of $CaCO_3$ throughout its length (Table 3.20), eventhough it comes from a depth closer to CCD (~3.5 km). Thus ,in this core too,the near absence of dissolution can be assumed.

Summarising dissolution effect, in SK-20-185 and SK-20-186 is probably insignificant. Bioturbation effect, though small in SK-20-185 and CD-17-30,might be important in SK-20-186. In addition, Holocene-LGM amplitudes in SK-20-185 and SK-20-186 (see next section) are similar to those obtained in the cores with high sedimentation rate from nearby locations (Duplessy 1982).Hence it is assumed that Holocen-LGM amplitudes are not altered by bioturbation or dissolution mechanism.If it is assumed that this is true for the last 120 kyr, then the enrichment of 5e stage relative to Holocene in SK-20-185 cannot be explained by

Table 3.13

Difference in $\delta^{18}O^{*}$ of two species having different solution susceptibilities in SK-20-185

Depth (cm)	$\Delta^{18}O$(Pull.-rub.) (‰)	$\Delta^{18}O$(men.-rub.) (‰)
2.5	-	1.06
4.5	1.30	1.42
6.5	1.27	1.21
8.5	0.86	1.16
10.5	1.31	1.68
12.5	-	1.02
14.5	1.34	0.93
16.0	1.33	1.33
18.0	-	1.25
20.0	1.33	1.36
22.0	1.27	1.23
24.0	1.30	1.26
26.0	1.24	1.08
28.0	1.27	1.01
30.0	-	1.40
32.0	1.88	1.15
34.0	1.80	1.32
37.5	1.23	1.08
42.5	-	0.99
47.5	1.58	1.42

* Calculated from values of Tables 3.14, 3.16 and 3.17.

the above-mentioned effects.It is suspected that this is an artifact of the sampling procedure. From 190 cm downward (see Table 3.9), this core is sampled at 10 cm intervals. Taking the sedimentation rate as 2.2 cm/kyr,this means,an averaging out of $\delta^{18}O$ signal over a period of 4.5 kyr.This is sufficient to 'reduce' the peak value of 5e stage by 0.5 $^{o}/oo$ which existed for 3 kyr only (Martinson et al. 1987).

Core SK-20-186 was also sampled at coarser levels beyond LGM. From 22 kyr (stage 1-2 boundary,i.e. 47 cm) to 124 kyr (stage 5-6 boundary,i.e. 197 cm) sampling is done at 5 cm intervals.From 197 cm below,sampling interval is 10 cm. Considering the sedimentation rate of 0.6 cm/kyr and 1.6 cm/kyr (see Fig. 3.2), this means an averaging of $\delta^{18}O$ record over 3-8 kyr period. Since peak 5e stage spanned about ~ 3 kyr (op. cit.),such coarse sampling can 'reduce' the 5e-6 amplitude by ~ 0.5 $^{o}/oo$ compared to LGM-Holocene amplitude. Similarly, reduced amplitude of 1 $^{o}/oo$ or less from stage 6 to 11 might have resulted from this coarse sampling. Superimposed on this coarse sampling,bioturbation (as has been mentioned earlier) might have some effect on $\delta^{18}O$ amplitudes in the deeper sections of this core.

Similar to the modification of the $\delta^{18}O$ amplitudes, against global cycles found beyond LGM, Holocene-LGM amplitudes in different cores also show considerable variations. This is inspite of the fact that $\delta^{18}O$ analysis is performed at a very close interval for this part in all the cores, so that the $\delta^{18}O$ signals are averaged out for only 1-2 kyr (considering their ^{14}C sedimentation rates,

also see section III.2.6).The following section discusses the implications of the variations in the Holocene-LGM $\delta^{18}O$ amplitudes.

III.2.5. The Holocene-LGM $\delta^{18}O$ Amplitudes

Estimation of this amplitude in various cores,depends on the $\delta^{18}O$ values corresponding to the Holocene and the LGM level which have to be independently established.But in practice the LGM in deep sea cores is assigned to the most recent level which shows a maximum enrichment in $\delta^{18}O$. Globally LGM is supposed to have occurred about 18 kyr ago (CLIMAP 1976). However, it has been shown earlier that $\delta^{18}O$ maxima levels always do not have 18 kyr age in the cores studied. Prell et al (1980) have shown that in Indian ocean this has a spread of ~ 1.5 kyr (18.6 $\pm$ 1.5 kyr).This spread is determined by the sediment mixing depth during rapid isotopic changes associated with fast deglaciation,rather than actual rate of change in the isotopic composition of ocean water (Shackleton and Opdyke,1976).Consequently,one has to be careful while selecting the LGM level.

In SK-20-185, the most enriched $\delta^{18}O$ level lies at 52.5 cm (~ 26 kyr) having a value ~ 0.4 °/oo and is taken as the LGM value.In CD-17-30,the most enriched levels of ~ 1 °/oo lies at 130 cm (~ 22 kyr) and is taken as representative of LGM. Note that 18 kyr (^{14}C) in both SK-20-185 (S = 2.2 cm/kyr, Table 3.1 and Table 3.9,see next section also) and CD-17-30 (S = 7.7 cm/kyr,Fig. 3.9) lie on $\delta^{18}O$ minima.

For SK-20-186, only one $\delta^{18}O$ maximum (0.13 °/oo) is

observed at 28.5 cm. This too, has been obtained by performing very close analyses at 2 cm interval between 11.5 cm and 32 cm. Lower glacial sedimentation rate is perhaps responsible for the confinement of enriched level in a very thin layer of sediment.CD-17-15 (piston core) does not yield a good oxygen isotope stratigraphy.Core top value is -0.08 °/oo and erratic excursion of $\delta^{18}O$ (Fig. 3.9) is seen all through the 300 cm analysed.This indicates that this core in all probability contains slumped material, which is consistent with the litholog showing distinct turbidite layers. However, the most enriched $\delta^{18}O$ value in this core is 0.9 °/oo corresponding to a depth of 77.5 cm. The most depleted value of -1.43 °/oo comes from 47.5 cm. depth of the box core part of CD-17-15 (Fig. 3.9).No foraminifera could be picked up from 0 - 45.0 cm depth in this box core where the sediments are sandy and clayey and perhaps derived from slumped materials of adjacent continental slopes.If these two extreme values are taken as representative LGM and Holocene,then the amplitude for this core is 2.33 °/oo.

In SK-20-185, CD-17-30 and SK-20-186,the most depleted $\delta^{18}O$ values are taken as Holocene values i.e. -1.72,-1.28 and -1.39 respectively. Consequently (GIA) amplitudes for these three core locations are calculated to be 2.12 °/oo, 2.28 °/oo and 1.52 °/oo respectively.Note that,even though CD-17-15 is a disturbed core, its estimated amplitude is close to that of CD-17-30.Both the cores came from nearby locations in the western Arabian sea.CD-17-32 shows a small

variation (0.5 °/oo) in $\delta^{18}O$ and does not reach the LGM level.

Before the possible causes of the amplitude differences among various cores are examined, it will be necessary to discuss the modern hydrological setting in northern Indian ocean and how it controls the $\delta^{18}O$ of planktonic foraminifera.

III.2.5.a. Modern Hydrological Conditions of Northern Indian Ocean related to Foraminiferal $\delta^{18}O$

The present day climatic condition over the Asian continent and the northern Indian ocean is dominantly controlled by seasonally varying insolation. In summer, the land is heated faster than ocean, resulting in the expansion of the overlying air. A pressure gradient from ocean to land is set; strong wind blows from the ocean to the continent, which carries moisture from ocean. This wind is deflected rightward due to the Coriolis force. Near the coast of Somalia and Arabia, this wind reaches a very high speed of about 5-10 m/sec during this period (Hasternath and Lamb 1979) causing intense upwelling due to Ekman transport (Prell and Streeter 1982). On the other hand, the moist air moving towards the Indian continent, rises up, water vapour condenses and causes heavy monsoon rains. Such a coupled system of monsoon and upwelling (Dietrich 1973; INDEX 1976) produces two changes in the Arabian sea. Firstly, the Arabian sea receives a large freshwater discharge, (due to heavy precipitation) through the west-bound rivers. Secondly, a

pronounced temperature decrease (~4°C) takes place along Somalian and the Arabian coasts due to the upwelling of cold bottom water. Horizontal advection and wind induced mixing also contribute towards cooling of the Arabian sea in summer. In general, the Arabian sea is dominated by a strong evaporation which increases from south to north producing a salinity gradient.Salinity during summer time, increases from 35 °/oo in the south to 36.5 °/oo in the north (Fig. 3.10a). Because of a large freshwater flow,the iso-haline contours, which run east-west in the central Arabian sea, are pushed northward along the west coast of India. In winter time, this gradient steepens, but has a similar north-south pattern (Fig. 3.10b).On the contrary, sea surface temperature (SST) during the monsoon period does not show any marked change or a gradient from south to north (Fig. 3.11a) except near Somalian and off the Arabian coasts where SST reduces due to intense upwelling.However, winter SST shows a gradient of 4°C (from 28°C in the south to 24°C in the north), with vanishing coastal upwelling centres (Fig. 3.11b). These patterns of salinity and temperature have a strong influence on the $\delta^{18}O$ composition of water and foraminiferal $CaCO_3$ respectively. $\delta^{18}O$ of the surface ocean water is mainly controlled by precipitation (freshwater), evaporation and mixing of different water masses (Craig and Gordon 1965).During evaporation process, isotopically lighter molecules i.e. $H_2{}^{16}O$ are preferentially removed and the remaining water becomes enriched in the heavier $H_2{}^{18}O$ molecules. On the contrary,precipitation adds

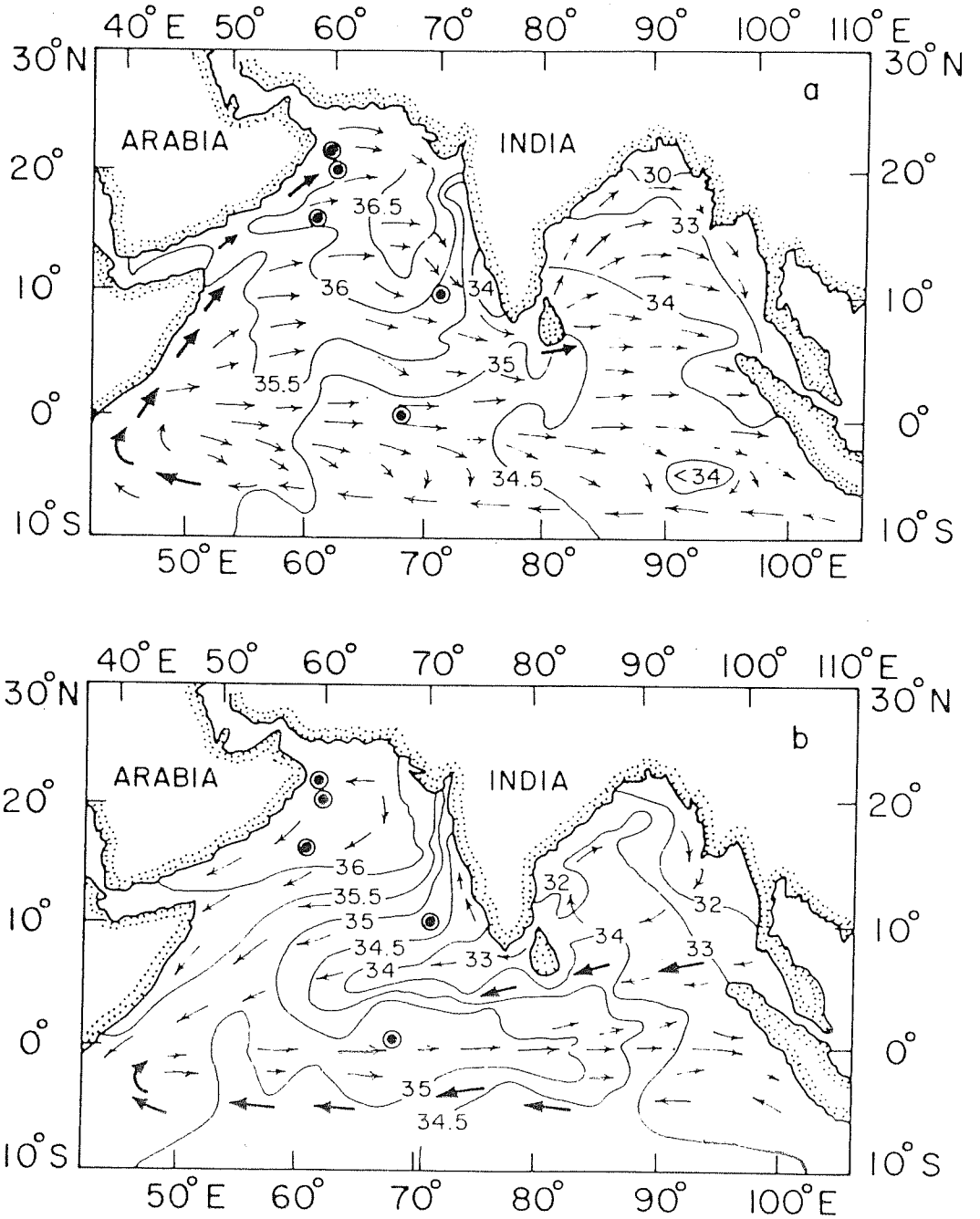

Fig. 3.10 : a. Surface salinity (in parts per mille) in July and August (SW monsoon period). Surface currents are shown by arrows. Also shown are the core locations.

b. Surface salinity in January and February (NE monsoon period).

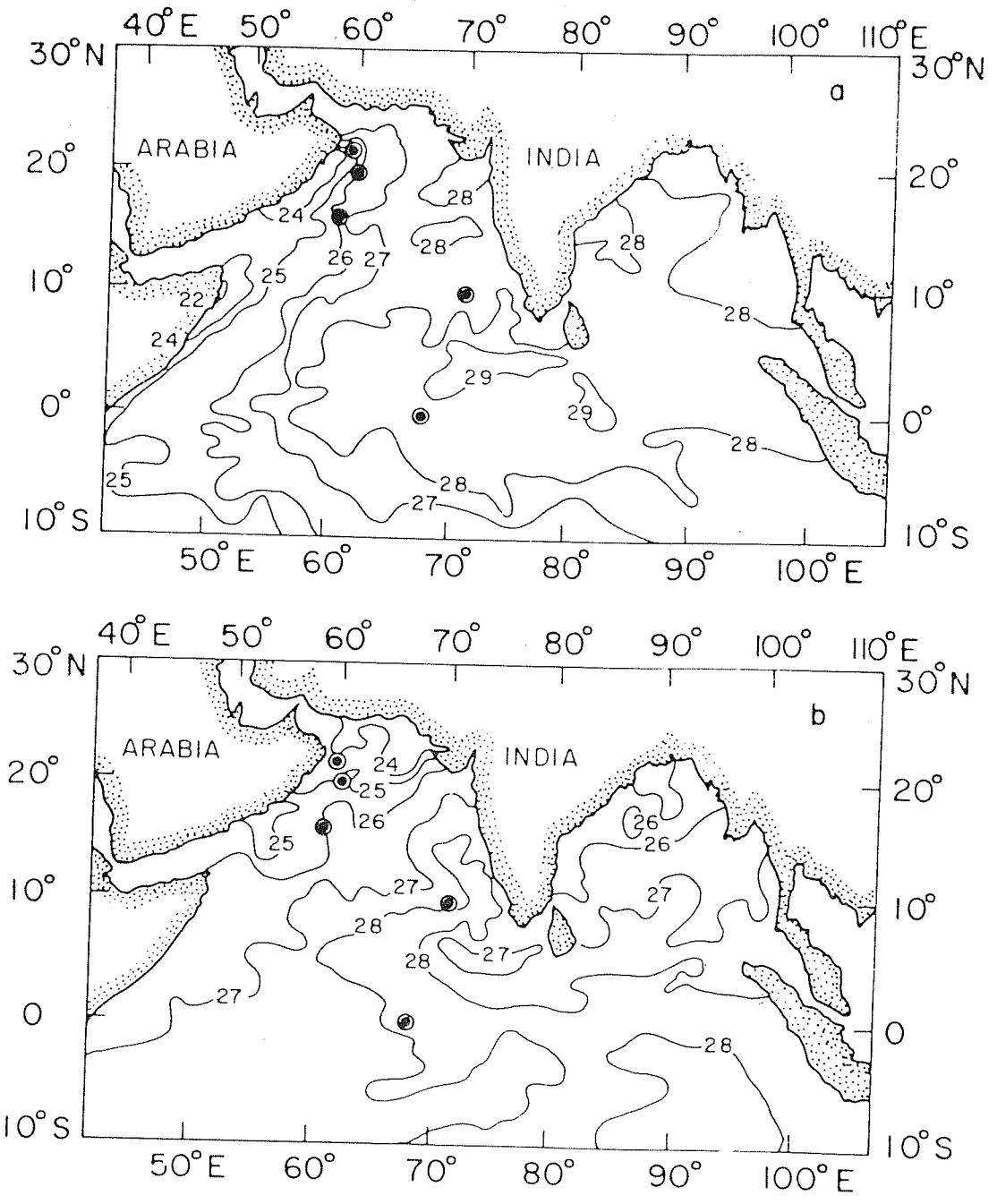

Fig. 3.11 : a. Sea surface temperature (SST in °C) in August (SW monsoon period) over northern Indian ocean, alongwith the core locations.

b. SST in February.

(Data for a and b from Wyrtki 1971)

water depleted in $\delta^{18}O$ to the oceans either through river discharge or by direct rainfall over the ocean. Besides changing the $\delta^{18}O$ composition of ocean water, evaporation and precipitation also cause marked changes in salinity. The former increases the salinity while the latter reduces it. Hence a linear relationship between sea-surface salinity and $\delta^{18}O$ is observed (Hoefs 1980) in most of the ocean basins. However, the slope of the line in $\delta^{18}O$-salinity plot differs from region to region and depends mainly on the $\delta^{18}O$ composition of freshwater input. For Arabian sea, water-$\delta^{18}O$ data are very meagre. Calculation of salinity-water $\delta^{18}O$ relation, from the available meagre data of Duplessy et al (1981a) from the Arabian sea shows that for a 1 °/oo change in salinity, $\delta^{18}O$ of water changes by about 0.32 °/oo.

The difference in core top $\delta^{18}O$ of G. sacculifer between the locations of cores SK-20-185 and CD-17-30 is 0.4 °/oo. The difference in mean annual SST between the locations of CD-17-30, 32 and 15 (16-22°N) and SK-20-185 (10°N) is 2°C, the northern part being cooler (Fig. 3.11). This can give rise to enriched core top value by ~ 0.4 °/oo in CD-17-30 relative to SK-20-185. On the other hand, difference in mean annual salinity between these locations is ~ 1.13 °/oo, the northern part being more saline (Fig. 3.10). Hence this salinity difference alone can also produce enriched value in CD-17-30 by ~ 0.4 °/oo. Therefore, lower SST and higher salinity in northern core locations relative to southern one, together should give a $\delta^{18}O$ value, 0.8 °/oo

higher. The observed difference of 0.4 °/oo is lower by a factor of two.A possible explanation of this discrepancy is that the foraminiferas in this region might have strong seasonal abundance (as has been found in other oceans, Williams et al 1979, 1981),thereby not recording the mean annual SST and salinity in these locations.Instead,their $\delta^{18}O$ composition might reflect surface water properties of particular season of the year.Additionally the foraminifera might vertically migrate in the water column,which has a gradient in temperature.Therefore,the small SST difference (of 2°C) between the two places may not be recorded in the foraminiferal $\delta^{18}O$.

III.2.5.b. Climate during the Last Glacial Maximum

Considering the global ice volume effect to be 1.6 °/oo the GIA values of 2.12 to 2.28 °/oo for the Arabian sea cores indicate extra 0.5 to 0.7 °/oo effect,which is local in nature.Such an enrichment during the last glacial period in both the northern and the southern cores indicates that the entire Arabian sea was in general more saline than today by about 1-2 °/oo (following the $\delta^{18}O$ salinity relation cited above,Duplessy et al.,1981a).In the next section, however,we show that there was a brief period when the surface water salinity at SK-20-185 location significantly reduced. When the Holocene core top-differences between northern and southern cores are compared with those during the LGM one,a small change is observed. The difference in $\delta^{18}O$ is found to have increased

during LGM. Against the Holocene difference of 0.4 °/oo,LGM difference between CD-17-30 and SK-20-185 is 0.6 °/oo. Similarly, Holocene difference of 0.3 °/oo between CD-17-15 and SK-20-185, increases to 0.5 °/oo during LGM.Considering the experimental error this difference is not very significant. However, earlier work by Duplessy (1982) also demonstrated such an increase in $\delta^{18}O$,from 0.6 °/oo in the Holocene to 1 °/oo during LGM in this region.Our result seems to be consistent with his observation.This difference cannot be attributed to any change in temperature due to the following reason. The upwelling during LGM reduced resulting in warmer SST in north-western Arabian sea (Prell 1978, 1984; Prell et al., 1980). This would deplete the foraminiferal $\delta^{18}O$.Thus the $\delta^{18}O$ difference between the two locations would decrease, rather than increase,as has been found. Hence upwelling (or temperature) change is not responsible for the observed difference.Therefore,we infer that salinity is the causative factor for this change. Salinity change can produce the observed effect in two ways:

1. A large amount of fresh water may be discharged during LGM, in southern (SK-20-185) Arabian sea, thereby increasing the difference in $\delta^{18}O$ with the northern part

2. A strong evaporation in northern Arabian sea relative to southern part,can take place during LGM.This would enhance the salinity (and $\delta^{18}O$) in northern part, thereby increasing the difference with southern region.

Earlier work in this region showed that freshwater discharge to the Arabian sea had considerably reduced during LGM (Duplessy 1982; Kale and Rajaguru 1987).This rules out the first possibility and we conclude that the difference is due to excess evaporation over northern Arabian sea during LGM.The effect of this evaporation (and enhanced salinity) was so strong that its signal is not masked by the compensating effect of warming due to the weaker upwelling.

A large body of palaeoclimatic evidence shows that during the LGM (18 kyr B.P.),extreme arid condition was prevailing over India,associated with stronger NE dry winds (Van Campo et al. 1982) and less rainfall in the northern plains (Duplessy 1982).As a result,large lakes in Rajasthan dried up (Singh et al. 1974).The west-bound rivers also became almost dry (Kale and Rajaguru 1987).Evidence of a strong NE monsoon circulation, by organic carbon isotopic measurements from Bay of Bengal has also been reported (Fontugne and Duplessy 1986). If true,then the dry trade winds associated with this NE monsoon,over the northern Arabian sea could have been responsible for the excess evaporation observed. This,coupled with a weaker SW monsoon (Prell 1978, Prell et al.,1980,Prell and Van Campo,1986), perhaps increased the salinity gradient from south to north. However, no $\delta^{18}O$ evidence for a stronger NE monsoon has so far been reported. In the next section we report some new

experimental evidence, based on foraminiferal $\delta^{18}O$ measurements which gives information about a short term intensification of NE monsoon during LGM compared to the present day. From the foregoing discussion,it is evident that global glacial-interglacial climatic cycles are considerably modified in the Arabian sea.

In comparison to the Holocene-LGM amplitude of 2.12, 2.28 $^{o}/oo$ in the Arabian sea,the Holocene-LGM amplitude in the equatorial core SK-20-186,is 1.5 $^{o}/oo$.Duplessy (1982) has also noted such a reduced amplitude in this region and commented that "this amplitude is lower than the ice volume effect alone (1.6 $^{o}/oo$) for south of 10^{o}N".According to him, this reduction is present even in cores with a high sedimentation rate,often going upto 1.27 $^{o}/oo$ and therefore cannot be an effect of bioturbation.He explained it to be due to a marked increase in the precipitation over oceanic regions south of 10^{o}N during LGM which depleted the $\delta^{18}O$ and decreased the amplitude. This interpretation, though supported by GCM simulation of Prell and Kutzbach (1988) indicating an increased precipitation over the western Indian ocean during LGM, however, still remains to be substantiated. Recent studies by Labeyrie et al. (1987) (the same French Laboratory) show that the global ice volume effect is only 1.1 $^{o}/oo$, contrary to 1.6 $^{o}/oo$ believed before. If true, then the 1.5 $^{o}/oo$ amplitude in SK-20-186 need not be taken as an indication of an increased oceanic precipitation as proposed by Duplessy. It can as well be explained by a combination of 1.1 $^{o}/oo$ ice volume effect

and a decrease in SST by ~ 2°C during LGM, at this equatorial region. However, Labeyrie et al.'s estimate of such a low ice volume effect is a radical proposition and still being debated.Their observation demands that the deep sea temperature was 2-3°C lower during LGM to be consistent with the results of benthic foraminifera.Such a relatively large reduction in deep sea temperature requires an increase in the rate of thermohaline overturn (Mix and Pisias 1988) during LGM.But the available data suggest that this rate was lower,associated with a reduction in the rate of deep water formation (Shackleton et al.,1983;Berger and Vincent 1986). In such a situation it is difficult to conclude which of the two factors, namely increased precipitation or a reduced ice volume effect coupled with 2°C cooler SST, is responsible for 1.5 °/oo LGM-Holocene amplitude in SK-20-186.

Summarising, individual shells of planktonic foraminifera show significant isotopic variability (probably due to seasonal change, depth stratification, ontogenic development, metabolic effect, etc.). However, analysis of large population as a whole does not show such variability mainly because the isotopic variations due to the factors cited above, are averaged out.In the northern Indian ocean, modern G. sacculifer from the core top sediments, have been found to grow in isotopic equilibrium with ambient water. Long term $\delta^{18}O$ stratigraphies from 5 cores based on analyses of G. sacculifer, give climatic records of the last 30 kyr to more than 400 kyr in the

northern Indian ocean. The major global $\delta^{18}O$ cycles and amplitudes in these records are present with some modifications. Holocene-LGM amplitudes in the Arabian sea cores are much higher than global ice volume effect, indicating that in general entire Arabian sea was 1-2 $^{o}/oo$ more saline than today. In addition, these cores show differences (where fine scale sampling was done to improve time resolution) among themselves, consistent with the proposed effect of increased salinity in the northern Arabian sea during LGM. Such a climatic condition was perhaps caused by a vigorous NE-monsoon circulation with simultaneous weakening of the SW-monsoon. The equatorial Indian ocean, on the contrary, was characterized by heavy precipitation or lower LGM-SST.

III.2.6. High Resolution $\delta^{18}O$ Study of the Cores from the Arabian Sea and the Equatorial Indian Ocean

Apart from the long term changes, palaeoclimatic records in the deep sea cores also contain high frequency events corresponding to short term phenomena. These include a sudden input of meltwater into the sea (meltwater spike, Kenneth and Shackleton 1975; Keigwin et al. 1984), stepwise deglaciation (Berger et al. 1985a,b; Duplessy et al. 1986) etc. Most of these transient climatic phenomena are lost, mainly due to the bioturbation on the sea floor (Bard et al 1987) in cores with a low sedimentation rate. Additionally, stable isotope analysis performed at large intervals (several thousand years) tend to average out these signals

(Shackleton and Opdyke 1976), thus either completely obliterating or making a substantial reduction in the amplitudes of these high frequency events.One common method, to recover these signals from the cores which show evidence of bioturbation, is to use the so-called "unmixing models" (Berger et al 1977a).But these models are successful only under suitable circumstances. In any case, when one is looking for short term events,it is essential that isotope analysis be performed at intervals as close as possible to improve the resolution.Such a high resolution (even upto 1 cm. level) stratigraphy has been successfully used earlier, to derive local climatic information (Johnson 1980;Berger et al. 1985a,b).However,obtaining a meaningful signal,from high resolution $\delta^{18}O$ analysis,specially in cores with a low sedimentation rate, requires that the core should be devoid of bioturbation (Jones and Keigwin 1988) in order to avoid spurious noise (Vincent et al. 1981). The best way of recovering short-term signals, is to use cores with high sedimentation rates, if available (Broecker 1988b).While it is difficult to obtain cores with high sedimentation rates from the deep sea,those raised from near the continents do often have considerable sedimentary flux due to high productivity and/or terrigenous input.However,one should be cautious while interpreting the data obtained from such cores since their records are substantially influenced by near coastal processes (Duplessy 1982).

In the present study,we have performed high resolution $\delta^{18}O$ analysis of 5 species of planktonic foraminifera from

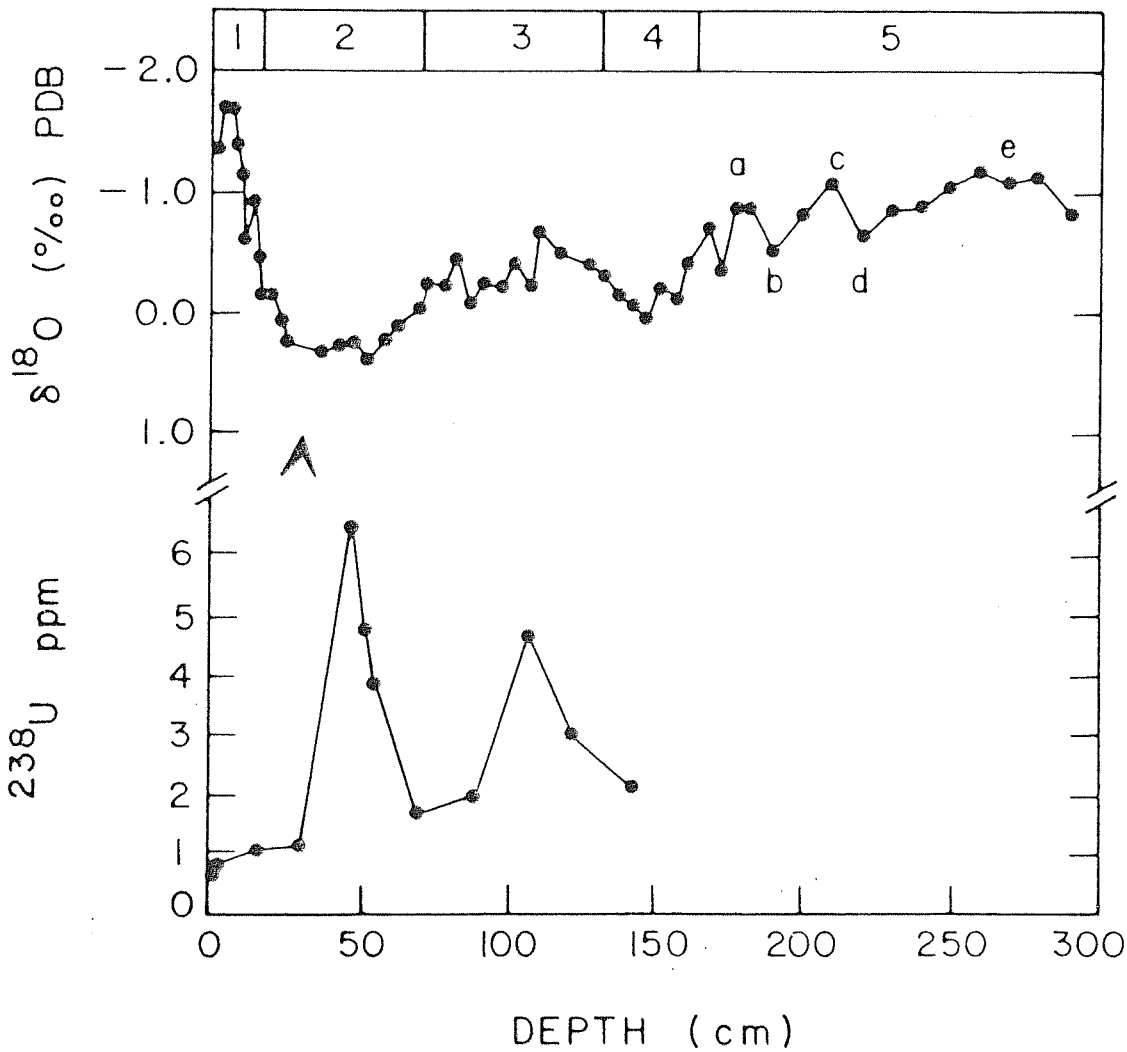

Fig. 3.12 : Variation of ^{238}U as a function of depth in core SK-20-185. $\delta^{18}O$ stratigraphy is also shown as time marker.

core SK-20-185 (Fig. 3.13).Before we discuss the climatic implication of these $\delta^{18}O$ data,it is important to show that the original signals of $\delta^{18}O$ and ^{14}C in this core are not significantly altered by processes like bioturbation or alteration of ^{14}C dates by contamination with external carbonates, changing the chronology of climatic events.We show below, based on the uranium data and ^{14}C ages of different fractions of sediments, that bioturbation and contamination are probably negligible in this core.

III.2.6.a. Uranium Analysis and Bottom Water Conditions

In section III.1.2, it has been shown that in core SK-20-185 ^{238}U concentration gradually increases below (29-31) cm with a corresponding decrease in the Th/U ratios. ^{238}U concentration in deeper layers is higher by factor of 2 to 10 relative to the core top sections. The high concentration of uranium results from its incorporation into the sediments from the sea water as evidenced from $^{234}U/^{238}U$ ratio > 1 (see Table 3.4). Fig. 3.12 shows downcore variation of total ^{238}U (in ppm) as against $\delta^{18}O$ stratigraphy of G. sacculifer. The maximum ^{238}U concentration of 6.4 ppm (in bulk sediments) is observed at (40-45) cm, which corresponds to ^{14}C age of ~ 22 kyr.On the other hand, Holocene sediment layers are characterised by lower concentration of ^{238}U.A second peak in the uranium concentration is found at (105-110) cm.

High concentration of uranium in sediment layers can come from the following sources:

1. Deposition of uranium rich hydrothermal materials (Cochran,1982).

2. Diagenetic effects, resulting in removal of ^{238}U from bottom water to sediments under suitable redox conditions (Cooley and Thompson 1985).

In addition,presence of coral debris containing uranium can produce false uranium enrichments in sediments,if its concentration is expressed on a carbonate free basis. Presence of such debris can be easily ascertained by looking for aragonite with XRD. Recently, Shankar et al (1987) have reported high uranium content in surface sediments close to the Laccadive ridge,a region adjacent to that of core SK-20-185. They obtained very high values of uranium concentration ranging from 12-16 ppm (on a $CaCO_3$ free basis) and explained it to be derived from coral debris. Since during glacial time the sea level was lower, terrigenous input was likely to be increased,bringing coral carbonates upto the present core location. However, all earlier studies showed that corals can contain a maximum of only 3 ppm of uranium.Additionally,U-content in corals has been shown to be remarkably constant for last 5 million years (Broecker and Peng 1982). Hence the uranium concentration of upto ~ 6.4 ppm (on bulk basis) in sediments cannot be explained by contributions from corals.

The site of core SK-20-185 is far away from any active

hydrothermal ridge systems and hence hydrothermal deposits are unlikely to be the cause of the observed high uranium layers.

That leaves the second mechanism to be responsible for high uranium concentration i.e. the removal of uranium from the sea water to the sediments under reducing conditions.In general, under oxidising conditions, U forms uranyl ion (UO^{+2}) in which U has a hexavalent state,and forms soluble complexes like $[(UO_2)(CO_3)]^{-4}$.Under reducing conditions in sediments, this hexavalent U (VI) is reduced to tetravalent state U (IV) (Weber and Sackett 1981;Faure 1986),which can be fixed into sediments more easily.However,there is some debate over the exact mechanism of this fixation.Uranium fixation may be due to the formation of an insoluble U^{+4} species or adsorption/complexation of U^{+4} by organic matter (Burton 1975; Dymond et al. 1973).The creation of reducing conditions in sediments would depend on many factors, important one among them being the flux of organic matter to the sediment surface.Therefore,a correlation may exist between U-concentration and organic matter in sediments. High U content from organic matter (OM) rich sediments from the coastal Arabian sea and several other shallow water sediments have been reported earlier (Borole et al. 1982b); they showed a positive correltion between U and OM.In core SK-20-185 also, we believe that the high uranium layers result from its incorporation into sediments from bottom waters. Such an incorporation would require these layers to be reducing so that uranium can be fixed into them in U^{+4}

state. The sediment accumulation rate of core SK-20-185 is nearly uniform over the past 30 kyr. However, the accumulation rate of $CaCO_3$ during the LGM stage was only 50% of that in Holocene (see section III.3) perhaps due to higher productivity during Holocene.If $CaCO_3$ is a measure of supply of organic matter to sediment surface,then it would require that organic matter supply to sediments was higher during the Holocene than during the LGM.Pore water oxygen may be consumed for this oxidation of OM in the Holocene sediments and an oxic/reducing boundary layer may have formed around the vicinity of the Holocene/LGM boundary (40 cm).This reducing layer would fix uranium from pore water to solid phase,thereby creating a concentration gradient in pore water uranium. The peak in ^{238}U concentration at various levels may arise because of change in the flux of organic matter.Presence of black coloured sediments around the depths where high uranium was observed indicates the presence of higher organic carbon content. This can be verified only by the measurement of total organic carbon in the sediments. Earlier, Fontugne and Duplessy (1986) recorded higher organic carbon content during LGM in the eastern Arabian sea.Our uranium data indicate that in the deeper layers of sediments a reducing condition is produced which provides a better preservation of organic matter, relative to the upper Holocene part.In addition, a low oxygenated condition in bottom water during LGM would have given rise to better preservation of organic matter. Recent work by Kallel et al (1988),based on the ^{13}C

analysis of benthics has recorded the development of a deep water mass (below 2000 m) depleted in oxygen during LGM.As a result glacial sediments below 2500 m in eastern Arabian sea do not contain sufficient benthic foraminifera (cibicides) which generally grow in well oxygenated water. Such a situation might have enhanced the preservation of organic matter in sediment layers during LGM which might have acted as a concentration sites for uranium.Furthermore, complexation of organic matter and uranium in a low oxygenated condition can also give rise to high uranium concentration during LGM.However,exact mechanism of uranium fixation is not very clear at the moment for which further close analysis of uranium all through this core is required. Occurrence of glacial low-oxygenated deep water has an important implication for retrieving climatic information based on the high resolution $\delta^{18}O$ record.Prevalence of low-oxygenated condition means the near absence of benthic fauna which in turn implies a negligible bioturbation at least in glacial sections. Consequently the transient climatic events during glacial periods can be recovered if high resolution analyses are performed.

The second problem that can affect the conclusions regarding past climates, is the uncertainty due to contamination in determining ^{14}C ages.

III.2.6.b. Reliability of the ^{14}C Ages:

Radiocarbon ages on bulk sediments are often subject to contamination by lateral advection of old fine grained

carbonate (Berger et al. 1985b),making the ^{14}C ages older by 2-4 kyr.This alters the chronology of climatic events.In the Arabian sea, radiocarbon ages are often biased towards older ages, because of the transport of dust carbonate particles from the continents to the ocean.This effect is most dominant near the coast of Arabia (J.C. Duplessy, personal communication, 24.3.1989). The best way to get rid of this problem is to date the same species of foraminifera by accelerator mass spectrometry (Duplessy et al. 1986),for which $\delta^{18}O$ analyses have been performed. The second alternative, which is less accurate but more viable,is to date coarse carbonate fraction (> 63 μm or > 150 μm) which is predominantly composed of foraminiferal specimens. Consequently, we have dated three different fractions of sediments in this core at three different depths:(0-2) cm, (23-25) cm and (40-45) cm (see Table 3.1) along with bulk sediments.As explained in Table 3.1,these 3 fractions are:

1. Size fraction > 63 μm, consisting of juvenile and mature forams

2. Size fraction > 150 μm, consisting of only mature forams,and

3. Size fraction < 63 μm, consisting of fine carbonate powder and nannoplanktons.

As can be seen,for (0-2) cm and (23-25) cm depths different fractions yield same age,within one standard deviation.At

(40-45) cm, fine fraction (< 63 μm) is older than the coarse (> 63 μm) fraction but not by a large amount considering the errors in the measurements. Hence we infer that in this core, ^{14}C ages are not significantly altered by fine older particle contamination and bulk ages can be taken as representative of the true ages.

Based on the above considerations we can safely conclude that neither the $\delta^{18}O$ record nor the ^{14}C ages are seriously degraded by bioturbation and/or contamination. The following section discusses the implication of high resolution studies in SK-20-185.

III.2.6.c. High Resolution $\delta^{18}O$ Studies in SK-20-185 and its Climatic Implication

Five planktonic species were chosen for analyses. These are Globigerinoides sacculifer, Globigerinoides ruber, Orbulina universa, Globorotalia menardii and Pulleniatina obliquiloculata. Anlyses have been done at 2 cm intervals from surface to 37.5 cm and at 5 cm intervals from 37.5 to 47.5 cm, corresponding to resolutions of 1 and 2 kyr respectively (based on a constant sedimentation rate of 2.2 cm/kyr upto 70 cm depth, see section III.1). All the species have been picked up from a narrow size range of (250-400) μm, excepting Orbulina universa (400-500 μm) in order to avoid the contribution due to ontogenic developments (Berger et al. 1978b). In all cases, 30-40 individuals were analysed per aliquot. Results of the analysis are given in Table 3.9 for G. sacculifer and Tables 3.14 to 3.17 for

Table 3.14

Oxygen and Carbon Isotope Data* on Core SK-20-185

Depth (cm)	$\delta^{18}O_{PDB}$ (°/oo)	$\delta^{13}C_{PDB}$ (°/oo)
2.50	-1.87	1.43
4.50	-2.24	1.32
6.50	-2.23	1.27
8.50	-1.90	1.01
10.50	-1.89	1.25
12.50	-1.17	1.17
14.50	-1.45	0.90
16.00	-1.37	0.84
18.00	-0.61	1.17
20.00	-1.21	0.96
22.00	-0.72	1.11
24.00	-0.48	1.21
26.00	-0.21	1.19
28.00	-0.42	1.30
30.00	-0.53	1.24
32.00	-0.75	1.21
34.00	-0.67	1.23
37.50	-0.28	1.04
42.50	-0.42	1.26
47.50	-0.63	0.85

* Measured on G. ruber (250-355) μm with 30-40 individuals per aliquot.

Table 3.15

Oxygen and Carbon Isotope Data* on Core SK-20-185

Depth (cm)	$\delta^{18}O_{PDB}$ (°/oo)	$\delta^{13}C_{PDB}$ (°/oo)
2.50	-1.49	1.94
4.50	-1.61	1.80
6.50	-1.44	1.50
8.50	-1.38	1.61
10.50	-0.69	1.62
12.50	-0.63	1.21
14.50	-0.52	1.34
16.00	0.01	1.45
18.00	0.08	1.44
20.00	-0.12	1.51
22.00	0.38	1.43
24.00	0.38	1.47
26.00	0.43	1.35
28.00	0.23	1.47
30.00	0.31	1.71
32.00	0.05	1.72
34.00	-0.69	1.66
37.50	0.65	1.58
42.50	0.20	2.01
47.50	0.22	1.94

* Measured on *O. universa* (400-500) μm with 30 individuals per aliquot.

Table 3.16

Oxygen and Carbon Isotope Data* on Core SK-20-185

Depth (cm)	$\delta^{18}O_{PDB}$ (°/oo)	$\delta^{13}C_{PDB}$ (°/oo)
4.5	-0.94	0.60
6.5	-0.96	0.58
8.5	-1.04	0.59
10.5	-0.58	0.57
14.5	-0.11	0.50
16.0	-0.04	0.59
20.0	0.12	0.65
22.0	0.55	0.65
24.0	0.82	0.67
26.0	1.03	0.92
28.0	0.85	0.62
32.0	1.13	0.76
34.0	1.13	0.76
37.5	0.95	0.70
47.5	0.95	0.70

* Measured on P. obliquiloculata (250-400)μm with 30-40 individuals per aliquot.

Table 3.17

Oxygen and Carbon Isotope Data* on Core SK-20-185

Depth (cm)	$\delta^{18}O_{PDB}$ (°/oo)	$\delta^{13}C_{PDB}$ (°/oo)
2.50	-0.81	1.37
4.50	-0.82	1.37
6.50	-1.02	1.34
8.50	-0.74	1.16
10.50	-0.21	1.21
12.50	-0.15	1.47
14.50	-0.52	1.13
16.00	-0.04	1.36
18.00	0.64	1.39
20.00	0.15	1.48
22.00	0.51	1.53
24.00	0.78	1.61
26.00	0.87	1.63
28.00	0.59	1.57
30.00	0.87	1.70
32.00	0.40	1.42
34.00	0.65	1.65
37.50	0.80	1.71
42.50	0.57	1.62
47.50	0.79	1.54

* Measured on G. menardii (250-400) μm with 30 individuals per aliquot.

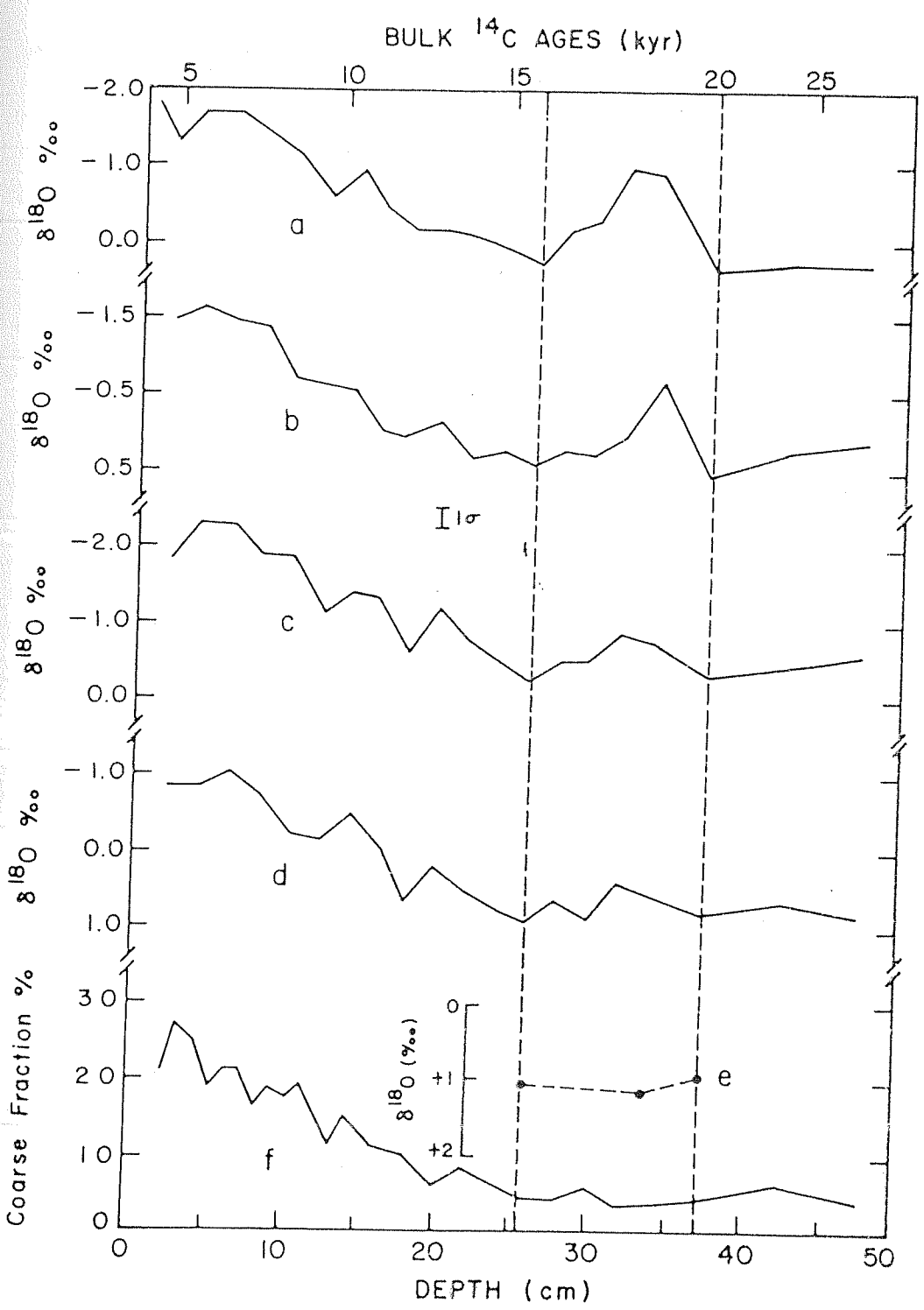

Fig. 3.13 : $\delta^{18}O$ values as a function of depth in core SK-20-185 for G. sacculifer (a), O. universa (b), G. ruber (c) and G. menardii (d). Percentage coarse fraction is also shown (f). Radiocarbon ages of the bulk sediments are shown on the top. $\delta^{18}O$ values of P. obliquiloculata are shown (e) for comparison

other species and plotted in Fig. 3.13.

Glacial to interglacial amplitude (GIA) in all the species excepting G. menardii, are ~ 2 °/oo and consistent with the earlier result (Duplessy 1982), from nearby locations. Holocene G. ruber value of -2.2 °/oo also agrees well with earlier measurements (op. cit.). Absolute $\delta^{18}O$ values in these species show an interesting sequence.For example, $\delta^{18}O$ values of shallow water species G. sacculifer are significantly more negative than the $\delta^{18}O$ values of deeper water species G. menardii, If the $\delta^{18}O$ differences are solely due to depth habitat, then the ranking,with increasing depth habitat,should be as follows:

G.sacculifer → O.universa → P.obliquiloculata

G.ruber G.menardii

The difference in $\delta^{18}O$ between G. sacculifer,G.ruber and G.menardii, P.obliquloculata is 0.8 to 1.3 °/oo,the second group being heavier. This indicates temperature difference of 4 to 6°C in their calcification zones.This ranking agrees with that observed from the Pacific (Berger et al. 1978b) and Indian oceans (Be 1977;Shackleton and Vincent 1978). Table 3.18 is a comparison of depth habitats of these species based on plankton tow and $\delta^{18}O$ data from the Indian ocean.

In Fig. 3.13, radiocarbon dates of bulk sediments are shown on the top. The ^{14}C age pips have been drawn to indicate integer values for clarity and the positions of the pips have been obtained roughly based on the actual

Table 3.18

Depth Habitats of Different Planktonic Foraminifera

Species	Depth	Reference
G.saculifer/G.ruber	0-50 m	Be, 1977
G.sacculifer	Within mixed layer	Duplessy et al., 1981a
G.sacculifer/G.ruber	Surface	Present work; Shackleton and Vincent, 1978
G.ruber/O.universa/P.obliquiloculata	No apparent depth preference	Duplessy et al. 1981a
O.universa/P.obliquiloculata	50-100m	Be, 1977, Shackleton and Vincent, 1978
O.universa	Deeper than G.ruber	Present work
P.obliquiloculata	Below mixed layer	Present work
G.menardii	Below mixed layer	Present work
G.menardii	Within mixed layer	Duplessy et al.1981a
G.menardii	> 100 m	Be, 1977
G.menardii	~ 200 m	Shackleton and Vincent, 1978

ages in Table 3.1.

The most notable feature of Fig. 3.13 (shown enclosed between two vertical dashed lines), is the negative excursion of $\delta^{18}O$ during LGM, lasting approximately for 4 kyr (16 to 20 kyr). Though all the four species show this, the magnitudes are different: ~ 1 °/oo in G. sacculifer and O. universa, ~ 0.6 °/oo in G. ruber and ~ 0.4 °/oo in G. menardii. The coarse fraction > 150 μm) mainly consisting of foraminiferal tests also reduced to a minimum of 5% (Fig. 3.13f) during this period indicating lesser productivity (section III.3). From 16 kyr upwards the curves follow a normal monotonous decrease in $\delta^{18}O$. Since the magnitude of the pulse is much less in G. menardii (a deeper dwelling planktonic species), it can be inferred that the mechanism responsible for this pulse was predominantly of surface origin. Also, no difference in $\delta^{18}O$ values between 'peak' (34 cm) and 'background' (26 cm and 37.5 cm, Table 3.9, Fig. 3.13) levels was found in another deep dwelling species P. obliquiloculata (Fig. 3.13e). Having the most enriched $\delta^{18}O$ values among these species, G. menardii does not record the variation of the salinity and temperature of the euphotic zone (Duplessy 1982) and so is the case with P. obliquiloculata.

The negative pulse in $\delta^{18}O$ was confirmed by repeated analyses of these species extracted from multiple aliquots of the sediments. Thus, there was a period of about 4 kyr during LGM, when surface dwelling foraminifera in this region secreted isotopically lighter $CaCO_3$ shells.

We have already shown that benthic mixing in this core duging LGM was small due to prevailing low oxygenated conditions.Even if some amount of benthic mixing took place, a signal can be detected if the mixing scale length is low or if the amplitude of the signal is large enough to escape a complete wash-out.In the present case,the signal shows up even without the use of any 'unmixing' precedure. Application of unmixing model will only sharpen the pulse (Guinasso and Schink 1975) apart from introducing some spurious noise (Jones and Ruddiman 1982).We have also shown earlier, that dissolution effect in this core is almost absent (section III.2.4b) and ^{14}C concentrations are uncontaminated. Consequently, the negative pulse during LGM, is considered to be a genuine climatic signal.

Modern hydrographic conditions at the core site indicate a decrease in SST by 1-2^{o}C during summer (SW) monsoon period,caused by the thickening of mixed layer from 20 m to 80 m induced by the SW monsoon (Nair et al.,1989). During winter time, the NE monsoon current transports low salinity water from the Bay of Bengal to the eastern Arabian sea via south of Sri Lanka (Wyrtki 1971),decreasing the surface salinity at the core location by about 1 ^{o}/oo (Fig. 3.10b).

Numerous studies have shown that SW monsoon was weaker during LGM (Chapter I; Prell et al. 1980;Van Campo et al. 1982; Duplessy 1982;Prell 1984;Prell and Van Campo 1986) and the upwelling diminished. As a result,the Arabian sea SST was higher (Prell et al. 1980).It may be suggested that the

observed negative pulse is essentially due to this warming. However, explaining the entire 1 ^{o}/oo signal to be due to increase in temperature, requires an abnormal increase in SST of about 5^{o}C during LGM, for which there is no evidence (CLIMAP 1976). At present there is record of a small scale upwelling only near Minicoy Island (~ 8^{o}N, 73^{o}E, Init. Rep. D.S.D.P. 1974) during winter time and not at our core location (10^{o}N, 71^{o}50'E). If at all, the core site experiences reduction in temperature by 1-2^{o}C due to minor upwelling or mixed layer thickening during the SW monsoon (Wyrtki 1971; Nair et al. 1989). Since the SW monsoon was weaker during LGM, the mixed layer thickness would be reduced and cold nutrient rich bottom water supply would be less. As a result, the SST would be relatively increased by 1-2^{o}C, resulting in a decrease in the $\delta^{18}O$ of planktonic foraminifera upto a maximum of 0.4 ^{o}/oo, thereby explaining only a part of the observed signal. For the remaining part, we propose another mechanism.

In Chapter I, it has been shown that along with a weaker SW-monsoon, evidences (non-isotopic) of a strong NE monsoon during LGM were also found. This conclusion was based on the percentage of quartz (Kolla and Biscaye 1977), pollen (Van Campo et al. 1982) and $\delta^{13}C$ of organic matter (Fontugne and Duplessy 1986). Today, the NE monsoon circulation brings low salinity water from the western Bay of Bengal to the eastern Arabian sea. If duirng LGM the NE monsoon was stronger, increased precipitation in the SE coast of India and increased run-off from the southern rivers, viz., Cauvery,

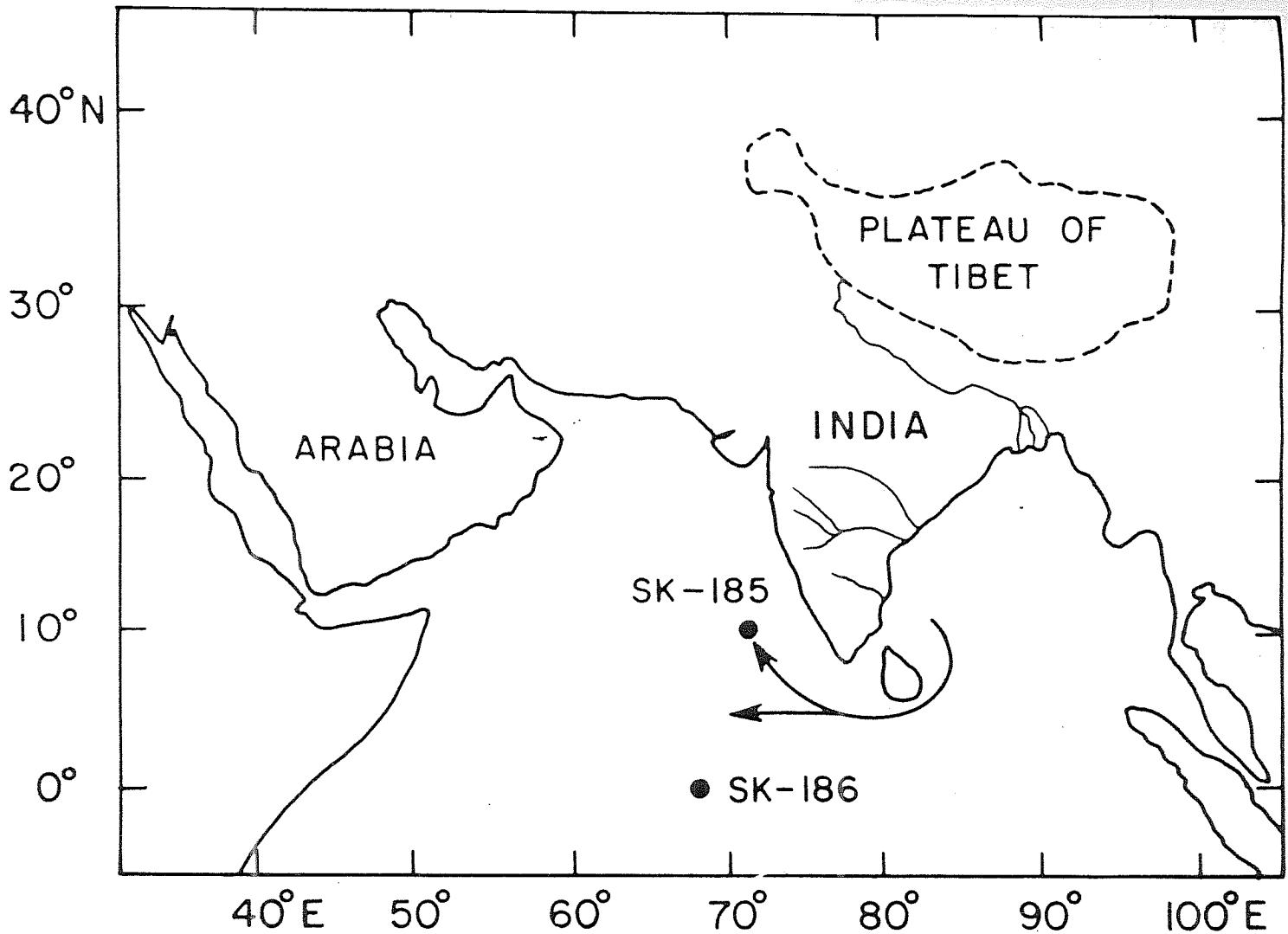

Fig. 3.14 : Inferred path of low salinity water (shown by arrows) transported from the Bay of Bengal to the eastern Arabian sea during winter time, by a reinforced north-east monsoon current. Note that the SK-20-186 location did not receive the low salinity water; it does not reach this location even today (Fig. 3.10b).

Godavari, etc., would result in a further lower salinity in the SW Bay of Bengal.Today,most of the annual rainfall in Tamilnadu and eastern Andhra Pradesh, is received during NE-monsoon which causes cyclonic storms and occasional floods in these regions.This,coupled with reinforced trade winds and atmospheric circulation (op. cit.), would intensify the NE monsoon oceanic current. As a result increased amount of low salinity water would have been transported to the core location.The inferred path of this transport of low salinity water is shown by the arrows in Fig. 3.14. The transport of low salinity water along this route takes place even today, however, its magnitude increased during LGM, due to the intensified NE-monsoon circulation.

To substantiate the above scenario we need to look critically at the available evidence on the salinity of the Bay of Bengal during LGM.It is known that the Bay of Bengal and the Arabian sea were more saline (compared to today) during LGM due to the decrease in the river water discharges caused by weaker SW monsoon system.However, between the two basins the Bay of Bengal was less saline. Unfortunately, the earlier work in this region was confined mostly to eastern and central Bay of Bengal and the evidence regarding salinity of western Bay of Bengal is lacking. Nevertheless,if the salinity difference between the two basins was similar to that of today,and the annual circulation in the eastern Arabian sea was dominated by the NE monsoon current the surface water at the core location

would have less salinity than otherwise expected.

Below we compute the probable effect of this salinity reduction on foraminiferal $\delta^{18}O$.

Present day salinity-$\delta^{18}O$ relation in eastern Arabian sea is given by the following equation (calculated from the data of Duplessy et al.1981a).

$$\delta^{18}O(\,^{o}/oo) = (0.32)S-10.97$$

where S is the salinity in $^{o}/oo$.

This relation implies that for a 1 $^{o}/oo$ drop in salinity, the $\delta^{18}O$ value will reduce by about 0.32 $^{o}/oo$ in this region. Assuming that this relation is valid for the LGM ocean, 0.6 $^{o}/oo$ of the total pulse 1 $^{o}/oo$ would require a salinity decrease (due to transport of low-salinity water) of about 2 $^{o}/oo$.

Thus, a total reduction of ~ 1 $^{o}/oo$ in $\delta^{18}O$ would result from a combination of temperature increase (~ 0.4 $^{o}/oo$) and salinity (~ 0.6 $^{o}/oo$) decrease due to transport of fresher water by increased NE monsoon circulation. *G. menardii* being deeper dwelling, records only the lack of mixed layer thickening (~ 0.4 $^{o}/oo$) whereas the other species show the full effect of ~ 1 $^{o}/oo$. *G. ruber*, though surface dwelling, has a lower pulse ~ 0.6 $^{o}/oo$. The negative $\delta^{18}O$ anomaly of varying magnitude in different planktonic components has been reported earlier (Showers and Margolis 1985) and has been attributed to migration of depth habitat. Currently no evidence exists to show that *G. ruber* depth habitat changed during LGM. Therefore the reduced magnitude could be due to

changes in seasonal abundances. G. ruber abundance peaks in summer and fall whereas O.universa has more or less uniform abundances throughout the year (Deuser 1978). G. sacculifer, though presumably has a higher summer abundance, may have some winter contribution as well, thus recording the salinity variation during LGM-winter. This record of SK-20-185 is compared with that of SK-20-186 in the following section.

III.2.6.d. Comparison with the High Resolution Stratigraphy of SK-20-186

Along with SK-20-185, high resolution $\delta^{18}O$ stratigraphy on G. sacculifer, was also performed in core SK-20-186. The close spaced analysis on this equatorial core was done from LGM to Holocene (Table 3.10). Considering the 2.4 cm/kyr sedimentation rate (Fig. 3.2) in the upper part, this means a climatic resolution of < 1000 years. A magnified plot of this core from the LGM to the Holocene (Fig. 3.15) shows the characteristic decrease in the $\delta^{18}O$ values due to deglaciation. The negative excursion of $\delta^{18}O$, as seen in SK-20-185, is, however, absent probably because the NE monsoon current did not reach this location. This is consistent with the ocean circulation pattern prevailing today, where the low salinity tongue does not reach upto this equatorial region (Fig. 3.10b).

The monotonous decrease in $\delta^{18}O$ in this core, halts at a depth of 19.5 cm and remains constant (or slightly enriched) upto 15.5 cm, indicating a quiescent stage in the

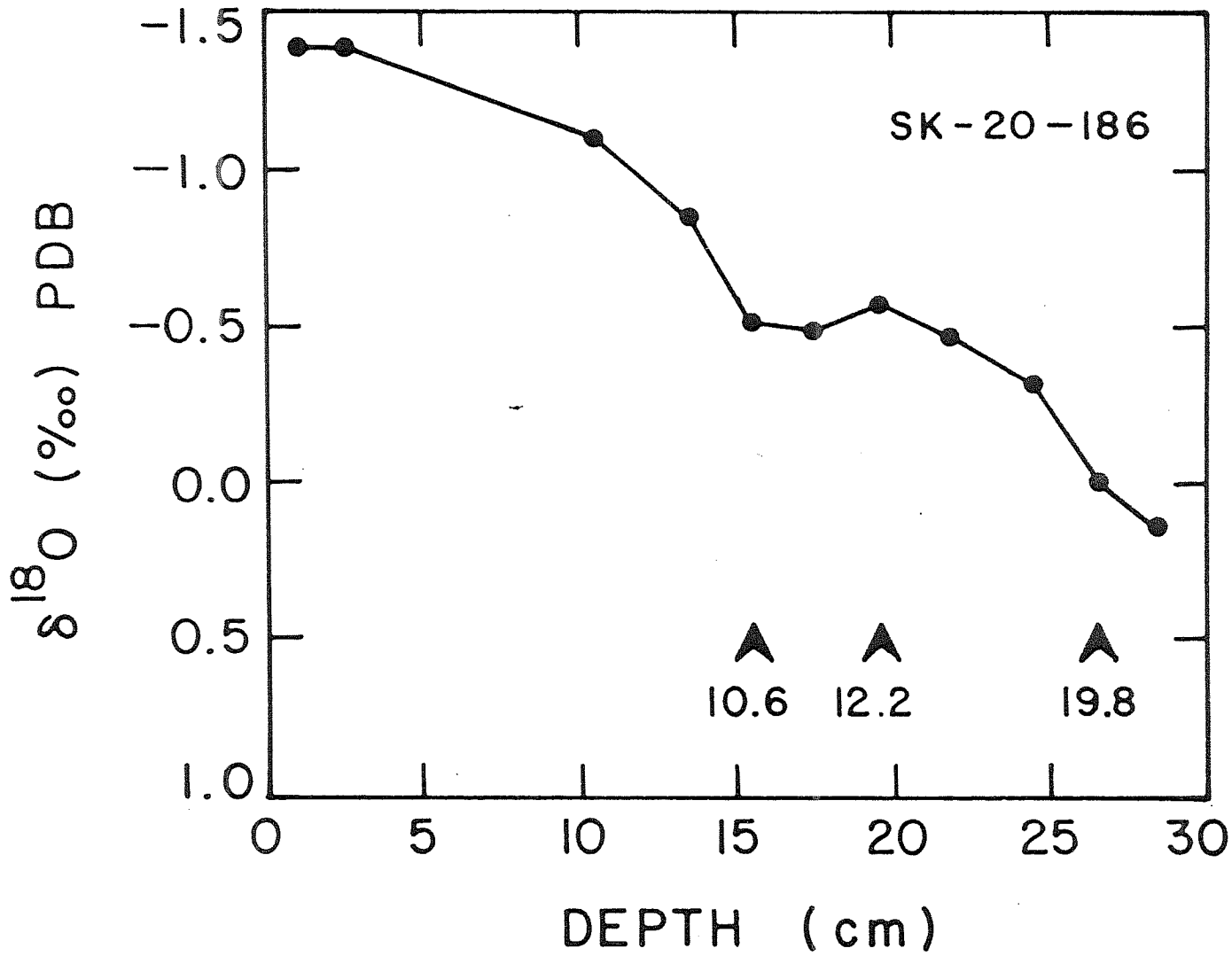

Fig. 3.15 : $\delta^{18}O$ values as a function of depth in SK-20-186. Exploded view from Holocene to LGM shows a two-step deglaciation (centered around 11 kyr), but not the negative excursion during LGM.

deglaciation (note that break and reduction in sedimentation rate in this core occur at 22-23 cm. depth below and not during the Holocene segment).This cessation of deglaciation is confined between 10-12 kyr (^{14}C age). Such a stepwise nature in the deglaciation associated with a brief period of cold condition has been reported from other oceans and correlated with the continental 'Younger Dryas' period (Ruddiman and Duplessy 1985;Berger et al. 1985a, b). Timing of this event has been a matter of controversy. Accelerator mass-spectrometer dating in recent years has substantially resolved this issue and the time bracket has been put as 10-11 kyr (Broecker et al. 1988a). As can be seen from the figure,the step in SK-20-186 is also centred around 11 kyr and thus can be correlated with 'Younger Dryas'. Similar step-wise deglaciation in high sedimentation rate cores, from the W-Arabian sea has also been noted by Prell (1984b).These observations contradict the idea that the 'Younger Dryas' event was a local one, strongest in the vicinity of N-Atlantic and weak or absent in records from south of $45^{o}N$ (Broecker et al. 1988a; Broecker et al. 1988b). Our data indicates the probable global nature of the effect of 'Younger Dryas' event.

III.2.6.e. Mechanism of Freshwater Intrusion at the site of SK-20-185 during LGM

At present, the intrusion of Bay of Bengal water during winter time, into the SE Arabian sea takes place along two routes,one along the west coast of India and the other along

$5^{o}N$ (Fig. 3.10b). The intrusion along $5^{o}N$ is mainly due to the NE monsoon circulation, which brings low salinity water to the southern Arabian sea. This low salinity water intrudes northward along the west coast (Fig. 3.10b) (SE-Arabian sea), by a strong thermohaline circulation, the mechanism of which is described below.

The pronounced density stratification, found in this region (SE-Arabian sea) is very well correlated with the salinity stratification, indicating that salinity controls the density field. During winter time salinity gradient (north-south) in this part, is higher than that in summer time (Fig. 3.10). This is because the NE-monsoon circulation brings low salinity water along $5^{o}N$ (in Arabian sea), which enhances the gradient. This produces a drop in sea surface dynamic height (density), and subsequent intrusion of low saline water northwards. Mass transport in such a case is expressed by (Pankajakshan and Rama Raju 1987):

$$T_S = \frac{g\Delta}{fk^2}\left[1 - \frac{1}{KD}(1-e^{-KD}) - \frac{S}{D}(1-e^{-KD})\right]$$

where, g = gravitational acceleration

f = coriolis parameter

$1/k$ = density gradient along depth

D = depth of the ocean

S = depth upto which transport takes place

and Δ = meridional density gradient at the surface.

Since $1/k$ and $S \ll D$,

$$T_s = g\Delta/fk^2$$

T_s can be compared with amount of surface Ekman transport due to strong wind stress.The Ekman transport is expressed by T_i/f,where T_i is longshore wind stress and f is coriolis parameter. During SW monsoon period, salinity gradient is less (i.e. Δ is less).Consequently $T_i/f > T_s$ and hence no thermohaline transport occurs. During NE monsoon, on the other hand, the salinity gradient is increased.Taking the winter time density (salinity) gradient $\Delta = 1.5.10^{-11}$ gm/cm, T_s has been calculated to be 9.10^3 gm/cm/sec.This is 3 times larger than the Ekman transport (T_i/f) value of $2.5.10^3$ gm/cm/sec, calculated for the same time (op. cit.). Hence, the thermohaline transport dominates over Ekman transport during winter period resulting in intrusion of low saline water further northward.

We assume that the salinity gradient in the Arabian sea increased by ~ 50% during LGM. Taking LGM Δ value as $2.25x10^{-11}$gm/cm and considering 1/k as of today, we calculate ~ 13.10^3gm/cm/sec value for T_s during LGM.This is 5 times larger than present day winter value of T_i/f,which either remained constant or reduced.Such a situation should make much stronger thermohaline circulation than today, taking more of the low salinity water north upto and beyond the present core site.

It can be however, argued that during LGM salinity of Bay of Bengal was higher due to lower river discharge from Ganges-Brahmaputra river system.A closer look at Duplessy's (1982) core sites would reveal that most of the cores are from eastern Bay of Bengal,while no core was raised from

western Bay of Bengal, where southern rivers drain their water. In this part a pronounced low salinity pocket (upto 32 $^{o}/oo$, Fig. 3.10b) is produced even today during NE monsoon season. During this season, Ganges has a total discharge of water upto about $2.4.10^{11}$ cubic meter (from December to May, 10 year-average,UNESCO 1971),into the Bay of Bengal. This is 10 times lower than the discharge during monsoon months ($\sim 2.2.10^{12}$ cubic meter,June to November,10 years average, op. cit.). In this respect, today's Ganges discharge during winter perhaps mimics the discharge during LGM-summer (Duplessy 1982). Even if we accept that Ganges discharge during LGM reduced by 50%,the salinity could not have been higher than 32-33 $^{o}/oo$. Hence, though today's assymetry in salinity between the Arabian sea and the Bay of Bengal reduced during LGM,we believe that Bay of Bengal was still less saline than the Arabian sea.This,coupled with increased precipitation along east-coast due to stronger NE-monsoon and increased evaporation-induced thermohaline circulation in Arabian sea perhaps,brought significant amount of the low salinity water to the present core site.

Our results, thus indicate that the phase during which the NE-monsoon was stronger,lasted for a maximum of 4 kyr during LGM. It is of interest to note that an indication of stronger NE monsoon circulation in this region was obtained by Van Campo et al (1982) based on pollen analysis of a core taken from western Arabian sea.Their studies indicate that during (19-25) kyr ago ther was a high relative

frequency of taxa from Mediterranean steppe, indicating strong NE trade winds. Considering the uncertainty of the dating and methodology, we think their study provides an independent evidence of the same phenomenon of particularly intense phase of NE monsoon circulation.This was possibly caused by the build up of glacial ice over Himalayas and Tibetan plateau, which enhanced the land to sea temperature contrast in winter and reduced it during summer (Duplessy 1982). Evidence based on terminal moraines,for the existence of huge ice sheets on Tibetan plateau has been reported (Kuhle 1987). The estimated areal extent of this ice sheet was 2-2.4 million sq. km. (larger than the Greenland ice cap, 1/3 of Laurentide ice sheet) with an average thickness of 700-1200 m. This is in contrast to the assumption of CLIMAP group that high Asia was little glaciated during LGM (CLIMAP 1976). As the ice sheet gradually built up,it reached a critical size,enough to energise the NE-monsoon, usually a weak one, to become highly active.As the global ice sheets melted,so did the Tibetan ice,bringing back the north-east monsoon to the present day levels. It is speculated that the peak seen in $\delta^{18}O$ (Fig. 3.13) between 26 and 37 cm in SK-20-185,is a crude measure of the excess ice that was required to increase the NE monsoon activity. The duration for which this excess ice lasted is not clearly known otherwise.Pollen evidence from north-western Himalaya (same latitude as Tibetan plateau) indicates that deglaciation started around 15 kyr B.P. (Singh and Agarwal 1976). It is therefore likely that the excess ice lasted for

about 3 kyr (18 to 15 kyr).

In conclusion, our study of high resolution $\delta^{18}O$ analyses on multiple species of planktonic foraminifera, on a core from SE Arabian sea shows an oxygen isotope evidence of a stronger NE-monsoon during the last glacial maximum. The spatial and temporal extent of this intensification should be further studied using cores raised from several locations in the southern Arabian sea and especially from the western Bay of Bengal and the south of Sri Lanka, where more significant $\delta^{18}O$ anomaly (and drop in salinity) is expected.

III.3. Carbon Isotope Studies of the Ocean Cores

$\delta^{13}C$ values for all the 5 cores are given in Tables 3.9 to 3.12. These measurements have been made on G. sacculifer. In addition, high resolution $\delta^{13}C$ analyses were made (along with simultaneous measurements of $\delta^{18}O$, see section III.2.6) on four other species viz., G. ruber, O. universa, P. obliquiloculata and G. menardii upto 47.5 cm depth (~ 25 kyr, ^{14}C age) in core SK-20-185. Data for these species are given in Tables 3.14 to 3.17.

In section III.2.1, it has been shown that the species G. sacculifer does not grow in isotopic equilibrium as far as carbon isotopes are concerned. If the calculated $\delta^{13}C$ value at the site of SK-20-185 (i.e. 3.77 $^{o}/oo$, Table 3.8) is compared with the core top $\delta^{13}C$ values of the four other species cited above, it is seen that none of them grows their shells in isotopic equilibrium with surface water

ΣCO_2. However, an apparent depth habitat is discernible from their absolute $\delta^{13}C$ values. The deep dwelling P. obliquiloculata is depleted by ~ 1 °/oo than the surface species G. sacculifer and G. ruber. This is consistent with the $\delta^{13}C$ ΣCO_2 profile in the water column (Chapter 1), which shows that the deep water is depleted with respect to surface water and confirms our previous inference from $\delta^{18}O$ data regarding depth habitat of different species. This simplified picture, however, does not fit with the observed values of O. universa and G. menardii. The former one is 0.2-0.4 °/oo enriched compared to G. ruber while the latter has the same $\delta^{13}C$ values as those of surface species. The $\delta^{18}O$ measurements, on the contrary, show greater depth habitats for both these species. This indicates that the magnitude of disequilibrium fractionation is not constant and perhaps species dependent (Grossman 1987). However, as discussed in Chapter 1, we consider that the extent of this vital effect, has remained constant in the past.

A plot of the $\delta^{13}C$ data against depth, for five planktonic species from SK-20-185, is shown in Fig. 3.16 where 9 kyr (early Holocene) and 20 kyr (glacial) periods (^{14}C ages) are indicated by bold arrows. As can be seen, all the top 3 species viz., G. sacculifer. G. ruber and O. universa show a more or less similar $\delta^{13}C$ stratigraphy. To remove the effect of single "wild" points, a 5 points moving average has been run to smooth out the data. Dashed lines in Fig. 3.16 represent the smoothed trends which reveal the following features:

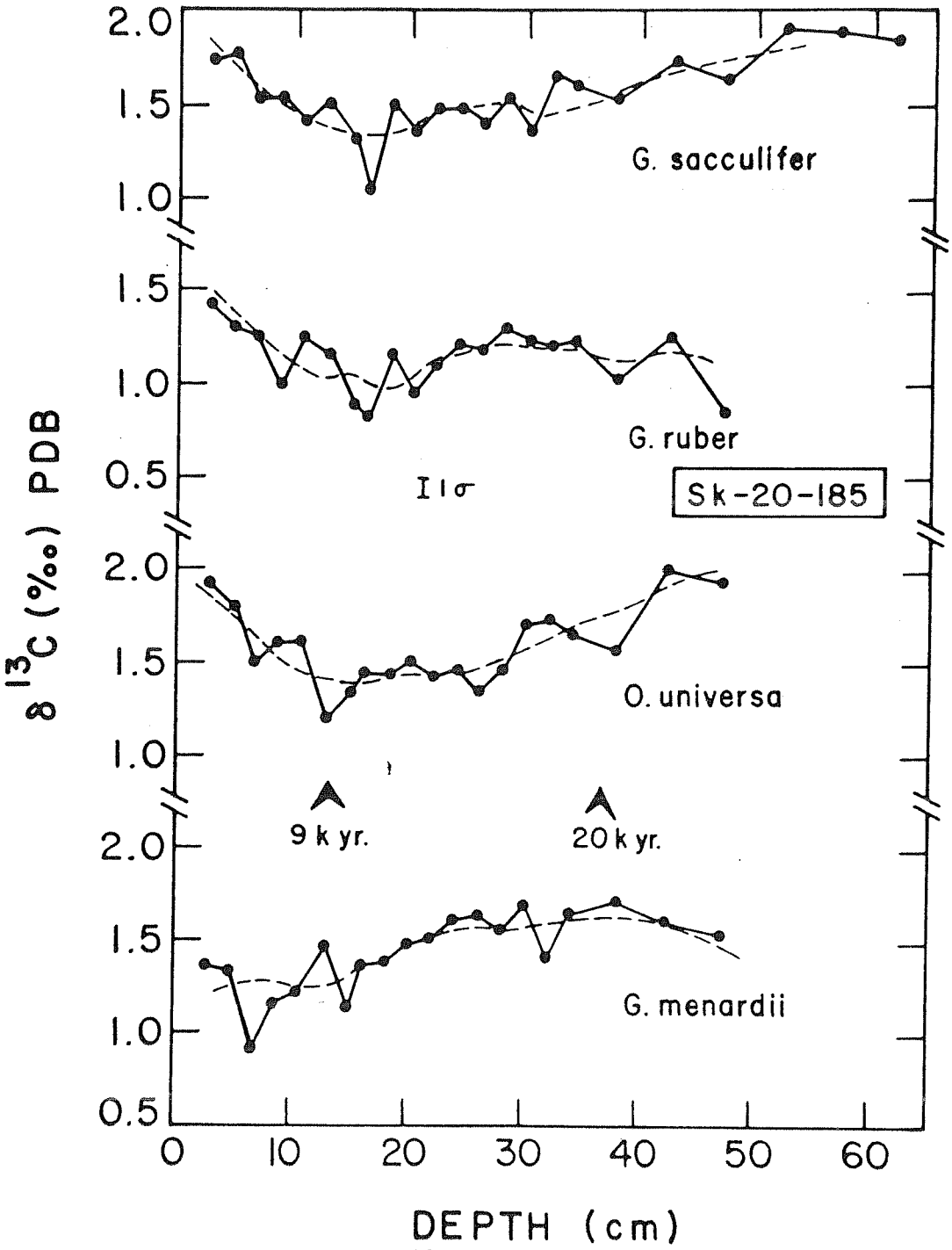

Fig. 3.16 : $\delta^{13}C$ values as a function of depth in SK-20-185 for 4 planktonic species. Glacial period (20 kyr) and early Holocene (9 kyr) periods are shown by bold arrows.

1. There are $\delta^{13}C$ minima in G. sacculifer, G. ruber and O. universa around 9 kyr period. The magnitude of these minima between surface to 9 kyr period is about (0.5 ± 0.1) °/oo.

2. With respect to 9 kyr B.P., glacial $\delta^{13}C$ values in these species show an enrichment by 0.2 °/oo (G. ruber) to 0.6 °/oo (O. universa).

3. For G. menardii, no difference in $\delta^{13}C$ value is seen between surface and 9 kyr B.P. level. However, glacial value is enriched relative to surface (present) by ~ 0.4 °/oo.

Additionally, P. obliquiloculata (not plotted in Fig. 3.16, Table 3.16) shows almost constant $\delta^{13}C$ (~ 0.66±0.1 °/oo) throughout this length. A plot of $\delta^{13}C$ of G. ruber against $\delta^{13}C$ of G. sacculifer (Fig. 3.17) shows that they are positively correlated (correlation coefficient r = 0.6 which is significant at 2.5% level). A similar plot between G. sacculifer and O. universa is shown in Fig. 3.18 and the down core $\delta^{13}C$ values for these two species are also positively correlated (r = 0.6; sig. level = 2.5%). Such a concomitant variation in down-core $\delta^{13}C$ in several species of planktonic foraminifera, indicates likely major changes in ΣCO_2 reservoir in the Arabian sea during the last 25 kyr. A large number of models have been proposed to explain the downcore $\delta^{13}C$ variations in foraminifera

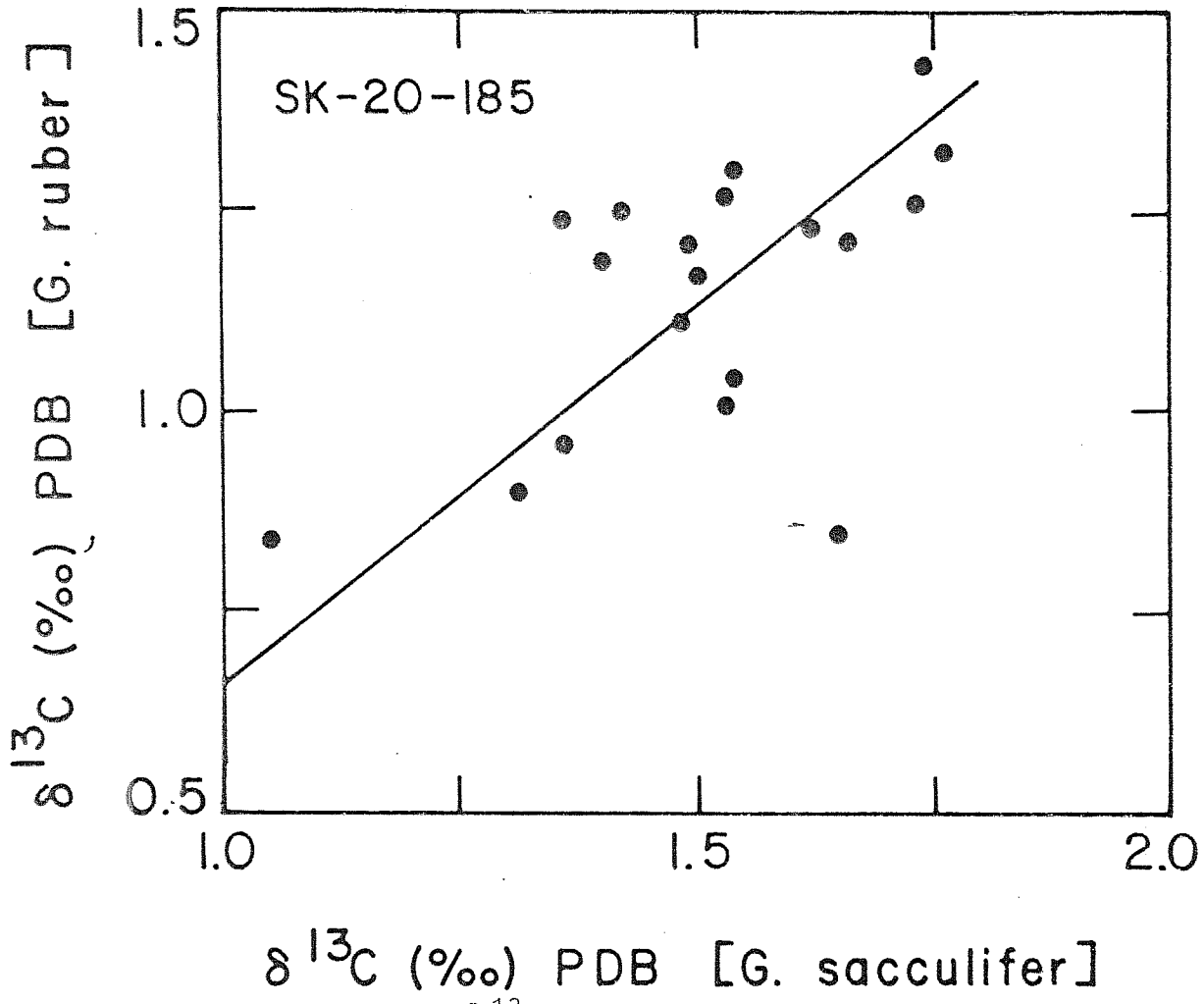

Fig. 3.17 : $\delta^{13}C$ values of G. ruber against G. sacculifer at various levels in SK-20-185 from glacial to Holocene. For the regression line shown in the figure, r = 0.6 and significant at 2.5% level.

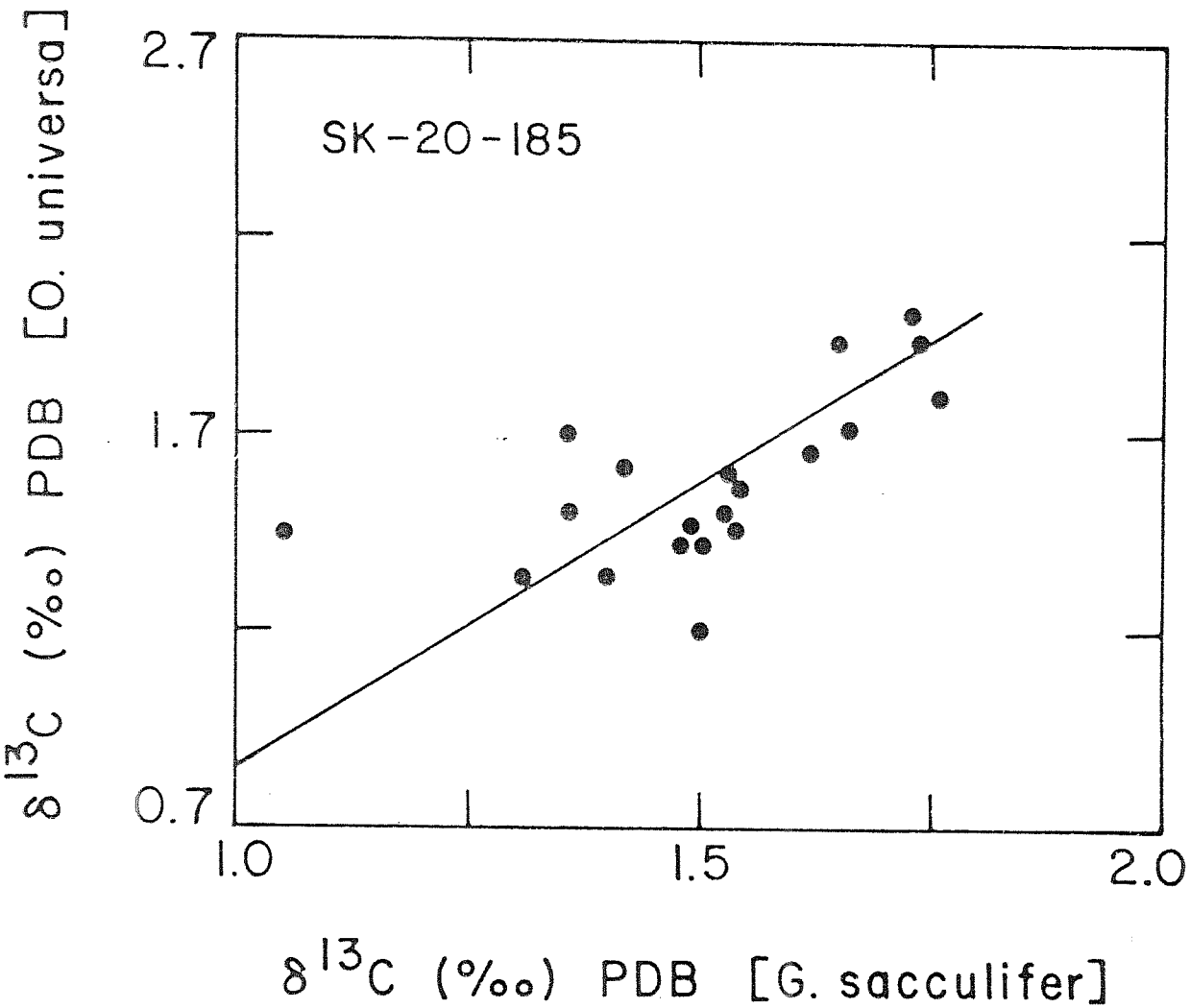

Fig. 3.18 : $\delta^{13}C$ values of O. universa against G. sacculifer at various levels in SK-20-185 from glacial to Holocene. For the regression line shown in the figure, r = 0.6 and significant at 2.5% level.

(Broecker and Peng, 1986). Recently Sarnthein et al. (1988) have made a strong case about the importance of biological productivity in the ocean in controlling the $\delta^{13}C$ of foraminifera and the variation in past atmospheric CO_2. In today's ocean, the productivity is largely controlled by mid and low latitude upwelling centres (op. cit.). In the Arabian sea also the copious productivity is mainly controlled by upwelling, which has varied in the past. We discuss below the downcore calcium carbonate measurements and show that a significant change in productivity had taken place in the past in the Arabian sea. Variation in $\delta^{13}C$ is then subsequently discussed in the context of this productivity change.

III.3.1. Calcium Carbonate and Palaeoproductivity

Two cores, SK-20-185 and SK-20-186, have been analysed for their calcium carbonate ($CaCO_3$) percentage. Data on $CaCO_3$ for these cores are given in Tables 3.19 and 3.20. Along with $CaCO_3$ percentage, coarse fraction (> 150 μm) is also measured. These are mainly mature foraminifera. The coarse fraction data are given in Tables 3.21 and 3.22.

Depth profiles of $CaCO_3$ and the coarse fraction abundances against depth for SK-20-185 is shown in Fig. 3.19. The $\delta^{18}O$ stages are also given in this figure for a chronological framework. Bold arrows indicate the 18 kyr level. $CaCO_3$ decreases from Holocene ~ 68% to LGM ~ 40%. $CaCO_3$ again increases to about 60% during the interglacial stage 5e. $CaCO_3$ and $\delta^{18}O$ exhibit a strong inverse

Table 3.19

Down Core $CaCO_3$ Data on SK-20-185

Depth (cm)	$CaCO_3$ (%)	Depth (cm)	$CaCO_3$ (%)
2.50	67.5	132.50	43.4
3.50	65.8	137.50	45.8
5.50	65.6	142.50	41.4
10.50	60.3	147.50	37.4
14.50	52.6	152.50	32.6
16.00	51.6	157.50	31.4
18.00	48.1	162.50	32.6
24.00	42.6	167.50	28.6
30.00	41.0	172.50	32.5
37.50	40.2	177.50	35.2
47.50	38.5	182.50	33.0
57.50	40.2	190.00	44.0
62.50	40.2	200.00	48.6
67.50	42.8	210.00	53.5
72.50	45.2	220.00	42.7
77.50	44.4	230.00	56.0
82.50	46.7	240.00	59.4
87.50	45.6	250.00	55.1
97.50	45.7	260.00	52.1
102.50	46.1	270.00	49.7
112.50	42.9	280.00	49.2
117.50	45.4	290.00	51.0
127.50	45.4		

Table 3.20

Down Core $CaCO_3$ Data on SK-20-186

Depth (cm)	$CaCO_3$ (%)	Depth (cm)	$CaCO_3$ (%)
2.50	87.8	21.50	81.8
3.50	87.1	22.50	80.2
4.50	89.0	23.50	88.5
5.50	80.1	24.50	82.5
6.50	86.7	25.50	83.2
7.50	85.8	26.50	82.2
8.50	86.4	27.50	81.4
9.50	86.4	28.50	82.0
10.50	83.8	29.50	81.8
11.50	87.9	30.50	81.3
12.50	84.9	31.50	82.0
13.50	82.0	32.50	83.7
14.50	82.6	33.50	82.8
15.50	83.3	34.50	82.6
16.50	77.8	35.50	82.7
17.50	84.3	36.50	86.0
18.50	83.3	37.50	82.7
19.50	82.5	38.50	82.6
20.50	83.4	39.50	83.7

Table 3.20 contd.

40.50	83.0	129.50	83.2
41.50	84.4	134.50	82.3
43.00	79.5	139.50	84.1
45.00	82.4	144.50	84.9
47.00	80.9	149.50	87.0
49.00	83.3	154.50	86.2
51.00	84.4	159.50	86.9
53.00	82.3	164.50	83.8
55.00	85.0	169.50	83.1
57.00	85.1	174.50	83.3
59.00	84.1	179.50	86.7
61.00	85.3	184.50	85.1
64.50	85.6	189.50	86.1
69.50	83.6	197.00	84.1
74.50	84.2	207.00	83.4
79.50	83.2	217.00	82.8
84.50	85.1	227.00	83.4
89.50	79.6	237.00	87.5
94.50	81.6	247.00	88.6
99.50	81.1	257.00	88.3
104.50	80.4	267.00	85.8
109.50	79.0	277.00	85.8
114.50	79.9	287.00	83.3
119.50	81.3	297.00	84.0
124.50	86.2	307.00	83.5

Table 3.20 contd.

317.00	83.3	407.00	87.1
327.00	83.4	417.00	86.4
337.00	83.7	427.00	87.5
347.00	82.8	437.00	86.5
357.00	83.5	447.00	86.7
367.00	85.6	457.00	87.1
377.00	88.9	467.00	87.9
387.00	81.5	477.00	88.7
397.00	85.5	487.00	84.1

Table 3.21

Down Core Coarse Fraction (> 150 μm) Data on SK-20-185

Depth (cm)	Coarse Fraction (%)	Depth (cm)	Coarse Fraction (%)
2.50	21.2	30.00	6.2
3.50	27.3	32.00	4.1
4.50	25.3	34.00	4.5
5.50	19.1	37.50	5.1
6.50	21.5	42.50	7.3
7.50	21.5	47.50	4.7
8.50	16.3	52.50	5.1
9.50	19.3	57.50	5.4
10.50	17.7	62.50	8.3
11.50	19.8	67.50	7.3
12.50	14.3	72.50	7.0
13.50	11.6	77.50	7.9
14.50	15.9	82.50	8.6
16.00	11.8	87.50	6.9
18.00	10.4	92.50	7.0
20.00	6.5	97.50	5.8
22.00	8.8	102.50	7.2
24.00	6.5	107.50	7.2
26.00	4.9	112.50	4.5
28.00	4.4	117.50	5.4

Table 3.21 contd.

122.50	11.5	182.50	3.5
127.50	8.2	190.00	3.4
132.50	8.3	200.00	8.9
137.50	9.1	210.00	13.3
142.50	5.4	220.00	5.2
147.50	3.9	230.00	5.0
152.50	4.8	240.00	5.0
157.50	2.7	250.00	9.5
162.50	1.9	260.00	8.4
167.50	1.5	270.00	6.4
172.50	1.9	280.00	3.9
177.50	2.0	290.00	3.1

Table 3.22

Down Core Coarse Fraction (> 150 μm) Data on SK-20-186

Depth (cm)	Coarse Fraction (%)	Depth (cm)	Coarse Fraction (%)
2.50	34.1	22.50	32.7
3.50	36.9	23.50	36.7
5.50	39.5	24.50	33.4
6.50	37.8	25.50	42.7
7.50	38.2	26.50	37.6
8.50	39.6	27.50	34.3
9.50	37.0	28.50	35.3
10.50	39.6	29.50	38.5
11.50	36.2	30.50	37.5
12.50	34.7	31.50	35.8
13.50	38.6	32.50	34.9
14.50	41.7	33.50	35.5
15.50	34.6	34.50	32.5
16.50	32.7	35.50	32.3
17.50	35.1	36.50	30.8
18.50	35.5	37.50	30.2
19.50	31.8	38.50	35.9
20.50	33.6	39.50	38.0
21.50	35.1	40.50	33.4

Table 3.22 contd.

41.50	33.3	134.50	21.9
43.00	33.2	139.50	23.0
45.00	27.7	144.50	20.4
47.00	32.3	149.50	23.5
49.00	30.4	154.50	28.3
51.00	33.7	159.50	35.4
53.00	34.0	164.50	32.9
55.00	29.2	169.50	25.2
57.00	33.6	174.50	22.9
59.00	35.1	179.50	33.0
61.00	28.8	184.50	28.2
64.50	35.5	189.50	28.1
69.50	28.7	197.00	28.7
74.50	34.0	207.00	31.5
79.50	32.3	217.00	27.9
84.50	36.3	227.00	16.2
89.50	33.2	237.00	10.2
94.50	30.2	247.00	15.6
99.50	31.5	257.00	21.4
104.50	34.7	267.00	22.3
109.50	37.3	277.00	29.7
114.50	34.8	287.00	17.6
119.50	36.5	297.00	15.3
124.50	34.2	307.00	14.6
129.50	30.8	317.00	19.3

Table 3.22 contd.

327.00	18.9	417.00	23.2
337.00	17.4	427.00	22.4
347.00	16.3	437.00	27.7
357.00	13.4	447.00	29.8
367.00	25.5	457.00	35.1
377.00	26.8	467.00	34.7
387.00	28.4	477.00	35.1
397.00	18.1	487.00	33.9
407.00	18.5		

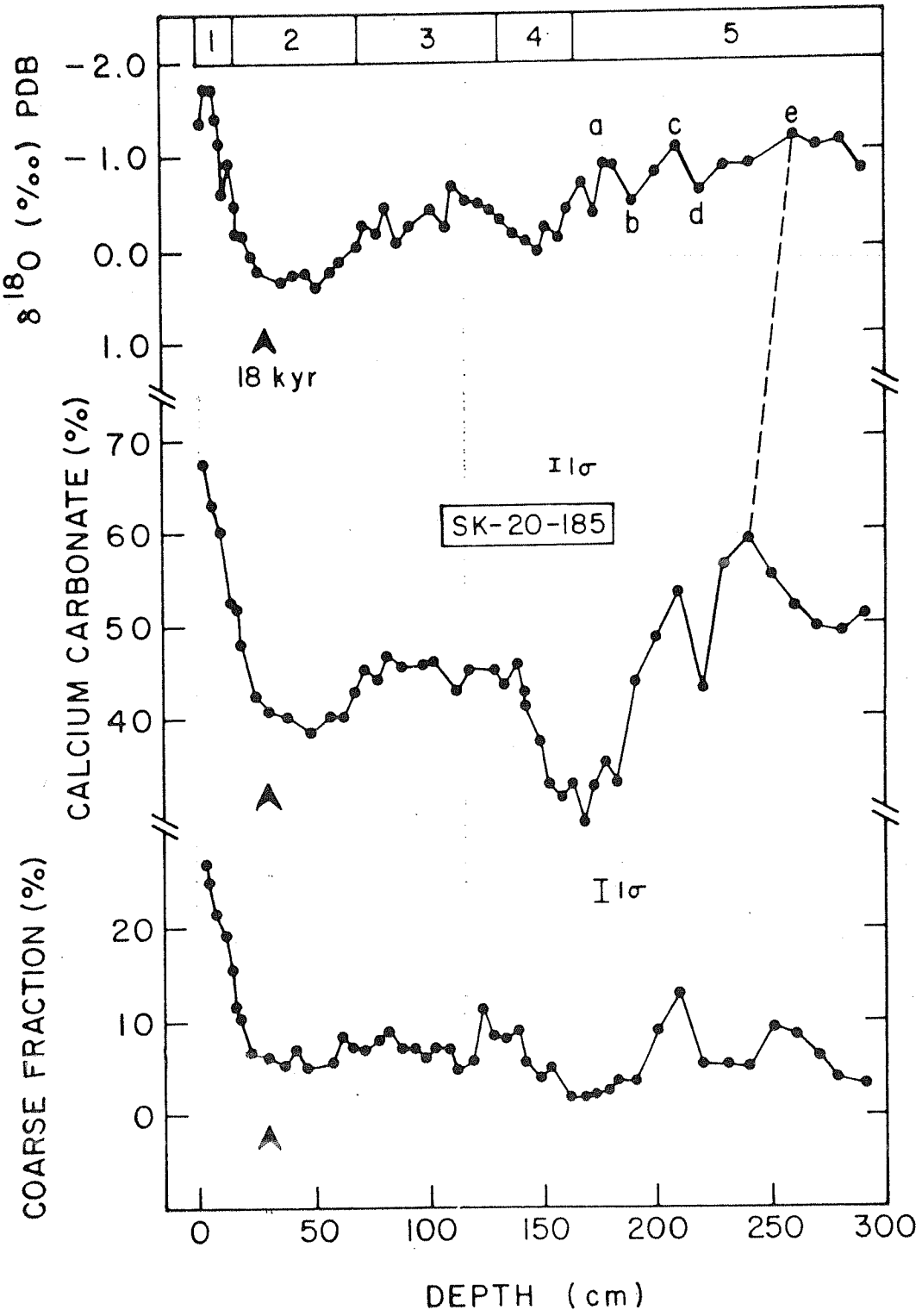

Fig. 3.19 : Depth distribution of calcium carbonate and coarse fraction in SK-20-185. $\delta^{18}O$ stratigraphy provides chronology. The 18 kyr level is shown by bold arrows.

correlation ($r = -0.6$) in this core, which is significant at 2.5% level (Fig. 3.20). Major $\delta^{18}O$ stages are also reflected in the $CaCO_3$ abundance profile. In stage 5e, however, only two $CaCO_3$ substages are found, against 5 substages in $\delta^{18}O$. As has been discussed in Section III.2.3, this can be due to the coarse sampling (at 10 cm intervals) below 150 cm depth. The coarse fraction amount also varies sympathetically with the $CaCO_3$ in this core. From 27% in Holocene, it decreases to 5% during LGM. During 5e stage, the coarse fraction does not increase to same degree as much as $CaCO_3$. Such a close parallelism between $CaCO_3$ and the $> 150\ \mu m$ fraction indicates that most of the $CaCO_3$ is biogenic in nature.

The depth profiles of $CaCO_3$ and the coarse fraction for the core SK-20-186, are plotted in Fig. 3.21 (along with $\delta^{18}O$). For the top 61 cm all the data points are not plotted in Fig. 3.21, but the general trend in $CaCO_3$ and coarse fraction abundance are shown. Unlike SK-20-185, the $CaCO_3$ variation in this core is only marginal. In general, the $CaCO_3$ % in this core is very high (~ 80%). Nevertheless, a Holocene value of 90% reduces to an LGM value of 80%. There exists an apparent correlation between $\delta^{18}O$ and $CaCO_3$ in this core as well (shown by dashed lines in Fig. 3.21). On the contrary, the coarse fraction percentage varies significantly with depth and does not show any relationship with either $\delta^{18}O$ or $CaCO_3$. A pronounced minimum in the coarse fraction % is found at 237 cm depth. Visual inspection under microscope shows that most of the coarse fractions in both the cores are composed of foraminifera

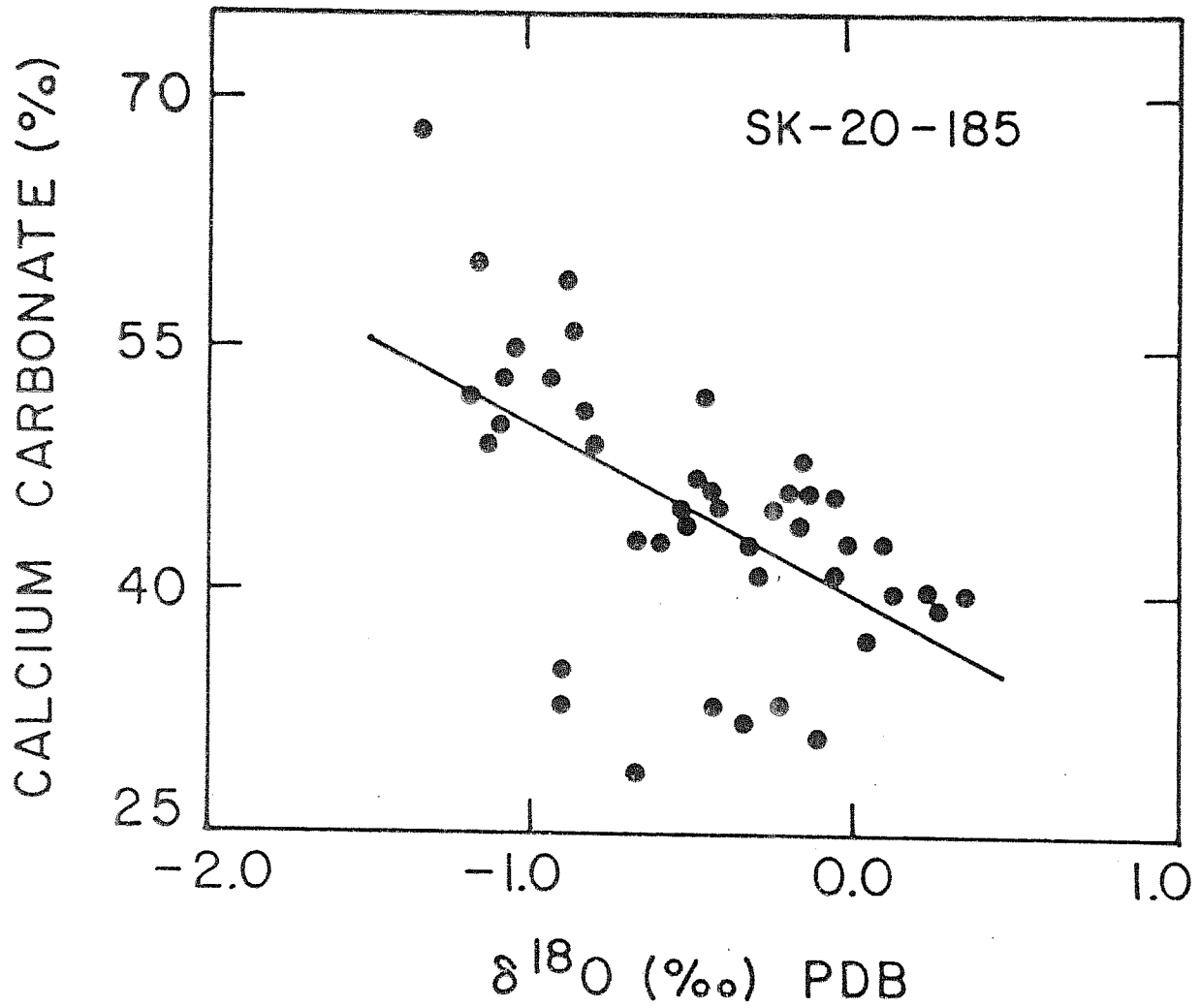

Fig. 3.20 : Scatter diagram of $CaCO_3$ vs. $\delta^{18}O$ for the entire length in SK-20-185. Best fit line indicates the negative correlation ($r = -0.6$, 2.5% level) between the two.

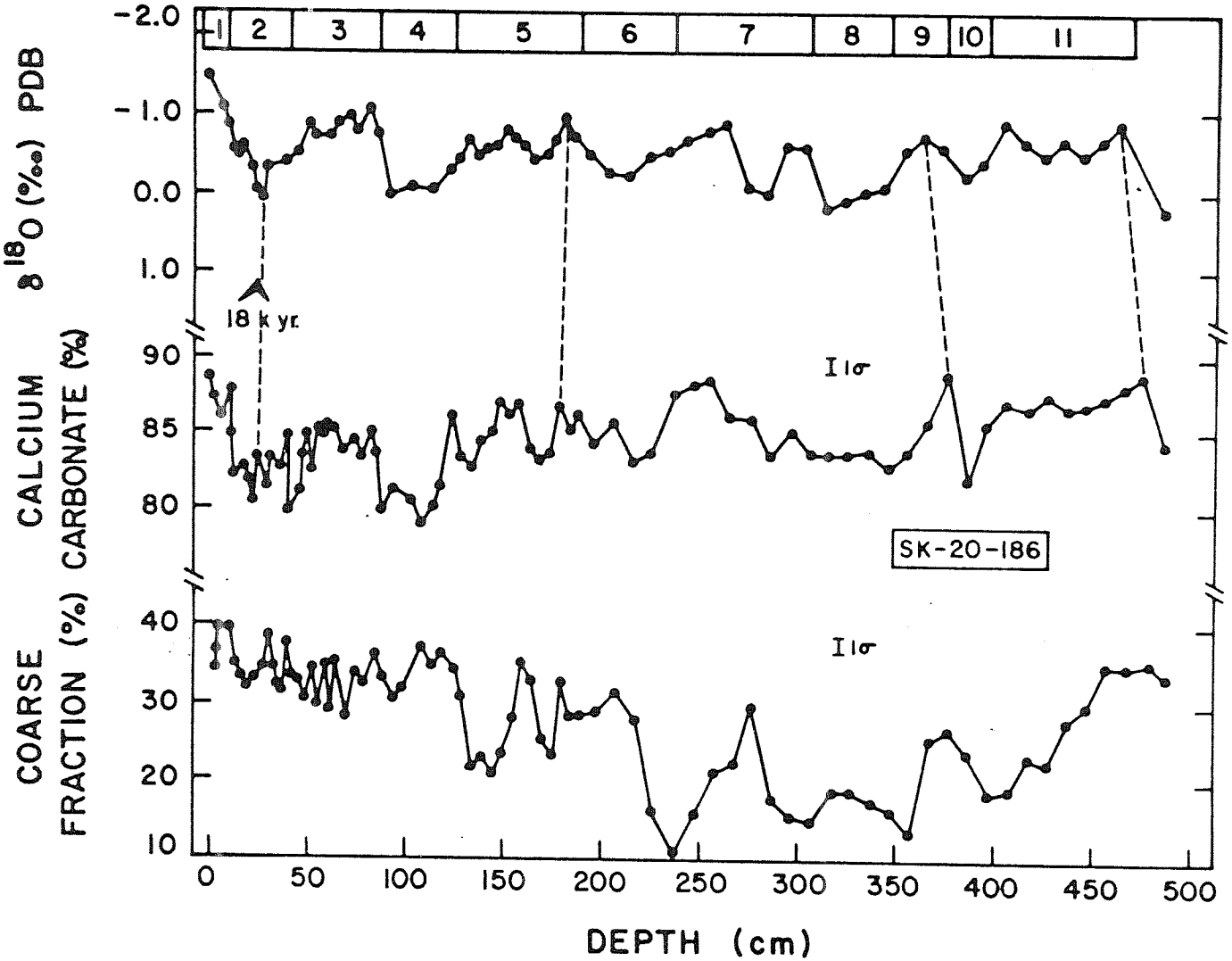

Fig. 3.21 : Calcium carbonate and coarse fraction abundance as functions of depth in SK-20-186. $\delta^{18}O$ stratigraphy and 18 kyr level (bold arrow) serve as time markers. Dashed lines indicate peak to peak correlation between $\delta^{18}O$ and $CaCO_3$.

and other form of carbonates are extremely small in proportion.

These fluctuations in downcore $CaCO_3$ can be due to three factors (Volat et al. 1980):

1. Variation in carbonate dissolution

2. Dilution by non-carbonate material i.e. variation in terrigenous input.

3. Variation in the biological productivity of calcareous planktons.

It is known for some time that variation in $CaCO_3$ in Pacific ocean is often a mirror image of the Atlantic pattern (Boyle 1983). While the interglacial in Atlantic ocean is represented by higher $CaCO_3$, that in the Pacific ocean shows low $CaCO_3$. Consequently the glacial Pacific has higher $CaCO_3$ content relative to interglacial (op. cit.). Berger (1968) found that in the Pacific, the ratio of solution susceptible to solution resistant species increased during glacial. This indicates that dissolution was lower in the Pacific during glacial period, resulting in a high $CaCO_3$ stage. Subsequently most of the explanations on $CaCO_3$ variation, was based on the change in dissolution intensity from interglacial to glacial period. In general, the Indian ocean shows a similar $CaCO_3$ pattern as that of the Pacific (Volat et al. 1980). A change in the global deep water circulation during the glacial period has been held responsible for such a pattern. For example, the formation of

North Atlantic Deep Water (NADW) makes the remaining North Atlantic surface water nutrient depleted. The nutrient rich NADW flows southward and becomes progressively enriched in CO_2 due to the respiration and oxidisation of benthic organisms. This CO_2 rich corrosive bottom water ultimately reaches the Pacific via the Indian ocean and enhances the dissolution of $CaCO_3$, producing lower $CaCO_3$ content in Pacific compared to Atlantic. Evidences are increasingly accumulating that production of NADW was much reduced during LGM (Berger and Vincent 1986). In such a case the $CaCO_3$ preservation cycle in two oceans would be reversed. This basin to basin fractionation, though held important, is not the only viable mechanism. Terrigenous input can also significantly dilute the $CaCO_3$ content. It is generally believed that the volume of eolian and fluvially transported material increased during the glacial period. Added to this was the effect of lowered sea-level, when more of terrigenous inputs could have reached the deeper basin (Volat et al. 1980).

Earlier we have shown (from $\delta^{18}O$ analysis of solution prone and solution resistant species) that dissolution was perhaps negligible for last 25 kyr in the core SK-20-185. The high $CaCO_3$ content of SK-20-186 perhaps also indicates insignificant dissolution, inspite of its depth being closer to CCD (~ 3.5 km). An earlier study by Luz and Shackleton (1975) in the tropical Pacific showed, that CCD plays an important role in controlling the $CaCO_3$ variation via dissolution. They observed that the $CaCO_3$ content during the

glacial and interglacial stages are similar in cores well above CCD, while the cores below it show significant fluctuations. In the present study, both the cores show almost similar downcore variation in $CaCO_3$ (i.e. glacial lower $CaCO_3$%) albeit their large differences in water depth. Consequently we consider that dissolution is probably unimportant for $CaCO_3$ variations in these cores.

During the LGM river discharge was much less in the Arabian sea. Also the Arabian basin received similar amount of continental detritus over last 18 kyr (J.C. Duplessy and R. Chesselet, preprint). The influence of terrigenous input can be estimated as follows. The amount of dilution by terrigenous material (non-carbonate) required to reduce an initial carbonate content C_i to some observed carbonate value C_f is given by (Gardner 1982):

$$\text{Addition of non-carbonate} = [(C_i/C_f)-1]/(1-C_i)$$

If we take surface $CaCO_3$ values for SK-20-185 and SK-20-186 as 68% and 90% respectively, and if we assume that the LGM value of 40% and 80% in them are purely due to dilution effect by terrigenous influx, then for SK-20-185, 220% and for SK-20-186, 125% increase in non-carbonate material are necessary to get the low $CaCO_3$ values in LGM. Such an increase would obviously change the bulk sedimentation rate at those places. The bulk sedimentation rate (^{14}C) of core SK-20-185 is 2.2 cm/kyr which remained constant for last 30 kyr and shows no major break during this period. SK-20-186

location receives very little terrigenous input today and bulk (^{14}C) rate shows a decrease by a factor of four during glacial period which is in opposite direction.Hence we infer, that variation in terrigenous input is unlikely to cause the down core change of $CaCO_3$ in these cores.

Therefore, we are left with the third option i.e. $CaCO_3$ variation is induced by a change in the productivity. Arrhenius (1952) proposed that higher $CaCO_3$ in glacial Pacific is mainly due to increased productivity caused by stronger oceanic circulation and increased upwelling.On the other hand, Atlantic workers hold a view of shifting the high productivity belt from polar to equatorwards,thus making low productivity (and low $CaCO_3$) stages in high and mid latitudes.

In the Arabian sea,however,the productivity variation is caused mainly by the change in upwelling intensity.In today's condition, though the strong centres of upwelling are known to occur only along coast off Arabia and Somalia, perhaps their effects are felt over most of the Arabian sea. The SST in the monsoon period (strong upwelling time) decreases by ~ $4^{o}C$ along the Arabian coast while over most of the Arabian sea ~ $1-2^{o}C$ drop in temperature is seen (Wyrtki 1971). This is due to the upwelling,horizontal advection and mixed layer thickening which supplies cold water to the surface rich in nutrient,thus supporting a high productivity. Recent sediment trap experiments by Nair et al. (1989) show that during the SW monsoon period,the total particle flux (mainly composed of biogenous

carbonates and opal) increases in most of the Arabian sea (east, central and west). Consequently,the weakening of SW monsoon (Duplessy 1982) and hence the upwelling and less thickening of mixed layer (Prell 1978) would decrease the productivity not only in the strong upwelling zones of today (Prell 1984a, b) but probably also in other parts of the Arabian sea.A decrease in the $CaCO_3$ during the glacial period in the cores from the NE Arabian sea has been reported earlier and was explained by a change in the productivity (Borole et al. 1982a).On the other hand,Nair and Hashimi (1980) have reported a high productivity in the west coast of India during the Holocene.The percentage of G. bulloides increased in the western Arabian sea around 9 kyr (Prell 1984b) indicating a stronger upwelling.This reinforced upwelling was caused by a stronger SW monsoon than today,when heavy rainfall produced high lake levels in surrounding continental areas (Street and Grove 1979).A vigorous SW-monsoon in this early Holocene period (~ 8-11 kyr) brought humid tropical pollen from Africa to Arabian sea (Van Campo et al. 1982) and sustained a luxuriant growth of Mangrove forest along the west coast of India (Van Campo 1986).Theoretical model simulations by Kutzbach (1981) and Kutzbatch and Otto-Bliesner (1982) indicate that the increased summer insolation around this period (~ 11 kyr) was responsible for such a stronger monsoon,when the temperature contrast between the Asian continent (Tibetan plateau) and the Arabian sea was enhanced. In section III.2.6.d we have shown that around 11 kyr B.P. there was a

pause in deglaciation (cold period?) in the $\delta^{18}O$ record of core SK-20-186. However,at this equatorial region monsoonal effect is absent. Additionally step in deglaciation ('Younger Dryas') is probably caused by some internal feedback mechanism unrelated to change in insolation (Broecker et al., 1988). Therefore, though the monsoon is directly linked to the northern hemispheric summer insolation, the cold 'Younger Dryas' stage is not. The enhanced land-ocean temperature contrast around 11 kyr produced by this insolation change, created low pressure cells over Asia, stronger than today, producing an intensified SW monsoon. Hence we find two climatic regimes in the Arabian sea for the last 25 kyr.Glacial weak monsoon, weak upwelling and low biogenic productivity and early Holocene (~ 9-11 kyr) intensified monsoon,stronger upwelling and higher productivity.We discuss below the effect of this change in upwelling and productivity on foraminiferal carbon isotope ratios, in relation to the downcore $\delta^{13}C$ variation in the different cores.

III.3.2. Upwelling,Productivity and $\delta^{13}C$

Phytoplanktons preferentially fix more ^{12}C than ^{13}C at the surface layer of the ocean.This carbon fixation makes the phytoplankton $\delta^{13}C$ ~ -19 to -26 °/oo,thereby enriching the ΣCO_2 of surface water by about ~ + 2 °/oo PDB (Kroopnick 1985). These organisms,after their death,settle down to deeper water.Their carbon is subsequently released by oxidation, making the deep water $\delta^{13}C\ \Sigma CO_2$ depleted.This

biologically controlled $\delta^{13}C \Sigma CO_2$ profile can be modified by disturbing the water column stability. For example, thickening of mixed layer and upwelling from deeper water may bring $\delta^{13}C$ depleted water up,which may deplete surface water $\delta^{13}C$. Consequently, in an upwelling dominated region, surface water $\delta^{13}C$ is a mixture of $\delta^{13}C$, induced by biological productivity and amount of water upwelled.

In today's condition,the surface water ΣCO_2 in Arabian sea has a $\delta^{13}C$ of ~ 1.6-1.8 °/oo (PDB) while that in the depth between 100 m and 200 m is 0-0.3 °/oo (PDB),(GEOSECS 1987). If upwelled water comes from a depth of 200 m or mixed layer thickening of 100 m takes place, then the maximum $\delta^{13}C$ difference between the upwelled water/water brought up by mixed layer thickening and the normal surface water would be ~ 1.5 °/oo. This difference is of course diluted by mixing within the water column, secondary production and the exchange of upwelled CO_2 with atmospheric CO_2.Hence one might expect a change in downcore $\delta^{13}C$ record upto ~ 0.5 to 1 °/oo (PDB),if any change in the upwelling took place in the past.

During the LGM, $\delta^{13}C$ values in different planktonic species show an enrichment by upto about 0.6 °/oo (Fig. 3.16) relative to the early Holocene (~ 9 kyr).We have shown earlier that the productivity in the Arabian sea was lower during glacial period,which should deplete the $\delta^{13}C$ of the $CaCO_3$.The fact that it shows an enrichment instead, indicates that the absence of upwelling masked the productivity effect. Less upwelling means less supply of

$\delta^{13}C$ depleted water to surface and consequent enrichment of $\delta^{13}C \Sigma CO_2$ of surface water. Similarly $\delta^{13}C$ depletion upto ~ 0.5 °/oo in 3 surface species (Fig. 3.16) around 9 kyr B.P. indicates a very strong upwelling caused by an intensified SW monsoon during this period. G. menardii, a deeper dwelling species shows a ~ 0.4 °/oo enrichment only during glacial period relative to 9 kyr period but no difference in the $\delta^{13}C$ is found between 9 kyr and present. This may be because of the deeper habitat of this species. If the upwelling around 9 kyr was essentially a surface phenomenon, G. menardii would not record its effect. During LGM, however, it records an enrichment which is an effect of lower glacial productivity, rather than upwelling. Lower glacial productivity would supply less organic matter to deeper level. Consequently the production of oxidised CO_2 would be less and $\delta^{13}C\Sigma CO_2$ would be enriched relative to today. P. obliquiloculata (with most depleted $\delta^{13}C$) has the deepest habitat (see section III.2.6) and is not affected by a change in the $\delta^{13}C$ gradient in upper water column, thereby not showing any change for last 25 kyr.

$\delta^{13}C$ values against depth, for the cores SK-20-186, CD-17-30 and CD-17-15 are plotted in Figs. 3.22 and 3.23. The $\delta^{13}C$ minimum around 9 kyr B.P. (as found in core SK-20-185) is not present in these cores. While SK-20-186 is far away from any upwelling centre, it is surprising that, a core (CD-17-30) nearer to the upwelling zone off Arabia, does not show any change in the $\delta^{13}C$ due to variation in upwelling. Prell and Curry (1981), however, observed that core

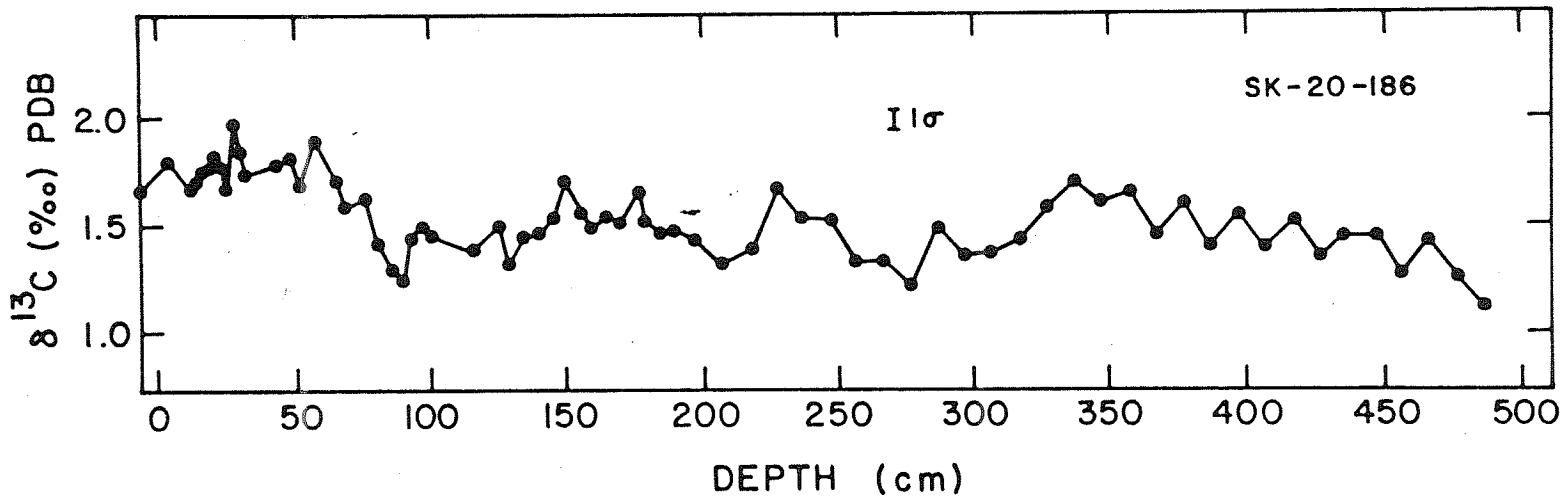

Fig. 3.22 : $\delta^{13}C$ values as a function of depth in SK-20-186.

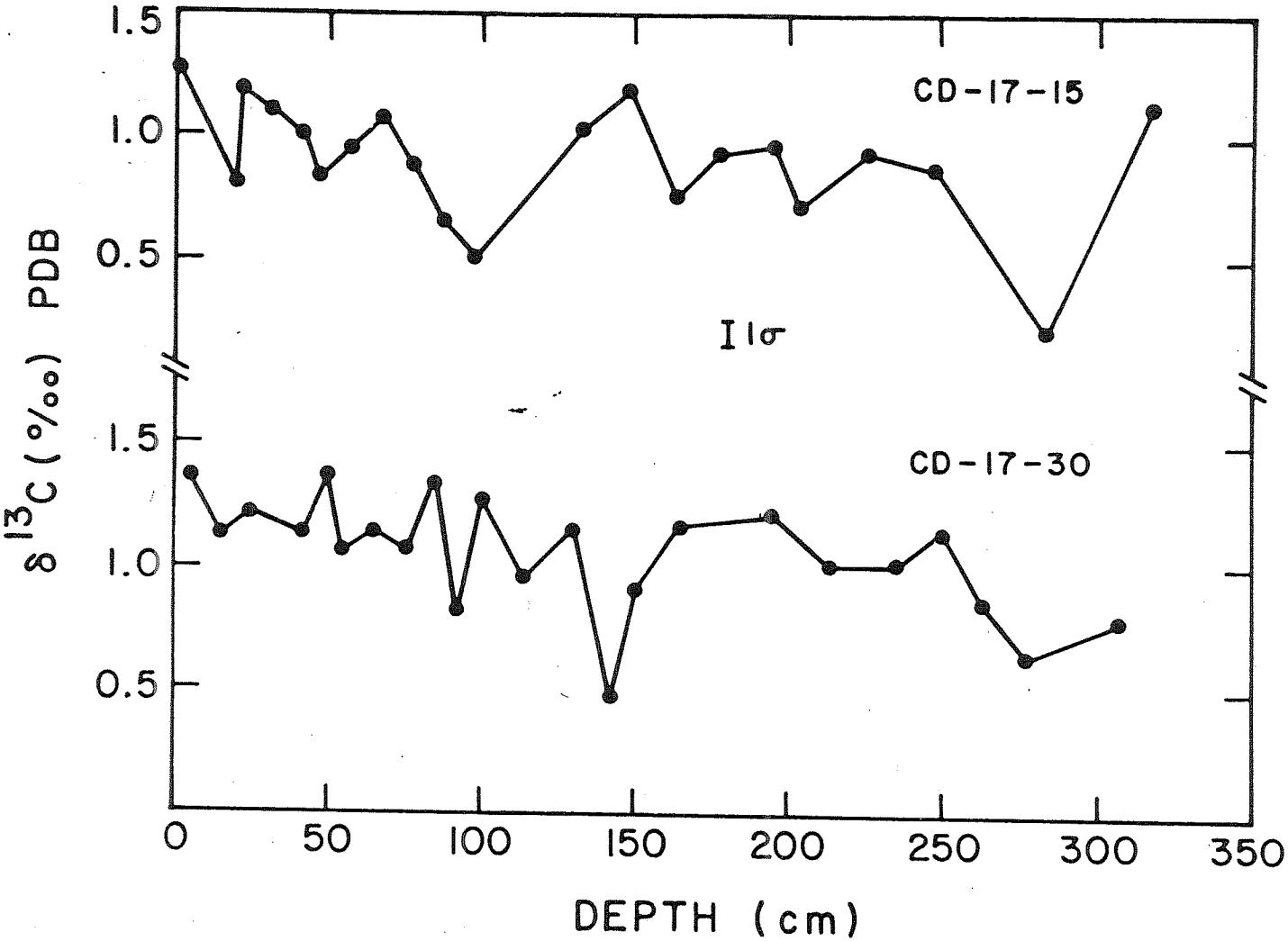

Fig. 3.23 : $\delta^{13}C$ values as functions of depth in CD-17-15 and CD-17-30

top foraminifera across this upwelling zone do not record any imprint of $\delta^{13}C$ change.It is possible,that owing to the vast nutrient supply in this zone, growth of planktonic foraminifera is very fast. Such fast growing species can suffer from severe disequilibrium "vital" effect (Berger et al. 1977b) which is not constant in magnitude, thus potentially damping the original signal.Further analysis of downcore $\delta^{13}C$ within and outside the upwelling zone would substantially help to resolve the issue.

The increase in the intensity of upwelling and productivity during post-glacial period indicates a major climatic change in the Arabian sea. Prell (1984a,b) has shown that G. bulloides percentage increased in the post-glacial period in the western Arabian sea,which was synchronous with the change in $\delta^{18}O$ (an ice volume index). Therefore, it is important to know the timing of this productivity change in various parts of Arabian sea.In the following discussion we make an attempt to find out the timing of this change.

III.3.3. Chronology of Productivity Change in the Arabian Sea

Considering that the $CaCO_3$ variation is an index of the productivity change,we have compared its temporal variation in SK-20-186 and SK-20-185 with the data from cores (ARB52, 54) of Borole et al. (1982a).These four cores span from 0^{o} to $19^{o}N$ and are probably representative cores for most of the Arabian sea.Plots of $CaCO_3$ variations with time,in them,

are shown in Fig. 3.24.In cores ARB-52 and 54,a rapid $CaCO_3$ change occurs within a very short time interval between 13-14 kyr. In SK-20-185 and SK-20-186 too 14 kyr levels (shown by bold arrows in Fig. 3.24) mark the change in $CaCO_3$, though the changes are not as rapid as ARB-52 and 54. In all the 4 cores in Arabian sea, by 10 kyr B.P. a significant increase in $CaCO_3$ productivity has taken place. The changes in productivity around 14 kyr B.P. are almost coincidental with the onset of the $\delta^{18}O$ depletion (deglaciation) in core SK-20-185 and SK-20-186 (see Tables 3.1, 3.2, 3.9 and 3.10) and is found in all cores irrespective of their sedimentation rates.Interestingly,the break in the sedimentation rate in SK-20-186 is also found around ~ 13-14 kyr. Therefore,we infer that perhaps there was a synchronous and ubiquitous change in productivity in most of the Arabian sea.Though no $CaCO_3$ data is available on core CD-17-30 at present (for which ^{14}C dates are obtained), from the study of the western Arabian sea cores, Prell and Curry (1981) observed that "carbonate content ..... is high during isotope stage 1 and decreases rapidly across the termination" which is likely to be due to low glacial productivity. Hence we see an uniform increase in productivity from glacial to Holocene in this region at around ~ 14 kyr B.P. This conclusion is consistent with the observation of Van Campo (1986),who states that the resurgence of monsoon (and upwelling and consequent productivity?) took place around 16.5 to 15.5 kyr ago. Evidence to the contrary comes from the study of

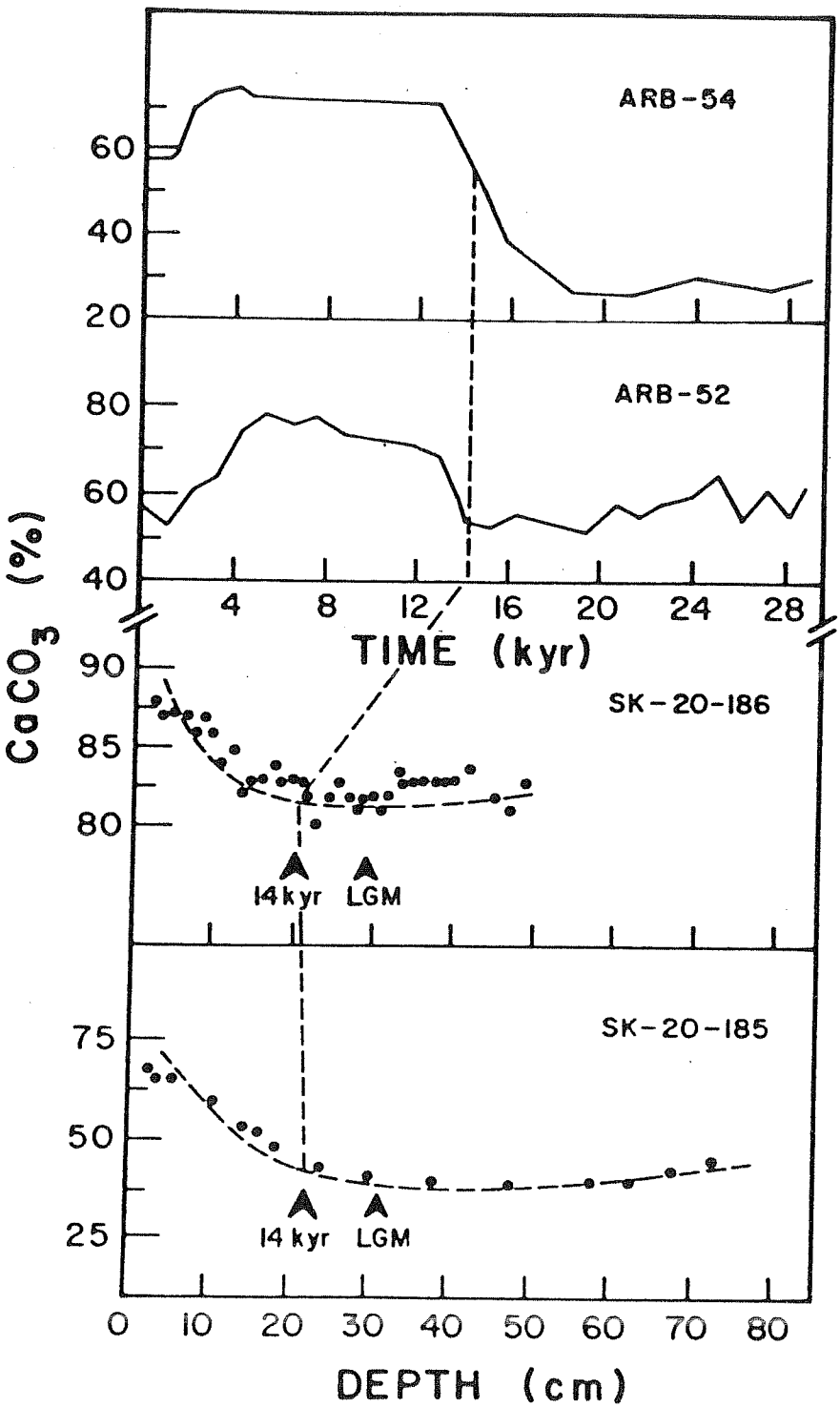

Fig. 3.24 : Variation of $CaCO_3$ with time in cores from the equatorial Indian ocean to the northern Arabian sea. Note that the transition period between high and low $CaCO_3$ lies around 14 kyr.

Sarnthein et al. (1988). Their study was based on the downcore variation of the total organic carbon (TOC) content and $\delta^{13}C$ of organic matter in this region.From the TOC content, these workers estimated a higher palaeoproductivity in the eastern Arabian sea during LGM.On the other hand, they conclude that in the western Arabian sea productivity decreased during the same time.Such an asymmetry within a small basin is difficult to visualize.We consider that the increase in TOC in eastern Arabian sea, during LGM is not due to high productivity but due to better preservation of organic matter.Earlier we have shown that either low-oxygen condition was prevailing during glacial period in the eastern Arabian sea or a reducing condition (redox front) in deeper part of sediment was established, which removed significant amount of uranium from sea water.We essentially attribute the high LGM-TOC to these mechanisms. Therefore, interpreting TOC in terms of productivity is not probably valid at least in the eastern Arabian sea. The productivity during glacial time can be better estimated by $CaCO_3$,which was indeed lower.

This change in productivity and upwelling might have been responsible for the down core $\delta^{13}C$ variation cited above. Upwelling,in particular,controls the productivity and the turnover of CO_2,ultimately controlling the $\delta^{13}C$ of the surface CO_2.

The $\delta^{13}C$ stratigraphy of core SK-20-185 is compared with that of another planktonic species Neogloboquadrina dutertrei from another ocean basin.Fig.

3.25 compares $\delta^{13}C$ stratigraphy of this species in a Pacific core V 19-30, analysed by Shackleton and Pisias (1985) with $\delta^{13}C$ stratigraphy of G. sacculifer for the entire length of core SK-20-185.In Fig. 3.25,all $\delta^{13}C$ data for the upper part of core SK-20-185 are not plotted and only the general trend is shown. $\delta^{18}O$ curve on core SK-20-185 is also shown in the upper panel for time framework. It is worthwhile to attempt a correlation only upto a depth of 132 cm in core SK-20-185,beyond which high resolution $\delta^{13}C$ measurements are not available.As can be seen, upto this depth i.e. for a period of about 60 kyr there is a good correlation between the two $\delta^{13}C$ variations. Dashed lines show that in both the cores glacial levels are enriched in $\delta^{13}C$ while early Holocene (~ 9-10 kyr) levels are depleted in it. The $\delta^{13}C$ enrichment in various oceans during glacial period has mostly been explained by increased productivity (Sarnthein et al. 1988).However,in the Arabian sea,productivity was lower during LGM and hence the observed enrichment is perhaps due to the cessation of upwelling as was discussed earlier. Therefore,eventhough variations in $\delta^{13}C$ in different ocean basins are in the same direction, causative mechanism might be different.Such a change in the $\delta^{13}C$ of different planktonic species in relation to the variation of upwelling (depleted $\delta^{13}C$ coupled with stronger upwelling and higher productivity) has also been reported from cores off NW-Africa (Berger et al. 1978a).

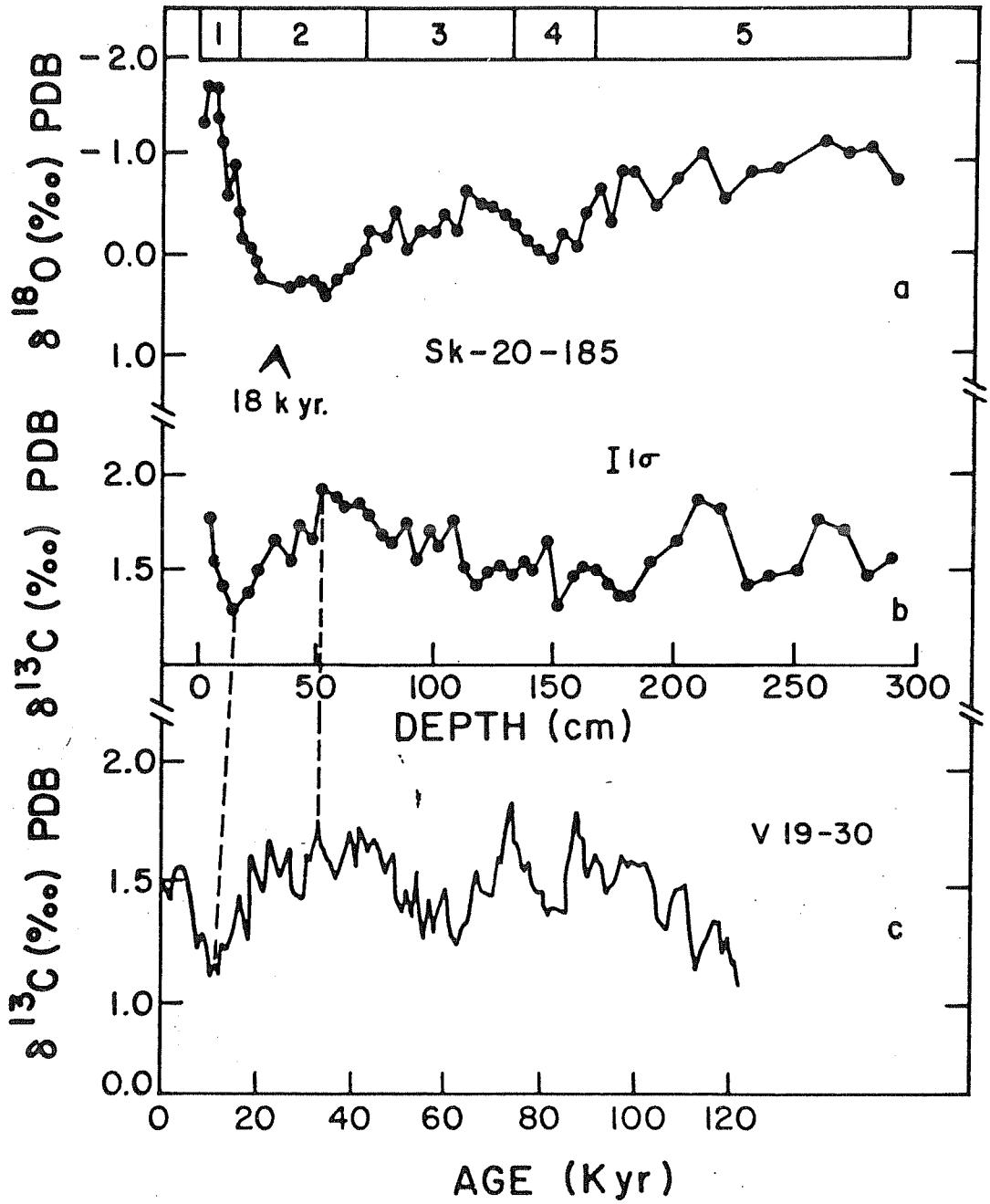

Fig. 3.25 : $\delta^{13}C$ stratigraphy of SK-20-185 (G. sacculifer) compared with that of N. dutertrei in V19-30 (Shackleton and Pisias, 1985) from Pacific. $\delta^{18}O$ stratigraphy and 18 kyr level (bold arrow) serve as time framework.

III.3.4. Periodicities in the Climatic Indices and their Inter-relationship

After Hays et al. (1976) reported that periodicities associated with earth's orbit are recorded in the oceanic $\delta^{18}O$ record, numerous other investigators supported their contention (Berger et al. 1982). According to the Milankovitch theory, these statistical correlations between astronomical forces and climatic index are caused by the change in the distribution of solar radiation over the earth. The orbital variations have mainly four frequencies e.g. 100 kyr eccentricity cycle,41 kyr obliquity cycle,23 and 19 kyr precessional cycles,with varying amplitudes and phases. It is, therefore, expected that if solar insolation changes in such a cyclic fashion,its imprint will be found on both $\delta^{18}O$, an ice volume indicator and $CaCO_3$, a productivity index.

In the previous section,we have seen that there was a significant variation of $CaCO_3$ productivity in both the Arabian sea and the equatorial Indian ocean in the past.We have also noted that an apparent correlation exists between $\delta^{18}O$ and $CaCO_3$ in both the cores SK-20-185 and SK-20-186 in this region. Therefore,an attempt has been made to find out the periodicities associated with these variations and their interrelationship. For this purpose, $\delta^{18}O$ and $CaCO_3$ records in these two cores have been converted to time series. Sampling interval (Δt) for SK-20-186 is 5 kyr and for SK-20-185 is 2 kyr.In cases,where actual measurements were not available, at these intervals (coarse sampling),

interpolated values were taken from the respective curves. The time control points in these cores are ^{14}C dates for the top part and $\delta^{18}O$ stratigraphies (compared with SPECMAP curve, Fig. 3.9) for the remaining part.Subsequently these time series were subjected to a power spectrum analysis. Spectral variances are obtained using Fourier transformations on autocorrelation calculations (Jenkins and Watts 1968). The coherency between two time series is calculated on the basis of cross-correlation which yields a cross-spectrum. A Tukey lag (one-third) window has been used in this calculation.Finally a phase spectrum between these two series is obtained (Shah,1988).

Fig. 3.26 shows the normalized variance density of both $\delta^{18}O$ (dotted line) and $CaCO_3$ (dashed line) for about ~ 430 kyr record of SK-20-186, also shown in this figure is the coherency spectrum (solid line) between $\delta^{18}O$ and $CaCO_3$. Variance spectra are plotted on an arbitrary log scale while coherency spectrum is plotted as hyperbolic arc tangent. Frequencies in cycle/kyr and periods in kyr are also shown. Examination of $\delta^{18}O$ and $CaCO_3$ spectra reveal peaks around 41 kyr and 45 kyr respectively. Second concentrations in variance occur at 23 kyr for both $\delta^{18}O$ and $CaCO_3$. We also note a significant 16 kyr peak in $CaCO_3$ spectrum and a weak 17 kyr peak in the $\delta^{18}O$ spectrum. Examination of cross-spectrum shows that $\delta^{18}O$ and $CaCO_3$ are coherent at 95% level over a frequency band of 50 kyr for which no peak exists. However,both are coherent at 23 kyr (80% level) and 15 kyr band. Fig. 3.27 shows the phase

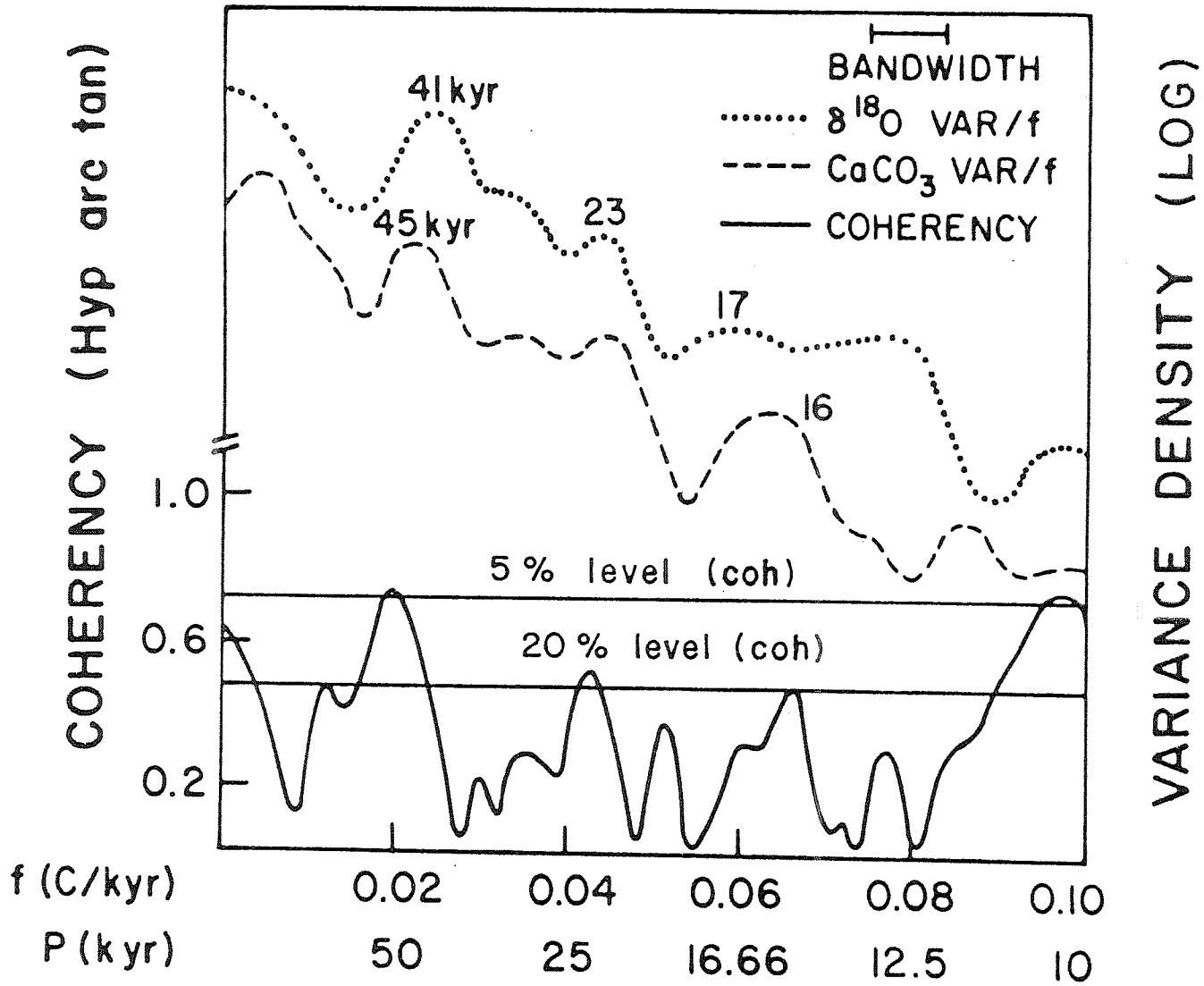

Fig. 3.26 : A normalized variance spectrum of $\delta^{18}O$ (dotted line) and percent $CaCO_3$ (dashed line) and the coherency spectrum (solid line) between them, for the period from 0 kyr to 425 kyr in SK-20-186. Critical values of non-zero coherence at the 80% and the 95% confidence levels are shown.

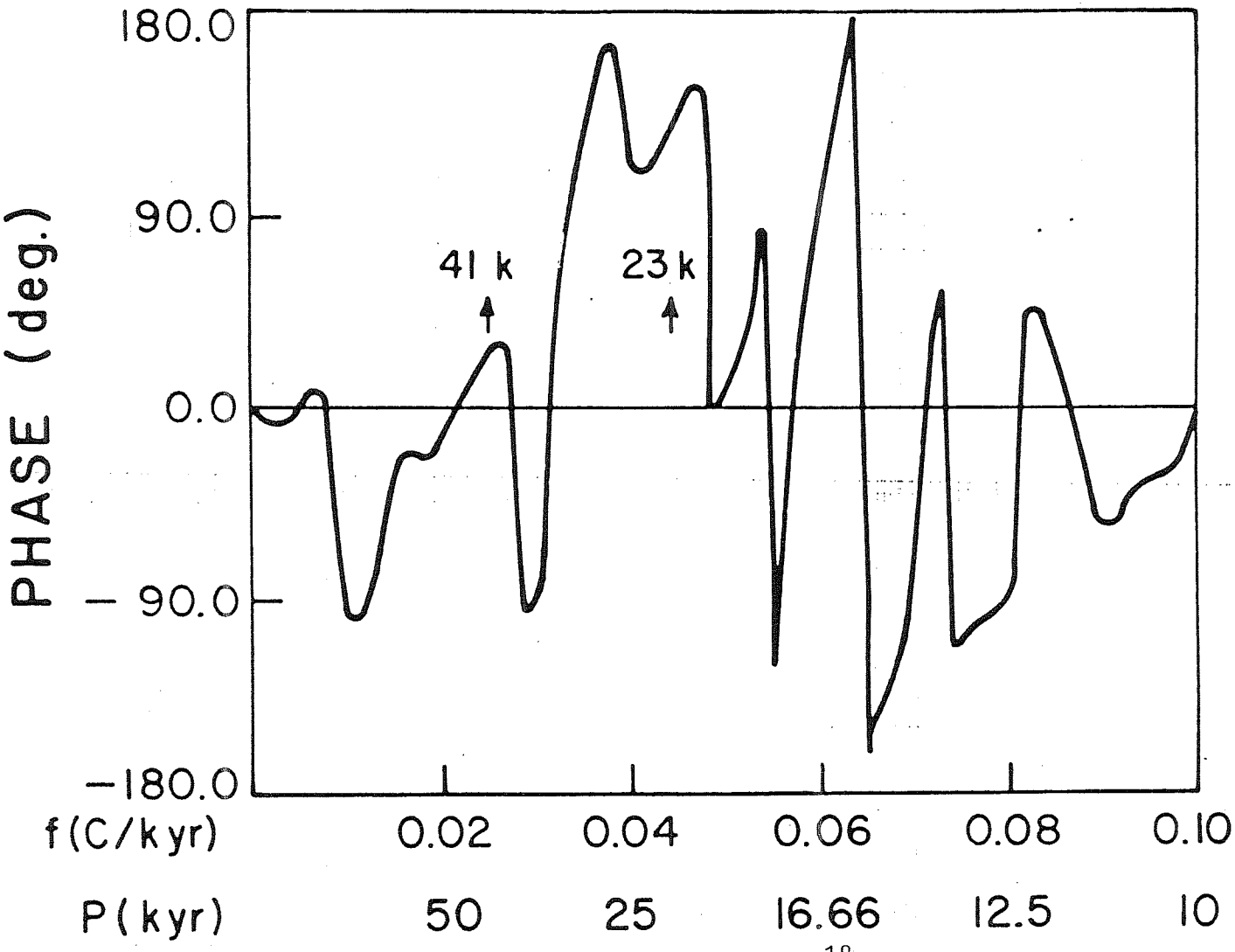

Fig. 3.27 : Phase spectrum of $\delta^{18}O$ vs. $CaCO_3$ in SK-20-186

spectrum between $\delta^{18}O$ and $CaCO_3$.Over 50 kyr band $\delta^{18}O$ lags $CaCO_3$ by merely 12° (~ 2 kyr). $CaCO_3$ lag $\delta^{18}O$ by 25° (equivalent to 1.5 kyr) over 41 kyr band and by 125° (~ 8 kyr) over 23 kyr frequency band.

Presence of 41 kyr and 45 kyr periods indicates the influence of the obliquity cycle. The 23 kyr periodicity shows the effect of the precessional frequency.16 kyr and 17 kyr periodicities perhaps indicate influence of 19 kyr precessinal cycle. Both $\delta^{18}O$ and $CaCO_3$ are coherent over 23 kyr precessional cycle but not on 41 kyr and 19 kyr.The distinct 100 kyr eccentricity cycle, found in many ocean cores, is not present in any of these records.For $\delta^{18}O$,it is perhaps due to the reduced peaks at stages 5e,7,9 and 11 (section III.2.2).

The lag of coarse fraction carbonate behind $\delta^{18}O$ by 5 kyr has been reported by Shackleton and Opdyke (1976).A lag of 1-5 kyr has also been reported by other workers (Luz and Shackleton 1975; Gardner 1982).However,at the present stage of our sampling interval of 5 kyr in SK-20-186,the observed lags between $CaCO_3$ and $\delta^{18}O$ of 1.5-8 kyr over obliquity and precessional bands,are not significant.Similar observations were made by Foucault and Fang (1987) from the Bay of Bengal, where both $\delta^{18}O$ and Carbonate along with terrigenous flux changed in phase with periodicities of 41 kyr and 22 kyr,for last 200 kyr.

The core SK-20-185,however,does not reveal any distinct peak at the orbital variations, perhaps due to its short length of time series (~ 120 kyr).Plot of $\delta^{18}O$ and $CaCO_3$

(Figs. 3.19 and 3.20) shows that they are correlated and perhaps in phase.

These observations along with that of Foucault and Fang (1987) indicate that in the northern Indian ocean climatic and productivity change are probably dominantly controlled by the obliquity and precessional cycles.

Summarising, biogenic productivity in the Arabian sea and the equatorial Indian ocean show a significant change around 14 kyr B.P. This change from glacial low productive ocean to Holocene high productivity stage, is almost coincidental with change in $\delta^{18}O$.The probable reason for this productivity change is the variation of upwelling in this region.During glacial period upwelling was weak due to a weak SW-monsoon. In the early Holocene upwelling was stronger due to a reinforced monsoon. These changes in upwelling intensity are recorded in the down core $\delta^{13}C$ values of different species in planktonic foraminifera.The variations in $\delta^{18}O$ (ice volume) and $CaCO_3$ (productivity) in northern Indian ocean are probably controlled by orbital variations in obliquity (41 kyr) and precessional (23 kyr) frequencies.

CHAPTER IV

CONCLUSIONS AND RECOMMENDATIONS FOR FUTURE WORK

CHAPTER IV

CONCLUSIONS AND RECOMMENDATIONS FOR FUTURE WORK

IV.1. Conclusions

The main aim of this thesis is to study palaeo-oceanographic and palaeoclimatic conditions in the northern Indian ocean (the Arabian sea and the equatorial Indian ocean) by using stable isotopes of oxygen ($\delta^{18}O$) and carbon ($\delta^{13}C$) in deep sea cores. For this purpose a CO_2 extraction system was fabricated which can anslyse foraminiferal samples consisting of 30-40 individual shells from these sediments with a high precision ($\pm$ 0.1 $^{o}/_{oo}$). Different absolute dating techniques (^{14}C, U-Th series isotopes) have been used to determine the timing of these climatic events. In addition, conventional studies like measurements of downcore $CaCO_3$, estimation of coarse fraction (> 150 μm), etc., were also carried out.The major conclusions obtained from this work are given below:

1. $\delta^{18}O$ stratigraphies from 5 deep sea cores from the eastern and the western Arabian sea as well as equatorial Indian ocean provide past climatic records of more than 400 kyr.In general,the entire Arabian sea was more saline than today.In the northern Arabian sea, excessive evaporation coupled with increased salinity gradient (than today) from south to north, characterised the last glacial maximum (~ 18 kyr B.P.) condition. These observations indicate,prevalance of a dry NE monsoon atmospheric circulation during the same period and a low river discharge in the Arabian sea due to a weak SW-monsoon.

2. High resolution $\delta^{18}O$ analyses in multiple species of planktonic foraminifera yield evidence of a stronger NE monsoon current which brought increasing amount of low salinity water from the western Bay of Bengal to the eastern Arabian sea during the LGM.

3. High resolution $\delta^{13}C$ analyses on multiple species of planktonic foraminifera show that upwelling in the Arabian sea was very strong around 9 kyr B.P. alongwith a probable weaker upwelling condition during last glacial period.

4. Biogenic productivity in the Arabian sea and the equatorial Indian ocean was lower during glacial period, due to the weaker upwelling.The increase in

productivity, from glacial to Holocene, took place around 14 kyr B.P. This change in productivity was perhaps synchronous in most of the Arabian sea and concomitant with deglaciation.This indicates that the variation in upwelling has probably a major role in controlling $\delta^{13}C \sum CO_2$ of ocean water.

5. Sedimentation rates for the cores from the eastern Arabian sea and the equatorial Indian ocean,based on ^{14}C agree quite well with $\delta^{18}O$ stratigraphies.In the Holocene, these rates are 2.2 to 2.4 cm/kyr,similar to those found in deep sea cores. The core from the upwelling zone of the western Arabian sea has a higher rate (~ 7.7 cm/kyr) indicating a higher productivity.

6. Sedimentation rates based on the ^{230}Th excess method agree with those based on ^{14}C method within a factor of two. In the eastern Arabian sea,the glacial period was characterised by a high deposition of authigenic uranium, indicating fixation of uranium from pore water to the sediments at these deeper levels and/or its removal under the low oxygenated bottom water condition.

7. Time series analysis of $CaCO_3$ (a productivity index and $\delta^{18}O$ (an ice value index) show that their variations are in phase and controlled by the change in obliquity (41 kyr) and precession (23 kyr) of the earth's axis.

IV.2. Recommendations

Though interesting information about past oceanographic and climatic conditions in the northern Indian ocean have been obtained during the present investigation,it has also raised several questions.

For example,the anomalous $\delta^{18}O$ depletion during LGM has been explained by the transport of low salinity water from the western Bay of Bengal to the eastern Arabian sea. However, to check this hypothesis,a few more strategically located cores should be studied from the western Bay of Bengal and the south of Sri Lanka where a more significant drop in salinity is expected. Apart from foraminiferal species, nannoplankton assemblages should also be analysed. Having the shallowest depth habitat,nannoplanktons should show the maximum effect of this surface process.

We have shown that an increase in the oceanic productivity took place around 14 kyr B.P. in these oceans. However, $\delta^{18}O$ and $CaCO_3$ measurements from high (> 10 cm/kyr) sedimentation rate cores from the eastern and the western Arabian sea should be done in conjunction with radiocarbon dating. This would tell us how rapid the change in productivity was and what was its exact time relationship with deglaciation.Broecker et al.(1988b) have reported from south China sea an abrupt increase in foraminiferal abundance (by 10 fold) within a period of 1000 years,

centered around 13-14 kyr. It would be interesting to see whether the observed productivity change in the Arabian sea is of such rapid nature.

The $\delta^{13}C$ signature of upwelling found in the core SK-20-185 was not found from the core raised near the upwelling region. Prell and Curry (1981) also observed that planktonic foraminifera in the upwelling zone do not record the imprint of the ΣCO_2 variation.The question is,does the foraminifera from strong upwelling zones,suffer from severe disequilibrium effect,so as to mask the ΣCO_2 variation?Fast growth (owing to a copious nutrient supply) might be the reason for such disequilibrium (Berger et al., 1977b). Studies of $\delta^{13}C$ in cores from within and out of upwelling centres would probably resolve the issue.

A significant enrichment in authigenic uranium has been observed which indicates uranium fixation from pore water under locally reducing condition or a low oxygenated bottom water condition. If removal or uranium is controlled by bottom water oxygen content then it supports the observation of Kallel et al. (1988) regarding a glacial deep water enriched in CO_2 and poor in O_2.However,from the limited data, it is difficult to ascertain whether the removal of uranium is climatically controlled.More high resolution analysis of uranium on the entire core SK-20-185 as well as other cores raised from south to north in the Arabian sea, is required to establish the causative mechanism and time variation of the authigenic removal of uranium.

REFERENCES

1. Arrhenius, G. 1952. Sediment cores from the East Pacific, Swedish Deep Sea Expedition 1947-1948,Rep. 5, 1-228.

2. Arrhenius, G. 1963. Pelagic sedimentation,in "The Sea", 3,(ed. M.N. Hill),John Wiley,New York 655-727.

3. Bard, E., Arnold,M,Duprat,J.,Moyes,J.,and Duplessy,J.C. 1987. Reconstruction of the last deglaciation : Deconvolved records of $\delta^{18}O$ profiles, micropalaeontological variations and accelerator mass spectrometric ^{14}C dating,Climate Dynamics,1,101-112.

4. Barnes, H. 1959. "Apparatus and methods of oceanography",Allen and Unwin. London.

5. Barrera, E. and Savin S.M. 1987. Effect of small sample preparation on the $\delta^{18}O$-value of fine grained calcite, Chemical Geology (Isotope Geoscience Section), 66, 301-305.

6. Be, A.W.H., and Duplessy, J.C. 1976. Subtropical convergence fluctuations and Quaternary climates in middle latitudes of Indian ocean,Science,194,419-422.

7. Be, A.W.H., 1977. An ecological, zoogeographic and taxonomic review of recent planktonic foraminifera,in

"Oceanic Micropalaeontology", (ed. A.T.S. Ramsay), Academic Press,1977,1-100.

8. Berger, A., Imbrie,J.,Hays,J.,Kukla,G.,and Saltzman,B., eds. 1982. Milankovitch and Climate, pt. 1 & 2,D. Riedel.

9. Berger, W.H. 1968. Planktonic Foraminifera: Selective solution and palaeoclimatic interpretation, Deep Sea Res. 15,31-43.

10. Berger, W.H. 1969: Ecologic patterns of living planktonic foraminifer,Deep Sea Res.,16,1-24.

11. Berger, W.H. and Killingley,J.S. 1977.Glacial Holocene transition in deep sea carbonates : Selective dissolution and the stable isotope signal,Science,197, 563-566.

12. Berger, W.H., Johnson, R.F. and Killingley,J.S. 1977a. 'Unmixing' of the deep sea record and the deglacial meltwater spike,Nature,269,661-663.

13. Berger, W.H., Killingley, J.S.,Vincent,E. 1977b. Carbon isotopic variations in planktonic foraminifera from the eastern equatorial Pacific, Geol. Soc. Amer. Abstracts,with program.

14. Berger, W.H. 1978. Oxygen-18 stratigraphy in deep sea sediments, Additional evidence for deglacial meltwater effect. Deep-Sea Research,25,473-480.

15. Berger, W.H., Diester-Haass, L., Killingley,J.S. 1978a. Upwelling off northwest Africa: The Holocene decrease as seen in carbon isotopes and sedimentological indicators. Oceanol. Acta.,1,1-7.

16. Berger, W.H., Killingley, J.S.,Vincent,E. 1978b. Stable isotopes in deep sea carbonates: Box core ERDC-92,west equatorial Pacific. Oceanol. Acta,1,No. 2,203-216.

17. Berger, W.H. Killingley,J.S.,Metzler,C.V. and Vincent, E. 1985a. Two step deglaciation: ^{14}C dated high resolution $\delta^{18}O$ records from the tropical Atlantic, Quat. Res.,23,258-271.

18. Berger, W.H., Killingley, J.S. and Vincent, E. 1985b. Timing of deglaciation from an oxygen isotope curve for Atlantic deep sea sediments,Nature,314,156-158.

19. Berger, W.H. and Vincent,E. 1986. Sporadic shutdown of North Atlantic deepwater production during the Glacial-Holocene transition?Nature,324,53-55.

20. Bonneau,M.C.,Vergnaud-Grazzini,C.,and Berger,W.H.,1980. Stable isotope fractionation and differential dissolution in recent planktonic foraminifera for Pacific box cores.Oceanol. Acta.,3,377-382.

21. Borole, D.V. 1980. Radiometric and trace elemental investigations on Indian estuaries and adjacent seas.

Ph.D. Thesis (unpublished), Gujarat University, Ahmedabad,India,pp. 155.

22. Borole, D.V., Rao, K.K., Krishnamurthy, R., V. and Somayajulu, B.L.K. 1982a. Late Quaternary faunal change in coastal Arabian sea sediments. Quat. Res., 18, 236-239.

23. Borole, D.V., Krishnaswami, S. and Somayajulu, B.L.K. 1982b. Uranium isotopes in rivers, estuaries and adjacent coastal sediments of western India: Their weathering, transport and oceanic budget, Geochim. Cosmochim. Acta,46,125-137.

24. Boyle, E.A. 1983. Chemical accumulation variations under the Peru current during the past 130,000 years, J. Geophys. Res.,88,7667-7680.

25. Broecker, W.S. and Van Donk,J.,1970,Insolation changes, ice volumes and the O-18 record in deep sea cores. Reviews in Geophysics and Space Physics,8,169-198.

26. Broecker, W.S. and Peng,T.H. 1982. Tracers in the sea Palisades,New York,Eldigio Press,pp. 690.

27. Broecker, W.S. and Peng,T.H. 1986. Carbon cycle 1985. Glacial to interglacial changes in the operation of the global carbon cycle. Radiocarbon,28,309-327.

28. Broecker, W.S. 1986. Oxygen isotope constraints on surface ocean temperatures Quat. Res.,26,121-134.

29. Broecker, W.S.. Andree,M.,Wolfli,W.,Oeshger,H.,Bonani, G., Kennett, J. and Peteet,D. 1988a. The chronology of the last deglaciation: Implications to the cause of the Younger Dryas event,Palaeoceanography,3,No. 1,1-19.

30. Broecker, W.S., Andree,M.,Klas,M.,Bonani,G. and Wolfli, W. 1988b. New evidence from the south China sea for an abrupt termination of last glacial period,Nature,333, 156-158.

31. Bryson, R.A. and Swain,A.M. 1981. Holocene variations of monsoon rainfall in Rajasthan, Quat. Res., 16, 135-145.

32. Burton, J.D. 1975. Radioactive nuclides in marine environments,Chp. 18,Chemical Oceanography,3,91-97.

33. CLIMAP Project Members 1976. The surface of the ice-age earth,Science,191,1131-1137.

34. Cochran, J.K. and Osmond, J.K. 1976. Sedimentation pattern and accumulation rate in the Tasmanian basin. Deep Sea Res. 23,193-210.

35. Cochran, J.K. 1982. The oceanic chemistry of the U- and Th-series nuclides, in "Uranium series disequilibrium Applications to environmental problems" (eds. Ivanovich, M. and Harmon,R.S.),384-430,Clarendon Press, Oxford.

36. COHMAP Members 1988. Climatic changes of the last 18, 000 years: observations and model simulations,Science, 241,1043-1052.

37. Cooley, S. and Thompson, J., 1985. Recurrent uranium relocations in distal turbidites emplaced in pelagic conditions.Geochim. Cosmochim. Acta 49,2339-2348.

38. Coplen, B.T., Kendall,C. and Hopple,J.,1983. Comparison of stable isotopic reference sample. Nature, 302, 236-238.

39. Craig, H. 1957. Isotopic standards for carbon and oxygen and correction factors for mass spectrometric analysis of carbon dioxide,Geochim. Cosmochim. Acta,12, 133.

40. Craig, H. and Gordon,L.I. 1965. Deuterium and oxygen-18 variations in the ocean and the marine atmosphere,in Stable isotopes in oceanographic studies and palaeotemperatures - A Symposium,Cons. Naz. Ric. Pisa. 9-130.

41. Craig, H. 1965. The measurement of oxygen isotope palaeotemperatures, in Tongiorgi,E.,ed. Stable isotopes in oceanic studies and palaeotemperatures. Third SPOLETO Conference on Nuclear Geology. Pisa,consiglio Nazionale delle Richerche, Laboratoire di Geologia Nucleare P. 161-181.

42. Cullen J.L. 1981. Microfossil evidence for changing salinity patterns in the Bay of Bengal over the last 20,000 years. Paleo. Paleo. Paleo.,35,315-456.

43. Curry, W.B. and Matthews, R.K. 1981. Palaeo-oceanographic utility of oxygen isotopic measurements on planktonic foraminifera,Indian Ocean core top evidence. Palaeo. Palaeo. Palaeo.,33,173-191.

44. Deuser, W.G. 1978. Stable isotope palaeoclimatology A possible meausre of past seasonal contrast from foraminiferal tests, in "Stable isotopes in Earth Sciences", (ed. Robinson,B.W.),DSIR Bulletin,220,55-60, (New Zealand department of Scientific and Industrial Research,Wellington,New Zealand).

45. Dietrich, G., 1973. The unique situation in the environment of the Indian ocean, in the Biology of Indian ocean, (ed.B. Zeitzschel), Springer-Verlag,New York,1-6.

46. Duplessy, J.C., Lalou, C., and Vinot, A.C. 1970. Differential isotopic fractionation in benthic foraminifera and palaeotemperature reassessed. Science 168,250-251.

47. Duplessy, J.C.,1970. Isotope studies in climatic change (ed. J. Gribbon),Cambridge University Press.

48. Duplessy, J.C., Be, A.W.H. and Blanc,P.L. 1981a. Oxygen and carbon isotopic composition and biogeographic distribution of planktonic foraminifera in the Indian ocean,Palaeo. Palaeo. Palaeo.,33,9-46.

49. Duplessy, J.C., 1982. Glacial to interglacial contrasts in the northern Indian ocean.Nature 295.

50. Duplessy, J.C., Shackleton,N.J.,Matthews,R.K.,Prell,W., Ruddiman, W.F., Caralp, M. and Hendy, C.H., 1984. ^{13}C record of benthic foraminifera in the last interglaciall ocean: Implications for the carbon cycle and the global deep water circulation. Quat. Res.,21, 225-243.

51. Duplessy, J.C., Arnold, M.,Maurice,P.,Bard,E.,Duprat,J. and Moyes,J. 1986. Direct dating of the oxygen isotope record of the last deglaciation by ^{14}C accelerator mass-spectrometry,Nature,320,350-352.

52. Dymond, J., Corliss, J.B., Heath,G.R.,Field,C.W.,Dasch, E.T. and Veeh, H.H. 1973. Origin of metalliferous sediments from the Pacific ocean,Geol. Soc. Am. Bull., 85,3355-3372.

53. Emiliani, C., 1954. Depth habitats of some species of Pelagic foraminifera as indicated by oxygen isotope ratios,Amer,J. Sci.,252,149-158.

54. Emiliani,C.,1955. Pleistocene temperatures,J. Geol.,63, 538-578.

55. Emiliani, C., 1966. Palaeotemperature analysis of Caribbean cores P6304-8 and P6304-9 and the generalised temperature curve for the past 425,000 years. J. Geol.,74, 109-196.

56. Emiliani, C., 1971. Depth habitats of growth stages of pelagic foraminifera. Science,173,1122-1124.

57. Emiliani, C., 1981. A new global geology,in:The Oceanic Lithosphere,(ed. Emiliani,C.),V.VII,The Sea.

58. Emrich, K., Ehalt, D.H.,Vogel,J.C. 1970. Carbon isotope fractionation during precipitation of calcium cabronate. Earth. Planet. Sci. Lett.,8,363-371.

59. Epstein, S., Buchsbaum, R.,Lowenstam,H.A. and Urey,H.C. 1953. Revised carbonate-water isotopic temperature scale. Bull. Geol. Sci. Am.,64,1315-1326.

60. Epstein, S. and Mayeda, T. 1953. Variation of $\delta^{18}O$ content of waters from natural sources. Geochim. Cosmochim. Acta,4,213.

61. Erez, J., 1979. Modification of the oxygen-isotope record in deep sea cores by pleistocene dissoluton cycles,Nature 281,535-538.

62. Erez, J. and Luz, B., 1983. Experimental palaeotemperature equation for planktonic foraminifera, Geochim. Cosmochim. Acta,47,1025-1031.

63. Fairbanks, R.G. Sverdlove,M.,Free,R.,Wiebe,P.H. and Be, A.W.H. 1982. Vertical distribution and isotopic compositon of living planktonic foraminifera from the Panama basin,Nature,298,841-844.

64. Faure, G. 1986. Principles of Isotope Geology, 2nd edition,John Wiley and Sons.

65. Fein, J.S. and Stephens, P.L. 1987. Monsoon dynamics, John Wiley and Sons.

66. Fontugne, M.R. and Duplessy, J.C. 1986. Variations of the monsoon regime during the upper Quaternary: Evidence from carbon isotopic record of organic matter in North Indian ocean sediment cores,Palaeo. Palaeo. Palaeo. 56,69-88.

67. Foucault, A. and Fang, N., 1987. Climatic control of Quaternary sedimentation in the gulf of Bengal,C.R. Acad. Sci. Paris,t. 305,series II,1383-1388.

68. Friedman, I. and O'Neil, J.R., 1977. Compilation of stable isotope fractionation factors of geochemical interest, in: Data Geochem. 6th ed.,Geol.Surv. Prof. Paper 440 KK.

69. Ganssen, G. and Sarnthein, M., 1983. Stable isotope compositon of foraminifers, the surface and bottom water record of coastal upwelling,in,Coastal Upwelling,

its sediment records. Pt. A., Responses of the sedimentary regime to present coastal upwelling,(eds. Suess,E. and Thiede,J.),New York,Plenum Press,99-121.

70. Gardner, J.V. 1982. High resolution carbonate and Quaternary organic-carbon stratigraphies for the late Neogene and Quaternary from the Western Caribbean and eastern equatorial Pacific. Init. Rep. D.S.D.P. 68, N.S.F. Washington,D.C.,347-364.

71. GEOSECS Atlantic, Pacific and Indian Ocean expeditons, 1987. (eds. Gote-Ostuland, H.,Craig,H.,Broecker,W.S., Spenser,D.),7,N.S.F.,Washington,D.C.

72. Goldberg, E.D. and Koide, M. 1962. Geochronological studies of deep sea sediments by ionium/thorium method. Geochim. Cosmochim. Acta,26,417.

73. Goldberg, E.D. 1968. Ionium/thorium. Geochronologies. Earth Planet. Sci. Lett.,4,17-21.

74. Grossman, E.L. 1984. Stable isotope fractionation in live benthic foraminifera from the southern California borderland. Palaeo. Palaeo. Palaeo.,47,301-327.

75. Grossman, E.L., 1987. Stable isotopes in modern benthic foraminifera : A study of vital effect. J. Foram. Res., 17,No. 1,48-61.

76. Grosswald, M.G. 1980. Late Weicheselian ice sheet of northern Eurasia. Quat. Res.,13,1-32.

77. Guinasso, N.L. and Schink D.R., 1975. Quantitative estimates of biological mixing rates in abyssal sediments. J. Geophys. Res.,80,3032-3043.

78. Hahn, D.G. and Manabe,S. 1975. The role of mountains in the south Asian monsoon circulation,J. Atmos. Sci. 32, No. 8,1515-1541.

79. Hasternath, S. and Lamb, P.J.,1979. Climatic Atlas of the Indian ocean. The University of Wisconsin Press, Madison,Wisconsin,97,charts,pp. 19.

80. Hays, J.D., Imbrie, J. and Shackleton, N.J., 1976. Variations in the earth's orbit,Pacemaker of the ice ages. Science,194,1121-1132.

81. Hoefs, J. 1980. Stable isotope geochemistry. IInd edition,Springer-Verlag,pp. 208.

82. Horibe, Y. and Oba, T., 1972. Temperature scales of aragonite-water and calcite-water systems. Fossiles, 23/24,69-74.

83. Huang, Y.C. 1973. in "Loess Deposits in China",(ed. Fairbridge,R.W.),63-76.

84. Imbrie, J., Hays, J.D., Martinson,D.G.,Mcintyre,A.,Mix, A.C.,Morley,J.J.,Pisias,N.G.,Prell,W.L. and Shackleton, N.J., 1984. The orbtial theory of pleistocene climate; support from a revised chronology of the marine $\delta^{18}O$

record, in,Milankovitch and Climate,pt. 1,(eds. Berger, A., Imbrie, J., Hays, J.D., Kukla, G. and Saltzman,B., Dordrecht,Reidel,269-305.

85. INDEX 1976. An oceanographic contribution to international programmes in the monsoon region of the Indian Ocean,NOVA/NYIT University Press.

86. Init. Rep. D.S.D.P. Site 219, 1974. Shipboard scientific party,N.S.F.,23,35-116.

87. Ivanovich, M. and Harmon, R.S. 1982. Uranium series disequilibrium Applications to environmental problems, Clarendon Press,Oxford.

88. Jenkins, G.M. and Watts, D.G. 1968. Spectral analysis and its applications. Holden Day,San Francisco,525.

89. Johnson, R.F., 1980. Ph.D. Thesis, Scripps Inst. of Oceanography,La Jolla,USA.

90. Jones, G.A. and Ruddiman, W.F., 1982. Assessing the global meltwater spike,Quat. Res.,17,148-172.

91. Jones, G.A. and Keigwin, L.D.,1988.Evidence from Fram strait (78^{o}N) for early deglaciation.Nature 336,56-59.

92. Kale, V.S. and Rajaguru, S.N. 1987. Late Quaternary alluvial history of the northwestern Deccan upland region. Nature,325,612-614.

93. Kallel, N., Labeyrie, L.D., Juillet-Leclere, A. and

Duplessy, J.C., 1988. A deep hydrological front between intemediate and deep-water masses in the glacial Indian ocean,Nature,333,651-655.

94. Keigwin, L.D., Corliss, B.H., Druffel,E.R.M. and Laine, E.P., 1984. High resolution isotopic study of the latest deglaciation based on Bermuda rise cores. Quat. Res.,22,383-386.

95. Kennett, J.P. and Shackleton,N.J.,1975. Laurentide ice sheet meltwater recorded in Gulf of Mexico deep sea cores. Science,188,147-150.

96. Killingley, J.S., Johnson, R.F. and Berger,W.H. 1981. Oxygen and carbon isotopes of individual shells of planktonic foraminifera from Ontong-Java plateau, equatorial Pacific. Palaeo. Palaeo. Palaeo., 33, 193-204.

97. Kolla, V. and Biscaye,P.E. 1977. Distribution of quartz in the sediments of the Indian ocean. J. Sediment. Petrol. 47,642-649.

98. Krishnaswami, S. and Sarin,M.,1976. Procedure for the simultaneous determination of Th,Pu,Ra isotopes, ^{210}Pb, ^{55}Fe, ^{32}Si, ^{14}C in marine suspended phases. Anal. Chim. Acta.,83,143-156.

99. Kroopnick, P. 1974. The dissolved O_2-CO_2-^{13}C system in the eastern equatorial Pacific,Deep Sea Research,21, 211.

100. Kroopnick, P.M. 1985. The distribution of $\delta^{13}C$ of ΣCO_2 in the world oceans, Deep Sea Res., 32, 57-84.

101. Ku, T.L., Broecker, W.S. and Opdyke, N., 1968. Comparison of sedimentation rates measured by palaeomagnetic and ionium method of age determination, Earth Planet. Sci. Lett., 4, 1-16.

102. Kuhle, M., 1987., Subtropical mountain and highland glaciation as ice age triggers and the waning of the glacial periods in the pleistocene, Geojournal, 4, 393-521.

103. Kutzbach, J.E., 1981. Monsoon climate of the early Holocene : Climatic experiment using the Earth's orbital parameters for 9000 years age, Science, 214, 59-61.

104. Kutzbach, J.E. and Otto-Bliesner, 1982. The sensitivity of African-Asian monsoonal climate to orbital parameter changes for 9000 years B.P. in a low resolution general circulation model. J. Atmos. Sci., 39, 1177-1188.

105. Kutzbach, J.E. and Guetter, P.J. 1986. The influence of changing orbital parameters and surface boundary conditions on climate simulations for the past 18,000 years. J. Atmos. Sci., 43, 1726-1759.

106. Labeyrie, L.D., Duplessy, J.C. and Blanc, P.L., 1987. Variations in mode of formation and temperature of oceanic deep waters over the past 125, 000 years. Nature,327,477-482.

107. Lighthill, J., and Pearce, R.P., eds. 1981. "Monsoon Dynamics",Cambridge University Press,735.

108. Locke, S.M. and Thunell,R.C.,1988. Palaeo-oceanographic record of the last glacial/interglacial cycle in the Red Sea and Gulf of Aden,Palaeo. Palaeo. Palaeo.,64, 163-187.

109. Luz, B. and Shackleton,N.J.,1975. $CaCO_3$ dissolution in the tropical east Pacific during the past 130,000 years, dissolution of deep sea carbonates,special publ. 13, (eds. Sliter, W.V., Be, A.W.H., and Berger,W.H.), Cushman Found. Foram. Res.,Washington,D.C.,142-150.

110. Manabe, S. and Hahn,D.G.,1977.,Simulation of tropical climate of an ice age. J. Geophys. Res.,82,3889-3911.

111. Martinson, D.G., Pisias,N.G.,Hays,J.D.,Imbrie,J.,Moore, T. and Shackleton, N.J., 1987. Age dating and the orbital theory of the ice ages : Development of a high resolution 0 to 300,000 year chronostratigraphy. Quat. Res. 27,1-29.

112. McCrea, J.M. 1950. On the isotopic chemistry of carbonates and a palaeotemperature scale, J. Chem. Phys.,18,849-857.

113. Miller, F.R. and Keshavamurty,R.N.,1968. Structure of an Arabian sea summer monsoon system. Internat. Indian Ocean Expedition Meteor. Monog. No. 1,East West Center Press,Honolulu,9.

114. Mix, A.C.,1987. The oxygen-isotope record of glaciation The geology of North America, North America and adjacent oceans during the last deglaciation. Geol. Soc. Am.,K-3,111-135.

115. Mix, A.C. and Pisias,N.G.,1988. Oxygen isotope analyses and deep-sea temperature changes Implications for rates of oceanic mixing,Nature,331,249-251.

116. Mook, W.G., 1968. Geochemistry of stable carbon and oxygen isotopes of natural waters in the Netherlands, Ph.D. Thesis,University of Groningen,Groningen,62.

117. Nair, R.R. and Hashimi, N.H., 1980. Holocene climatic inferences from the sediments of the western Indian continental shelf. Proc. Ind. Acad. Sci.,89A,299-315.

118. Nair, R.R., Ittekkot, V., Manganini, S.J.,Ramaswamy,V., Haake, B., Degens, E.T., Desai, B.N. and Honjo,S. 1989. Increased particle flux to the deep ocean related to monsoons,Nature,338,749-751.

119. Oba, T., 1969. Biostratigraphy and isotope palaeotemperature of some deep sea cores from the

Indian ocean,Science Reports of the Tohuku University, 42,129-195.

120. O'Neil, J.R., Clayton,R.N. and Mayeda,T.K.,1969. Oxygen isotope fractionation in divalent metal carbonates. J. Chem. Phys.,51,5547-5558.

121. Pankajakshan, T. and Rama Raju,D.V.,1987. Intrusion of Bay of Bengal water into Arabian sea along the west coast of India during North East monsoon, in: Contributions to Marine Sciences, Dr. S.Z.S. Qasim Felicitation Volume, (ed. T.S.S. Rao),237-244,National Institute of Oceanography,Goa.

122. Prell, W.L., 1978. Glacial-interglacial variability of monsoonal upwelling Western Arabian sea,in:Int. Conf. Evolution of Planetary Atmospheres and Climatology of the Earth. Centre National d'Etude Spatiales, Nice, 149-156.

123. Prell, W.L., Hutson, W.H., Williams, D.F., Be, A.W.H., Geitzenauer, W. and Molfinos, B., 1980. Surface circulation of the Indian ocean during the last glacial maximum approximately 18,000 yrs. B.P. Quat. Res.,14,309-336.

124. Prell, W.L. and Curry, W.B.,1981. Faunal and isotopic indices of monsoonal upwelling Western Arabian sea. Oceanol. Acta,4,91-98.

125. Prell, W.L. and Streeter, H.F., 1982. Temporal and

spatial patterns of monsoonal upwelling along Arabia A modern analogue for the interpretation of Quaternary SST anomalies. Journ. Mar. Res.,40,143-155.

126. Prell, W.L.,1984a. Monsoonal climate of the Arabian sea during the late Quaternary : A response to changing solar radiation. (eds. A.L. Berger et.al.), Milankovitch and Climate pt. 1,D. Riedel,349-366.

127. Prell, W.L., 1984b. Variation of monsoonal upwelling a response to changing solar radiation, in climate processes and climate sensitivity, Geophys. Monogr. Ser.,29,A.G.U.,Washington,D.C.,USA.

128. Prell, W.L. and Van Campo,E.V.,1986. Coherent response of the Arabian sea upwelling and pollen transport to late Quaternary monsoonal winds,Nature,323,526-528.

129. Prell, W.L. and Kutzbach,J.E.,1987. Monsoon variability over the past 150, 000 years. J. Geophys. Res.,92, 8411-8425.

130. Rajagopalan, G. and Vishnu-Mittre, 1977. Radiocarbon dating programme at the Birbal Sahni Institute of Palaeobotany, Lucknow. Int. Conf. Low Radioactivity measurements and applications,Proc. High tatras,6-10, Oct. 1975,335-340.

131. Ruddiman, W.F. and Glover,L.K.,1972. Vertical mixing of ice rafted volcanic ash in north Atlantic sediments. Geol. Soc.Am. Bull.,83,2817-2836.

132. Ruddiman, W.F. and Duplessy, J.C. 1985. Conference on the last deglaciation Timing and mechanism,Quat. Res., 23,1-17.

133. Sarin, M.M., Borole, D.V., Krishnaswami, S., 1979. Geochemistry and geochronology of sediments from the Bay of Bengal and equatorial Indian ocean. Proc. Ind. Acad. Sci. 88,pt. II,131-154.

134. Sarnthein, M.,1978. Sand deserts during glacial maximum and climatic optimum,Nature,272,43-46.

135. Sarnthein, M.,Winn,K.,Duplessy,J.C.,and Fontungne,M.R., 1988. Global variations of surface ocean productivity in low and mid latitudes : Influence on CO_2 reservoirs of the deep ocean and atmosphere during the last 21, 000 years,Palaeo-oceanography,3,361-399.

136. Savin, S.M. and Douglas,R.G.,1973. Stable isotope and magnesium geochemistry of recent planktonic foraminifera from the south Pacific. Geol. Soc. Am. Bull.,84,2327-2342.

137. Shackleton, N.J., 1967. Oxygen isotope analyses and pleistocene temperatures,reassessed. Nature,215,15-17.

138. Shackleton, N.J. and Opdyke,N.D.,1973. Oxygen isotope and palaeomagnetic stratigraphy of equatorial Pacific core V28-238; oxygen isotope temperatures and ice

volumes on a 10^5 and 10^6 year scale. Quat. Res.,3, 39-55.

139. Shackleton, N.J., 1974. Attainment of isotopic equilibrium between ocean water and the benthonic foraminifera genus Uvigerina : Isotopic changes in the ocean during the last glacial,in:Variation du Climat au Cours du Pleistocene,C.N.R.S.,Paris,203-209.

140. Shackleton, N.J. and Opdyke,N.D.,1976. Oxygen isotope and palaeomagnetic stratigraphy of Pacific core V28-239, late pliocene to latest pleistocene. Geol. Soc. of Am. Mon.,45,449-464.

141. Shackleton, N.J.,1977. The oxygen isotope stratigraphic record of late pleistocene. Phil. Trans. R. Soc. Lond. B. 280,169-182.

142. Shackleton. N.J. and Vincent,E.,1978. Oxygen and carbon isotope studies in recent foraminifera from the southwest Indian ocean. Marine Micropalaeoontology,3, 1-13.

143. Shackleton, N.J., Imbrie, J. and Hall,M.A.,1983. Oxygen and carbon isotope record of East Pacific core V19-30: Implications for the formation of deep water in the late Pleistocene North Atlantic. Earth Planet. Sci. Lett.,65,233-244.

144. Shackleton, N.J. and Pisias, N.G., 1985. Atmospheric carbon dioxide, orbital forcing, and climate,in:"The

Carbon Cycle and Atmospheric CO_2: Natural Variations Archean to Present",Geophy. Monogr.,32,303-317.

145. Shah, S.K. 1988. A software package for cross spectral analysis employing the difference method. Technical Note,Physical Research Laboratory,No. TN-88-61,pp.14.

146. Shanker, R., Subbarao, K.V. and Reddy, G.R., 1987. Distribution and origin of uranium in surficial sediments from the Arabian sea.Chemical Geology 63, 217-223.

147. Showers, W.J. and Margolis, S.V. 1985. Evidence for a tropical freshwater spike during the last glacial/interglacial transition in the Venezuela basin $\delta^{18}O$ and $\delta^{13}C$ of calcareous plankton. Marine Geology, 68,145-165.

148. Singh, G., Joshi. R.D.,Chopra,S.K. and Singh,A.B.,1974. Late Quaternary history of vegetation and climate of Rajasthan desert,India. Phil. Trans. Roy. Soc.,London, B. Biol. Sci.,889,467-501.

149. Singh, G. and Agarwal,D.P.,1976. Radiocarbon evidence for deglaciation in northwestern Himalaya,India,Nature, 260,232.

150. Street, F.A. and Grove, A.T., 1979. Global maps of lake-level fluctuations since 30, 000 kyr B.P. Quat. Res. 12,83-118.

151. Such, J.E. 1971. Linear polyphosphoric acids,in:Mellors comprehensive treatise on inorganic and theoretical chemistry, (eds. Eldridge,A.A.,Dyson,G.M.,Welch,A.J.E. and Pantony, D.A.), V.VIII, Suppl. III,Wiley,New York, 726-753.

152. Suess, E. and Thiede, J. 1983. Coastal upwelling,its sediment record. Pt. A. Responses of the sedimentary regime to present coastal upwelling. NATO Conference Series IV Marine Sciences,10a,Plenum Press,New York.

153. Thiede, J., and Suess, E., 1983. Coastal upwelling,its sediment record. Pt. B. Sedimentary records of ancient coastal upwelling. NATO Conference Series IV Marine Sciences,10b,Plenum Press,New York.

154. Thunell, R.C., Locke, S.M. and Williams, D.F., 1988. Glacio-eustatic sea-level control on Red sea salinity, Nature,334,601-604.

155. UNESCO, 1971.Discharge of selected rivers of the world, Vol.II,Paris,Imprimeries Reunics S.A.,Lausanne.

156. Urey, H.C., 1947. The thermodynamic properties of isotopic substances. J. Chem. Soc. 169-182.

157. Van Campo, E., Duplessy, J.C. and Rossignol-Strick,M., 1982. Climatic conditions deduced from a 150 kyr oxygen isotope-pollen record from the Arabian sea. Nature,296,56-59.

158. Van Campo, E.,1986. Monsoon fluctuations in two 20,000 yr B.P. oxygen-isotope/pollen records off southwest India,Quat. Res.,26,376-388.

159. Vergnaud-Grazzini, C., 1975. $\delta^{18}O$ changes in foraminiferal carbonate during the last 10^5 years in the Mediterranean sea. Science,190,272-274.

160. Vergnaud-Grazzini, C., 1976. Non-equilibrium isotopic compositions of shells of planktonic foraminifera in the Mediterranean sea., Palaeo. Palaeo. Palaeo.,320, 263-276.

161. Vincent, E., Killingley, J.S. and Berger, W.H.,1981a. Stable isotope composition of benthic foraminifera from the equatorial Pacific.,Nature 289,639-643.

162. Vincent, E., Killingley, J.S. and Berger, W.H.,1981b. Stable isotope in benthic foraminifera from Ontong-Java plateau, Box cores ERDC 112 and 113., Palaeo. Palaeo. Palaeo.,33,221-230.

163. Volat, J., Pastouret, L. and Vergnaud-Grazzini,C.,1980. Dissolution and carbonate fluctuations in pleistocene deep-sea cores A review. Marine Geology,34,1-28.

164. Wachter, E.A., and Hayes,J.M.,1985. Exchange of oxygen isotopes in carbon dioxide - phosphoric acid systems. Chemical Geology (Isotope Geoscience Section), 52, 365-374.

165. Wasson,R.J.,Rajaguru,S.N.,Misra,V.N.,Agarwal,D.P.,Dhir, R.P., Singhvi, A.K. and Kameswara Rao, K., 1983. Geomorphology, late Quaternary stratigraphy and palaeoclimatology of Thar dune field. Z. Geomorph. N.F. 45,117-151.

166. Weber, F.F. and Sackett,W.M.,1981. Uranium geochemistry in Orca basin. Geochim. Cosmochim. Acta,45,1321-1329.

167. Weser, O.E., 1974. Sedimentological aspects of strata encountered on Leg 23 in the northern Arabian sea. Init. Rep. D.S.D.P.,23,503-526.

168. Williams, D.F., Sommer, M.A. and Bender,M.,1977. Carbon isotopic composition of recent planktonic foraminifera of the Indian ocean. Earth Planet. Sci. Lett.,36, 391-403.

169. Williams, D.F., Be, A.W.H. and Fairbanks, R.G., 1979. Seasonal oxygen isotope variations in living planktonic foraminifera, off-Bermuda, Science, 206, 447-449.

170. Williams, D.F., Be, A.W.H. and Fairbanks, R.G., 1981. Seasonal stable isotopic variations in living planktonic foraminifera from Bermuda plankton tows. Palaeo. Palaeo. Palaeo.,33,71-102.

171. Wyrtki, K., 1971. Oceanographic Atlas of the International Indian Ocean Expedition, N.S.F., Washington,D.C.,U.S.A.,531.

LIST OF PUBLICATIONS OF THE AUTHOR

1. Cretaceous-Tertiary boundary - an enigma in earth sciences. A. Sarkar, Ind. Jour. Earth Sc. 1,1986.

2. $\delta^{18}O$ in dinosaur eggshells from India - a clue to Palaeowind. A. Sarkar and S.K. Bhattacharya, Terra Cognita 6, no. 2,1986.

3. Cretaceous-Tertiary boundary marine extinctions : The Russian platform record. Y. Herman, S.K. Bhattacharya, K.P. Nelson, A. Sarkar,L.F. Kopaevitch,D.P. Naidin,V.T. Frolov,J.D. Jeffers. Revista Espanola de Paleontologia, n. Extraordinario, 31-40, 1988, Palaeontology and Evolution-Extinction Events.

4. Mean proloculus size, $\delta^{13}C$ and $\delta^{18}O$ variations in recent benthic foraminifera from the West Coast, India : Climatic implications. Rajiv Nigam and A. Sarkar, Jour. Geol. Soc. India (in press).

5. $\delta^{18}O$ evidence for a stronger north-east monsoon current during the last glaciation. A. Sarkar, R. Ramesh, S.K. Bhattacharya and G. Rajagpopalan. Submitted to Nature.

6. Stable isotope studies in Indian carbonatites. A. Sarkar et. al. Paper presented at the 3rd National Symposium of Mass Spectrometry,Hyderabad,1985.

7. Intercluth $\delta^{18}O$ variations in dinosaurian egg-shells - a clue to Palaeoclimatic study. A. Sarkar et. al. Presented at Symposium on Isotope based studies on problems of Indian Geology, Calcutta, 1986.

8. Geochronological studies of some deep sea cores from Arabian sea and Indian ocean. Paper presented at Arabian Sea Geology Symposium, Mangalore, August, 1987.

9. An on-line CO_2 extraction system for stable Isotope analysis of carbonates. A. Sarkar and S.K. Bhattacharya. Paper presented at the 4th National Symposium of Mass Spectrometry, Bangalore, January 1989.

10. Carbonatites from Bermer and Mundwara alkaline complex, Rajasthan, India. R.K. Srivastava, A. Sarkar and S.K. Bhattacharya (under publication).

11. Petrographic and Isotopic studies of some Eocene Assilina Marlites of western Kutch-evidence of a highly reducing environment. A. Sarkar, A.K. Roy and C.C. Ghosh (under publication).